MODEL PREDICTIVE CONTROL (MPC) FOR CONSTRAINED NONLINEAR SYSTEMS

Thesis by

Simone Loureiro de Oliveira

In Partial Fulfillment of the Requirements

for the Degree of

Doctor of Philosophy

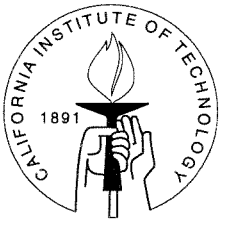

California Institute of Technology

Pasadena, California

1996

(Submitted March 5, 1996)

Acknowledgements

I wish to express my deepest gratitude to my advisor Manfred Morari for his continuous guidance, care and support throughout this work. His insightful criticism, comments, suggestions and his overall friendly style contributed decisively to the development of this work and to the enjoyment of my academic life both at Caltech and at ETH. I am mostly grateful for the ample freedom he allowed me in conducting my research. Many thanks also to the members of the thesis committee, John Doyle, Richard Murray, Stephen Wiggins and George Gavalas, for their time and valuable suggestions.

I would like to acknowledge the always beneficial interaction with the faculty of the Departments of Chemical, Mechanical and Electrical Engineering at Caltech especially during my course work and in the early stages of research.

The discussions with Frank Doyle, Frank Allgöwer, John Doyle and Wei-Min Lu on nonlinear control in 1991/92 were very helpful in starting me off in my research project and introducing me to new concepts and ideas in control theory.

Great support and encouragement were given to me by professors Evaristo Chalbaud Biscaia Jr. and Argimiro Secchi at the Federal Universities of Rio de Janeiro (UFRJ) and Rio Grande do Sul (UFRGS), respectively, and I would like to thank them in a very special way.

Thanks to my colleagues Iftikhar, Carl and Matt for making lunch time fun at ETH. A very special thanks to Mayuresh for his relentless care, support and understanding. For the last two and a half years, he has certainly been my favorite person and closest, dearest friend.

To my parents, what can I say? Words cannot express my gratitude to these two wonderful people who I had the privilege to have as parents. They kept my motivation alive in the worst times and, of course, they made it all possible.

Finally, the financial support from the Coordenadoria de Aperfeiçoamento de Pes-

soal de Nível Superior (CAPES), the US Department of Energy, the National Science Foundation and, in the last year, from the Swiss Federal Institute of Technology (ETH), is gratefully acknowledged.

Abstract

This thesis addresses the development of stabilizing model predictive control algorithms for nonlinear systems subject to input and state constraints and in the presence of parametric and/or structural uncertainty, disturbances and measurement noise.

Our basic model predictive control (MPC) scheme consists of a finite horizon MPC technique with the introduction of an additional state constraint which we have denoted *contractive constraint.* This is a Lyapunov-based approach in which a Lyapunov function chosen a priori is decreased, not continuously, but discretely; it is allowed to increase at other times (between prediction horizons). We will show in this work that the implementation of this additional constraint into the on-line optimization makes it possible to prove rather strong stability properties of the closed-loop system. In the nominal case and in the absence of disturbances, it is possible to show that the presence of the contractive constraint renders the closed-loop system exponentially stable. We will also examine how the stability properties weaken as structural and/or parametric model/plant mismatch, disturbances and measurement noise are considered.

Another important aspect considered in this work is the computational efficiency and implementability of the algorithms proposed. The MPC schemes previously proposed in the literature which are able to guarantee stability of the closed-loop system involve the solution of a nonlinear programming problem at each time step in order to find the optimal (or, at least, feasible) control sequence. Nonlinear programming is the general case in which both the objective and constraint functions may be nonlinear, and is the most difficult of the smooth optimization problems.

Due to the difficulties inherent to solving nonlinear programming problems and since MPC requires the optimal (or feasible) solution to be computed on-line, it is important that an alternative implementation be found which guarantees that the problem can be solved in a finite number of steps. It is well-known that both linear

and quadratic programming (QP) problems satisfy this requirement.

If a standard quadratic objective function is used and the input/state constraints are linear in the decision variables, then the contractive constraint (which is originally a quadratic constraint) can be implemented in such a way that the optimization problem to be solved in the prediction step of the MPC algorithm is reduced to a QP. Having linear input/state constraints means that a linear approximation of the original nonlinear system has to be used in the prediction as well as in the computation of the contractive constraint. Thus, in order to make the algorithm more easily implementable we introduce the difficulty of having to handle the mismatch between the real nonlinear system and its linear approximation which is used for prediction. In other words, we now have a robust MPC control problem at hand. In this case, it is the contractive constraint which comes to the rescue and allows the MPC controller to stabilize the closed-loop system in spite of the linear/nonlinear mismatch, for certain choices of the contractive parameter (the parameter which defines how much "shrinkage" of the states is required during one prediction horizon).

In summary, this thesis is an application of contractive principles to model predictive control and it is dedicated to robust stability analysis, design and implementation of state and output feedback "contractive" MPC schemes.

Contents

List of Figures

Chapter 1 Introduction

The vast majority of industrial processes is typically operated using linear controllers, although it is well known that many of these processes are highly nonlinear. The major difficulty in the design of feedback control laws for nonlinear systems arises from the necessity to explore the whole state space. The problem of the design of feedback controls for nonlinear systems has found a general solution only in the case of systems which are feedback equivalent to linear systems. The fact that most nonlinear systems are not feedback equivalent to linear ones has motivated the study of alternative control techniques which do not require construction of diffeomorphic state-feedback transformations. One of these techniques is model predictive control (MPC) - an optimal control based method for the construction of stabilizing feedback control laws.

A key feature contributing to the success of model predictive control is that various process constraints can be incorporated directly into the on-line optimization performed at each time step. In other words, model predictive control has the potential, not easily possessed by other methods, to globally stabilize linear and nonlinear systems subject to control and/or state constraints. This is undoubtedly a very important feature since many practical control problems are dominated by constraints. In [89], Mayne and Polak state:

> "It can be argued that the most urgent, unresolved control problem is an effective, practical method for the design of feedback controllers for **constrained** dynamic systems, linear or nonlinear."

Other important features of MPC are its ability to handle multi-input multi-output

(MIMO) systems with very little changes in the formulation compared to the single-input single-output (SISO) case, and its variable structure in the event of faults.

Besides being subject to input/state constraints, most real systems are represented by process models which are not accurate. Furthermore, they are invariably subject to disturbances of various kinds. Due to these practical problems, it is important for the controllers designed to be *robust* (i.e., take into account the model/plant mismatch which may exist and guarantee satisfactory stability and performance properties of the closed-loop system) and present good *disturbance rejection* properties.

Regarding robustness, a very extensive theory [102] has been developed for the robust control of linear systems without constraints. This theory has been proven successful when applied to a number of academic case studies such as, e.g., high purity distillation columns (see [116]), with process constraints not taken into consideration. The neglect of constraints has made this robust control theory unsuitable for industrial applications. When constraints are considered, even if the plant is linear, the overall control problem becomes nonlinear and this is the reason why constrained problems are so much harder to deal with than unconstrained ones.

In spite of MPC's considerable practical importance and extensive use, there is in fact very little theory to guide the design and tuning of these controllers for stability, performance and robustness, especially in the nonlinear case. Moreover, the existing stability and robustness analysis of MPC applied to nonlinear systems is rather complicated and non-intuitive and the resulting controllers hardly implementable.

It is the goal of this thesis to develop a general theory for designing controllers for nonlinear continuous-time systems subject to constraints with robust stability and robust performance guarantees. Several different problems will be considered, such as output feedback, parametric model/plant mismatch, disturbance rejection, structural model/plant mismatch, etc. One of the main concerns throughout this work is to develop nonlinear MPC (NLMPC) controllers which involve a reasonable computational effort and can be easily implemented.

1.1 Motivation

Most practical control problems are dominated by process constraints and nonlinearities. The most common process constraints are constraints on the manipulated and/or state variables. Regarding the nonlinear character of most real systems, nonlinearities can be quantified as "weak" or "strong" (see [5, 6]) and it may be that while a linear controller design is satisfactory for a "weakly nonlinear" system it will most probably be inappropriate for a system with stronger nonlinearities.

With respect to process constraints, constraints on the manipulated variables are present in the vast majority of processes and they result from physical limitations of the actuators which cannot be exceeded under any circumstances. Safe operation of a plant very often requires limitations on states as well, such as velocity, acceleration, temperature and pressure. State constraints are also a natural way to express control performance objectives in many applications. Although most control constraints should be respected throughout the operation (hard constraints), it may be unavoidable to exceed the state constraints for some time, especially if the system is subjected to disturbances not accounted for in advance. Therefore, the constraints imposed on states and output variables are most often soft constraints.

Regarding system nonlinearities and model error (be it parametric and/or structural), most model predictive control designs do not take these factors into account. The presence of unmodeled nonlinearities and unknown parameter values can make the tuning of MPC controllers for certain stability and performance requirements quite cumbersome, if not impossible. In fact, if uncertainty in the structure of the nonlinearities and/or in the parameter values is not properly accounted for, the performance on the real system can be arbitrarily poor (the result could even be an unstable closed-loop system). Therefore, since exact modeling of a plant is not feasible in most practical cases, the controller must be designed to show very little sensitivity to model uncertainty.

A rich theory has been developed to address the robustness issue in unconstrained linear systems (as will be discussed in the next section). For constrained and uncertain linear systems the scope of results is not so vast. And, as one would expect, for constrained and uncertain nonlinear systems results are few and incomplete. One can surely say that the theory on constrained control of nonlinear systems (be it the nominal or robust case) is still in its infancy. It is the goal of this thesis to add a contribution to this area.

1.2 Previous work

1.2.1 A general look

Open-loop optimal feedback, dating back to a 1963 seminal paper by Propoi, [108], is a general approach for the construction of stabilizing feedback laws for systems subject to input constraints and other nonlinearities. Originally, it was based on the idea that in a sampled-data system, the control to be applied between sampling times can be determined by solving a fixed horizon open-loop optimal control problem with or without constraints. Over the years, open-loop optimal feedback has been explored under the names of *model predictive control* (to mention a few references, see [48, 49, 50, 51, 73, 94, 107]) and *moving horizon control* (see, e.g., [62, 68, 69, 71, 81, 82, 83, 84, 85, 95]).

The literature dealing with linear MPC presents an enormous amount of results on issues such as stability, reference trajectory tracking and constant disturbance rejection capabilities of the resulting feedback systems, under the assumption that control and state variables are unconstrained (see, e.g., [33]). Nominal stability results for constrained linear systems can be found in [31, 101, 91, 109], for robust analysis see [66, 122, 127].

As far as moving horizon control is concerned, it has not always been realized that

a naive application of the strategy can lead to instability. The early literature dealt with the stabilizing properties of moving horizon control laws based on open-loop optimal control for finite horizon optimal control problems with quadratic criteria and no input constraints. More recently, [66, 69, 71, 128] dealt with linear time-varying (LTV) systems, [1, 2, 3, 62, 92, 91] dealt with nonlinear discrete-time systems and [28, 81, 82, 83, 84, 85] have established the stability properties of nonlinear, continuous-time systems with moving horizon control in the presence of constraints. In [95] Mayne and Michalska examined the robust stability of a moving horizon control, although the analysis is somewhat involved and the resulting *hybrid control law* (a nonlinear MPC controller is used to drive the states to a small neighborhood of the origin and the control law switches over from MPC to a linear controller which is then used to drive the states asymptotically to the origin) is hard to implement even for simple examples. [83, 85] took into account the non-trivial time needed for the computation of the open-loop control law even in the nominal case. [125] analyzed the robust stability problem by discretizing the problem into multiple linear feedback control systems.

Dealing with the nonlinear control and estimation problems simultaneously we can find [87], although the stability analysis presented in that work is quite complicated and incomplete.

An adaptive receding horizon control scheme for constrained nonlinear systems can be found in [88] although we can clearly say that adaptive control theory for constrained systems (linear or nonlinear) is still in its infancy and this is only a very preliminary work in the area.

1.2.2 MPC and its different implementations

The basic formulation of an MPC problem for a nonlinear plant of the form

$$\dot{x}^p(t) = f^p(x^p(t), u(t), t), \quad x^p(t_0) =: x_0^p \tag{1.1}$$

$$y(t) = g^p(x^p(t), u(t), t) \tag{1.2}$$

is the following:

$$\min_{u(t)} \Phi[x(t), u(t)] \tag{1.3}$$

subject to:

$$\dot{x}(t) = f(x(t), u(t), t), \quad \text{with } x(t_0) = x_0 \text{ and } t \in [t_0, t_0 + PT] \tag{1.4}$$

$$\kappa(x(t), u(t), t) = 0 \tag{1.5}$$

$$h(x(t), u(t), t) \geq 0 \tag{1.6}$$

where:

Φ := performance criterion (a positive definite function)

f, f^p := model and plant dynamics, respectively

g^p := output model

κ, h := equality and inequality time-varying mixed input/state nonlinear constraints (in the most general case), respectively

$x^p(t)$:= state vector of the plant

$y(t)$:= output vector

$x(t)$:= state vector of the model

$u(t)$:= control vector

P := prediction horizon; an integer number which can be finite or infinite

x_0^p, x_0 := initial condition of the plant and model states, respectively

t_0 := initial time of computation

T := sampling time

PT := prediction time

Throughout this thesis the symbol ":=" means that the left-hand side is defined to be equal to the right-hand side; the reverse holds for "=:".

The control sequence $u(t)$ is computed for $t \in [t_0, t_0 + PT]$ but only $u(t)$ restricted to $t \in [t_0, t_1 := t_0 + T]$ is actually applied to the real plant (1.1). At time t_1 a measurement $y(t_1)$ is obtained, the states of the plant are estimated (in the case where not all states can be directly measured at sampling times) and with this new initial condition $x_1 := \hat{x}(t_1)$ (where $\hat{x}(t)$ represents the estimated states of the plant at time t) a new optimization problem is solved at time t_1. This is known as a receding horizon implementation of the control law.

The plant (1.1) is linear if its dynamics is given by:

$$\dot{x}^p(t) = f^p(x^p(t), u(t), t) := A^p(t)x^p(t) + B^p(t)u(t) \tag{1.7}$$

$$y(t) = C^p(t)x^p(t) + D^p(t)u(t) \tag{1.8}$$

If all the matrices $A^p(t), B^p(t), C^p(t)$ and $D^p(t)$ are constant, the linear system (1.7), (1.8) is said to be time-invariant (LTI system); if one or more of them vary in time, we have a linear time-variant (LTV) system.

Let the linear model used in the prediction be given by:

$$\dot{x}(t) = f(x(t), u(t), t) := A(t)x(t) + B(t)u(t) \tag{1.9}$$

If $f(x(t), u(t), t)$ ($\{A(t), B(t)\}$) differ from $f^p(x^p(t), u(t), t)$ ($\{A^p(t), B^p(t)\}$) for some $t \in [t_0, \infty)$ we have a nonlinear (linear) *robust* control problem at hands.

In general, the performance criterion Φ is given by:

$$\Phi[x(t), u(t)] := \int_{t_0}^{t_P := t_0 + PT} \phi[t, x(t), u(t)]dt \; + \; \varphi[t_0, x(t_0), t_P, x(t_P)] \tag{1.10}$$

where the functions $\phi : \Re \times \Re^n \times \Re^m \to \Re$ and $\varphi : \Re \times \Re^n \times \Re \times \Re^n \to \Re$ are positive (semi-)definite functions of their arguments.

Most commonly, ϕ is a time-invariant quadratic function of its arguments, i.e.,

$$\phi[t, x(t), u(t)] = x(t)'Qx(t) + u(t)'Ru(t)$$

with Q, R positive definite matrices, and $\varphi = 0$.

Within the context of the preceding formulation, MPC algorithms can be divided into the following main categories:

(1) Finite prediction horizon [$P \in (0, \infty)$] for:

- Linear plants [27, 35, 49];
- Nonlinear plants [19, 20, 39, 48];

(2) Infinite prediction horizon [$P \to \infty$] for:

- Linear plants [66, 109, 127];
- Nonlinear plants [1, 3, 92];

(3) Finite prediction horizon with end constraints[1] (also known as stability constraints) for:

- Linear plants [13, 23, 32, 52, 69, 101, 122, 123, 127];
- Nonlinear plants [1, 2, 28, 62, 63, 81, 82, 83, 84, 85, 91, 95, 96, 124].

In the first category a simple finite horizon objective function is employed which does not, per se, guarantee stability. This means that closed-loop stability cannot be assumed simply because the on-line optimization finds a solution. The issue of closed-loop stability is complicated by two facts: first, there is always uncertainty associated with the model used in the prediction; second, the presence of constraints in the optimization problem results in a nonlinear closed-loop system even if the model and plant dynamics are linear. In [22] the authors underlined the poor stability properties of finite prediction horizon schemes.

In the second category, [92, 109] propose a control algorithm which minimizes an infinite horizon objective function subject to the constraint that the unstable modes of the plant are set to zero at some finite time. This kind of control algorithm has desirable stability properties in the nominal case but it cannot be extended in a straightforward manner to plants with uncertainty. In [66], the authors propose a technique which deals explicitly with model/plant uncertainty in LTV plants. The goal in this technique is to design, at each time step, a state feedback control law which minimizes a "worst-case" infinite horizon objective function, subject to constraints on the control inputs and plant outputs. The problem of minimizing an upper bound on the "worst-case" objective function subject to constraints is reduced to a convex optimization involving linear matrix inequalities (LMIs). It is shown that the feasible receding horizon state feedback control design robustly stabilizes the set of uncertain plants. In [1, 3], discrete-time nonlinear systems are considered and global stability of the infinite prediction horizon scheme is shown under certain stabilizability assumptions.

[1]By end constraint we mean any state constraint imposed at the end of the prediction horizon.

It should be pointed out that one of the great restrictions of infinite prediction horizon schemes (even with finite control horizons) is naturally computational.

The third category is the one with most of the desirable stability and robustness characteristics. In the nonlinear context, MPC for discrete-time systems with mixed state/control constraints is discussed in an important paper by Keerthi and Gilbert [62]. The control action is determined by minimizing, at each k^{th} time step, a nonlinear cost function over the horizon $[k, k + P_k]$ (here the horizon P is not constant, instead it is included as a decision variable in the optimization together with the control and represented by P_k) subject to the mixed state/control constraints and the terminal equality constraint $x(k + P_k|k) = 0$ and setting the current control equal to the first element of the minimizing sequence. Keerthi and Gilbert show that this control is, under certain conditions, stabilizing. The finite horizon approach for nonlinear discrete-time systems proposed in [1, 2] is very similar to this found in [62], the only apparent difference being that certain observability assumptions on the system can be relaxed because the performance criterion is defined in terms of states and inputs (instead of outputs and inputs as in [62]). In [91] the same end equality constraint is used to show stability using Lyapunov arguments. The authors show in that paper that systems which are feedback linearizable can be asymptotically stabilized with MPC. They also find discrete-time systems which cannot be stabilized with continuous feedback and they show that MPC generates a discontinuous feedback which stabilizes such systems.

Model predictive control for nonlinear time-invariant continuous-time systems is introduced in [28] but Mayne and Michalska [81, 82, 83, 84, 85] appear to provide the first rigorous analysis. Here the value function for the (open-loop) finite horizon control problem, which is continuously solved, is employed as a Lyapunov function for the closed-loop system. In order to apply standard Lyapunov theory, fairly strong assumptions (including controllability of both the nonlinear system and its linearization about every trajectory) are made to establish continuous differentiability of the value function. The latter property is relaxed in [85] where only Lipschitz continuity of the

value function is required, allowing for less strict assumptions on the behavior of the linearized system. In each case, the finite horizon control requires exact solution, at each time instant k, of a finite horizon nonlinear control problem with the terminal equality constraint $x(k + P_k|k) = 0$.

In [82] a relaxed version of the stability constraint for continuous-time nonlinear systems is presented, i.e., instead of $x(k+P_k|k) = 0$, the authors use $x(k+P_k|k) \in W$ (where W is some neighborhood of the origin). Since the terminal constraint has been relaxed, the MPC strategy loses its stabilizing properties inside W. To compensate for this effect, a linear, locally stabilizing controller designed for the linearized system is used inside W. The resulting "hybrid" controller is shown to be globally stabilizing.

One common factor in the stability proofs of all MPC schemes mentioned here is that the questions related to feasibility are eluded through the assumption that the constrained control problem always remains solvable. In [113], it is argued that the issue of feasibility is in fact central to the question of stability and that, therefore, the feasibility assumption is inappropriate. In that work, a technique for systematic handling of infeasibilities is proposed which is such that its use allows stability guarantees obtained under the assumptions of feasibility to be carried over to the usual case when feasibility cannot be guaranteed (details of this technique are not found in [113] but the authors claim that they will be published in the Ph.D. thesis of P. Scokaert).

A rather comprehensive review of all these methods can be found in [70].

1.3 Thesis overview

1.3.1 General contents

In chapter 2, we give a brief tutorial review of the state space formulation of MPC for both linear and nonlinear systems. There we concentrate on the stability results found in the literature for the three main classes of linear/nonlinear constrained MPC controllers:

(1) Finite prediction horizon MPC.

(2) Infinite prediction horizon MPC.

(3) Finite prediction horizon MPC with (stabilizing) end constraints.

We see that for class **(1)** there are no stability guarantees. For class **(2)** the controller is stabilizing if the optimization is feasible. And, finally, for class **(3)**, even though the prediction horizon is finite, the end constraints add stability (and sometimes robustness) to the controller.

In chapter 3, we introduce our so-called *Contractive MPC* scheme. Contractive MPC is a finite horizon nonlinear MPC algorithm which is stabilized through the addition of an end constraint called *contractive constraint*. In that chapter, we introduce the formulation, implementation and basic philosophy of the contractive MPC scheme and discuss its stability properties in the nominal case and in the absence of disturbances. The results show that the contractive constraint exponentially stabilizes the closed-loop system when model uncertainty and disturbances are absent. We also discuss the conditions under which the chosen standard quadratic objective function is a Lyapunov function for the closed-loop system. Finally, four examples are introduced:

(1) A nonholonomic system (the model of a car)

(2) A fluidized catalytic cracking unit (FCCU)

(3) A 2-degree of freedom robot

(4) A continuous stirred tank reactor (CSTR) + flash unit

We apply our contractive MPC scheme to these four examples which are of very different natures and present varied levels and sources of difficulties (that are discussed there) and the obtained simulation results are compared with a standard finite prediction horizon nonlinear MPC algorithm. Moreover, in the case of the car, we also present a comparison of our results with some analytical control design techniques derived especially for nonholonomic systems.

In chapter 4, we examine how the stability results are modified when the system is subjected to an asymptotically decaying disturbance of bounded energy. Our results demonstrate that the closed-loop system becomes uniformly asymptotically stable in the presence of this class of disturbances (thus, the exponential stability properties of contractive MPC are weakened to uniform asymptotic stability). We also show that this kind of disturbance can be caused by introduction of an asymptotically convergent observer into the closed-loop for purposes of state estimation. We then derive sufficient conditions under which the association of an exponentially stable controller (such as contractive MPC) with an asymptotically convergent observer, generates an asymptotically stable closed-loop system. Furthermore, we design such an observer for a continuous-time system with discrete observations and prove its asymptotic convergence properties. The results reveal that if the outputs are measured continuously, then this nonlinear observer has its convergence properties strengthened as it becomes exponentially stabilizing.

At the end of that chapter, we perform simulations for the so-called *van der Vusse* reactor, a benchmark CSTR system. We study the closed-loop response under exponentially decaying disturbances and the results are compared with the ones obtained with a standard NLMPC algorithm. Then we design a discrete version of the nonlin-

ear state estimator proposed in that chapter (the reason we use this discrete version of the observer instead of the original mixed continuous/discrete one is to reduce the differential Riccati equation to an algebraic Riccati equation) for the example mentioned above and examine the behavior of the closed-loop system generated by the resulting output feedback controller.

In chapter 5, we first look into the state feedback control problem when persistent, bounded and non-additive disturbances affect the nonlinear dynamics of the system. In the nonlinear context, the problem posed by disturbances of this kind is equivalent to having parameter uncertainty only (i.e., model and plant are matched in the nonlinear structure, only some - or all - parameters are unknown). We demonstrate that the most which can be guaranteed under non-additive bounded disturbances or constant parameter mismatch, is that the states are driven to a control invariant set whose size is proportional to the magnitude of the disturbances or parameter deviation. Then, we examine how these results change when the states are also unknown (which constitutes the output feedback case) if the parameters are unknown but constant. We use a moving horizon-based least-squares estimator for state estimation. Additionally, we study in that chapter how the results are modified if both states and parameters are unknown, the parameters are time-varying, the system is subjected to additive disturbances and the moving horizon least-squares estimation procedure seeks to estimate states, disturbances and parameters.

The example used to test the robust state and output feedback contractive MPC controllers proposed in chapter 5 is a biochemical reactor with substrate inhibition. There we study how the closed-loop behaves when there is a constant parameter deviation between the model used for prediction, computation of the contractive constraint and estimation and the real nonlinear system.

The MPC schemes in chapters 3, 4 and 5 involve the solution of a nonlinear programming problem at each time step to find the optimal (or, at least, feasible) control sequence. Nonlinear programming is known to be the most difficult of the smooth

optimization problems. Indeed there is no general agreement on the best approach to be used for its solution and much research is still to be done. Due to the difficulties inherent to solving nonlinear programming problems and since MPC requires the optimal (feasible) solution to be computed on-line, we propose in chapter 6 an alternative implementation which guarantees that the problem can be solved in a finite number of steps. It is well-known that quadratic programming (QP) problems satisfy this requirement. Thus, we show in that chapter how to pose the optimization problem as a QP by means of using a linear approximation of the original nonlinear system in the prediction step of the MPC control algorithm and by implementing the contractive constraint in an appropriate way. We propose three different ways of implementation of the contractive constraint, namely, the "approximate (or conservative) approach", the "penalty function approach" and the "approach based on sensitivity analysis of the QP". We also show how to pose the problem as a QP by appropriately defining the Hessian matrix, the gradient vector and the constraint matrices.

Still in chapter 6, we describe the formulation, implementation and basic philosophy of this computationally simplified but harder to analyze controller. The reason why the analysis of the contractive MPC controller, under the local linear approximation of the original nonlinear system, becomes more involved, comes from the fact that the linearization introduces a structural mismatch between the plant and the model used in the control computations (it is basically a linear/nonlinear mismatch, if no other types of uncertainties are considered). Therefore, the controller must be robust with respect to this mismatch (i.e., the controller must stabilize the states of the plant even though nonlinearities are ignored in the prediction). Under certain assumptions on this model/plant mismatch (a growth condition on the nonlinear terms of the model), we show that the states of the plant can be driven to a control invariant set whose size depends on how "strongly nonlinear" the system is. We also include bounded disturbances and parameter mismatch in this analysis.

Finally, at the end of chapter 6, we present simulation results for this more computationally efficient contractive MPC algorithm applied to the 2-degree of freedom robot,

the nonholonomic system/car, the FCCU, the CSTR + flash unit (all of these introduced in chapter 3) and the van der Vusse reactor(introduced in chapter 4) and we compare the results with the ones previously obtained for when the nonlinear system itself is used in the prediction step of the MPC control algorithm.

1.3.2 List of theorems in the thesis

Chapter 3 State Feedback Contractive NLMPC: Nominal Case

Theorem 3.1 Exponential stability of the closed-loop system.

Theorem 3.2 Conditions for the objective function to be a Lyapunov function for the closed-loop (not necessary for exponential stability).

Chapter 4 Output Feedback Contractive NLMPC: Nominal Case

Theorem 4.1 Uniform asymptotic stability of the closed-loop system in the presence of asymptotically decaying disturbances in the state feedback case.

Theorem 4.2 Feasibility condition (sufficient condition on the magnitude of the asymptotically decaying disturbances so that feasibility can be assured).

We then discuss how these asymptotically decaying additive disturbances can be caused, for example, by introduction of an asymptotically stable state estimator into the closed-loop. We propose a mixed continuous/discrete-time nonlinear observer and examine its stability properties.

Theorem 4.3 Computation of a stability region for the nonlinear observer proposed in this chapter. The observer is shown to provide asymptotically convergent state estimates for a certain set of initial state estimation errors and for systems with "not very strongly nonlinear" dynamic and output maps.

Theorem 4.4 Closed-loop stability in the output feedback case. The association of the asymptotically convergent nonlinear observer proposed in this chapter with the exponentially stabilizing contractive MPC controller is shown to originate an asymptotically stable closed-loop.

Chapter 5 Robust Output Feedback Contractive NLMPC: Parameter Uncertainty

Theorem 5.1 Computation of a bound on the difference between model and plant states at the end of prediction horizons, in the presence of parameter uncertainty and in the state feedback case.

Theorem 5.2 Stabilizing properties of the state feedback controller in the presence of parameter uncertainty.

Theorem 5.3 Feasibility condition (sufficient condition on the magnitude of the parameter uncertainty so that feasibility can be assured).

Theorem 5.6 Computation of a bound on the difference between true and estimated states in the presence of parameter uncertainty. The state estimator is a moving horizon-based least squares estimation (LSE) procedure.

Theorem 5.7 Stabilizing properties of contractive MPC in the presence of parameter uncertainty and in the output feedback case.

Theorem 5.8 Feasibility condition (sufficient condition on the magnitude of the parameter uncertainty so that feasibility can be assured in the presence of state estimation errors).

Theorem 5.9 Using the LSE moving horizon-based procedure for both state and parameter estimation, we compute a bound on the difference between true and estimated "augmented" states (i.e., newly defined states which comprise the states and parameters of the plant) at the beginning of the estimation window.

Chapter 6 Contractive NLMPC reformulated as a Quadratic Programming (QP) Problem

Here, local linear approximations of the nonlinear system are used for prediction and in the computation of the contractive constraint, in order to reduce the optimization to a simple QP problem. Thus, we proceed to show how the stability properties of the closed-loop are modified when this structural model/plant (linear/nonlinear) mismatch is introduced. The presence of disturbances and parameter uncertainty is also taken into consideration in our results.

Theorem 6.2 Computation of a bound on the difference between the states of the nonlinear system and of its local linearization at the beginning of prediction horizons.

Theorem 6.3 Feasibility condition (sufficient condition on the structural model/plant mismatch and on the magnitude of possible parameter uncertainty and disturbances, so that feasibility can be assured).

Theorem 6.4 Derivation of finite bounds on the norm of the continuous state trajectory generated by the controller for all time $t \geq 0$, demonstrating its well-posedness.

Theorem 6.5 Feasibility conditions for systems with stable Jacobian in the whole state space (derivation of a lower bound on the contractive parameter so that feasibility can be assured) in the absence of parameter uncertainty or disturbances.

Theorem 6.6 Stability and feasibility properties of the output feedback scheme when the controller has to deal with the mismatch between the linear system used in the control computations and the real nonlinear system, and the nonlinear observer is asymptotically convergent. Parameter uncertainty and disturbances are not considered here.

Chapter 2 MPC: An Overview

2.1 Implementation aspects

A tutorial review of the state space formulation of Model Predictive Control for both linear and nonlinear systems is presented in this chapter.

The various implementations of MPC are identical in their global structure but differ in the details. The general structure of MPC schemes is shown in figure 2.1.

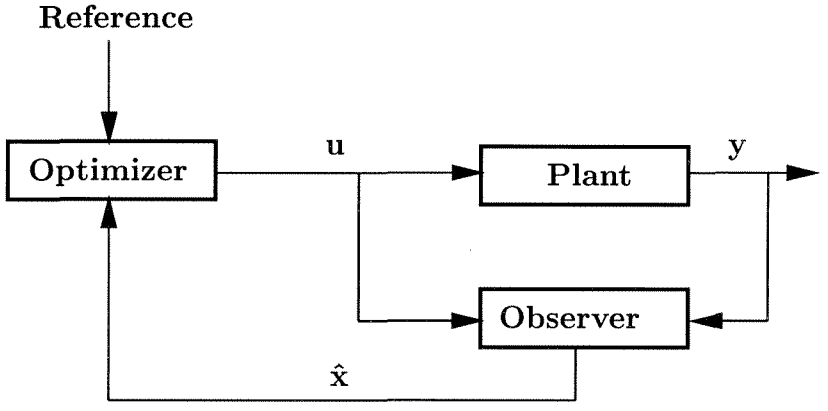

Figure 2.1: Inherent structure in all MPC schemes.

The selected observer uses the input and output information (u and y, respectively) and computes the state estimate $\hat{x}$. With this estimate, one can use an optimization scheme to predict the trajectory of the controlled variables y over some prediction (or output) horizon P with the manipulated variables u changed over some control (or input) horizon M ($M \leq P$). This prediction step is represented in figure 2.2.

At time step k, the optimizer is used to compute the present and future manipulated variable moves $u(k|k), \ldots, u(k+M-1|k)$ such that the predicted outputs follow

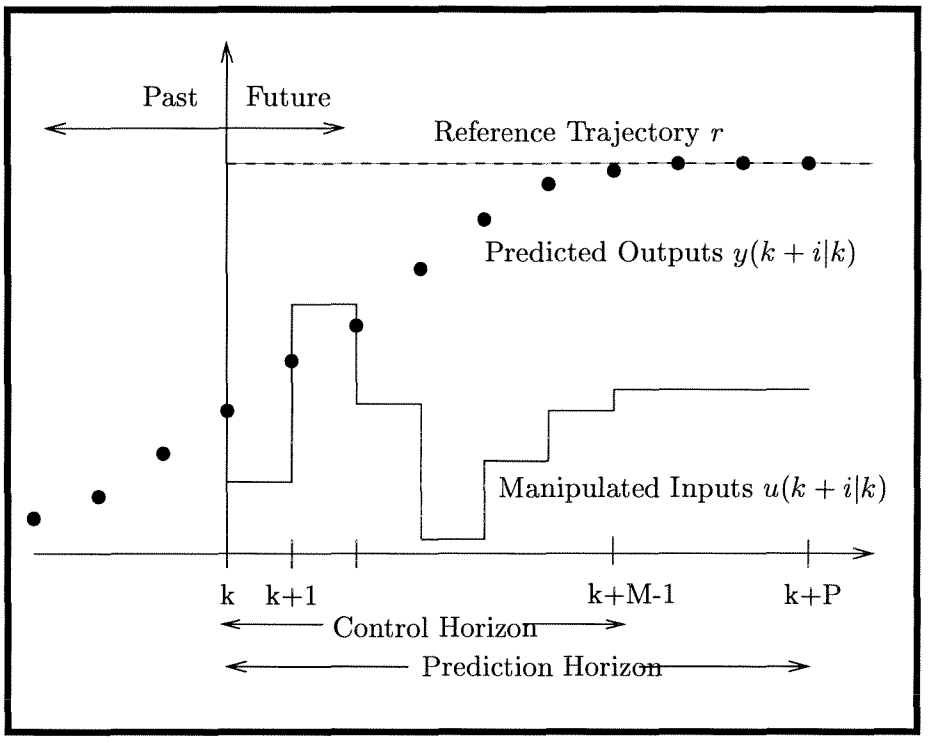

Figure 2.2: Optimization problem at time k.

the selected reference trajectory in a satisfactory manner. The optimizer takes into account the input and output constraints which may exist, by incorporating them directly into the optimization. For linear systems, if a linear or quadratic objective function is considered, the resulting optimization is a linear or a quadratic programming problem, respectively. For nonlinear systems, independent of the chosen performance criterion, the optimization becomes a nonlinear programming problem which is non-convex in the majority of cases.

Only $u(k|k)$, the first control move of the sequence, is implemented on the real plant from time step k to $k+1$. At time step $k+1$ the measurement $y(k+1)$ is used together with $u(k|k)$ by the observer to compute the new estimate $\hat{x}(k+1)$, the horizons M and P are shifted ahead by one step and a new optimization problem is solved at time step $k+1$ with the new initial condition $\hat{x}(k+1)$. This procedure results in a so-called *moving horizon* or *receding horizon* type of strategy. For computational reasons, the

values of the horizons M and P are generally finite. However, it has been observed that it is very hard to provide stability guarantees for an MPC scheme with finite output horizon P (see [22]). Stability results can be obtained when P is infinite, keeping M finite. It has been shown that such selection of controller parameters makes it possible to guarantee certain stability properties of the closed-loop system while keeping the computation effort reasonable in most cases.

2.2 Basic formulation

A very general and not very detailed formulation of the prediction step in MPC algorithms was given in chapter 1. Here we will go into more details regarding the shape of the objective function, prediction models, state estimators and constraints.

2.2.1 Prediction models

(1) Continuous-Time Systems

Linear: In its most general form, a linear prediction model is given by:

$$\dot{x}(t) = A(t)x(t) + B(t)u(t) + E(t);\ x(0) =: x_0 \text{ given} \tag{2.1}$$

$$y(t) = C(t)x(t) + D(t)u(t) \tag{2.2}$$

where $x(t) \in \Re^n$ denotes the state at time t, $u(t) \in \Re^m$ the manipulated variables (or inputs) and $y(t) \in \Re^p$ the controlled variables (or outputs). Here we have not included the disturbance or the noise that the actual plant may be subjected to.

In most cases, the independent term $E(t)$ is not included. If any of $A(t), B(t), C(t)$ or $D(t)$ are functions of time the linear system is called

time-varying (LTV), if they are all constant we have a linear time-invariant (LTI) system.

Nonlinear:

$$\dot{x}(t) = f(x(t), u(t), t); \quad x(0) = x_0 \text{ given} \tag{2.3}$$

$$y(t) = g(x(t), u(t), t) \tag{2.4}$$

In most cases, the nonlinear system is time-invariant, that is, $f(.) : \Re^n \times \Re^m \times \Re \rightarrow \Re^n$ and $g(.) : \Re^n \times \Re^m \times \Re \rightarrow \Re^p$ are not explicit functions of time. Usually, f and g are assumed to be continuously differentiable functions.

(2) Discrete-Time Systems

Linear:

$$x(k+1) = \Phi(k)x(k) + \Gamma(k)u(k) + \eta(k); \; x(0), u(0) \text{ given} \tag{2.5}$$

$$y(k) = C(k)x(k) + D(k)u(k) \tag{2.6}$$

The matrix $\Phi(k)$ is known as *state transition matrix.*

When the continuous-time linear system (2.1) is time-invariant, the discrete form (2.5) can be easily obtained from that system by having $\Phi(k)$, $\Gamma(k), \eta(k)$ given by:

$$\Phi(k) := e^{AT} \tag{2.7}$$

$$\Gamma(k) := \int_0^T e^{A(T-t)}Bdt \tag{2.8}$$

$$\eta(k) := \int_0^T e^{A(T-t)}Edt \tag{2.9}$$

where T is the sampling time.

Nonlinear:

$$x(k+1) = F(x(k), u(k), k);\ x(0), u(0) \text{ given} \tag{2.10}$$

$$y(k) = G(x(k), u(k), k) \tag{2.11}$$

In general, it is not possible to obtain a closed form solution of a general continuous-time nonlinear system as given by (2.3) (the solution has to be computed numerically), which means that F and G are not know explicitly for most systems modeled originally in continuous-time form.

2.2.2 State estimators

In general, state estimators have the following form:

Continuous-Time Systems:

$$\dot{\hat{x}}(t) = \hat{f}(\hat{x}(t), u(t), t) + K(t)\,[y(t) - \hat{y}(t)] \tag{2.12}$$

$$\hat{y}(t) = \hat{g}(\hat{x}(t), u(t), t) \tag{2.13}$$

Discrete-Time Systems:

$$\dot{\hat{x}}(k) = \hat{F}(\hat{x}(k), u(k), k) + K(k)\,[y(k) - \hat{y}(k)] \tag{2.14}$$

$$\hat{y}(k) = \hat{G}(\hat{x}(k), u(k), k) \tag{2.15}$$

In the case where $\hat{f}(.)$ is continuous (discrete) and linear, either because the plant is linear or because we are using a linearized estimator for a nonlinear plant, $K(t)$ (or $K(k)$) is determined from the solution of a differential (algebraic) Riccati equation.

2.2.3 Objective function

Various objective functions can be chosen depending on one's goal in using MPC. The most common one applies the 2−norm both spatially and temporally.

For continuous-time systems the following objective function is commonly used:

$$V_k := V(t_k, x_k) := \int_{t_k}^{t_k+P_kT} [\,\| x_k(t) \|_Q^2 + \| u_k(t) \|_R^2\,]\, dt \tag{2.16}$$

where $\| \cdot \|$ denotes the Euclidean norm of a vector and $\| x \|_{\hat{P}} := \sqrt{x' \hat{P} x}$, with $\hat{P} \in \Re^{n \times n}$ positive definite, is the weighted Euclidean norm of $x \in \Re^n$. $\| \cdot \|$ also denotes the Euclidean norm of a matrix. More generally, $\| \cdot \|_p$, $p \geq 1$, denotes the *Hölder* or p-norm of a vector or matrix (note that when $p = 2$ the p−norm becomes the Euclidean norm) and is given by:

$$\| x \|_p := (|x_1|^p + \ldots + |x_n|^p)^{\frac{1}{p}}, \quad \forall x \in \Re^n, \quad p \geq 1 \tag{2.17}$$

$$\| A \|_p := \sup_{x \neq 0,\, x \in \Re^n} \frac{\| Ax \|_p}{\| x \|_p}, \quad \forall A \in \Re^{m \times n} \tag{2.18}$$

where $|x_i|$ denotes the absolute value of $x_i \in \Re$, $\forall i = 1, \ldots, n$.

If we make $p = 2$ in definition (2.18) and $A \in \Re^{n \times n}$ ($C^{n \times n}$, in the general case of complex matrices and vectors) we have the so-called *induced (matrix) norm* of A corresponding to the Euclidean vector norm $\| \cdot \|$ on $\Re^n$ (C^n):

$$\| A \| := \sup_{x \neq 0,\, x \in \Re^n} \frac{\| Ax \|}{\| x \|} = \sup_{\|x\| = 1} \| Ax \| = \sup_{\|x\| \leq 1} \| Ax \| \tag{2.19}$$

The p-norms satisfy certain important properties which will be used here and that can be found in most books on matrix computations and numerical analysis (see, e.g.,

[54, 58]).

Besides the Euclidean and Hölder norms of vector and matrices, we will define $|||\ .\ |||$ to be the induced norm on tensors. Let $\|\ .\ \|$ be a given norm on $\Re^n$ (C^n). Then, for each tensor $\tilde{T} \in \Re^{n\times n\times n}$ ($\tilde{T} \in C^{n\times n\times n}$), the quantity $|||\tilde{T}|||$ defined by

$$|||\tilde{T}||| := \sup_{x,y\neq 0,\, x,y\in\Re^n} \frac{\| y'\tilde{T}x \|}{\| y \| \| x \|} = \sup_{\|x\|=\|y\|=1} \| y'\tilde{T}x \| = \sup_{\|x\|\leq 1,\, \|y\|\leq 1} \| y'\tilde{T}x \| \tag{2.20}$$

is called the *induced (tensor) norm* of $\tilde{T}$ corresponding to the vector norm $\|\ .\ \|$.

The notation used in (2.16) is the following: x_k are the states of the system at time t_k (in the output feedback case we would have $\hat{x}_k$, that is, the estimate of x_k); to keep coherent with the discrete case, P_k is the output or prediction horizon (which is a decision variable, together with the control, in some algorithms and therefore we are allowing it to be a function of k); T is the sampling time; $x_k(t)$ represents the state trajectory of the model for all $t \in [t_k, t_k + P_kT]$ given the initial condition x_k at t_k; $u_k(t)$ is the control trajectory to be computed for the same time interval and initial condition; Q and R are positive definite matrices and they are controller tuning parameters (known as *weights* in the objective function).

For simplified computation, most implementations of MPC generate a sequence of M[1] discontinuous control moves, $\{u(k|k), \ldots, u(k+M-1|k)\}$, instead of a continuous trajectory $u_k(t)$. In other words, these controllers require that $u_k(t) = u(k+i|k)$ for all $t \in [t_k+iT, t_k+(i+1)T)$ and $i \in [0, M-1]$, and $u_k(t) = 0$ for $t \in [t_k+MT, t_k+P_kT]$. In this case, the objective function can be rewritten as:

[1] In the implementations where the output horizon is a decision variable there is no difference between input and output horizons.

$$V_k := V(t_k, x_k) := \int_{t_k}^{t_k+P_kT} x_k(t)' Q x_k(t)\, dt \; + \; T \sum_{i=0}^{M-1} u(k+i|k)' R u(k+i|k) \quad (2.21)$$

If the system is linear or has a closed form solution it is possible to express the states $x_k(t)$ and, consequently, the objective function, as an explicit function of the control moves.

From this point forward we will consider P as a pre-specified tuning parameter, constant throughout the computations, in order to simplify the notation (unless otherwise necessary to make the distinction).

For discrete-time systems the most commonly used objective function is the quadratic one given by:

$$\begin{aligned} V_k \; := \; & \sum_{i=1}^{P} x(k+i|k)' Q x(k+i|k) + \sum_{i=0}^{M-1} u(k+i|k)' R u(k+i|k) + \\ + \; & \sum_{i=0}^{M-1} \Delta u(k+i|k)' S \Delta u(k+i|k) \end{aligned} \quad (2.22)$$

where:

S is a positive definite matrix

$\Delta u(k|k) := u(k|k) - u(k-1|k-1)$

$\Delta u(k+i|k) := u(k+i|k) - u(k+i-1|k),\ i \in [1, M-1]$

In general, one can choose the weights Q, R and S to be time-varying (i.e. functions of k). For simplicity they are assumed to be time-invariant here.

Other popular but non-differentiable choices for the objective function are the $1-1$ norm, the $\infty - 1$ norm, the $\infty - \infty$ norm and the $1 - \infty$ norm (where the first is the spatial norm and the second the temporal norm). A good description of the

advantages of using each of these, as well as some other special objective functions can be found in [26].

2.2.4 Constraints

The optimization or prediction step in MPC can be subject to general mixed state/control constraints of the form:

Equality Constraints:

$$\kappa(x(t), u(t), t) = 0 \tag{2.23}$$

Inequality Constraints:

$$h(x(t), u(t), t) \geq 0 \tag{2.24}$$

Inequality constraints are found much more often than equality constraints. In a nonlinear setting equality constraints can never be satisfied in a finite number of algorithm iterations and are therefore avoided.

In most MPC problem formulations, the only two types of constraints considered are input and state (in particular, output) constraints. The constraints on the input variables are in general hard constraints which impose lower and upper bounds on these variables, that is,

$$u(t) \in \mathcal{U} := \{u \in \Re^m : u_{min} \leq u \leq u_{max}\}, \quad \forall t \in [0, \infty) \tag{2.25}$$

To make the control problem meaningful $\mathcal{U}$ must contain the origin.

Other very commonly used constraints are bounds on the rate of change of the manipulated variables given by:

$$|\Delta u_j(k+i|k)| \leq \Delta u_{max,j},\ \forall i = 0,\ldots,M-1,\ k \geq 0,\ \text{with } \Delta u_{max,j} > 0,\ \forall j = 1,\ldots,m \tag{2.26}$$

where $\Delta u_j(k+i|k)$, $\Delta u_{max,j}$, $j = 1,\ldots,m$, are the components of the vectors $\Delta u(k+i|k)$, Δu_{max}, respectively. We will express these constraints in the following vector form:

$$|\Delta u(k+i|k)| \leq \Delta u_{max},\ \forall i = 0,\ldots,M-1,\ k \geq 0,\ \Delta u_{max} > 0 \tag{2.27}$$

where we have committed some abuse of notation since $\Delta u(k+i|k)$ is a vector and we have defined $|.|$ to be a scalar norm. The reason for this notation is that we do not want the norm used here (which is linear in the components of the vectors $\Delta u(k+i|k)$) to be confused with the $2-$norm.

The output constraints are in general of the form:

$$y_{min} \leq y(k+i|k) \leq y_{max},\ \forall i = 1,\ldots,P,\ k \geq 0 \tag{2.28}$$

or in the "soft" format:

$$y_{min} - \epsilon \leq y(k+i|k) \leq y_{max} + \epsilon,\ \forall i = 1,\ldots,P,\ k \geq 0 \tag{2.29}$$

where ϵ is an additional decision variable whose weighted quadratic norm is added to the objective function. This formulation allows the bounds y_{min} and y_{max} to be violated by at most ϵ whenever the problem with hard constraints is not feasible. The norm of ϵ is added to the objective function so as to minimize the violation of these bounds.

In addition to input and output constraints, the optimization may be subject to physical constraints on the state variables (e.g., mole fractions have to lie between 0 and 1, temperatures in Kelvin degrees have to be always positive, concentrations are always non-negative, etc). Other useful state constraints are constraints imposed at the end of the (finite) prediction horizon known as *end constraints*. Some of these constraints are used, for example, to guarantee stability of the closed-loop as we will see later.

Two well-known "stabilizing" end constraints are:

Equality End Constraint:

$$x(k+P|k) = 0, \quad \forall k \geq 0 \tag{2.30}$$

Inequality End Constraint:

$$x(k+P|k) \in W, \quad \forall k \geq 0 \tag{2.31}$$

where W is some compact and convex "small" neighborhood of the origin.

2.3 State of the art on stability analysis of MPC: main results

2.3.1 MPC for constrained linear plants: nominal case

For constrained linear systems, stability has been proven in two different cases: by use of *infinite prediction horizon* [66, 109, 127] or *finite prediction horizon with end constraint* [13, 23, 32, 52, 69, 101, 122, 123, 127]. For the still very popular MPC formulation with finite prediction horizon no stability properties can be assured in

the presence of constraints. Now we will briefly describe the stability results in the cases of infinite prediction horizon and finite prediction horizon with end constraints.

Infinite prediction horizon MPC

Infinite horizon MPC with mixed state/control constraints for completely known discrete-time LTI systems (i.e., no model/plant uncertainty) has been explored in [109, 127].

Here we will reproduce the main results found in [109] due to their simplicity and importance. In that work, an objective function of the type

$$V_k := \sum_{i=0}^{\infty} [x(k+i|k)' Q x(k+i|k) + u(k+i|k)' R u(k+i|k)] \tag{2.32}$$

is considered with $u(k+i|k) = 0$ for $i \geq M$, where M is the *finite* control horizon. Thus, even though the problem has infinite prediction horizon, the number of decision variables is kept finite and the optimization can be solved on line as a quadratic program (QP).

The plants considered are discrete-time LTI of the following form:

$$x(k+i+1|k) = Ax(k+i|k) + Bu(k+i|k), \quad i \in [0, \infty), \quad k \geq 0 \tag{2.33}$$

In the *absence of constraints* we have the following results:

Theorem 2.1 (Open-Loop Stable Plants) *For stable A and $M \geq 1$, the receding horizon controller with objective function (2.32), is stabilizing.*

Theorem 2.2 (Open-Loop Unstable Plants) *For stabilizable $\{A, B\}$ with r unstable modes and $M \geq r$, the receding horizon controller with objective function (2.32), is stabilizing.*

When input and state constraints of the kind

$$Du(k+i|k) \leq d, \quad i \in [0,\infty), \quad k \geq 0 \tag{2.34}$$

$$Hx(k+i|k) \leq h, \quad i \in [1,\infty), \quad k \geq 0 \tag{2.35}$$

are considered, the stability results are as follows:

Theorem 2.3 (Open-Loop Stable Plants) *For stable plants, the input constraints are feasible independent of* $\{A,B\}, x_0 := x(0|0)$ *and* M. *These input constraints can obviously be converted into a finite set because of the form of the input,*

$$Du(k+i|k) \leq d, \quad i \in [0, M-1], \quad k \geq 0 \tag{2.36}$$

The state constraints may be infeasible, but they can be converted into a feasible set by removing them for small k,

$$Hx(k+i|k) \leq h, \quad k = k_1, k_1+1, \ldots \tag{2.37}$$

with k_1 *given by:*

$$k_1 := max\{ln(\frac{h_{min}}{\| H \| K(T) \| x_0 \|})/ln(\lambda_{max}), 0\} \tag{2.38}$$

in which $K(T)$ *is the condition number of* T *(where* $A = TJT^{-1}$ *and* J *is the Jordan form of* A*),* $h_{min} := \min_i \ h_i$ *and* $\lambda_{max} := \max_i \ |\lambda_i(A)|$. *Thus, for stable* A *and* $M \geq 1$, $x_k = 0$ *is an asymptotically stable solution of the closed-loop receding horizon controller with objective function (2.32) and feasible constraints (2.36), (2.37).*

Theorem 2.4 (Open-Loop Unstable Plants) *For stabilizable* $\{A, B\}$ *with* r *unstable modes and* $M \geq r$, $x_k = 0$ *is an asymptotically stable solution of the closed-loop receding horizon controller for the feasible quadratic program represented by equations (2.32), (2.36), (2.37) and the additional constraints*

$$x^u(k+M|k) = 0 \tag{2.39}$$

where x^u *are the unstable modes of the system. This constraint establishes that the unstable modes of the system are brought to zero in* M *steps in the optimization (although they only approach* 0 *asymptotically in the moving horizon implementation of MPC) and the stable modes are left to approach* 0 *asymptotically.*

In constraint (2.37) k_1 *is now given by:*

$$k_1 := M + max\{ln(\frac{h_{min}}{\| H \| \| T \| \| x^s(k+M|k) \|})/ln(\lambda_{max}), 0\} \tag{2.40}$$

where x^s *are the stable modes of the system.*

Finite prediction horizon MPC with end constraints

In order to prove stability for the finite horizon MPC formulation, some additional constraints may have to be introduced. Several researchers ([13, 32, 62, 69, 101], etc) have proposed explicitly to include an additional constraint called "end constraint". The idea here is to force the state at the end of the prediction horizon to zero, i.e., $x(k+P|k) = 0, \forall k \geq 0$.

This idea seems to have been originated by Kwon and Pearson [69] for the unconstrained case. Keerthi and Gilbert [62] proved that closed-loop stability can be guaranteed with this type of controller in the presence of input and output constraints

provided that the resulting optimization problem is feasible. One of the requirements for the end constraint to be feasible is that the system described by (2.33) be controllable.

One can actually show that with state feedback, feasibility of the optimization problem at $k = 0$ implies feasibility for all future sampling times. However, this may not hold true any longer when the state has to be estimated and/or when there are disturbances present.

Other types of end constraints have been proposed in [122, 123, 127]. Instead of forcing the states to zero at the end of the prediction horizon, they require the states to "shrink" at some future time step $k+L$ ($L \leq P$) with respect to the states at time step k. This "shrinkage" condition is expressed as an inequality end constraint which has been shown in these works to guarantee asymptotic stability of the closed-loop system.

2.3.2 MPC for constrained linear plants: robust case

Robust stability results for discrete-time LTI systems are presented in [66, 101, 122, 127].

Infinite prediction horizon MPC

In [66], an MPC-based technique for the control of LTV plants with uncertainties is proposed. This technique is motivated by recent developments in the theory and application (to control problems) of optimization involving linear matrix inequalities (LMIs). The resulting LMI-based optimization to be solved at each time step can be solved in polynomial time and can therefore be implemented on line. Thus, from the computational point of view, we need to solve an LMI problem instead of a linear or quadratic programming problem, which normally result from classical linear MPC

implementations. The use of an infinite prediction horizon formulation guarantees stability and since the minimization is performed over the "worst-case" objective function, the resulting algorithm enjoys certain desirable robustness properties.

Finite prediction horizon MPC with end constraints

In [101], a preliminary investigation of the robustness properties of the MPC algorithm with equality end constraints on the outputs for LTI plants was performed by exploring its strict relations with infinite horizon predictive control.

Since the robust stability results found in [122, 127] are of very similar nature, we have chosen to present here some of the main results in the latter work.

Once again, consider the discrete-time LTI system (2.33) and let us denote the nominal model by (A_0, B_0) and the real plant by (A_p, B_p). The actual plant (A_p, B_p) is assumed to lie in some known completely arbitrary set, i.e., $(A_p, B_p) \in (\mathcal{A}, \mathcal{B})$. The goal is to design an MPC controller such that closed-loop stability is guaranteed for all plants in the set.

The proposed controller structure is given by:

Step 0: Input the data.

Step 1: Set $k_0 = k$ and $i = 1$, where k denotes the current time step.

Step 2: The current control move $u(k)$ equals the first element $u(k|k)$ of the sequence $\{u(k|k), \ldots, u(k+M-1|k)\}$ which is the minimizer of the optimization problem

$$V_k = \min_{u(k|k),\ldots,u(k+M-1|k),\epsilon(k)} V_k(A_0, B_0) \tag{2.41}$$

subject to

$$\begin{cases} u(k+j|k) \in \mathcal{U} & j = 0, 1, \ldots, M-1 \\ |\Delta u(k+j|k)| \leq \Delta u_{max} & j = 0, 1, \ldots, M-1 \\ \Delta u(k+j|k) = 0 & j = M, M+1, \ldots, \infty \\ x(k+j|k) \in \mathcal{X}_{\epsilon(k)} & j = 0, 1, \ldots, \infty \end{cases} \tag{2.42}$$

and the robust stability constraint

$$\sup_{(A,B)} \| A^L x(k_0) + C_L U(k_0|i) \|_{\hat{P}} \leq \lambda \| x(k_0) \|_{\hat{P}}, \quad \lambda \in [0, 1) \tag{2.43}$$

where the idea of "softening" (relaxing) state constraints with the extra decision variable $\epsilon(k)$ has been introduced. $\mathcal{X}_{\epsilon(k)}$ is the time-varying set within which the states are required to remain between k and $k+1$. The input constraint set $\mathcal{U}$ has been defined in (2.25).

In this problem formulation, we have the following definitions:

$$\begin{aligned} V_k(A,B) &:= \sum_{i=1}^{P} \| x(k+i|k) \|_Q^2 + \sum_{i=0}^{M} [\| u(k+i|k) \|_R^2 + \| \Delta u(k+i|k) \|_S^2] + \\ &+ \| \epsilon(k) \|_{Q_\epsilon}^2 \end{aligned} \tag{2.44}$$

and

$$C_L := [A^{L-1}B \; A^{L-2}B \; \ldots \; B]$$

$$U(k_0|i) := \begin{bmatrix} u(k_0) \\ \vdots \\ u(k_0+i-2) \\ u(k_0+i-1|k_0+i-1) \\ \vdots \\ u(k_0+L-1|k_0+i-1) \end{bmatrix}$$

P, Q_ϵ $>$ 0 are weighting matrices

L := location of placement of stability constraint

Step 3: Set $k = k + 1$. If $i = L$ or $\| x(k_0 + i) \|_{\hat{P}} \leq \lambda \| x(k_0) \|_{\hat{P}}$, go to **Step 1**; otherwise, set $i = i + 1$ and go to **Step 2**.

This robust controller optimizes nominal performance subject to a robust stability constraint. The stability result for this robust MPC scheme can be summarized in the following lemma and theorem:

Lemma 2.1 (Feasibility Condition) *Assume that A is stable for all $A \in \mathcal{A}$. Then there exist an integer L and a constant $\lambda^*(L, \hat{P}) \in [0, 1)$ such that the optimization problem in* **Step 2** *is feasible for all $\lambda \in [\lambda^*(L, \hat{P}), 1)$.*

Theorem 2.5 (Robust State Feedback) *Assume that A is stable, then for all $\lambda \in [\lambda^*(L, \hat{P}), 1)$, the closed-loop system with state feedback is globally asymptotically stable with the given robust controller for all $(A, B) \in (\mathcal{A}, \mathcal{B})$.*

Here we have not gone into the notational details of the original work and the interested reader is encouraged to refer to [127] or [128] for better understanding of the previously described robust MPC algorithm. The main idea, however, is that the states of all the models in the set $(\mathcal{A}, \mathcal{B})$ (which include the real plant (A_p, B_p)) are "contracted" by a factor of $\lambda \in [0, 1)$ with respect to the measured states at time step k_0. The robust stability constraint remains the same for a particular k_0 while i varies from 1 to L. When $i = L$, the stability constraint is redefined with respect to the states measured at $k_0 + L$, $x(k_0 + L)$, and imposed at $k_0 + 2L$.

This is one of the robust stability results in [128]. Extensions to the output feedback case, e.g., can be found in this work but will not be mentioned here for lack of space.

2.3.3 MPC for constrained nonlinear plants: nominal case

Nominal stability results for constrained nonlinear systems can be found in [1, 2, 3, 62, 92] (discrete-time) and in [28, 63, 82] (continuous-time). In both cases, the basic

suggested MPC algorithm is the same with finite prediction horizon and equality end constraint $x(k+P_k|k) = 0,\ \forall k \geq 0$. Note that the prediction horizon is allowed to be time-varying (i.e., P is a function of k). This type of MPC implementation is known as *Variable Horizon MPC*. Now since the plant is nonlinear the optimization problem is in general non-convex and one can expect at best to find a local optimal solution.

Let $\mathcal{P}(k, x_k)$ denote the optimization problem at sampling time k with initial condition x_k. The problem formulation at time step k for the continuous-time case is given by:

$$\mathcal{P}(k, x_k) : \min\{V(t_k, x_k) | u_k(t) \in \mathcal{U}, P_k \in [0, P_{max}], x(t_{k+1} := t_k + P_k T; x_k, t_k) = 0\} \tag{2.45}$$

With certain controllability and observability assumptions and Lipschitz continuity of the system dynamics and of the output map, the following results hold:

- for all $x_k \in \mathcal{X}$, $\lim_{i\to\infty} x_{k+i}(k, x_k) = 0$;
- $x = 0$ is the only equilibrium state of the system with the computed control law and it is *uniformly asymptotically stable*,

where the set $\mathcal{X}$ is defined by:

$$\mathcal{X} = \{x_k : \mathcal{P}(k, x_k) \text{ has an admissible sequence for which } V_k := V(t_k, x_k) \text{ is finite}\} \tag{2.46}$$

Another form of guaranteeing stability for a constrained nonlinear system has been presented in [83, 95] and it consists of imposing an *inequality* end constraint of the type $x(k+P_k|k) \in W_\alpha$, where W_α is a small neighborhood of the origin whose "size" is specified by the parameter α. In this case, the controller loses its stabilizing properties within W_α. In order to compensate for that and to guarantee asymptotic stability to the origin, a stabilizing linear control law must be used inside W_α. Thus, once the states of the system lie inside the region W_α one must switch over from MPC to a

linear robustly asymptotically stabilizing controller. This kind of implementation of MPC is known as *hybrid or dual-mode MPC*. The major difficulty lies in computing the set W_α so it is a Lyapunov set for the nonlinear system and for its linearization around the origin. This is a general problem of constructing local Lyapunov functions for nonlinear systems for which there is no established methodology.

The advantages of using an inequality instead of an equality end constraint are twofold: first, in a nonlinear programming problem equality constraints can never be satisfied in a finite number of algorithm iterations (which does not happen with most inequality constraints) and, second, a conservative form of this type of inequality constraint (e.g., $x(k+P_k|k) \in W_{\alpha/2}$) can be used to introduce robustness into this MPC formulation as we will see in the next section.

As previously mentioned, the problem is posed with a time-varying prediction horizon $P_k,\ k \geq 0$. In [82, 83, 95] the horizon is considered as an additional decision variable $P_k \in [0, P_{max}]$ (where P_{max} is a chosen upper bound to $P_k,\ \forall k \geq 0$, which determines a balance between the control effort in solving the problem and the feasibility of the constraints) so as to add more possibilities for making the constraints feasible.

The optimal control problem at time t_k is defined in the following way:

$$\mathcal{P}(k, x_k) : \min\{V(t_k, x_k)|u_k(t) \in \mathcal{U}, P_k \in [0, P_{max}], x(t_{k+1} := t_k + P_k T; x_k, t_k) \in W_\alpha\} \tag{2.47}$$

An important feature of this variable horizon MPC with end constraint (be it equality or inequality constraint) is that optimality is not required for stability, only feasibility. Moreover, if a feasible solution is found for the first optimal control problem, restrictions of this solution to smaller time intervals are feasible solutions of the optimization problems at subsequent time steps. This means that, in the absence of disturbances, if $\mathcal{P}(0, x_0)$ is feasible, feasibility of $\mathcal{P}(k, x_k),\ k > 0$, is ensured. Of course, one can improve on this solution at time step k by computing a control-horizon pair $\{P_k, u_k(t)\}$ that results in a smaller value of the cost function $V(t_k, x_k)$.

2.3.4 MPC for constrained nonlinear plants: robust case

Robust stability results for nonlinear plants can be found in [95]. In the first case, in order to add robustness to the hybrid or dual-mode MPC algorithm a conservative end inequality constraint is imposed in the optimization step. The motivation behind this idea is to require the states of the model used in the prediction to be inside a smaller set at the end of the prediction horizon ($W_{\alpha/2}$, for example) so that, if the model/plant mismatch is not very large, the states of the plant will be within the bigger set W_α. Inside W_α a *robust* linear stabilizing controller is used in order to drive the states of the plant asymptotically to the origin. It is clear that the synthesis of such a linear controller is not a trivial task, especially due to the model uncertainty. W_α now has to be a Lyapunov region for the real plant, the nonlinear model used in the prediction and its linearization around the origin.

Also here, the prediction horizon is an additional decision variable and the problem formulation is as follows:

$$\mathcal{P}(k, x_k) : \min\{V(t_k, x_k) | u_k(t) \in \mathcal{U}, P_k \in [0, P_{max}], x(t_{k+1} := t_k + P_k T; x_k, t_k) \in W_{\alpha/2}\} \tag{2.48}$$

Let $f^p(.)$ and $f(.)$ denote the dynamics of the plant and of the model, respectively. Then robust stability can be shown under the following conditions on f^p and f:

- f^p is continuously differentiable;
- $\| f^p(x,u) - f(x,u) \|_{\hat{P}} \leq \beta \| (x,u) \|_{\hat{P}}$ for all $(x,u) \in \mathcal{X} \times \mathcal{U}$, $\hat{P} > 0$;
- f is Lipschitz continuous on $\mathcal{X} \times \mathcal{U}$,

where the set $\mathcal{X}$ is defined as in (2.46).

If state constraints are present, a conservative version of such constraints should be used in the optimization to account for the model uncertainty. For example, if in the nominal case $\mathcal{P}(k, x_k)$ would be given by:

$$\begin{aligned}\mathcal{P}(k, x_k): \quad & \min\{V(t_k, x_k) | u_k(t) \in \mathcal{U}; P_k \in [0, P_{max}]; x(s; t_k, x_k) \in \mathcal{E}, \\ & \forall s \in [t_k, t_k + P_k T];\ x(t_{k+1} := t_k + P_k T; x_k, t_k) \in W_\alpha\} \end{aligned} \tag{2.49}$$

The robust version of the problem would be as follows:

$$\begin{aligned}\mathcal{P}(k, x_k): \quad & \min\{V(t_k, x_k) | u_k(t) \in \mathcal{U}; P_k \in [0, P_{max}]; x(s; t_k, x_k) \in \mathcal{E}_\epsilon, \\ & \forall s \in [t_k, t_k + P_k T];\ x(t_{k+1} := t_k + P_k T; x_k, t_k) \in W_{\alpha/2}\} \end{aligned} \tag{2.50}$$

where the sets $\mathcal{E}$ and $\mathcal{E}_\epsilon$ are closed subsets of $\Re^n$ defined by:

$$\mathcal{E} := \{x | g^j(x) \leq 0, j \in \mathbf{p}\};\ \ \mathbf{p} := \{1, \ldots, p\} \tag{2.51}$$

$$\mathcal{E}_\epsilon := \{x | g^j(x) \leq -\epsilon, j \in \mathbf{p},\ \epsilon > 0\} \tag{2.52}$$

and contain the origin in their interiors. Thus we can see that ϵ allows a margin of error so that if the states of the prediction model are required to stay within $\mathcal{E}_\epsilon$ the states of the plant remain inside $\mathcal{E}$, a larger set.

Chapter 3 State Feedback Contractive NLMPC: Nominal Case

3.1 Introduction

As we have mentioned before, there are no stability guarantees for finite horizon MPC. The two alternative approaches proposed so far which ensure stability of the closed-loop system under reasonable assumptions are infinite horizon MPC (for discrete-time constrained linear systems) and finite horizon MPC with end constraints (for continuous- and discrete-time constrained linear and nonlinear systems). These new formulations of MPC have allowed for a relatively easy analysis of the closed-loop behavior which had not been possible under the framework of finite horizon MPC.

The present work is devoted to the control of constrained nonlinear systems by using a finite horizon MPC technique with the introduction of an additional state constraint which we have denoted *contractive constraint.* This is a Lyapunov-based approach in which a Lyapunov function chosen a priori is decreased, not continuously, but discretely; it is allowed to increase at other times (between prediction horizons). This is also an approach where stability is guaranteed by introducing an inequality end constraint in a finite horizon MPC framework. As we will see later, the introduction of this additional constraint into the on-line optimization makes it possible to prove quite strong stability properties of the closed-loop system. In the nominal case and in the absence of disturbances, it is possible to show that the presence of the contractive constraint renders the closed-loop system exponentially stable. We will also examine how the stability properties weaken as structural and/or parametric model/plant mismatch, disturbances and measurement errors are considered. In the presentation

of our results, we will begin with the basic idea in the simplest context (state feedback + no model uncertainty + no disturbances) and then develop into the more complex situations showing that, in each case, some form of stability of the closed-loop system can be obtained.

Another important aspect considered in this work is the computational efficiency and implementability of the algorithms proposed. The previous work on stability analysis of MPC applied to nonlinear systems (see [82, 95]) addresses only partially the issue of the computational effort required in the controller implementation. These algorithms require only feasibility and not optimality of the control problem, which is also true for our *Contractive MPC* (finite horizon MPC + contractive constraint). However, the ideas presented by Mayne and Michalska in [82, 95] with their variable horizon MPC approach have the following limitations:

- in the nonlinear context, the equality end constraint, namely $x(k + P_k|k) = 0$, can never be satisfied in a finite number of algorithm iterations;
- the hybrid controller which results from imposing the inequality end constraint, $x(k + P_k|k) \in W$, and using a linear stabilizing controller inside W is theoretically sound but the computation of the region W and of the gain of the linear stabilizing controller is a major difficulty in real implementation.

Another relevant negative aspect of such controllers is the fact that, in general, the resulting optimization step is a non-convex problem. Even if only feasibility is required for stability, the performance may suffer quite a lot by using feasible solutions only. More serious yet is the fact that in nonlinear programming even the computation of feasible solutions may be quite cumbersome, if not all together impossible.

In this work much attention was devoted to the implementation aspects of the contractive MPC controller. We will show later that if a linear approximation of the original nonlinear system computed at each sampling time $k \geq 0$ is used in the prediction step, the contractive constraint can be implemented in such a way that the

resulting optimization problem is reduced to a quadratic programming (QP) problem. And, as we well know, there are many efficient and well-established algorithms in the market today devoted to solving quadratic programs. This implementation of MPC with local linearization of the nonlinear plant was first proposed by Garcia in [48] and subsequently used by Ricker and Lee in [74, 110].

We will progress to this computational aspect later because in order to make the controller computationally simpler we also need to make it robust (since a linear model is used in the prediction of the states of the real nonlinear plant). Initially we will be concerned only with the nominal stability analysis per se, without taking into account the fact that the resulting controller involves the solution of a nonlinear programming problem at each time step. The extensions to the basic problem will be added with each chapter.

Problem 1 : *State feedback, nominal case and no disturbances*

3.2 Description of the contractive MPC algorithm

3.2.1 Description of the system

In this chapter we assume that the plant is nonlinear time-invariant (NLTI) and described by the following differential equation:

$$\dot{x}(t) = f(x(t), u(t)) \tag{3.1}$$

where $f : \Re^n \times \Re^m \rightarrow \Re^n$ is continuously differentiable.

Throughout this thesis we will assume that the manipulated variables $u(t)$ are subject to the following hard constraints:

$$u(t) \in \mathcal{U} := \{u \in \Re^m : u_{min} \leq u \leq u_{max}\}, \quad \forall t \in [0, \infty) \tag{3.2}$$

Linear constraints on the rates of change of the manipulated variables are also commonly present, as we have pointed out in chapter 2 (see equations 2.26 and 2.27).

The solution of (3.1) at time t, corresponding to the initial time/state pair $\{t_0, x_0\}$ and the input $u(\tau)$, $\tau \in [t_0, t]$, is denoted by $x(t, t_0, x_0, u)$ or, in a simplified notation, $x_0(t)$.

3.2.2 Optimization step

Given any sampling time $t_k^0 := t_k := t_0 + kPT$, $k \in [0, \infty)$, and $t_k^j := t_k + jT$, $j \in [0, P]$, with $t_k^P = t_{k+1}^0 = t_{k+1}, \forall k \geq 0$, let us adopt the following notation $x_k := x_k^0 := x(t_k^0, t_0, x_0, u)$, $x_k^j := x(t_k^j, t_k, x_k, u)$, $x_k^j(t) := x(t, t_k^j, x_k^j, u)$ and $u_k^j(t)$ is the continuous control law for $t \in [t_k^j, t_k^j + PT]$. In order to conform to MPC's usual implementation scheme, let us consider a discontinuous control law of the kind $u_k^j(t) = u(kP+j+i|kP+j)$ for $t \in [t_k^j + iT, t_k^j + (i+1)T]$, $i \in [0, P-1]$, i.e., $u_k^j(t)$ is constant during one sampling time. Moreover, $u(kP + j + i|kP + j) = u(kP + j + M - 1|kP + j)$, $\forall i \in [M, P-1]$. Then the optimization problem at time t_k^j, namely, $\mathcal{P}(t_k^j, x_k^j)$, $\forall j \in [0, P-1]$, $k \in [0, \infty)$, is represented by:

$$\min_{u_k^j(t)} \int_{t_k^j}^{t_k^{j+P}} [x_k^j(t)' Q x_k^j(t) + u_k^j(t)' R^* u_k^j(t) + \dot{u}_k^j(t)' S^* \dot{u}_k^j(t)] \, dt \tag{3.3}$$

or, equivalently,

$$\min_{u(kP+j|kP+j),\ldots,u(kP+j+M-1|kP+j)} \int_{t_k^j}^{t_k^{j+P}} \| x_k^j(t) \|_Q^2 \; dt +$$
$$+ \sum_{i=0}^{P} \| u(kP+j+i|kP+j) \|_R^2 + \sum_{i=0}^{M-1} \| \Delta u(kP+j+i|kP+j) \|_S^2 \quad (3.4)$$

where $R := \frac{R^*}{T}$ and $S := \frac{S^*}{T^2}$.

subject to:

$$\begin{cases} \dot{x}_k^j(t) = f(x_k^j(t), u_k^j(t)), \;\; x_k^j := \text{ measured states at } t_k^j \\ u_{min} \leq u(kP+j+i|kP+j) \leq u_{max}, \;\; i \in [0, M-1] \\ |\Delta u(kP+j+i|kP+j)| \leq \Delta u_{max}, \;\; i \in [0, M-1] \\ \Delta u(kP+j+i|kP+j) = 0, \;\; i \in [M, P-1] \\ \| \bar{x}_k^j(t_k^P) \|_{\hat{P}} \leq \alpha \| x_k \|_{\hat{P}}, \quad \alpha \in [0,1), \quad \hat{P} > 0 \end{cases} \quad (3.5)$$

where

$$\dot{\bar{x}}_k^j(t) = f(\bar{x}_k^j(t), u_k^j(t)), \text{ with } \bar{x}_k^0 := x_k \text{ and } \bar{x}_k^j = \bar{x}_k^{j-1}(t_k^j), \text{ for } j \geq 1 \quad (3.6)$$

is the trajectory of the model which is not updated with the states of the plant at t_k^j for $j \in [1, P-1]$. The states $\bar{x}_k^j(t)$ are only updated with the states of the plant at $t = t_k + PT =: t_k^P$, i.e., at intervals of one prediction horizon.

3.2.3 MPC algorithm implementation

The controller is implemented according to the following scheme:

Control Algorithm 1

Data: *Initial Conditions:* t_0 *and* x_0*; Controller Parameters: horizons* P, M $(M \leq P)$*, weights* $Q, R, S, \hat{P} > 0$*, contractive parameter* $\alpha \in [0,1)$*, sampling time* T *and control constraints* $u_{min}, u_{max}, \Delta u_{max}$.

Step 0: *Set* $k = 0,\ j = 0$.

Step 1: *Assuming that the optimal control problem* $\mathcal{P}(t_k^j, x_k^j)$ *is feasible for the chosen set of parameters, then at* $t = t_k^j$ *solve* $\mathcal{P}(t_k^j, x_k^j)$ *specified by the sets of equations (3.4), (3.5) and (3.6). Local optimal solutions or even feasible solutions are accepted. The result of this step is an optimal (or feasible) sequence of control moves* $\{u(kP+j|kP+j), \ldots, u(kP+j+M-1|kP+j)\}$.

Step 2: *Apply the first control move,* $u(kP+j|kP+j)$, *to the plant (3.1) for* $t \in [t_k^j, t_k^{j+1}]$ *and measure the states at* t_k^{j+1}. *Set* x_k^{j+1} *equal to the measured states and* $\bar{x}_k^{j+1} = \bar{x}_k^j(t_k^{j+1})$.

Step 3: *If* $j < P-1$, *set* $j = j+1$ *and go back to* **Step 1**. *If* $j = P-1$ *set* $x_{k+1}^0 =: x_{k+1} = x_k^P, t_{k+1}^0 = t_{k+1} = t_k^P, k = k+1, j = 0$, *and go back to* **Step 1**.

Remark 3.1 *Notice that both the contractive constraint and its location (at time* $t = t_k + PT$ *and with respect to* x_k*) do not change for a fixed* k *as* j *varies in the interval* $[0, P-1]$. *This means that if at time* t_k *it is possible to find a control sequence which makes the objective function finite and satisfies all the constraints (i.e.,* $\mathcal{P}(t_k, x_k)$ *is feasible) and if the constraints remain unaltered for a fixed* k *while* j *varies from* 0 *to* $P-1$, *then the subsequent* $P-1$ *control problems (corresponding to the different values of* j*) will be feasible as well. So, all we need to be concerned about is the feasibility of* $\mathcal{P}(t_k, x_k)$, $\forall k \geq 0$.

Due to the absence of model/plant mismatch and disturbances the following remarks can be made:

Remark 3.2 *The receding or moving horizon implementation of the control law generated by* **Control Algorithm 1** *is not necessary for* **Problem 1**. *We could just implement all the control moves* $\{u(kP|kP), \ldots, u(kP+M-1|kP)\}$ *from* t_k *to* t_k+PT *and only solve a new control problem with a new initial condition,* x_{k+1}, *at the end of*

the horizon. Here we have chosen to present this moving horizon formulation because this is the most usual one in the MPC context and will be adopted throughout this thesis. In the presence of any uncertainty or disturbance, this approach can significantly enhance the performance of the closed-loop response due to the feedback provided by measurements at each sampling time (instead of leaving the plant open-loop for the period of a whole prediction horizon).

Therefore, for **Problem 1**, *the previously presented receding horizon MPC scheme is equivalent to the following simpler implementation (only one optimization problem, namely $\mathcal{P}(t_k, x_k)$, is solved for a whole prediction horizon):*

Control Algorithm 2

Data: *Same as in* **Control Algorithm 1**.

Step 0: *Set* $k = 0$.

Step 1: *Assuming that $\mathcal{P}(t_k, x_k)$ is feasible for the chosen set of parameters, then at $t = t_k$ solve $\mathcal{P}(t_k, x_k)$, which is specified by:*

$$\min_{u(kP|kP),\ldots,u(kP+M-1|kP)} \int_{t_k}^{t_k^P} \| x_k(t) \|_Q^2 \, dt + \sum_{i=0}^{P} \| u(kP+i|kP) \|_R^2 + \sum_{i=0}^{M-1} \| \Delta u(kP+i|kP) \|_S^2 \tag{3.7}$$

subject to:

$$\begin{cases} \dot{x}_k(t) = f(x_k(t), u_k(t)), \;\; x_k \text{ measured} \\ u_{min} \leq u(kP+i|kP) \leq u_{max}, \;\; i \in [0, M-1] \\ |\Delta u(kP+i|kP)| \leq \Delta u_{max}, \;\; i \in [0, M-1] \\ \Delta u(kP+i|kP) = 0, \;\; i \in [M, P-1] \\ \| x_{k+1} \|_{\hat{P}} := \| x_k(t_k^P) \|_{\hat{P}} \leq \alpha \| x_k \|_{\hat{P}}, \;\; \alpha \in [0, 1) \end{cases} \tag{3.8}$$

Step 2: *Apply the computed sequence of control moves* $\{u(kP|kP), \ldots, u(kP+M-1|kP)\}$ *to the system (3.1) for* $t \in [t_k, t_{k+1}]$, *and set* x_{k+1} *equal to the states of the system at* t_{k+1}.

Step 3: *Set* $k = k+1$ *and go back to* **Step 1**.

3.2.4 Basic assumptions and definitions

Without loss of generality, let us consider the regulation problem where the desired operating point is the origin $(x, u) = (0, 0)$. Then, the following assumptions are needed to ensure local stability:

Assumption 3.1 $(x, u) = (0, 0)$ *is an equilibrium point of (3.1), i.e.,* $f(0, 0) = 0$.

Assumption 3.2 *The linearization of the model dynamics around the origin is stabilizable, i.e.,* $\{\frac{\partial f}{\partial x}(0,0), \frac{\partial f}{\partial u}(0,0)\}$ *is a stabilizable pair.*

Assumption 3.3 *We assume that there exists a* $\rho \in (0, \infty)$ *such that for all* $x_k \in B_\rho$, *the optimization problem at* t_k, $\mathcal{P}(t_k, x_k)$, *is feasible. In other words, for all* $x_k \in B_\rho$, *we can find a contractive parameter* $\alpha \in [0, 1)$ *so that with the chosen finite horizon* P *all the constraints on the inputs and states can be satisfied and the objective function is finite.*

Remark 3.3 *Assumption 3.3 is not very restrictive since all that it establishes is that there exists a non-empty convex and compact set of initial conditions for which the optimization problem at every* P *time steps is feasible.*

For nonlinear systems with a unique globally exponentially stable equilibrium (which obviously include open-loop stable linear systems), since all trajectories in $\Re^n$ *satisfy*

the condition of exponential decay, it is always possible to find P so that the states at the end of P steps are contracted by a factor $\alpha \in [0,1)$ with respect to the initial states.

For general nonlinear systems, if $\left[\begin{array}{cc} \frac{\partial f}{\partial x} & \frac{\partial f}{\partial u} \end{array}\right] \in \Omega, \ \forall x, \ u$ *(where* $\Omega \subseteq \Re^{n\times(n+m)}$*), then there exists a matrix* $G(x,u) \in \Omega$ *such that:*

$$f(x,u) = G(x,u)\left[\begin{array}{c} x \\ u \end{array}\right]$$

In other words, the nonlinear system can be replaced by a time-varying linear system (idea which is implicit in the early work on absolute stability originating in the Soviet Union; see the works of Lur'e and Postnikov [79, 80] and Popov [106]) and this approach is known as global linearization. Of course, approximating the set of trajectories of the nonlinear system via linear differential inclusions (LDIs) can be very conservative, i.e., there are many trajectories of the LDI which are not trajectories of the nonlinear system. However, once the nonlinear system is represented in LDI form, sufficient conditions for satisfaction of assumption 3.3 can be stated (see [17], where sufficient conditions for exponential stability and an induced L_2-norm performance objective are given) by using a single quadratic Lyapunov function approach. The unique quadratic Lyapunov function decreases along the trajectories of the LDIs and, therefore, of the nonlinear system, which means that exponential stability is guaranteed and we can always find an $\alpha \in [0,1)$ such that the states of the nonlinear system are contracted by this factor in only one time step.

Remark 3.4 *In remark 3.2 we pointed out that due to the absence of model uncertainty or disturbances it follows that* $x_{k+1} = x_k^{P-1}(t_k^P)$ *and, therefore, due to the contractive constraint, we have* $\| x_{k+1} \|_{\hat{P}} \leq \alpha \| x_k \|_{\hat{P}}$*. This means that if* $x_0 \in B_\rho$*, then* $x_k \in B_{\alpha^k\rho} \subset B_\rho$ *(since* $\alpha \in [0,1)$*). Thus, with our condition for feasibility given in assumption 3.3, if* $\mathcal{P}(t_0,x_0)$ *is feasible (or equivalently, if* $x_0 \in B_\rho$*) then the sequence of control problems* $\mathcal{P}(t_k,x_k)$*,* $\forall k > 0$*, is feasible as well.*

Assumption 3.4 *We assume that if* $x_k \in B_\rho$, $\forall k \geq 0$ *(with* $\rho \in (0, \infty)$ *defined in assumption 3.3), then there exists a constant* $\beta \in (0, \infty)$ *so that the transient states of the model used in the computation of the contractive constraint (which is equal to the prediction model and the plant for* **Problem 1***) remain inside the set* $B_{\beta \| x_k \|_{\hat{P}}}$, *i.e.,* $\| \bar{x}_k^j(t) \|_{\hat{P}} \leq \beta \| x_k \|_{\hat{P}} \leq \beta\rho$, $\forall j = 0, \ldots, P-1$, $k \geq 0$.

Remark 3.5 *Since* u *is constrained, assumption 3.4 is always satisfied except for systems with finite escape time. So, nonlinear systems with finite escape time are ruled out from our investigation.*

Definition 3.1 *Under assumption 3.3, the reachable set* $\mathcal{X}$ *is defined by:*

$$\mathcal{X} := \{x(t) \in \Re^n \mid x(t) = x(t, t_0, x_0, u),\ t \in [t_0, \infty);\ x_0 \in B_\rho,\ u \in \mathcal{U}\} \tag{3.9}$$

Remark 3.6 *Under assumption 3.4 and since we are addressing the nominal case in the absence of disturbances, the reachable set* $\mathcal{X}$ *is equal to* $B_{\beta\rho}$.

3.2.5 Basic philosophy of the controller design

Figures 3.1 and 3.2 illustrate the behavior of the closed-loop system generated by the contractive MPC controller when no model/plant mismatch is present and no disturbances affect the system, as specified in **Problem 1**.

Thus, while the optimization problem remains at constant size P for different values of j and for a constant k, the number of steps between the beginning of the prediction and the location of the contractive constraint is equal to $P-j$ and therefore decreases as j increases as we can clearly see in figure 3.1.

The exponential decay of the state trajectory is illustrated in figure 3.3.

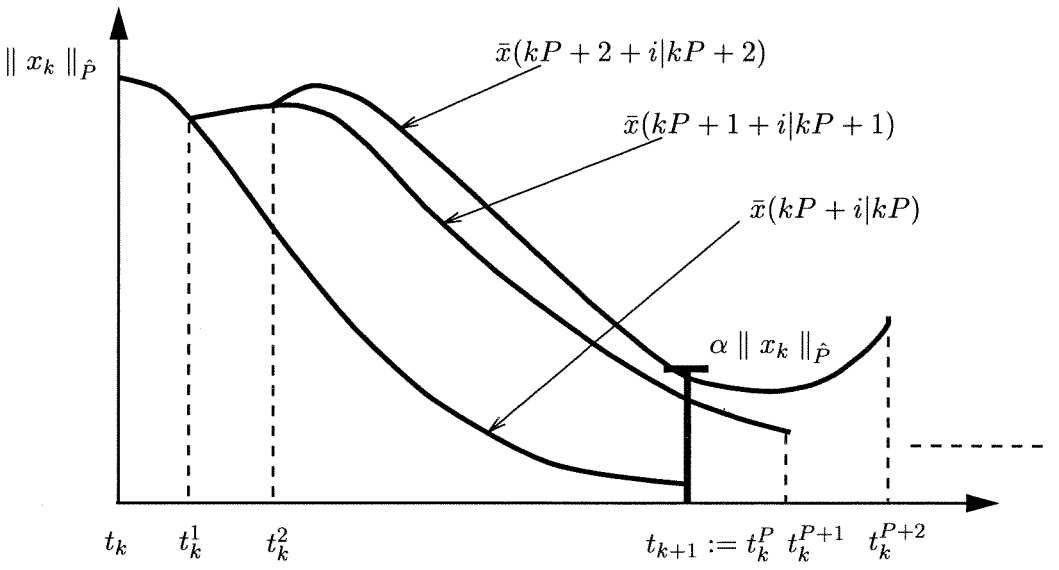

Figure 3.1: P control problems for a fixed k. Predicted trajectories generated by contractive MPC for a fixed k and j varying in the interval $j = 0, \ldots, P-1$.

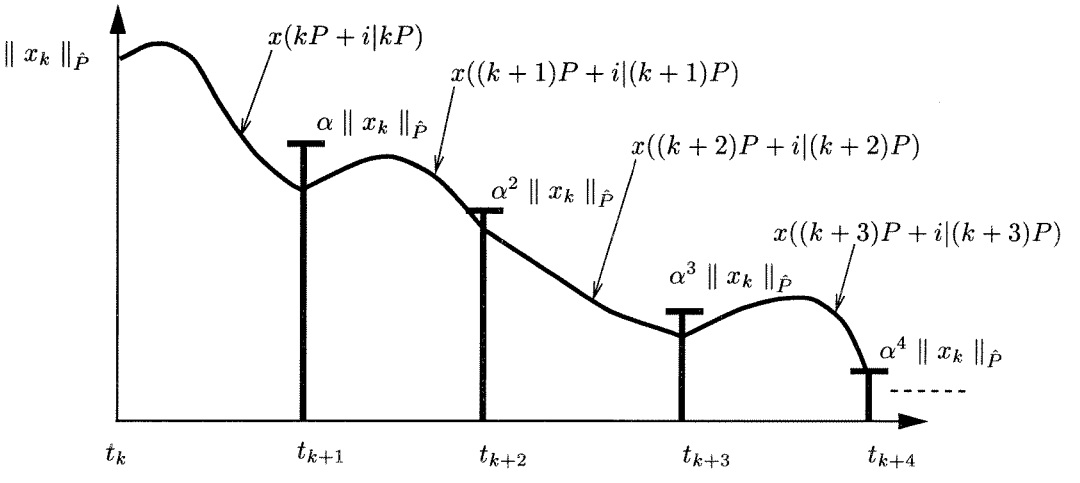

Figure 3.2: Exponential decay of the state trajectory.

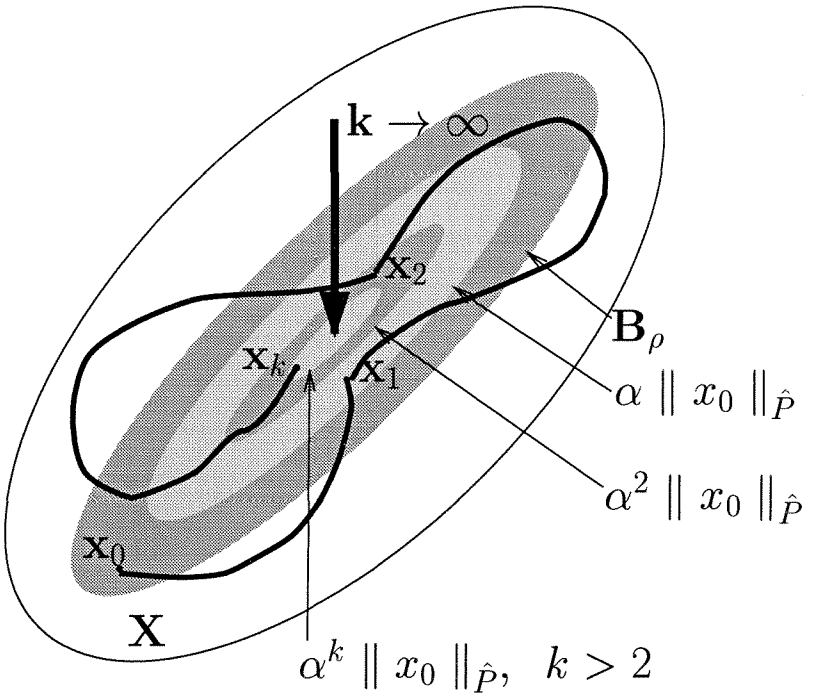

Figure 3.3: State trajectory generated by the contractive MPC scheme.

3.3 Stability analysis of contractive MPC

Theorem 3.1 (Exponential stability) *Given $\alpha \in [0,1)$ and ρ, $\beta \in (0,\infty)$ satisfying assumptions 3.3, 3.4,* **Control Algorithm 1** *(and, consequentely,* **2***) renders the closed-loop system exponentially stable on the set B_ρ, i.e., for any $x_0 \in B_\rho$, the resulting trajectory $x(t) := x(t, t_0, x_0, u)$ satisfies the following inequality:*

$$\| x(t) \| \leq a \| x_0 \| e^{-(1-\alpha)\frac{(t-t_0)}{PT}}, \qquad with \quad a \geq \beta e^{1-\alpha} \tag{3.10}$$

Proof: *From assumption 3.3 we have that the optimal control problems $\mathcal{P}(t_k, x_k)$, $\forall k \geq 0$, are feasible for all initial conditions $x_0 \in B_\rho$. So, this means that all the input/state constraints in (3.5) are satisfied at each sampling time $t_k^j, j \in [0, P-1]$, $k \geq 0$. In the absence of model/plant mismatch or disturbances it immediately follows*

that:

$$\| x_k \|_{\hat{P}} \leq \alpha^k \| x_0 \|_{\hat{P}}, \quad \forall k \geq 0 \tag{3.11}$$

and, therefore, for all $t \in [t_k, t_{k+1} := t_k + PT]$, $x_k(t)$ *satisfies the following inequality:*

$$\| x_k(t) \|_{\hat{P}} \leq \beta \alpha^k \| x_0 \|_{\hat{P}}, \ \forall k \geq 0, \ t \geq t_0 \tag{3.12}$$

Now, since $e^{(\alpha-1)} - \alpha \geq 0 \iff \alpha^k \leq e^{-(1-\alpha)k}$, $\forall \alpha \in [0,1)$ *and* $\forall k \geq 0$, *it results that:*

$$\| x_k \|_{\hat{P}} \leq \| x_0 \|_{\hat{P}} \, e^{-(1-\alpha)k} \tag{3.13}$$

$$\| x_k(t) \|_{\hat{P}} \leq \beta \| x_0 \|_{\hat{P}} \, e^{-(1-\alpha)k} \tag{3.14}$$

Notice that the bounds (3.13) and (3.14) are independent of the performance criterion. The performance criterion influences only the feasibility question but if the problem is feasible, stability is determined exclusively by the contractive constraint.

Although (3.14) establishes an exponentially discretely decaying bound on the states for all times $t \geq t_0$, *our proof of exponential stability for the continuous-time system (3.1) is not yet concluded.*

The condition for exponential stability for continuous-time systems is given by: the equilibrium 0 *is (locally) exponentially stable if there exist* $\rho, a, b > 0$ *such that*

$$\| x(t, t_0, x_0, u) \| \leq a \| x_0 \| \, e^{-b(t-t_0)}, \ \forall t > t_0 > 0, \ \forall x_0 \in B_\rho \tag{3.15}$$

We can see that this is not quite what we have in (3.14) since that is a discrete bound which remains constant for the period of a sampling time. So, we must find an exponentially continuously decaying function which bounds $\beta e^{-(1-\alpha)k}$ *for all* $t \in [t_k, t_{k+1}]$, *and for all* $k \geq 0$.

The discrete bounds on the states, (3.13) and (3.14), and the continuous upper bound are graphically represented in figure 3.4.

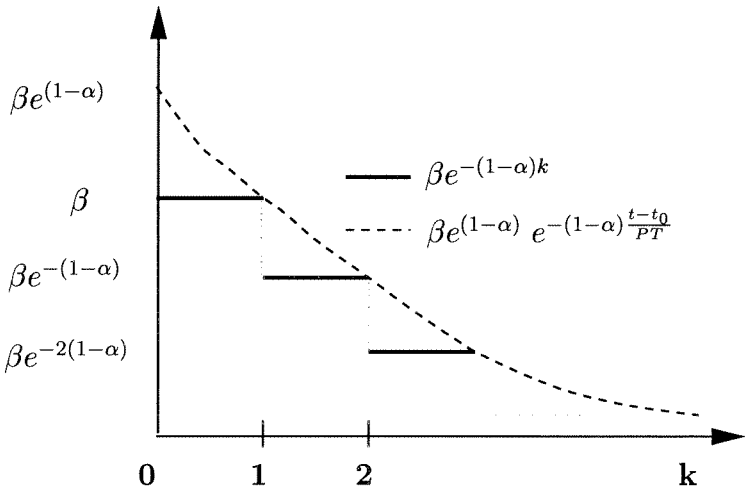

Figure 3.4: Discrete and continuous-time exponentially decaying upper bounds for the state trajectory.

So, as shown in figure 3.4, we want to find the least conservative continuously exponentially decreasing bound which matches the discrete bound exactly at the end of horizons.

Since $k = \frac{t_k - t_0}{PT}$ *and* $\frac{t-t_0}{PT} < \frac{t_k - t_0}{PT}$, $\forall t \in [t_0, t_k)$, *we can easily see that:*

$$\beta e^{-(1-\alpha)k} \leq a e^{-(1-\alpha)\frac{(t-t_0)}{PT}}, \quad \forall\ a \geq \beta e^{1-\alpha} \tag{3.16}$$

Thus, using equations (3.14) and (3.16) we finally have:

$$\| x(t) \| \leq a \| x_0 \| e^{-(1-\alpha)\frac{(t-t_0)}{PT}}, \qquad with \quad a \geq \beta e^{1-\alpha} \tag{3.17}$$

which is what we wanted to prove. This means that if $x_0 \in B_\rho$*, then the sequence of optimal control problems* $\mathcal{P}(t_k, x_k)$*,* $k \geq 0$*, is feasible and the origin is an exponentially stable equilibrium point inside the reachable set* $\mathcal{X} = B_{\beta\rho}$*.*

□

Now that exponential stability has been proven, we will show that, under certain assumptions on the control law originated by MPC, the objective function minimized in (3.7) is a Lyapunov function for the closed-loop system.

Before we start showing the conditions under which this is true, let us point out that the objective function being a Lyapunov function is not a necessary condition for stability of the closed-loop under the contractive MPC controller, as it may be for other moving horizon-based MPC schemes. The closed-loop is stabilized by the contractive MPC controller because the quadratic function which defines the contractive constraint is itself a Lyapunov function which decreases discretely, not continuously, at intervals of prediction horizons.

We will see in the next theorem that, in order for the objective function to be a Lyapunov function as well, stronger assumptions are needed on the computed control law and on the dynamics of the nonlinear system to be controlled. Here we want to establish which and how strong these assumptions are because they are *necessary* in proving exponential stability of the MPC scheme which uses the equality end constraint $x(k+P|k) = 0$ (see [114]). In other words, we want to emphasize that we are able to prove exponential stability of the closed-loop system under much less restrictive assumptions when the contractive constraint, rather than the end equality constraint, is used.

Theorem 3.2 (Objective function as a Lyapunov function) *Consider the system (3.1) and take into account the simpler implementation of MPC presented in remark 3.2. Suppose that f is C^q for some integer $q \geq 1$, and that $f(0,0) = 0$.*

Let $u_k(t) = \{u(kP|kP) \ldots, u(kP+M-1|kP)\} =: \eta(x_k) =: \{\eta_0(x_k), \ldots, \eta_{M-1}(x_k)\}$ be the feedback law applied to the system for $t \in [t_k, t_{k+1}]$, $\forall k \geq 0$, and for all $x_k \in B_\rho$. Then, let us define $F(x_k) := f(x_k, \eta(x_k))$.

Let us assume that the sequence of control moves computed at t_k is such that $\eta_i(0) = 0$, $\forall i \in [0, M-1]$, and $\{\eta_0, \ldots, \eta_{M-1}\}$ is Lipschitz continuous inside B_ρ, which means that there exists $L > 0$ such that:

$$\| \eta_i(x) - \eta_i(y) \|_{\hat{P}} \leq L \| x - y \|_{\hat{P}}, \quad \forall x, y \in B_\rho \text{ and } \forall i \in [0, M-1] \tag{3.18}$$

Finally, suppose that, for some finite constant $\lambda \geq 0$,

$$\| \frac{df}{dx_k}(x_k, \eta(x_k)) \|_{\hat{P}} =: \| \frac{dF}{dx_k}(x_k) \|_{\hat{P}} \leq \lambda, \quad \forall x_k \in B_{a\rho}, \quad \text{with } a \geq \beta e^{1-\alpha} \tag{3.19}$$

Under these conditions, the quadratic objective function at time t_k defined as:

$$V(t_k, x_k) := \int_{t_k}^{t_k+PT} [x_k(t)' Q x_k(t) + u_k(t)' R^* u_k(t)] \, dt \tag{3.20}$$

(i.e., we considered equation (3.3) with $S^* = 0$ for simplicity), is a Lyapunov function for the closed-loop system. This means that there exist constants $c, d, e, l > 0$ such that:

1. $c \| x_k \|_{\hat{P}}^2 \leq V(t_k, x_k) \leq d \| x_k \|_{\hat{P}}^2$,
2. $\dot{V}(t_k, x_k) := \frac{\partial V}{\partial t_k}(t_k, x_k) \leq -e \| x_k \|_{\hat{P}}^2$,

3. $\| \frac{\partial V}{\partial x_k}(t_k, x_k) \|_{\hat{P}} \leq l \| x_k \|_{\hat{P}}, \quad \forall k \geq 0, \forall x_k \in B_\rho.$

Proof: *The proof is constructive, i.e., we will compute the constants $c, d, e, l > 0$ such that the statement of the theorem holds.*

Because the control law is discontinuous, equation (3.20) is equivalent to:

$$V(t_k, x_k) := \int_{t_k}^{t_k+PT} x_k(t)' Q x_k(t)\, dt + \sum_{i=0}^{P} u(kP+i|kP)' R u(kP+i|kP), \quad \text{with } R := \frac{R^*}{T} \tag{3.21}$$

This is the form of $V(t_k, x_k)$ which we will use next to compute our lower and upper bounds.

- **Upper Bound on $V(t_k, x_k)$:** *Let us first derive an upper bound for $V(t_k, x_k)$, i.e., let us compute a possible value for $d > 0$. Due to the constraint $\| x_k(t) \|_{\hat{P}} \leq \beta \| x_k \|_{\hat{P}}, \ \forall t \in [t_k, t_{k+1}]$, we have that*

$$V(t_k, x_k) \leq \frac{\lambda_{max}(Q)}{\lambda_{min}(\hat{P})} \beta^2 PT \| x_k \|_{\hat{P}}^2 + \sum_{i=0}^{P} u(kP+i|kP)' R u(kP+i|kP) \tag{3.22}$$

Now, since $\| u(kP+i|kP) \|_{\hat{P}} := \| \eta_i(x_k) \|_{\hat{P}} \leq L \| x_k \|_{\hat{P}}, \ \forall i \in [0, M-1]$ (this inequality follows directly from (3.18) and from the fact that $\eta_i(0) = 0$), we have our desired upper bound on $V(t_k, x_k)$:

$$V(t_k, x_k) \leq \frac{P}{\lambda_{min}(\hat{P})} [\lambda_{max}(Q)\beta^2 T + \lambda_{max}(R) L^2] \| x_k \|_{\hat{P}}^2 =: d \| x_k \|_{\hat{P}}^2 \tag{3.23}$$

- **Upper Bound on the Gradient of $V(t_k, x_k)$, $\dot{V}(t_k, x_k)$:** *Taking the derivative from (3.20) we have that*

$$\dot{V}(t_k, x_k) = \| x_k(t_k + PT) \|_Q^2 - \| x_k \|_Q^2 + \| u_k(t_k + PT) \|_{R^*}^2 - \| u_k \|_{R^*}^2 \quad (3.24)$$

In our discontinuous control law notation we have:

$$\begin{aligned} \dot{V}(t_k, x_k) &= \| x_{k+1} \|_Q^2 - \| x_k \|_Q^2 + \| u(kP + P - 1|kP) \|_{R^*}^2 - \\ &- \| u((k-1)P + P - 1|(k-1)P) \|_{R^*}^2 \end{aligned} \quad (3.25)$$

Due to the contractive constraint, it follows that:

$$\begin{aligned} \dot{V}(t_k, x_k) &\leq -\frac{\lambda_{min}(Q)}{\lambda_{max}(\hat{P})}(1 - \alpha^2) \| x_k \|_{\hat{P}}^2 + \| u(kP + P - 1|kP) \|_{R^*}^2 - \\ &- \| u((k-1)P + P - 1|(k-1)P) \|_{R^*}^2 \end{aligned} \quad (3.26)$$

Now, if instead of imposing $u(kP+i|kP) = u(kP+M-1|kP), \ \forall i \in [M, P-1]$, *we have* $u(kP + i|kP) = 0, \ \forall i \in [M, P-1]$, *and* $M < P$ *(i.e., M is strictly smaller than P), then it immediately follows from (3.26) that:*

$$\begin{aligned} \dot{V}(t_k, x_k) &\leq -\frac{\lambda_{min}(Q)}{\lambda_{max}(\hat{P})}(1 - \alpha^2) \| x_k \|_{\hat{P}}^2 - \\ &- \| u((k-1)P + P - 1|(k-1)P) \|_{R^*}^2 \leq \\ &\leq -\frac{\lambda_{min}(Q)}{\lambda_{max}(\hat{P})}(1 - \alpha^2) \| x_k \|_{\hat{P}}^2 =: -e \| x_k \|_{\hat{P}}^2 \end{aligned} \quad (3.27)$$

- **Upper Bound on** $\frac{\partial V}{\partial x_k}(t_k, x_k)$**:** *From (3.20) it follows that*

$$\begin{aligned} \frac{\partial V}{\partial x_k}(t_k, x_k) &= \int_{t_k}^{t_{k+1}} [\frac{d \| x(t, t_k, x_k) \|_Q^2}{dx} \frac{\partial x(t, t_k, x_k)}{\partial x_k} + \\ &+ \frac{d \| u(t, t_k, x_k) \|_R^2}{du} \frac{\partial u(t, t_k, x_k)}{\partial x_k}] dt \end{aligned} \quad (3.28)$$

Thus,

$$\| \frac{\partial V}{\partial x_k}(t_k, x_k) \|_{\hat{P}} \leq \lambda_{max}(\hat{P})^{\frac{1}{2}} \int_{t_k}^{t_{k+1}} [\frac{d \| x_k(t) \|_Q^2}{dx} \| \frac{\partial x_k(t)}{\partial x_k} \|_{\hat{P}} + + \frac{d \| u_k(t) \|_R^2}{du} \| \frac{\partial u_k(t)}{\partial x_k} \|_{\hat{P}}] dt \tag{3.29}$$

Then, it results that:

$$\begin{aligned} \| \frac{\partial V}{\partial x_k}(t_k, x_k) \|_{\hat{P}} &\leq \frac{2\lambda_{max}(\hat{P})^{\frac{1}{2}}}{\lambda_{min}(\hat{P})^{\frac{1}{2}}} \int_{t_k}^{t_{k+1}} [\lambda_{max}(Q)^{\frac{1}{2}} \| x_k(t) \|_{\hat{P}} \lambda_{max}(\hat{P})^{\frac{1}{2}} e^{\lambda(t-t_k)} + \\ &+ \lambda_{max}(R)^{\frac{1}{2}} L \| u(t, t_k, x_k) \|_{\hat{P}}] dt \\ &\leq \frac{2\lambda_{max}(\hat{P})^{\frac{1}{2}}}{\lambda_{min}(\hat{P})^{\frac{1}{2}}} [\lambda_{max}(Q)^{\frac{1}{2}} \lambda_{max}(\hat{P})^{\frac{1}{2}} \beta \frac{(e^{\lambda PT} - 1)}{\lambda} + \\ &+ \lambda_{max}(R)^{\frac{1}{2}} L^2] \| x_k \|_{\hat{P}} =: l \| x_k \|_{\hat{P}} \end{aligned} \tag{3.30}$$

This follows from the fact that:

1. $$x_k(t) = x_k + \int_{t_k}^{t} F[x(\tau, t_k, x_k)] d\tau \tag{3.31}$$

   which means that

   $$\frac{\partial x_k(t)}{\partial x_k} = 1 + \int_{t_k}^{t} \frac{dF(x_k(\tau))}{dx} \frac{\partial x_k(\tau)}{\partial x_k} d\tau \tag{3.32}$$

   Thus,

$$\begin{aligned} \| \frac{\partial x_k(t)}{\partial x_k} \|_{\hat{P}} &\leq \lambda_{max}(\hat{P})^{\frac{1}{2}} + \int_{t_k}^{t} \| \frac{dF}{dx}(x_k(\tau)) \|_{\hat{P}} \| \frac{\partial x_k(\tau)}{\partial x_k} \|_{\hat{P}} d\tau \leq \\ &\leq \lambda_{max}(\hat{P})^{\frac{1}{2}} + \lambda \int_{t_k}^{t} \| \frac{\partial x_k(\tau)}{\partial x_k} \|_{\hat{P}} d\tau \end{aligned} \tag{3.33}$$

Using the Bellman-Grownwall (BG) inequality, it follows that:

$$\| \frac{\partial x_k(t)}{\partial x_k} \|_{\hat{P}} \leq \lambda_{max}(\hat{P})^{\frac{1}{2}} e^{\lambda(t-t_k)} \tag{3.34}$$

and

2. *Since* $u(t, t_k, x_k) = \eta_i(x_k), \ \forall t \in [t_k + iT, t_k + (i+1)T]$, *and* $\forall i \in [0, M-1]$, *and* η_i *is Lipschitz continuous for all* $i \in [0, M-1]$, *it results from (3.18) that:*

$$\| u(t, t_k, u_k) \|_{\hat{P}} \leq L \| x_k \|_{\hat{P}} \tag{3.35}$$

$$\| \frac{\partial u(t, t_k, x_k)}{\partial x_k} \|_{\hat{P}} \leq L \tag{3.36}$$

- **Lower Bound on** $V(t_k, x_k)$**:** *As a result of condition (3.19) we have:*

$$\begin{aligned} \| x_k(t) \|_{\hat{P}} &\geq \| x_k \|_{\hat{P}} - \lambda \int_{t_k}^{t} \| x_k(\tau) \|_{\hat{P}} \, d\tau \\ &\geq [1 - \lambda\beta(t - t_k)] \| x_k \|_{\hat{P}} \end{aligned} \tag{3.37}$$

It then follows, for example, that:

$$\| x_k(t) \|_{\hat{P}} \geq \frac{\| x_k \|_{\hat{P}}}{2} \quad for \ t \in [t_k, t_k + \frac{1}{2\lambda\beta}] \tag{3.38}$$

Thus, we have two cases to consider:

1. $t_{k+1} \leq t_k + \frac{1}{2\lambda\beta} \iff PT \leq \frac{1}{2\lambda\beta}$

   In this case,

$$\begin{aligned} V(t_k, x_k) &\geq \int_{t_k}^{t_{k+1}} \frac{[\lambda_{max}(Q) + 4L^2\lambda_{max}(R)]}{4\lambda_{min}(\hat{P})} \| x_k \|_{\hat{P}}^2 \, dt \geq \\ &\geq \frac{PT[\lambda_{max}(Q) + 4L^2\lambda_{max}(R)]}{4\lambda_{min}(\hat{P})} \| x_k \|_{\hat{P}}^2 \end{aligned} \tag{3.39}$$

2. $t_{k+1} \geq t_k + \frac{1}{2\lambda\beta} \iff PT \geq \frac{1}{2\lambda\beta}$

In this case,

$$\begin{aligned} V(t_k, x_k) &\geq \int_{t_k}^{t_k+\frac{1}{2\lambda\beta}} \frac{[\lambda_{max}(Q) + 4L^2\lambda_{max}(R)]}{4\lambda_{min}(\hat{P})} \parallel x_k \parallel^2_{\hat{P}} dt \geq \\ &\geq \frac{[\lambda_{max}(Q) + 4L^2\lambda_{max}(R)]}{8\lambda_{min}(\hat{P})\lambda\beta} \parallel x_k \parallel^2_{\hat{P}} \end{aligned} \tag{3.40}$$

Thus, it follows that:

$$\begin{aligned} V(t_k, x_k) &\geq \min\{\frac{PT[\lambda_{max}(Q) + 4L^2\lambda_{max}(R)]}{4\lambda_{min}(\hat{P})}, \frac{\lambda_{max}(Q) + 4L^2\lambda_{max}(R)}{8\lambda_{min}(\hat{P})\lambda\beta}\} \times \\ &\times \parallel x_k \parallel^2_{\hat{P}} =: c \parallel x_k \parallel^2_{\hat{P}} \end{aligned} \tag{3.41}$$

So, we have shown that, under the assumptions in the statement of the theorem, the quadratic performance criterion (3.3) subject to the constraints (3.5), with $u(kP + i|kP) = 0$ *for* $i \in [M, P-1]$ *and* $M < P$*, is a Lyapunov function for the closed-loop system.*

□

3.4 Algorithm implementation

Next we will show simulation results for various examples adopting the proposed MPC algorithm. This algorithm was implemented using a preliminary version of the MPC package in MATLAB written as the result of a semester thesis developed at the Institute of Automatic Control at the Swiss Federal Institute of Technology (ETH). This package is a combination of the well-known codes DASSL ([104]) and NPSOL ([53]) in MATLAB. DASSL is used for integration of the sets of algebraic and ordinary differential equations which describe the nonlinear dynamics of the model and the plant and NPSOL is used for solving the nonlinear optimization problem.

This code has not yet been optimized and our experience with it shows that a large amount of the time spent in the computations is devoted to calling functions in MATLAB which describe the model dynamics, the Jacobian of these dynamics, nonlinear constraints (such as the contractive constraint) and the Jacobian of these constraints. Therefore, it is likely that if DASSL and NPSOL are compiled together outside MATLAB, the computation time would be reduced significantly. So, the CPU time which we provide later for simulations of some examples only gives a rough idea of the order of magnitude of the time spent in the computations and should be interpreted with caution.

3.5 Example: A Nonholonomic System (Car)

3.5.1 Car (or "kinematic wheel") dynamics

The example considered here is a nonholonomic system which is the model of a car with no trailers. This system can be represented by the following set of equations:

$$\dot{x} = cos\theta \ v \tag{3.42}$$

$$\dot{y} = sin\theta \ v \tag{3.43}$$

$$\dot{\theta} = w \tag{3.44}$$

where (x, y) represents the Cartesian position of the center of mass of the car, θ is the inclination of the car with respect to the horizontal axis and v and w are its forward and angular velocities, respectively. The coordinate system for the car is illustrated in figure 3.5. Forward and angular motion of the car is achieved by changing the relative angular velocities of the wheels. Each wheel is driven by a stepper motor and any desired wheel angular velocity is achieved by commanding the motors to turn the

appropriate number of steps per second.

The inputs determined by the control law are v and w and the outputs are the state variables x, y and θ. The objective is to drive the system from any given initial condition to the origin with a satisfactory level of performance.

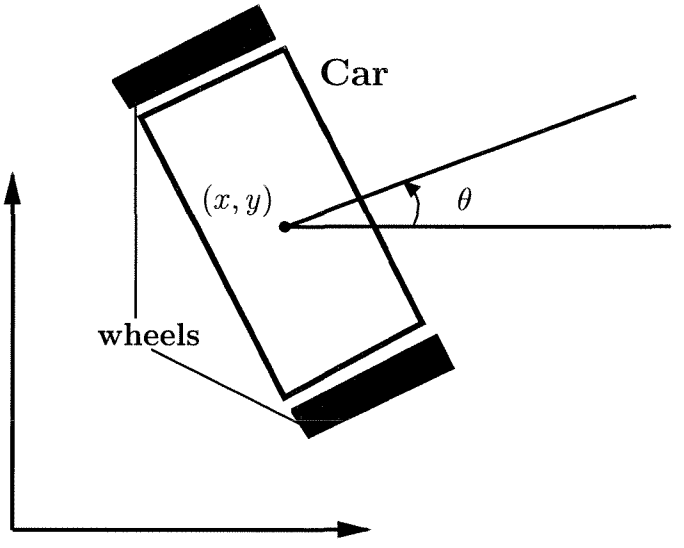

Figure 3.5: Coordinate system for the car.

This system violates Brockett's necessary condition for smooth or even continuous stabilization [24] and that is what makes the control design problem for this system (and nonholonomic systems, in general) a real challenge. Since MPC can automatically generate a discontinuous control law, we expect this controller to be suited for the class of nonholonomic systems. Moreover, this system is not controllable on the manifold of its equilibrium points, which also represents a difficulty from the control point of view. We will see later what difficulties are encountered by our contractive MPC scheme due to this fact.

Here the results obtained by using the proposed contractive MPC (CNTMPC) algorithm will be compared to the standard finite horizon nonlinear MPC (SNLMPC) scheme, the smooth controller found in [120], the homogeneous controller proposed by M'Closkey and Murray in [90], Pomet's controller [105] and, especially, the dis-

continuous controller proposed by Astolfi in [10, 11] (these last four techniques are analytic control designs devoted especially to nonholonomic systems).

3.5.2 Simulation results

Comparison between CNTMPC and Astolfi's discontinuous controller (unconstrained case)

In the plots shown in this section, the angle θ at all initial conditions is equal to $\theta_0 = 0$ (i.e., the car is parallel to the $x-$axis) and the angle at the origin is equal to $\theta_f = \frac{\pi}{2}$ (i.e., the car is parallel to the $y-$axis). We have adopted this convention because Astolfi's controller is analytically constructed to handle the output regulation problem with $(x, u, \theta) = (0, 0, \frac{\pi}{2})$ (and not $(x, u, \theta) = (0, 0, 0)$) as its target coordinate.

CNTMPC

Figure 3.6 shows the resulting paths in the $xy-$plane of the controlled car using CNTMPC in the unconstrained case.

The controller parameters used in these simulations are given by:

Controller Parameters (figure 3.6)		
$Q = \text{diag}([1\ \ 1\ \ 0])$	$R = 0$	$S = 0$
$P = 5$	$M = 3$	$\alpha = 0.9$

In all simulations for the car example the sampling time is equal to $T = 0.1$.

Astolfi's discontinuous controller

The same kind of plot in the $xy-$plane for the controlled car was presented in [10] (page 36) and we reproduce it in figure 3.7 with the same control gains, for purpose of comparison.

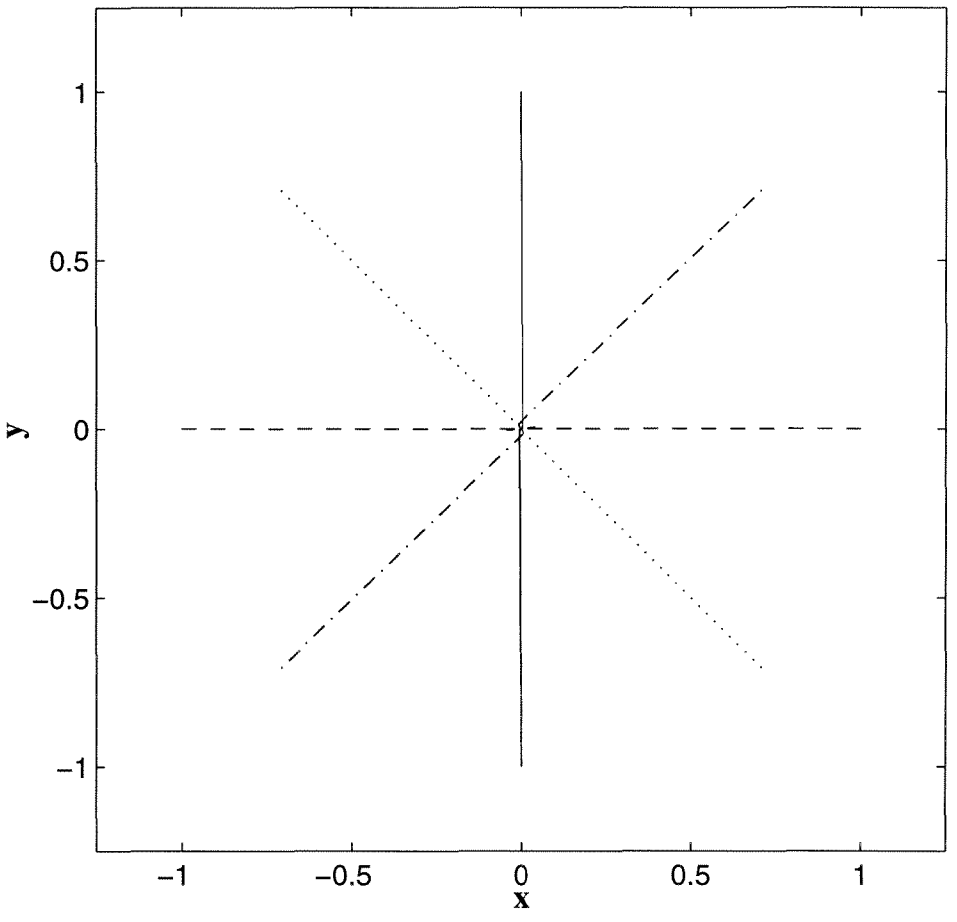

Figure 3.6: Resulting paths in the $xy-$plane using CNTMPC when the car is initially on the unit circle and parallel to the $x-$axis.

Comparison of results in figures 3.6 and 3.7

We should emphasize that the time taken by Astolfi's analytic discontinuous controller to compute these trajectories is less than a second, while CNTMPC took between 9 and 12 minutes on average (using the non-optimized MPC package which we discussed in section 3.4).

Moreover, because of the lack of controllability of this system at the origin, the contractive MPC algorithm is only able to drive the system to a very close neighborhood of the origin and then it stops (this effect cannot be really noticed

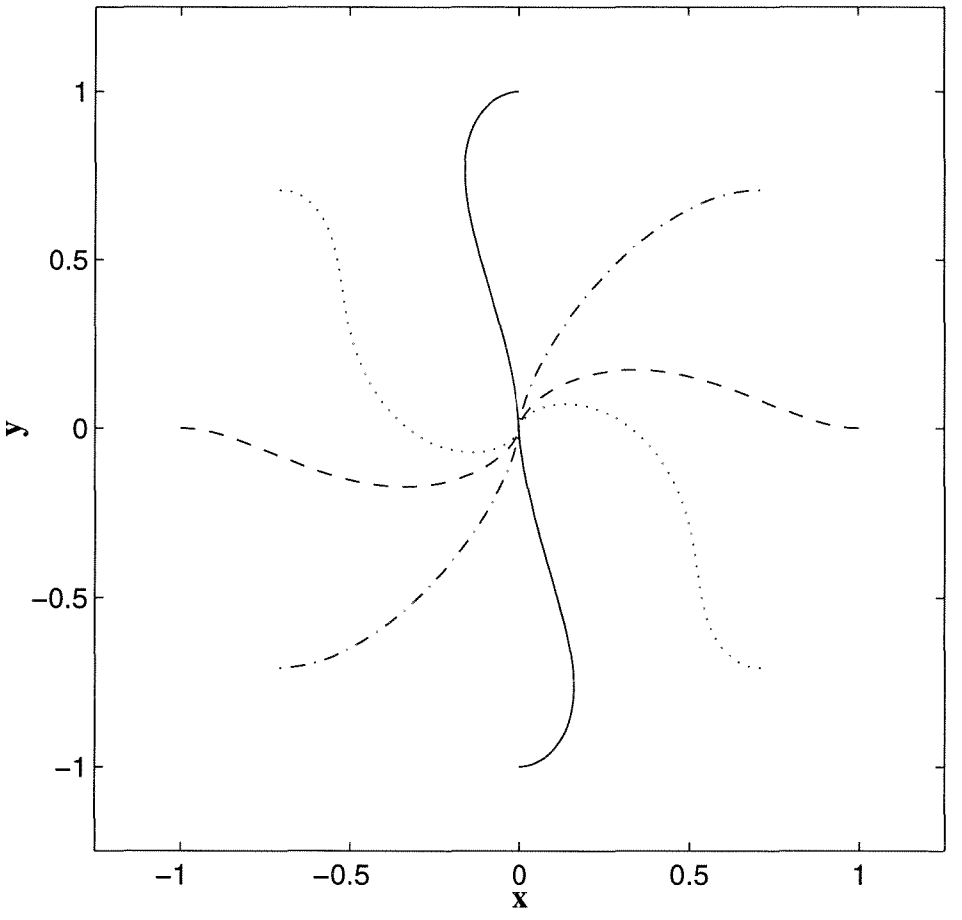

Figure 3.7: Resulting paths in the $xy-$plane using the analytic discontinuous controller when the car is initially on the unit circle and parallel to the $x-$axis.

in figure 3.6 due to scales). What happens is that, once the car is driven very near to the origin, the control action generated in the optimization step is very large - due to the lack of controllability - and the integration of the model equations with such control value cannot be carried out by the integrator.

We can see from figures 3.6 and 3.7 that for both controllers the car performs its maneuver towards the origin of the coordinate system in a very natural way and without ever inverting its motion. Hence, the floor trajectories do not contain any cusps. This response can be anticipated for the analytic discontinuous controller because the control signal v is constructed to always have a constant

sign. In the case of CNTMPC, the controller just automatically generates such a response.

We also observe that CNTMPC generates trajectories which approach the origin in an almost straight path. It is clear that the analytic discontinuous controller cannot match this performance. This is not surprising since the construction of the analytic controller does not take into account performance but only stabilization. CNTMPC, on the other hand, minimizes a performance criterion at every time step and the contractive constraint takes care of the stability issue.

Comparison between CNTMPC and SNLMPC (unconstrained and constrained cases)

Now that we have shown that CNTMPC performs satisfactorily in the unconstrained case, we will compare the performance and stability properties of a standard nonlinear MPC (SNLMPC) algorithm with CNTMPC in order to examine more closely the influence of the contractive and input constraints on the closed-loop response. The chosen initial condition is one used by M'Closkey in his experiments with the car at the Department of Mechanical Engineering at Caltech in 1993:

Initial Condition		
$x_0 = -0.5945$	$y_0 = 0.3299$	$\theta_0 = 0.8262$

Unconstrained case

The unconstrained responses for SNLMPC and CNTMPC can be found in figure 3.8.

The controller parameters used in these simulations are given by:

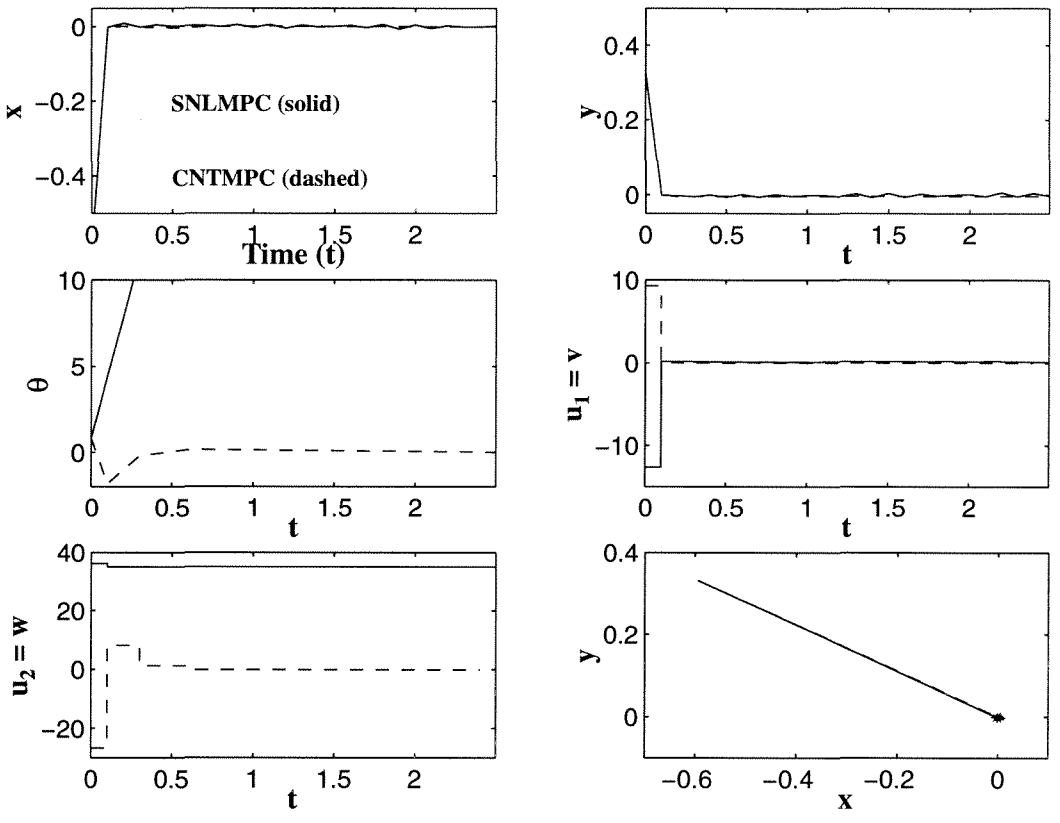

Figure 3.8: Car: State and control responses for SNLMPC and CNTMPC in the unconstrained case.

Controller Parameters (figure 3.8)		
$Q = \text{diag}([1\ \ 1\ \ 0])$	$R = 0$	$S = 0$
$P = 5$	$M = 3$	$\alpha = 0.9$

Naturally, the contractive parameter α is used only by the CNTMPC controller.

We notice that since the angle θ and the second input variable w are not weighted in the objective function, and since the system has two inputs and three outputs, the SNLMPC controller cannot stabilize θ which grows indefinitely. The other two states, x, y, reach the origin quickly but then they oscillate about it.

The CNTMPC controller is able to stabilize θ (even though the system has more states than inputs) due to the introduction of the contractive constraint.

Besides, the settling time of the other variables is not increased (they reach the origin after only one sampling time without further oscillations). Therefore, we see that SNLMPC cannot stabilize θ with the given controller parameter choices but the contractive constraint makes it possible, without degrading the performance of the response for the other state variables.

Constrained case

Case 1

The constrained responses for SNLMPC and CNTMPC can be found in figure 3.9.

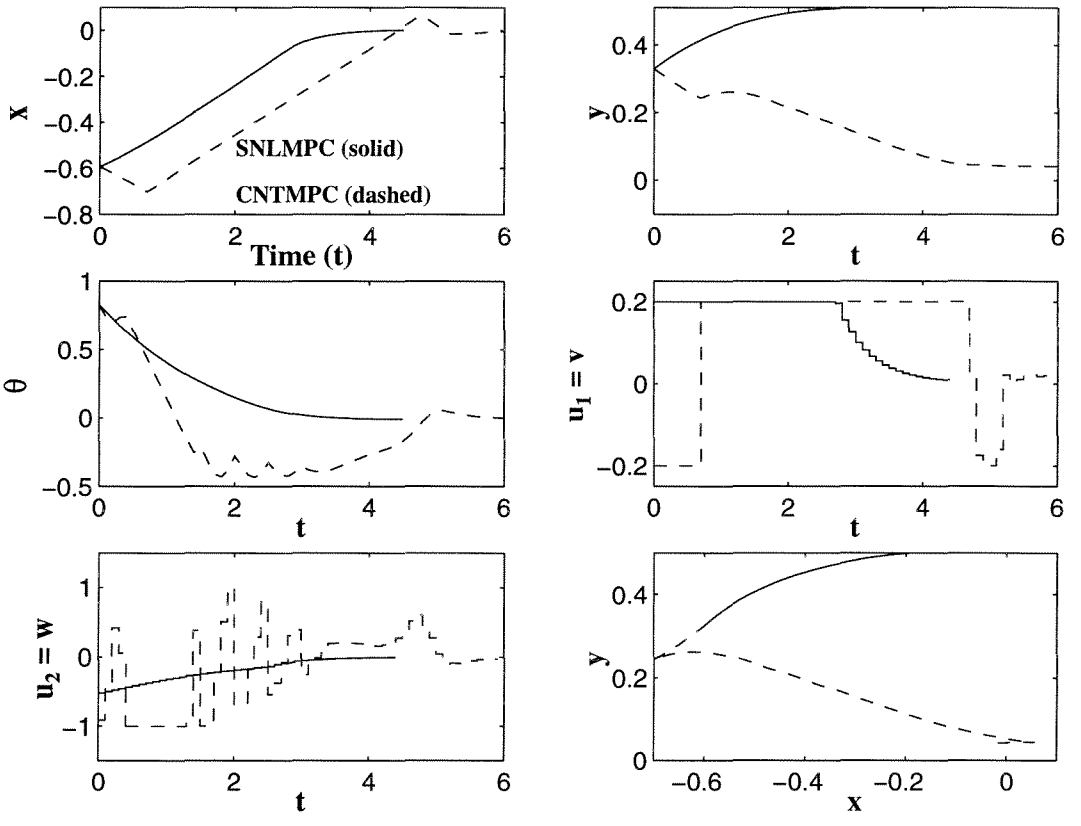

Figure 3.9: Car: State and control responses for SNLMPC and CNTMPC in the constrained **Case 1**.

The controller parameters in **Case 1** are the following:

Controller Parameters (figure 3.9)		
$Q = \text{diag}([1 \;\; 1 \;\; 0.1])$	$R = 0.1\, I_m$	$S = 0$
$P = 8$	$M = 5$	$\alpha = 0.9$
$u_{min} = [-0.2 \quad -1.0]$	$u_{max} = [0.2 \quad 1.0]$	

The control bounds u_{min} and u_{max} represent physical bounds on v and w which were encountered by M'Closkey in his experiments with the car at Caltech in 1993.

We can see from figure 3.9 that the Cartesian position y cannot be stabilized by SNLMPC with the given controller parameter choices. It will not reach the origin, even when given more time, because since v is already settling to 0, $\dot{y}$ is approaching 0 as well (as we can see from the model equation (3.44)).

CNTMPC stabilizes the system but y shows a small offset due to the lack of controllability of the car near the origin. This is a difficulty which causes the code to stop before the origin is reached.

Case 2

From the results in **Case 1**, we would expect to stabilize the $y-$response by adding more weight to this state in the objective function. Indeed, the response improves if the controller parameters are selected as in:

Controller Parameters (figure 3.10)		
$Q = \text{diag}([1 \;\; 5 \;\; 0.1])$	$R = 0.01\, I_m$	$S = 0$
$P = 8$	$M = 5$	$\alpha = 0.9$
$u_{min} = [-0.2 \quad -1.0]$	$u_{max} = [0.2 \quad 1.0]$	

The response with this new set of parameters can be found in figure 3.10. Here the responses obtained with SNLMPC and CNTMPC have approximately the same characteristics with the exception that the $y-$response

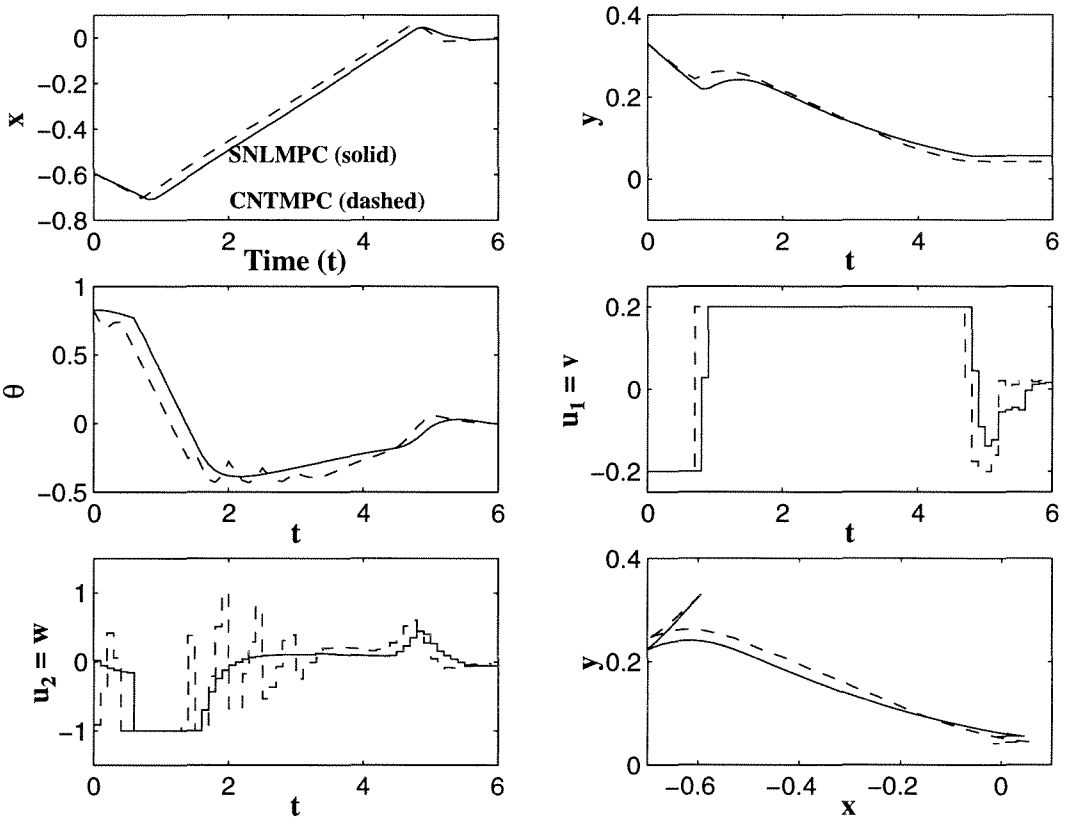

Figure 3.10: Car: State and control responses for SNLMPC and CNTMPC in constrained **Case 2**.

obtained with CNTMPC has a smaller offset than with SNLMPC. Because the system loses controllability at the origin and it has three states and two inputs, a certain amount of offset remains in generally only one variable.

Comparison between CNTMPC and some classic controllers (constrained case)

Here we want to compare the closed-loop response obtained by use of our CNTMPC controller in the presence of input constraints with some classic analytic control design techniques for nonholonomic systems. These techniques do not take into account process constraints but, since the response for the given initial condition remains between the bounds we used in our simulations with the CNTMPC controller, the

comparison is fair.

The simulation results are shown in figures 3.11 (state response), 3.12 (control response) and 3.13 (plots in the $xy-$plane).

The controller parameters used in the simulations with CNTMPC are:

Controller Parameters (figures 3.11, 3.12 and 3.13)		
$Q = \text{diag}([1 \;\; 8 \;\; 0.1])$	$R = 0.01\, I_m$	$S = 0$
$P = 20$	$M = 6$	$\alpha = 0.9$
$u_{min} = [-0.2 \quad -1.0]$	$u_{max} = [0.2 \quad 1.0]$	

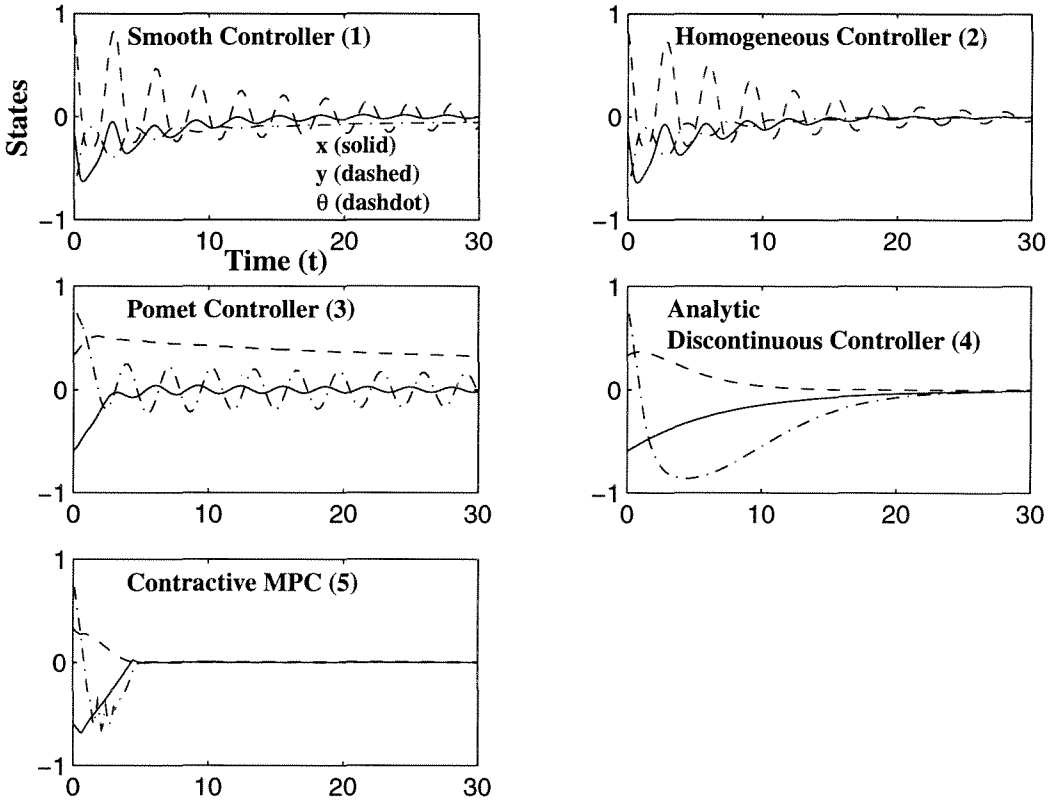

Figure 3.11: Car: Comparison of CNTMPC with other classic controllers for nonholonomic systems (state response).

From figures 3.11, 3.12 and 3.13, we can see that the smooth control law is not able to stabilize the car since it violates Brockett's necessary condition for stabilization of this

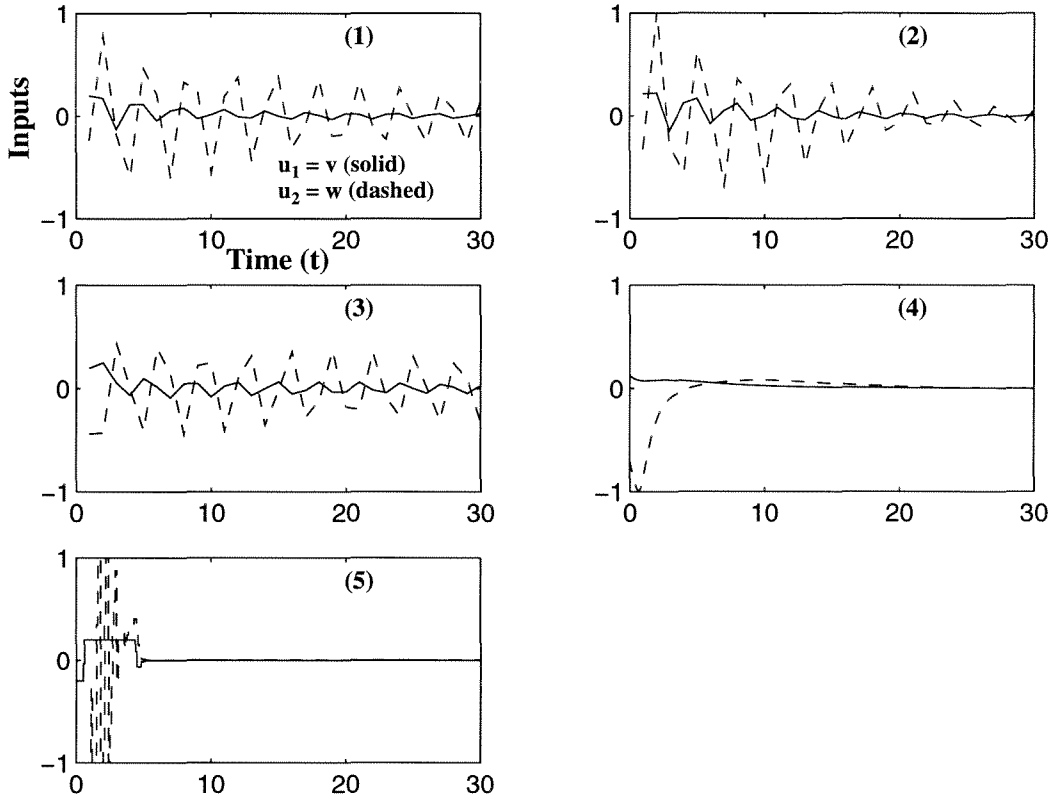

Figure 3.12: Car: Comparison of CNTMPC with other classic controllers for non-holonomic systems (control response).

class of systems. The angle θ oscillates indefinitely and so does the x coordinate (with oscillations of smaller magnitude). Pomet's controller suffers from similar drawbacks and while the angle θ and the x coordinate oscillate indefinitely, the y position has a very long settling time. The homogeneous controller performs better than the two previous controllers but once again the states oscillate indefinitely (even though with oscillations of much smaller magnitude than for the other two techniques). Astolfi's analytically constructed discontinuous controller is undoubtedly the best amongst these four analytic control design techniques and it can actually stabilize the system to the origin without oscillations. However, the comparison with the CNTMPC controller shows that the response time is five times longer within approximately the same control bounds. Therefore, we can conclude that the CNTMPC controller (and the SNLMPC as well, for certain parameter choices) performs significantly better

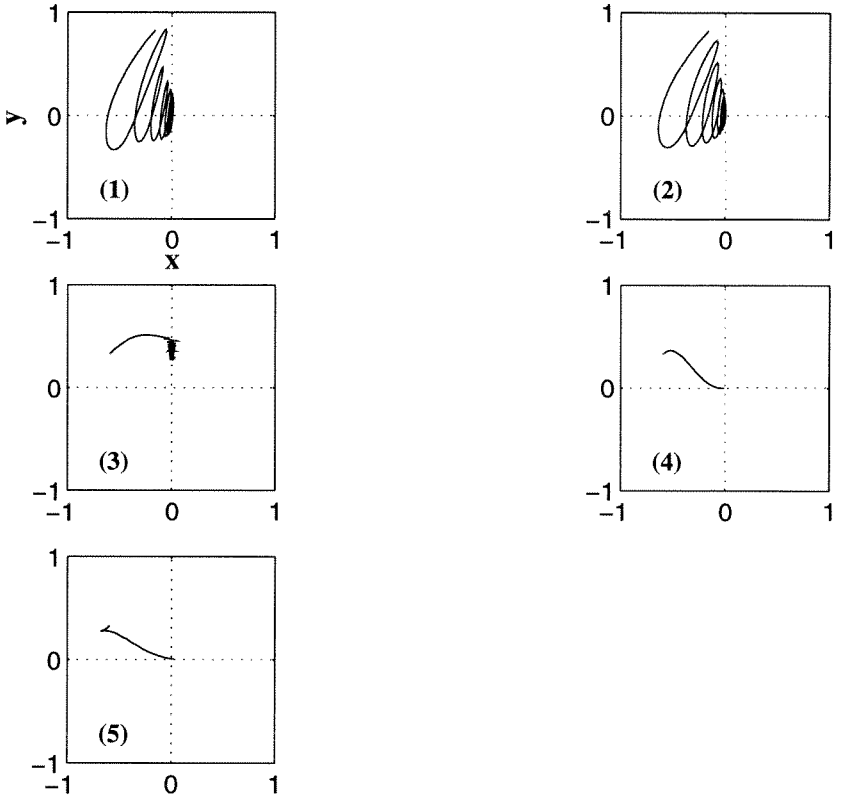

Figure 3.13: Car: Comparison of CNTMPC with other classic controllers for nonholonomic systems (plots in the $xy-$plane).

than the classic analytic techniques showing, as we expected, that MPC is a successful control technique for the class of nonholonomic systems. The introduction of the contractive constraint only adds more reliability to it, guaranteeing stability as long as feasibility can be assured.

3.6 Example: Fluid Catalytic Cracking Unit

3.6.1 Description of the system

Fluid catalytic cracking units (FCCUs) are commonly used to convert heavy petroleum feed-stocks into lighter hydrocarbon products, a key step in actual petroleum refining.

Significant practical incentives exist for the real-time optimization and improved control of these units, because of the large volume of raw material processed, together with their widespread use (see [12]). A schematic representation of the process is presented in figure 3.14.

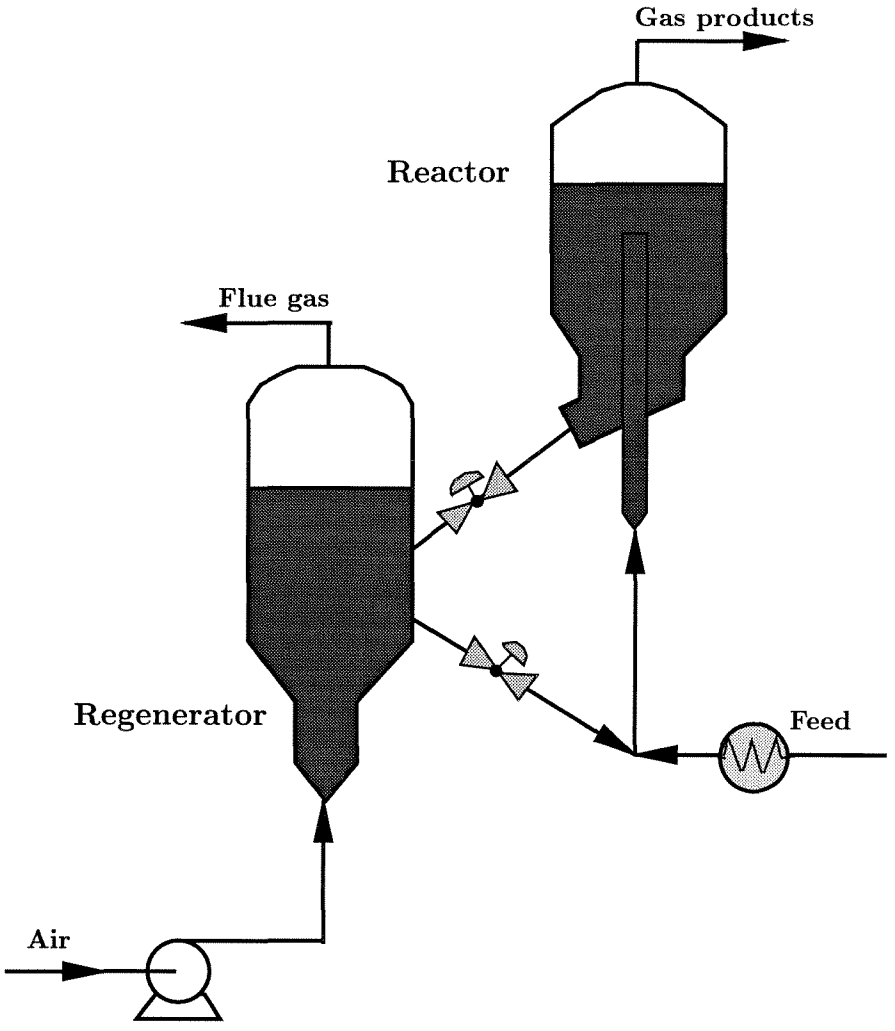

Figure 3.14: Schematic diagram of the FCCU.

This unit is composed of two vessels, a reactor where reaction and separation of products occur and a regenerator, where the catalyst is regenerated by burning the carbon deposits formed on its surface. After being vaporized, the feed is put in contact with hot catalyst in the riser and converted into gasoline, distillates and light olefins. All of these products exit the reactor in the gas phase. During this

process, carbonaceous deposits also form on the surface of the catalyst particles. These deposits considerably decrease the catalyst activity, introducing the need for its regeneration in the adjoint vessel (also a fluidized bed) where the deposits are burnt before the catalyst is recirculated back to the reactor. Because of the fast kinetics involved, a high recirculation rate for the catalyst is required, causing the mean catalyst residence time in the reactor to be typically on the order of seconds (as reported in [12]). This introduces a significant interaction between the dynamics of the two vessels. The temperature distribution and flow regime in the riser also have a major impact on the product distributions obtained at the exit of the reactor. Due to the nature of these interactions and their considerable nonlinear behavior, FCCUs have been considered amongst the most complex and challenging processes in modern refineries [57]. These characteristics make this process well-suited for testing more advanced control structures such as MPC. The controllability of FCC units has been studied in [59].

The interest in the more efficient control of these units is reflected by the large number of different controller design approaches proposed for these processes. A few of the main references in the area are [8, 25, 57, 55, 60, 103, 112].

3.6.2 FCCU dynamics

Here we will use the same semi-empirical model of FCCUs presented in [36] which is a modification of the original model of Lee and Kugelman [75]. It consists of balance equations for the mass of coke (carbonaceous material) and energy, both in the reactor and in the regenerator vessels. The main assumptions are a constant hold up in both vessels (maintained by the use of equal spent and regenerated catalyst flow rates), perfect mixing, physical properties independent of the temperature and negligible heat loss to the surroundings. The state variables are C_{sc} (coke content in the spent catalyst), T_{rx} (reactor bed temperature), C_{rg} (coke content in the regenerated catalyst) and T_{rg} (regenerator bed temperature). The model also considers five main

input variables which are F_a (air flow rate), T_a (air temperature), F_t (feed rate), T_f (feed temperature) and F_c (catalyst recirculation rate). The equations which describe the model are ([36, 75]):

Reactor coke balance:

$$\frac{d(H_{rx}C_{sc})}{dt} = F_c(C_{rg} - C_{sc}) + R_{cf}(T_r) \tag{3.45}$$

Reactor energy balance:

$$\frac{d(H_{rx}C_{pc}T_{rx})}{dt} = F_cC_{pc}(T_{rg}-T_{rx})+F_tC_{pf}(T_f-T_{rx})-F_t(\lambda_0+\epsilon(T_{rx})\Delta H_{cr}) \tag{3.46}$$

Regenerator coke balance:

$$\frac{d(H_{rg}C_{rg})}{dt} = F_c(C_{sc} - C_{rg}) - R_{cb}(T_{rg}, C_{rg}) \tag{3.47}$$

Regenerator energy balance:

$$\frac{d(H_{rg}C_{pc}T_{rg})}{dt} = F_cC_{pc}(T_{rx} - T_{rg}) + F_aC_{pg}(T_a - T_{rg}) + R_{cb}(T_{rg}, C_{rg})Q_{cb} \tag{3.48}$$

where:

Rate of carbon formation:

$$R_{cf}(T_r) = a_{cc}\, e^{-\frac{E_{cc}}{RT_r}}\, t_c^n F_c \tag{3.49}$$

Rate of cracking:

$$\epsilon(T_r) = \frac{A(1 - e^{-\lambda})}{\lambda + A(1 - e^{-\lambda})} \tag{3.50}$$

Rate of coke burning:

$$R_{cb} = \frac{F_aM_c}{\alpha_{CO}M_g}\,(0.21 - C_{O_2}) \tag{3.51}$$

Intermediate quantities:

$$C_{O_2} = 0.21\, e^{\left(-\frac{a_{cb}e^{\left(-\frac{E_{cb}}{RT_{rg}}\right)}C_{rg}M_g\alpha_{CO}H_{rg}}{0.21F_aM_c}\right)} \tag{3.52}$$

$$A = C_1 e^{-\frac{Q_1}{RT_r}} \tag{3.53}$$

$$\lambda = t_c C_2 e^{-\frac{Q_3}{RT_r}} \tag{3.54}$$

$$t_c = \frac{H_{rx}}{F_c} \tag{3.55}$$

$$T_r = 0.6T_r + 0.4T_{mix} \tag{3.56}$$

$$T_{mix} = \frac{C_{pc}F_cT_{rg} + C_{pf}F_tT_f - F_t\lambda_0}{C_{pc}F_c + C_{pf}F_t} \tag{3.57}$$

The nomenclature for this FCC model can be found in [75]. The numerical values for the model parameters are given by:

Parameter and steady state input values for the FCC	
$a_{cb} = 1.404 \times 10^{11}\ \ h^{-1}$	$a_{cc} = 0.0195$ lb coke/ lb cat. h^{-1}
$C_1 = 6990$	$C_2 = 111.1$
$C_{pc} = 0.28$ Btu/ lb.^0F	$C_{pf} = 0.75$ Btu/ lb.^0F
$C_{pg} = 0.2405$ Btu/ lb.^0F	$E_{cb} = 3.76 \times 10^4$ cal/gmol
$E_{cc} = 2450$ cal/gmol	$F_t = 8.97 \times 10^5$ lb/h
$H_{rg} = 4.0 \times 10^5$ lb	$H_{rx} = 1.0 \times 10^5$ lb
$M_c = 13$ lb/lbmol	$M_g = 29.2$ lb/lbmol
$n = -0.07$	$Q_1 = 1.0 \times 10^5$ cal/gmol
$Q_3 = -1.7 \times 10^3$ cal/lbmol	$Q_{cb} = 1.37 \times 10^4$ Btu/lb
$R = 1.986$ cal/gmol.^0C	$T_a = 90^0$ F
$T_f = 440^0$ F	$\alpha_{CO} = 1$
$\Delta H_{cr} = 120$ Btu/lb	$\lambda_0 = 95$ Btu/lb

3.6.3 Computation of steady states

Let us now examine the steady state characteristics of the given FCC model, in particular, the possibility of existence of multiple steady states. Such occurrences are common in nonlinear processes where exothermic reactions take place, and have in fact been identified in similar models of FCC units [7, 8, 42].

The steady states can be computed more easily by first eliminating some of the unknowns in the model equations. For example, from the reactor and regenerator coke balances we obtain:

$$C_{sc} = C_{rg} + \frac{R_{cb}(T_{rg}, C_{rg})}{F_c} \tag{3.58}$$

$$R_{cb}(T_{rg}, C_{rg}) = R_{cf}(T_{rx}) \tag{3.59}$$

From the regenerator energy balance it results that:

$$T_{rx} = T_{rg} - \frac{F_a C_{pg}(T_a - T_{rg}) + R_{cb}(T_{rg}, C_{rg}) Q_{cb}}{F_c C_{pc}} \tag{3.60}$$

And, finally, by substituting equation (3.60) into the regenerator energy balance, at steady state, we obtain:

$$\begin{aligned} [F_a C_{pg}(T_a - T_{rg}) + R_{cb}(T_{rg}, C_{rg}) Q_{cb}] \left(1 + \frac{F_t C_{pf}}{F_c C_{pc}}\right) + F_t C_{pf}(T_f - T_{rg}) - \\ - F_t(\lambda_0 + \epsilon(T_{rx}) \Delta H_{cr}) = 0 \end{aligned} \tag{3.61}$$

Further elimination of variables becomes difficult due to the complexity of expression (3.61).

By varying F_a and F_c in a range of $\pm 5\%$ around their nominal values while keeping the other potential inputs, F_t, T_f, F_c, at their nominal values, one "hot" open-loop (OL) stable and one OL unstable stationary point can be calculated and their coordinates are given by:

Steady state values for the FCC		
Variables	**unstable (1)**	**stable (2)**
F_a (lb/h)	6.8×10^5	7.2×10^5
F_c (lb/h)	8.95×10^6	9.48×10^6
C_{sc} (lb coke/ lb cat)	7.985×10^{-3}	7.173×10^{-3}
T_{rx} (^0F)	957.62	1149.88
C_{rg} (lb coke/ lb cat)	2.347×10^{-3}	3.571×10^{-4}
T_{rg} (^0F)	1163.46	1398.04

Previous studies (e.g., [42, 75]) have reported the possibility of existence of unstable steady states for similar FCC units where it was noted that the system tended to drift either to a state of complete combustion or to extinction. This fact together with the significant nonlinear nature of the process makes the application of linear controller design techniques for this system a significant challenge. Therefore, this kind of system is a natural candidate for application of nonlinear MPC techniques.

Standard nonlinear MPC techniques have been applied previously to this process and have been shown to perform rather well in the stable region of the state space for specific controller parameter choices (see [36]). In the unstable region difficulties were encountered due to the ill-conditioning of the nonlinear state space equations which describe the model for this system.

As pointed out by Arbel et al. in [9], operation in the unstable region is not considered important in most applications since this is a region where the temperatures in the reactor and regenerator are lower than they are in one of the "hot" stable regimes (the unstable equilibrium point is found between two stable equilibria, a "hot" and

a "cold"). There is no practical cold state in an FCC. Although one can compute a cold state, the temperature is so low that the feed will not be vaporized. There will be no reaction and no catalyst flow. The unit will merely fill up with unvaporized feed.

Since the open-loop unstable steady state is always an intermediate state between the desirable hot state and the unoperational cold one, the most important control task in this unit is, if the operation conditions are changed (manually or due to disturbances) and the stable hot steady state is lost, the control circuit should be able to act immediately, bringing the operation back to the hot steady state.

Thus, maintaining operation around the unstable steady state is not really the objective in these FCC units. The main interest is to design a controller which can restore the unit from the unstable region back to the "hot" stable one. However, since stabilizing the system around the unstable steady state is a challenging control problem, we will consider it here just for the sake of studying the stabilizing properties of the proposed contractive MPC controller under such unfavorable and challenging conditions.

Here we will adopt F_c and F_a as the manipulated variables (inputs). Thus, this is a 4-state 2-input system and, in this chapter, we consider that all the states are measurable and the measurements are noise-free. In practice, T_{rx} and T_{rg} are the controlled variables (outputs) since they can be easily measured and C_{sc} and C_{rg} are estimated states.

3.6.4 Simulation results

Our goal in the simulations that follow is to test the stability and performance characteristics of the proposed contractive MPC (CNTMPC) scheme against those of a finite horizon standard nonlinear MPC (SNLMPC) algorithm.

Here we will study two different steady state transitions:

Transition 1: a step change in the state values from steady state (**1**) (unstable) to steady state (**2**) (stable),

Transition 2: a step change in the state values from steady state (**2**) (stable) to steady state (**1**) (unstable).

Our results will reveal that while SNLMPC performs well in **Transition 1** (even though, as we will be showing, it can go unstable for certain controller parameter choices), we could not find a set of parameters for which SNLMPC generated a stable closed-loop system in **Transition 2**. On the other hand, CNTMPC is able to handle the step change to the unstable region due to the stabilizing effect of the contractive constraint.

The difficulty in operating in the unstable region comes from the fact that the model equations become much more ill-conditioned than they are in the neighborhood of the stable steady state. This behavior introduces difficulties in the convergence of the control response of the nonlinear algorithm, due to the extreme sensitivity of the equations to input changes.

The input and state variables which will be plotted for the FCC example are the deviation variables with respect to the desired steady state values.

Transition 1

Case 1

The simulation for **Transition 1** under no input constraints is illustrated in figure 3.15 for both SNLMPC and CNTMPC. For the chosen controller parameters, the responses are equal and in this transition to the stable

steady state, the beneficial stabilizing effects of the contractive constraint cannot be felt.

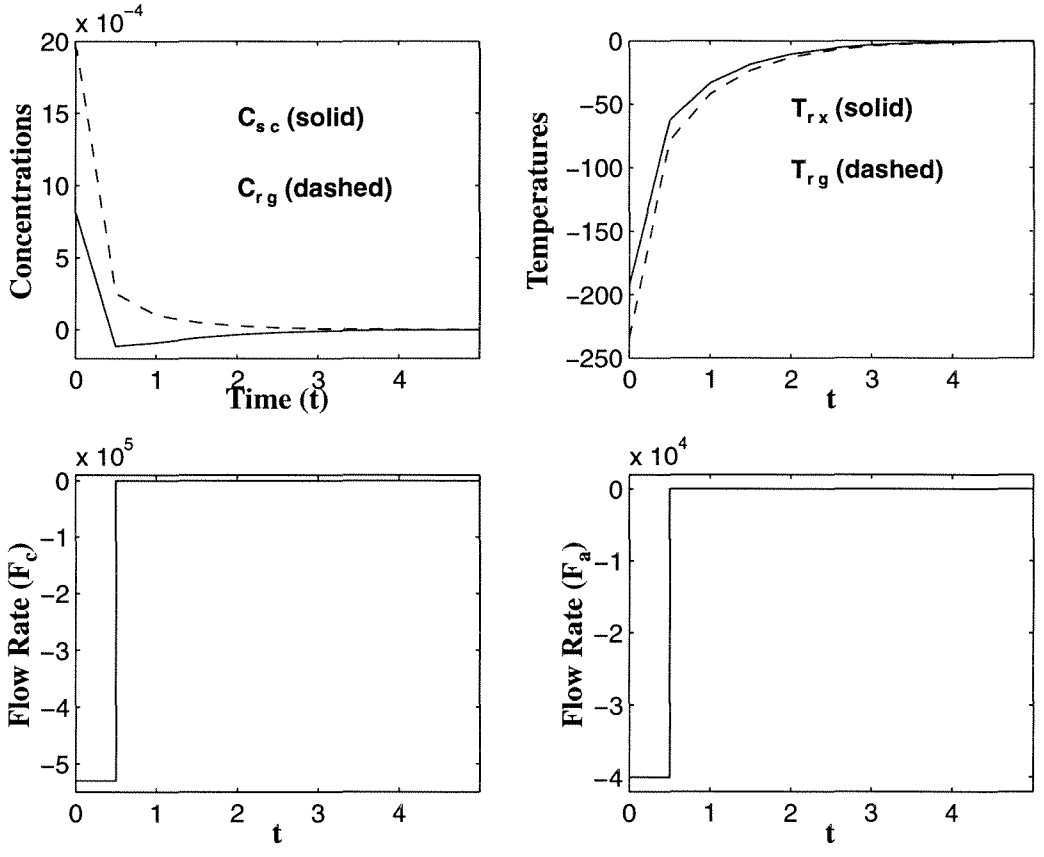

Figure 3.15: FCCU: State and control responses for SNLMPC/CNTMPC in the unconstrained **Case 1** (**Transition 1**).

The controller parameters used in **Case 1** are given by:

Controller Parameters (figure 3.15)		
$Q = \text{diag}([0 \;\; 10^{-3} \;\; 1 \;\; 0])$	$R = 0.1\, I_m$	$S = 0$
$P = 5$	$M = 5$	$\alpha = 0.9$

In all simulations for this example we used a sampling time $T = 0.5$ h.

Case 2

Now we want to show that, even when the desired steady state is open-loop stable, the response obtained with SNLMPC can be easily made unstable.

Our results will reveal that if no weights are added to the inputs in the objective function (i.e., $R = 0$), the manipulated variables settle to high values and cannot be brought to zero. Meanwhile, the temperatures T_{rg} and T_{rx} show a large offset and the concentrations C_{rg} and C_{sc} go unstable. These simulations are illustrated in figure 3.16.

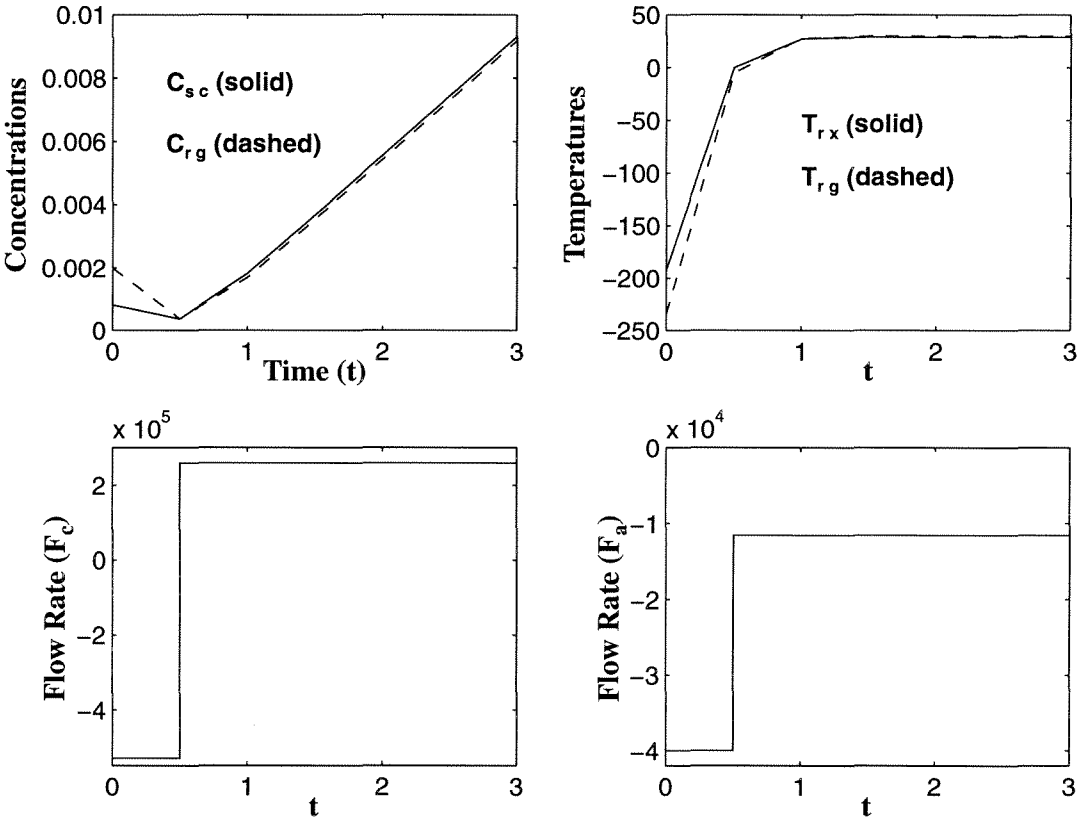

Figure 3.16: FCCU: State and control responses for SNLMPC in the unconstrained **Case 2** (**Transition 1**).

The controller parameters used in **Case 2** are given by:

Controller Parameters (figure 3.16)		
$Q = \text{diag}([0 \;\; 10^{-3} \;\; 1 \;\; 0])$	$R = 0$	$S = 0$
$P = 5$	$M = 3$	

Since the control effort is very little in **Case 1**, where both SNLMPC and CNTMPC

are stable (due to the weight on u in the objective function), there is no need to analyze the constrained case. Therefore, we will move straight into **Transition 2**.

Transition 2

SNLMPC

In this case, the control problem is much harder and the SNLMPC algorithm produces unstable responses as we can see from figures 3.17 (**Case 1**) and 3.18 (**Case 2**). **Case 1** and **Case 2** represent simulations with SNLMPC for different sets of controller parameters:

Controller Parameters (figures 3.17 and 3.18)		
Case 1		
$Q = \text{diag}([10^{-2}\ \ 10\ \ 0.1\ \ 10^{-2}])$ $P = 8$	$R = 0$ $M = 5$	$S = 0$
Case 2		
$Q = \text{diag}([10^{-4}\ \ 10^{-2}\ \ 1\ \ 10^{-4}])$ $P = 15$	$R = 0.01\ I_m$ $M = 5$	$S = 0$

In **Case 1** (figure 3.17), the state responses are highly oscillatory and show significant offset. The manipulated variables oscillate around their stable steady state values.

In **Case 2** (figure 3.18), T_{rx}, T_{rg} have large offsets once again (this time without oscillatory behavior) and C_{rg}, C_{sc} go unstable, increasing indefinitely. Meanwhile, the manipulated variables settle to zero in only one sampling time, leaving the system open-loop.

Thus, the parameter change from **Case 1** to **Case 2** causes a very different unstable closed-loop response.

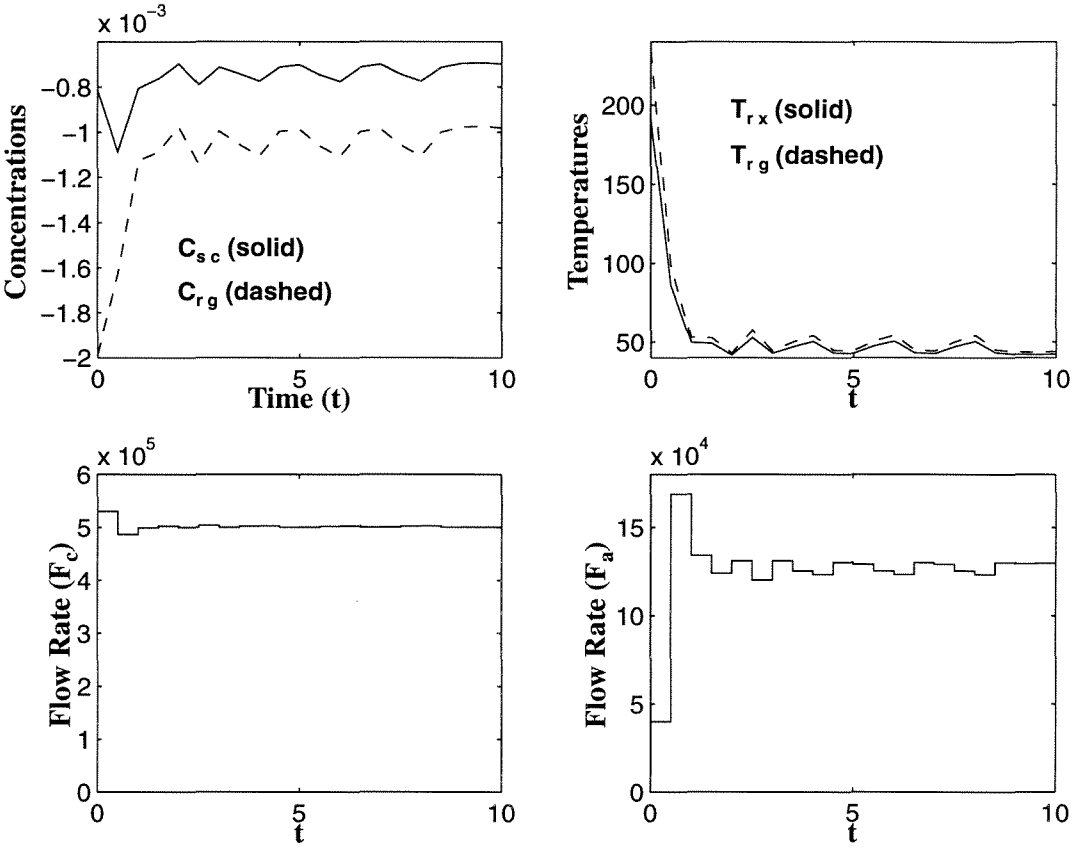

Figure 3.17: FCCU: State and control responses for SNLMPC in the unconstrained **Case 1 (Transition 2)**.

CNTMPC

CNTMPC generates a stable closed-loop with the state variables settling to the desired steady state in approximately eight sampling times ($t = 4$ h). The results are depicted in figure 3.19.

The controller parameters used in these simulations are given by:

Controller Parameters (figure 3.19)		
$Q = \text{diag}([10^{-6} \;\; 10^{-2} \;\; 1 \;\; 10^{-6}])$	$R = 0.01\, I_m$	$S = 0$
$P = 12$	$M = 6$	$\alpha = 0.9$

Due to the severe degree of difficulty in this control problem, we will not be considering the influence of input constraints. The main challenge which

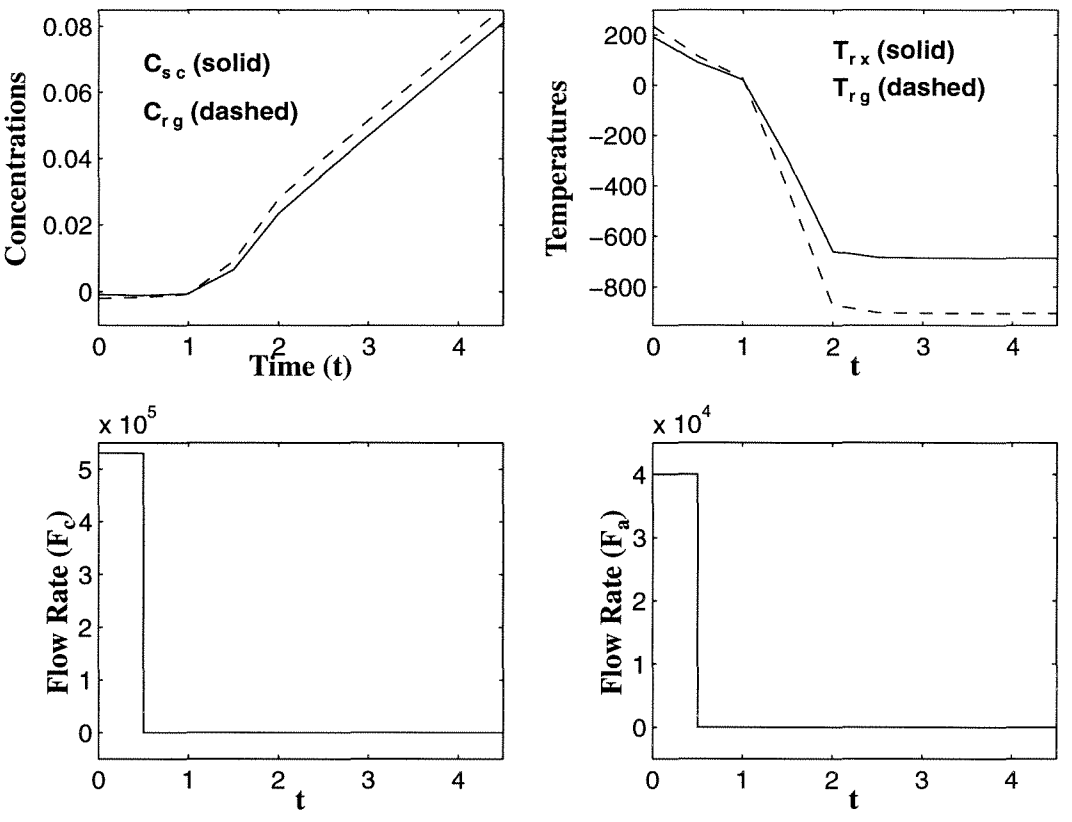

Figure 3.18: FCCU: State and control responses for SNLMPC in the unconstrained **Case 2 (Transition 2)**.

we have found in this case is to find a set of control parameters for which the optimization is feasible in the vicinity of the unstable operating point.

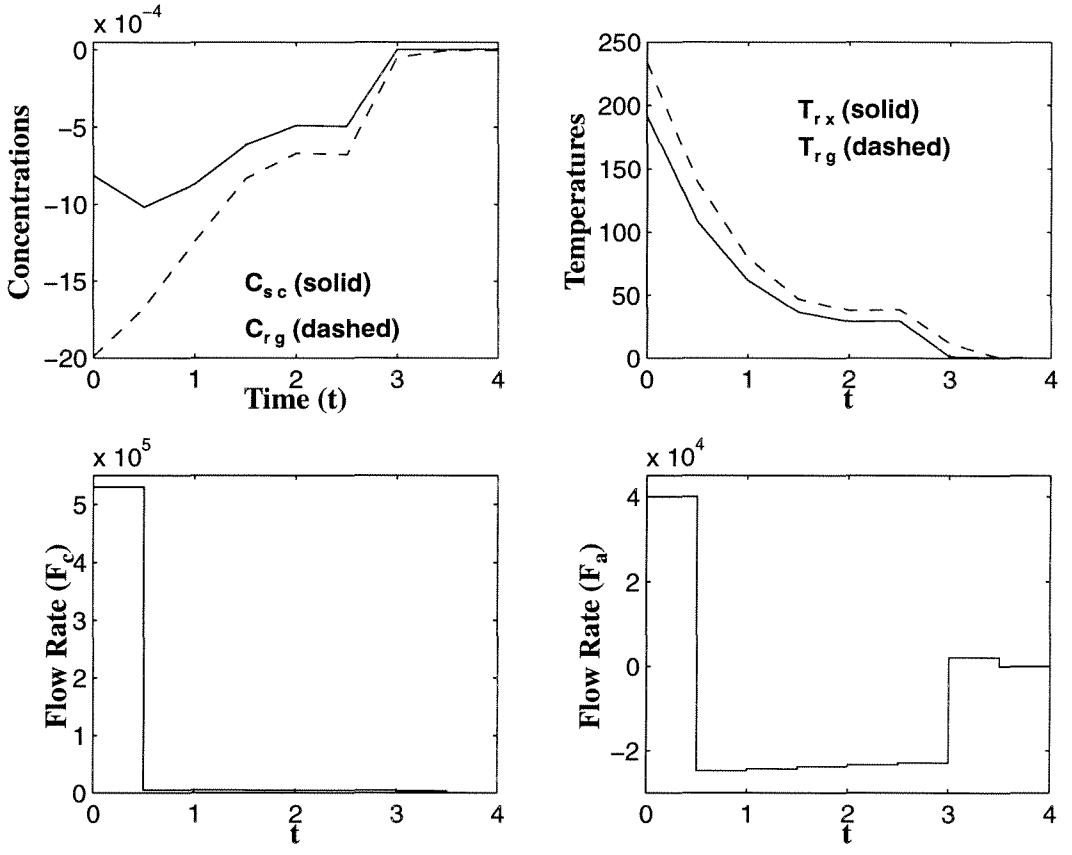

Figure 3.19: FCCU: State and control responses for CNTMPC in the unconstrained case (**Transition 2**).

3.7 Example: 2-Degree of Freedom Robot

3.7.1 Robot dynamics

The top view and cross section of the robot are shown in figure 3.20. The workspace of the robot is illustrated in figure 3.21.

The dynamics of the robot is represented by the following equations:

$$(J + mr^2)\ddot{\phi} + 2mr\dot{r}\dot{\phi} = T_1 \tag{3.62}$$

$$\rho m\ddot{r} - \rho mr\dot{\phi}^2 = T_2 \tag{3.63}$$

Introducing $\tilde{T}_2 = T_2/\rho$ the following matrix description results:

$$\underbrace{\begin{bmatrix} J + mr^2 & 0 \\ 0 & m \end{bmatrix}}_{M(q)} \cdot \underbrace{\begin{bmatrix} \ddot{\phi} \\ \ddot{r} \end{bmatrix}}_{\ddot{q}} + \underbrace{\begin{bmatrix} mr\dot{r} & mr\dot{\phi} \\ -mr\dot{\phi} & 0 \end{bmatrix}}_{C(q,\dot{q})} \cdot \underbrace{\begin{bmatrix} \dot{\phi} \\ \dot{r} \end{bmatrix}}_{\dot{q}} = \underbrace{\begin{bmatrix} T_1 \\ \tilde{T}_2 \end{bmatrix}}_{T} \tag{3.64}$$

where:

m	mass of the cart
J	the joint moment of inertia
$\phi(t)$	position of the robot arm $\phi \in [0° \ldots 270°]$
$r(t)$	position of the cart r∈[0.27m...1m]
$T_{1,2}(t)$	the torque of the arm and the cart, respectively
$q(t)$	the state vector $[\phi\ r]'$

Therefore, equations (3.62) and (3.63) can be rewritten as:

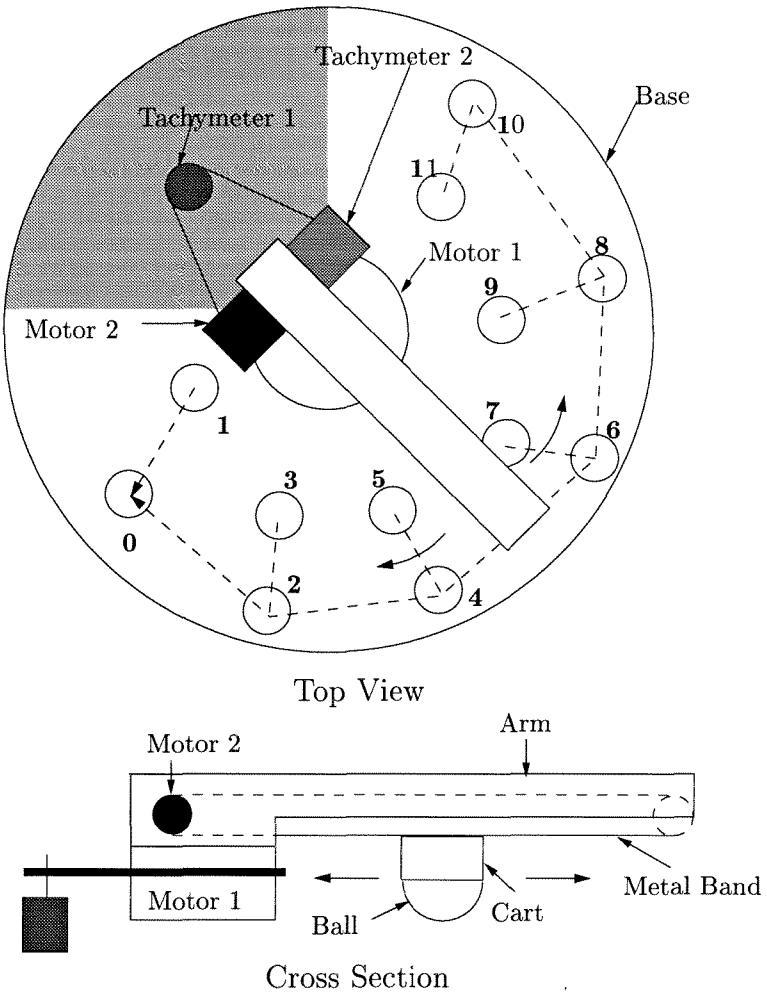

Figure 3.20: Top view and cross section of the robot.

$$M(q) \cdot \ddot{q} + C(q, \dot{q}) \cdot \dot{q} = T \tag{3.65}$$

The states of the system are: the position $q(t)$, the velocity $\dot{q}(t)$ and the acceleration $\ddot{q}(t)$ of the arm and the cart.

The parameters used in the simulations performed here are given by:

Parameters for the robot		
$m = 1.0$	$J = 6.43141$	$\rho = 1.0$

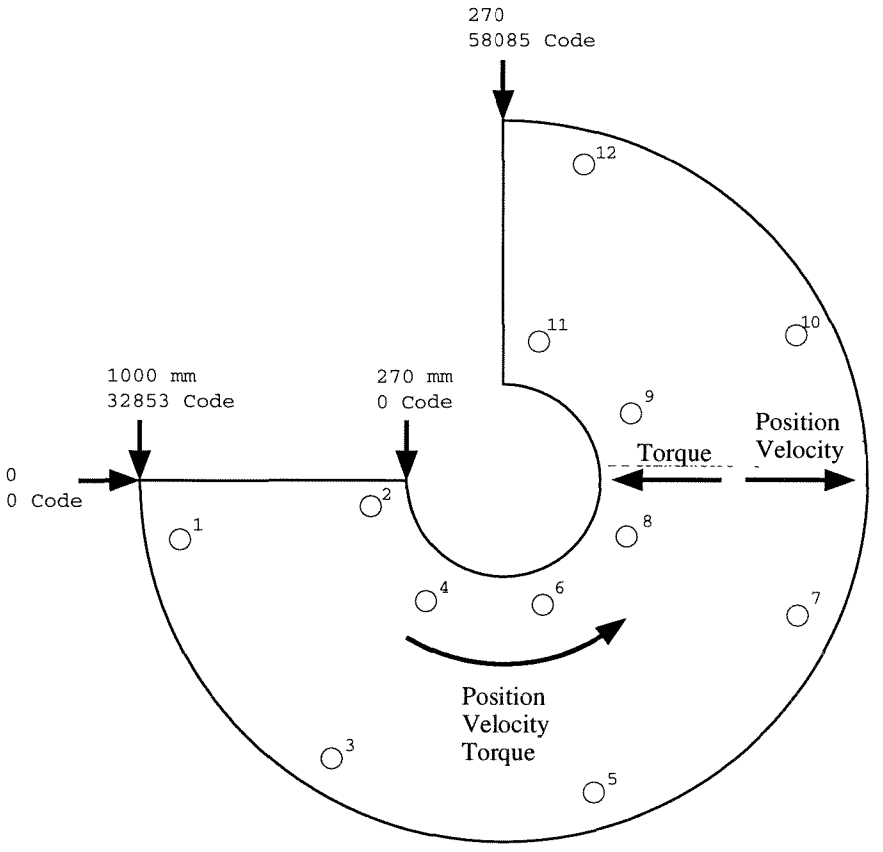

Figure 3.21: The robot workspace.

3.7.2 Simulation results

In this mechanical system, our goal is to take the robot arm to a specified position and angle beginning at the origin. In other words, we have a setpoint tracking problem at hand. This is a 2-input 2-output system where the outputs are the angle ϕ and the position r and the inputs are the torques $u := [T_1 \ T_2]$.

The desired setpoint in these simulations is given by:

Setpoint			
$\phi_0 = \frac{\pi}{2}$	$r_0 = 0.8$	$\dot{\phi}_0 = 0$	$\dot{r}_0 = 0$

The initial condition is the origin.

The unconstrained and constrained responses of our contractive MPC (CNTMPC) algorithm will be compared to those produced by a standard nonlinear finite horizon (SNLMPC) scheme, as we did for the previous examples.

Unconstrained case

Case 1

The comparison between the results obtained with SNLMPC and CNTMPC can be found in figure 3.22.

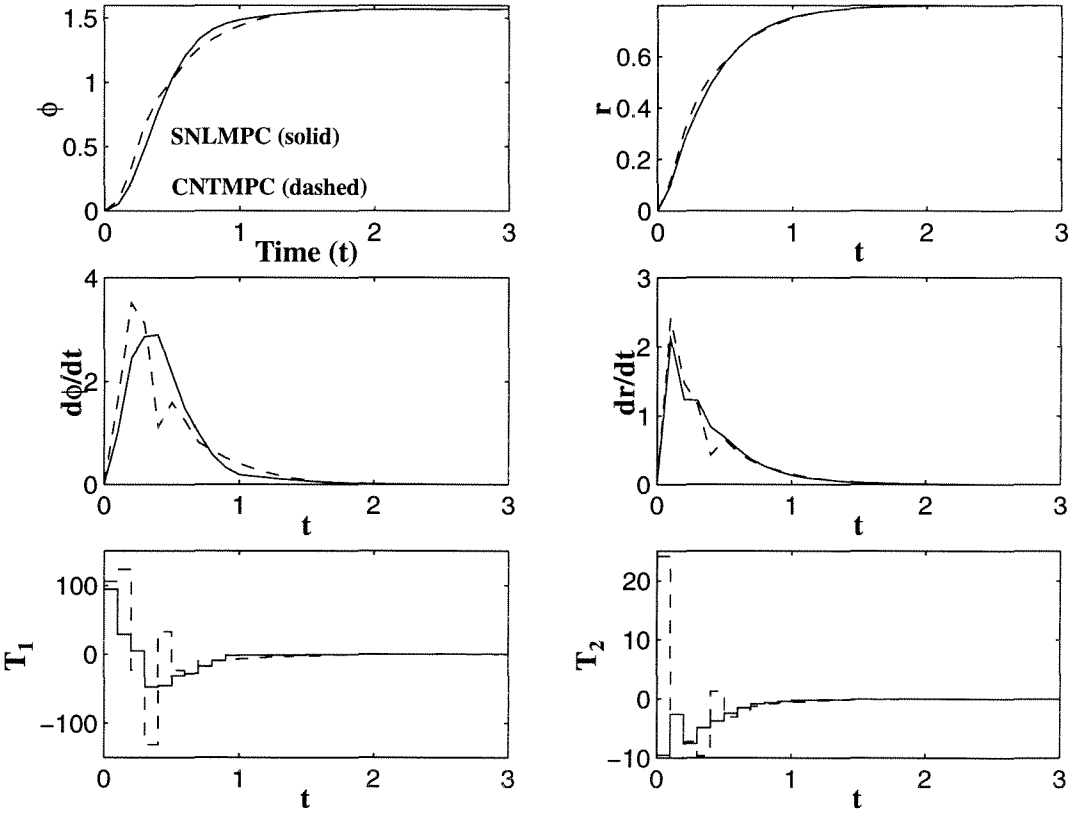

Figure 3.22: Robot: State and control responses for SNLMPC and CNTMPC in the unconstrained **Case 1**.

The controller parameters used in **Case 1** are given by:

Controller parameters (figure 3.22)		
$Q = \text{diag}([10\ \ 10\ \ 1\ \ 1])$	$R = 0$	$S = 0$
$P = 6$	$M = 4$	$\alpha = 0.8$

In all the simulations for this example, the sampling time is equal to $T = 0.1$.

We notice from figure 3.22 that the same response speed is obtained with both algorithms at the expense of a slightly higher control effort from CNTMPC (especially for $u_1 := T_1$).

Case 2

The speed of the response obtained with CNTMPC can be increased if we decrease the value of α. This effect is illustrated in figure 3.23, where the results obtained with $\alpha = 0.8$ are compared to the ones obtained with $\alpha = 0.3$, while keeping the remaining control parameters unchanged.

We see that the response speed for $\alpha = 0.3$ has improved at the expense of a higher control effort in comparison with the results obtained with $\alpha = 0.8$. Thus, α is not only a parameter for stability guarantee but it also strongly influences the performance.

Constrained case

The simulation results for SNLMPC and CNTMPC are illustrated in figure 3.24.

The controller parameters used in these simulations are as follows:

Controller parameters (figure 3.24)		
$Q = \text{diag}([10\ \ 10\ \ 1\ \ 1])$	$R = 0$	$S = 0$
$P = 7$	$M = 5$	$\alpha = 0.9$
$u_{min} = [-10\ \ -5]$	$u_{max} = [10\ \ 5]$	

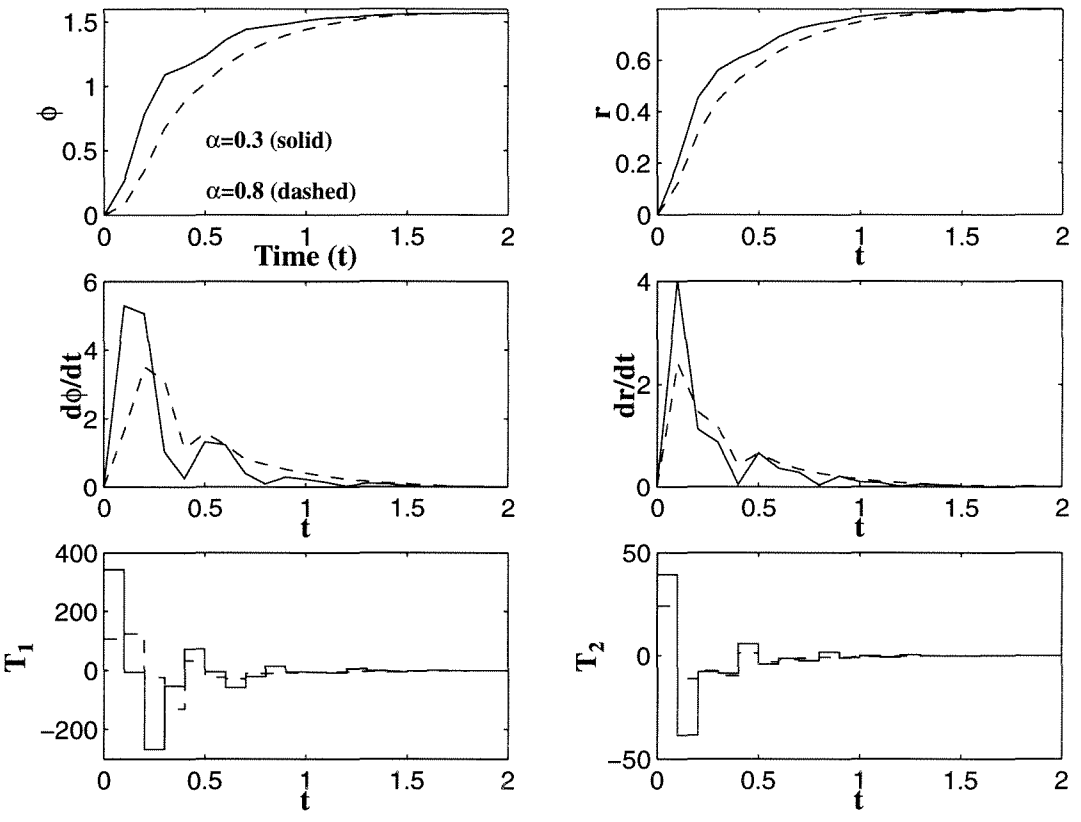

Figure 3.23: Robot: State and control responses for SNLMPC and CNTMPC in the unconstrained **Case 2**.

The results show that the two controllers behave very similarly, with CNTMPC being slightly more aggressive (within the constraint bounds) due to the presence of the contractive constraint.

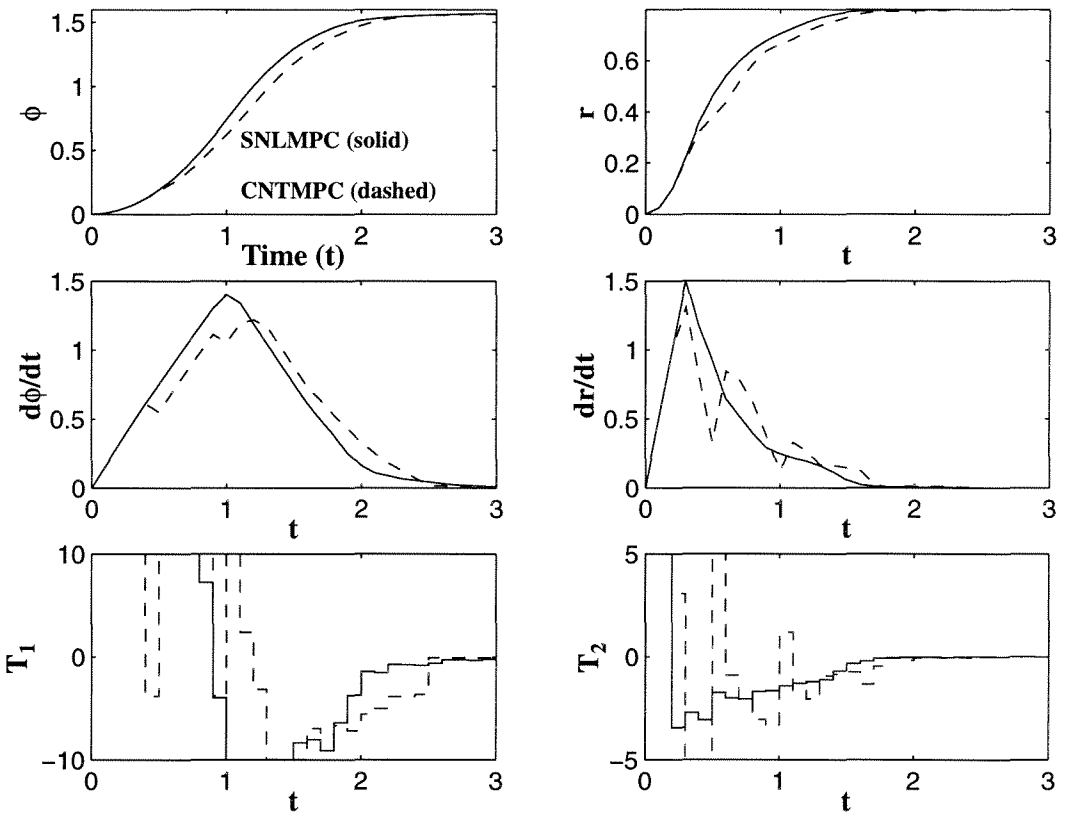

Figure 3.24: Robot: State and control responses for SNLMPC and CNTMPC in the constrained case.

3.8 Example: Continuous Stirred Tank Reactor (CSTR) + Flash Unit

3.8.1 Description of the system

We consider now the application of our contractive MPC scheme to the process represented in figure 3.25.

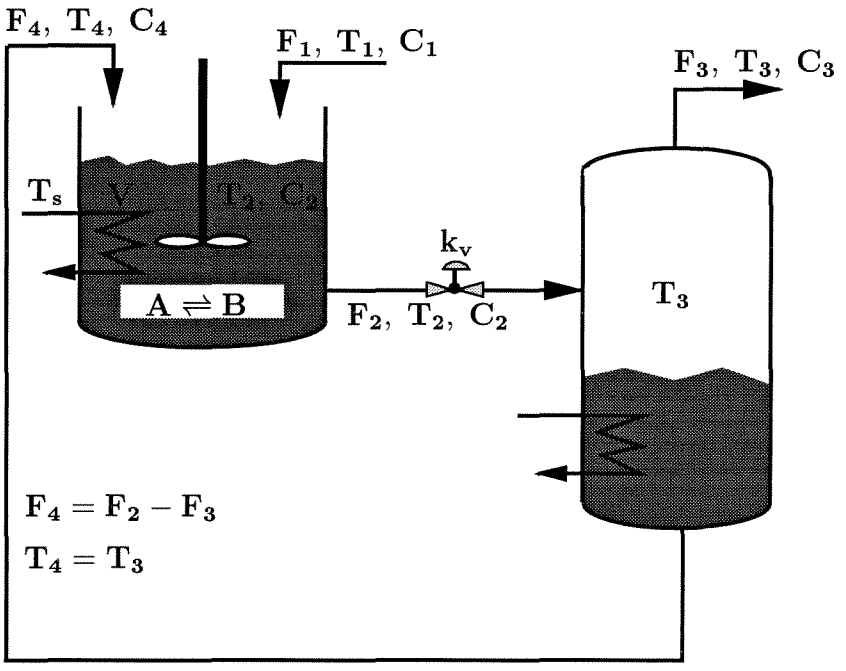

Figure 3.25: Schematic diagram of the CSTR and flash unit.

This process includes a continuous stirred tank reactor and a flash unit with a recycle stream. The reactor model is based on an example of Economou in [41] where a first-order endothermic reversible reaction is assumed to occur.

In figure 3.25 the variables C_i, $i = 1, 2, 3, 4$, are concentrations of B given in $\frac{\text{gmol B}}{l}$ and F_i, $i = 1, 2, 3, 4$, are the flow rates given in $\frac{\text{l}}{\text{s}}$. For simplicity, we will consider that all the streams have the same density $\rho = 1\ \frac{g}{l}$ and that the concentrations are equal to the molar fractions of A and B (this would be the case if the molecular

weights of A and B are the same and equal in value to the density of the streams). In this case, feed stream 1 contains $F_1 C_1 \frac{\text{gmol B}}{\text{s}}$ and $F_1(1 - C_1) \frac{\text{gmol A}}{\text{s}}$. In the reactor, A is decomposed into B in a reversible reaction. B is the product in which we are interested.

Accumulation in the reactor is possible in the transient phase. The flash is assumed to operate at steady state (i.e., $F_2 = F_3 + F_4$) and no reaction takes place in it. Stream 2 enters the flash where B, being a more volatile species, can be obtained with higher degree of purity in stream 3 than in the feed stream 2, depending on the operating conditions. Ideally, stream 4 contains mostly A and small amounts of B.

The flash drum is also assumed to operate at constant pressure and temperature. The liquid-vapor equilibrium constant for component B is assumed to depend only on the temperature in the separator, T_3. We assume that the fluid properties are preserved in the recycled stream and that no time delays are present in the material recirculation.

Our intention with the introduction of the flash and the recycle stream, is to increase the molar fraction of B in the final product (stream 3, in this case) compared to its molar fraction in the reactor C_2. We will see that depending on the operating conditions, the obtained product can be very significantly purified.

This is a SISO system where the output is C_3, the input is T_3 and the three states are V, C_2, T_2. The control objective is to operate the system at the point of maximum conversion of B in stream 3. The coordinates of V, C_2, T_2 and T_3 at the equilibrium point of maximum conversion can be computed by using the three equations of the model and the condition of optimality, namely $\frac{dC_3}{dT_3} = 0$. Thus, this optimal operating point is a point of zero steady state gain, which makes it difficult for linear controllers to stabilize the system around this point with satisfactory performance.

We will see that while the manipulated variable T_3 does not have much influence on the value of C_2, it can increase C_3 to much higher levels. In other words, the output

is highly sensitive to input values.

3.8.2 CSTR + flash dynamics

The dynamic model of the process, including dynamic balance equations for the reactor and algebraic equations for the connecting streams, is described by:

Reactor equations:

$$\frac{dV}{dt} = F_1 + F_4 - F_2 \tag{3.66}$$

$$\frac{d(VC_2)}{dt} = F_1C_1 + F_4C_4 - F_2C_2 + V\, r(T_2, C_2) \tag{3.67}$$

$$\frac{d(VT_2)}{dt} = F_1T_1 + F_4T_3 - F_2T_2 + V\, \frac{(-\Delta H)}{C_p}\, r(T_2, C_2) - \\ - \frac{U\, A}{C_p}\, (T_2 - T_s) \tag{3.68}$$

These equations can be re-written in a simplified form as:

$$\frac{dV}{dt} = F_1 + F_4 - F_2 \tag{3.69}$$

$$\frac{dC_2}{dt} = \frac{(F_1C_1 + F_4C_4 - F_2C_2)}{V} + r(T_2, C_2) - C_2\frac{(F_1 + F_4 - F_2)}{V} \tag{3.70}$$

$$\frac{dT_2}{dt} = \frac{(F_1T_1 + F_4T_3 - F_2T_2)}{V} + \frac{(-\Delta H)}{C_p}\, r(T_2, C_2) - \\ - \frac{U\, A}{C_p}\, \frac{1}{V}\, (T_2 - T_s) - T_2\frac{(F_1 + F_4 - F_2)}{V} \tag{3.71}$$

Flash equations:

$$C_3 = K_e(T_3)\, C_4 \tag{3.72}$$

$$F_2 = F_3 + F_4 \tag{3.73}$$

$$F_2C_2 = F_3C_3 + F_4C_4 \tag{3.74}$$

Mixed equations:

$$r(T_2, C_2) = K_{r1}(T_2)\,(1 - C_2) - K_{r2}(T_2)\,C_2 \tag{3.75}$$

$$K_{r1}(T_2) = A_1\, e^{-E_{a1}/T_2} \tag{3.76}$$

$$K_{r2}(T_2) = A_2\, e^{-E_{a2}/T_2} \tag{3.77}$$

$$K_e(T_3) = a\, 10^{-b/T_3} \tag{3.78}$$

$$F_2 = k_v\, V \tag{3.79}$$

$$F_4 = \beta\, F_1, \quad \text{with } \beta \geq 0 \tag{3.80}$$

The numerical values of the parameters used in the simulations are (for a compatible set of units which are omitted here):

Parameters for the CSTR + flash unit	
$C_1 = 0$	$T_1 = 4.5$
$F_1 = 1.79 \times 10^{-2}$	$a = 2.11 \times 10^4$
$A_1 = 5.0 \times 10^3$	$b = 18.5$
$A_2 = 1.0 \times 10^6$	$(\frac{-\Delta H}{C_p}) = 5.0 \times 10^{-2}$
$E_{a1} = 45$	$(\frac{UA}{C_p}) = 1.35 \times 10^{-3}$
$E_{a2} = 75$	$\beta = 1.32$
$T_s = 6.0$	$k_v = 0.5$

3.8.3 Computation of steady states

The first step in the study of this system is the computation of steady states. Given a steady state input value $u^{ss} = T_3^{ss}$ we can then compute the steady state coordinates through the following equations:

$$V^{ss} = \frac{F_1}{k_v}\,(1 + \beta) \tag{3.81}$$

$$C_2^{ss} = \frac{K_{r1}(T_2^{ss}) + \frac{C_1 k_v}{1+\beta}}{K_{r1}(T_2^{ss}) + K_{r2}(T_2^{ss}) + k_v(\frac{K_e(T_3^{ss})}{K_e(T_3^{ss})+\beta})} \tag{3.82}$$

$$0 = (\frac{-\Delta H}{C_p})\,(\frac{1+\beta}{k_v})\,r(T_2^{ss}, C_2^{ss}) - [1+\beta+(\frac{UA}{C_p})\,\frac{1}{F_1}]\,T_2^{ss} + \\ + (\frac{UA}{C_p})\,\frac{T_s}{F_1} + T_1 + \beta\,T_3^{ss} \tag{3.83}$$

Thus, the volume V^{ss} and reactor temperature T_2^{ss} are computed directly through equations (3.81) and (3.83), respectively. The concentration $C_{2^{ss}}$ can be computed through equation (3.82) once T_2^{ss} is known.

For the chosen plant parameters and for T_3^{ss} in the operating region of interest, we have verified that the computed steady state is unique and stable. Besides, for given steady state coordinates V^{ss}, C_2^{ss}, T_2^{ss}, there is only one corresponding input value T_3^{ss}.

In spite of the absence of steady state multiplicity, one of the interesting features of this example is the high sensitivity of the output (C_3) with respect to the input (T_3).

The output C_3 is computed by:

$$C_3 = \frac{C_2}{1 + \frac{\beta F_1}{k_v V}\,\frac{K_e(T_3)-1}{K_e(T_3)}} \tag{3.84}$$

At steady state, equation (3.84) reduces to:

$$C_3^{ss} = C_2^{ss}\,\frac{K_e(T_3^{ss})\,(1+\beta)}{K_e(T_3^{ss})+\beta} \tag{3.85}$$

From equation (3.85) we see that, for $K_e = 1$ (which implies that $T_3 = \frac{b}{\log_{10} a} =: T_3^* = 4.2782$), we have $C_3^{ss} = C_2^{ss}$, which means that there is no advantage in having the separation unit after the reactor. If $K_e < 1$ (or $T_3 < T_3^*$) we have $C_3^{ss} < C_2^{ss}$. Therefore, we are only interested in operating the plant at $T_3 > T_3^*$.

From equation (3.85) we also notice that, $C_3^{ss} = C_2^{ss}$ if $\beta = 0$. Large values of β will increase the value of C_3^{ss} for high values of T_3. However, if T_3 is low, $\lim_{\beta \to \infty} C_3^{ss} = 0$.

The coordinates V, C_2, $T2$, T_3 of the point of maximum conversion are computed by using equations (3.81, 3.82, 3.83) and the following equation:

$$\frac{dC_3}{dT_3} = \left(\frac{1+\beta}{K_e+\beta}\right)\left[K_e \frac{dC_2}{dT_2}\frac{dT_2}{dT_3} + \beta \frac{C_2}{K_e+\beta}\frac{dK_e}{dT_3}\right] = 0 \tag{3.86}$$

where:

$$\frac{dK_e}{dT_3} = K_e \frac{\log_{10} a}{T_3^2}$$

$$\frac{dC_2}{dT_2} = \frac{K_{r1}}{T_2^2(K_{r1}+K_{r2}+k_v\frac{K_e}{K_e+\beta})^2}\left[K_{r2}(E_{a1}-E_{a2}) + \frac{E_{a1}k_vK_e}{K_e+\beta} - \frac{k_vC_1}{1+\beta}\left(E_{a1}+E_{a2}\frac{K_{r2}}{K_{r1}}\right)\right]$$

$$\frac{dT_2}{dT_3} = \frac{\left(\frac{\beta}{1+\beta}\right) + \left(\frac{-\Delta H}{C_p}\right)\frac{K_{r1}\beta(K_{r1}+K_{r2})}{[(K_e+\beta)(K_{r1}+K_{r2})+k_vK_e]^2}\frac{dK_e}{dT_3}}{1+\left(\frac{UA}{C_p}\right)\frac{1}{F_1(1+\beta)} + \left(\frac{-\Delta H}{C_p}\right)\frac{K_{r1}K_e}{T_2^2[(K_e+\beta)(K_{r1}+K_{r2})+k_vK_e]^2}[K_{r2}(K_e+\beta)(E_{a2}-E_{a1}) - k_vK_eE_{a1}]}$$

For the chosen plant parameters, the steady state of maximum conversion has the following coordinates:

Steady state values for the CSTR + flash unit	
$T_3^{ss} = 6.109444$	$V^{ss} = 8.3056 \times 10^{-2}$
$C_2^{ss} = 0.459498$	$T_2^{ss} = 5.454972$
$C_3^{ss} = 0.999338$	

Thus, operation at the steady state of maximum conversion gives us a product containing 99.93% of B.

Our control objective is to drive the system to the operating point of maximum conversion and keep it there starting from arbitrary initial conditions or from steady states of low conversion of B.

3.8.4 Simulation results

In the following simulations we will demonstrate the stabilizing properties of contractive MPC (CNTMPC) for this chemical process example.

Case 1

In **Case 1**, we will perform a steady state change from a steady state of low flash temperature $T_3^{ss} = T_3^*$, which means that $C_3^{ss} = C_2^{ss}$, to the optimal operating point. The results will reveal a high sensitivity of C_3 to T_3 while C_2 varies very little in this operating range.

We will examine the situation where the system is operating initially at the following steady state:

Initial condition	
$T_{3,0} = 4.278166$	$V_0 = 8.3056 \times 10^{-2}$
$C_{2,0} = 0.428721$	$T_{2,0} = 4.43389$
$C_{3,0} = 0.428721$	

Thus, the system operates initially in a very undesirable regime with $C_{3,0} = C_{2,0} < 45\%$. In this operating region, one can see no advantage in using the separation unit after the reactor.

Notice that since the parameters and operational variables are the same for the chosen initial condition (which is a steady state) and the target steady state, the initial and final volumes are also the same (see equation 3.81, where it is shown that the steady state value of the volume does not depend on the input or the other states).

The input and state variables which will be plotted for the CSTR+flash example are the deviation variables with respect to the desired target steady state values. However, for better illustration of the behavior of the output C_3 in comparison

with the concentration in the reactor C_2, the real values of these variables will be plotted in the same graph.

The simulation results in the unconstrained case can be found in figure 3.26.

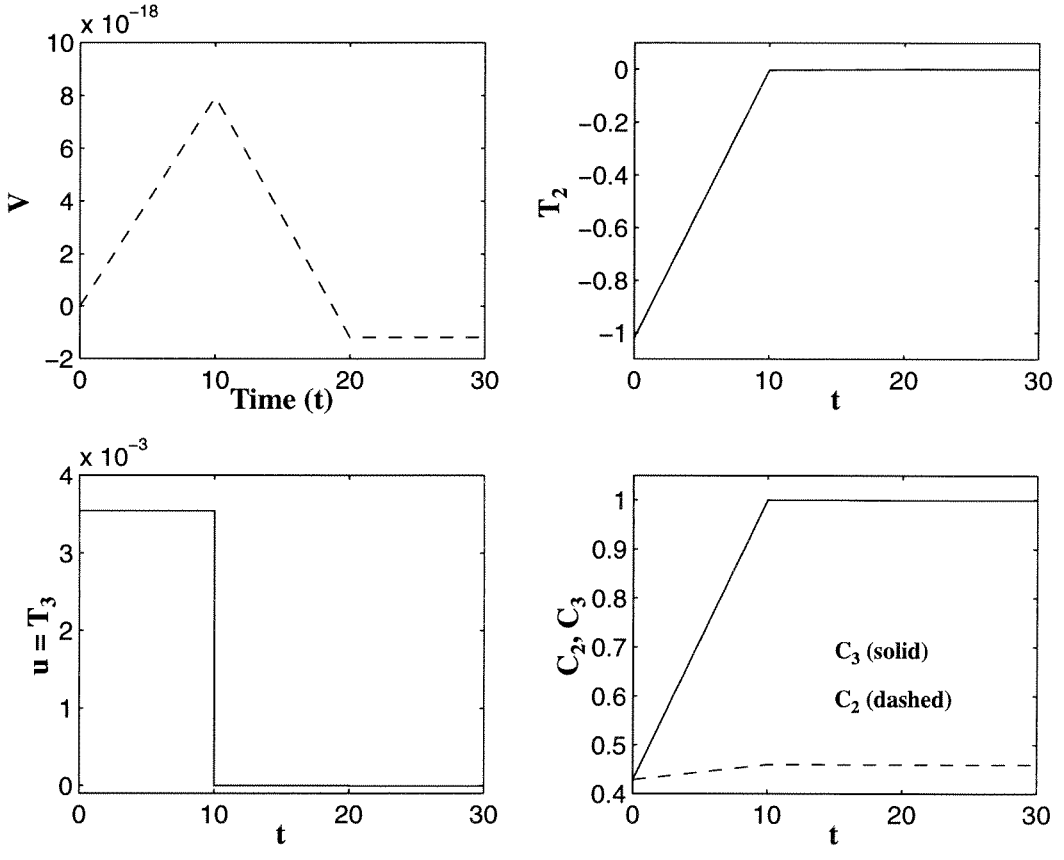

Figure 3.26: CSTR + Flash: State and control responses **Case 1**.

The controller parameters used in **Case 1** are given by:

Controller parameters (figure 3.26)		
$Q = \text{diag}([1 \;\; 100 \;\; 1])$	$R = 0$	$S = 0$
$P = 1$	$M = 1$	$\alpha = 0.1$

In the simulations for this example the sampling time is equal to $T = 10$.

As we can see from figure 3.26, the controller performs a very smooth transition to the steady state of maximum conversion and the response occurs in two sampling times with very little control effort involved.

Notice that since the point of maximum conversion is open-loop stable, we were able to impose a very tight contraction requirement ($\alpha = 0.1$) in only one time step.

Case 2

Since the control effort involved in **Case 1** was very small and we could not examine the influence of input constraints, let us now consider the following initial condition:

Initial condition	
$T_{3,0}$ = arbitrary	$V_0 = 1$
$C_{2,0} = 0$	$T_{2,0} = 0$
$C_{3,0} = 0$	

A comparison of the results obtained in the unconstrained and constrained cases can be found in figure 3.27.

The controller parameters used in **Case 2** are given by:

Controller parameters (figure 3.27)		
Q = diag([1 100 1])	$R = 0$	$S = 0$
$P = 1$	$M = 1$	$\alpha = 0.4$
$u_{min} = 0$	$u_{max} = 0.05$	

From figure 3.27 we can see that tight input constraints do not delay the response, the system still responds in two samples. This fact is due mostly to the fact that the optimum is an OL stable equilibrium. The plot of C_2, $C_3 \times t$ shows that the sensitivity of C_3 to variations in T_3 in this transition is more than twice that of C_2.

In conclusion, our contractive MPC scheme is able to perform the transition from arbitrary initial conditions to the point of maximum conversion, where almost pure

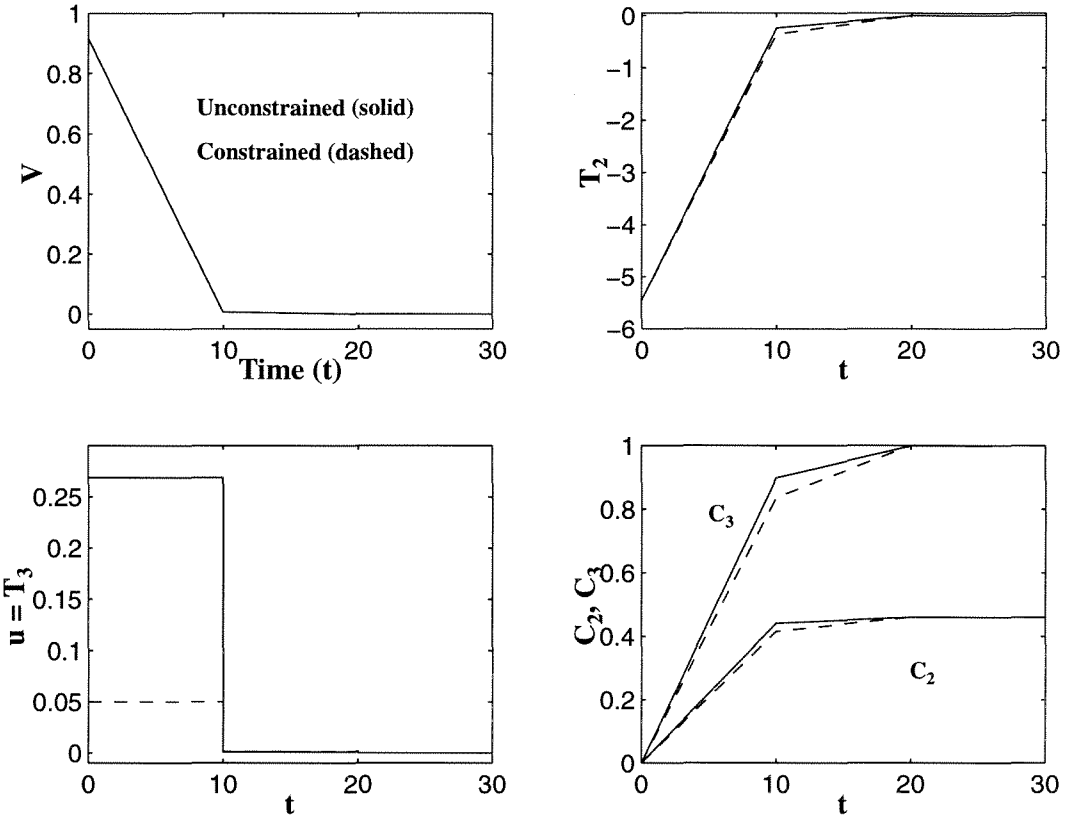

Figure 3.27: CSTR + Flash: State and control responses in **Case 2**.

B is produced in the distillate of the flash drum, in spite of the high sensitivity of the model to the input values of T_3.

Chapter 4 Output Feedback Contractive NLMPC: Nominal Case

In this chapter we will be dealing initially with the following control problem:

Problem 2 : *State feedback, nominal case and asymptotically decaying disturbance*

Later we will show that this problem is equivalent to dealing with the output feedback case when the state estimator is asymptotically convergent.

4.1 Introduction

In the previous chapter we have shown that, in the case of no model/plant mismatch, state feedback and no disturbances, the contractive constraint makes the closed-loop exponentially stable for all initial conditions $x_0 \in B_\rho$. It has been proven that if the sequence of optimal control problems $\mathcal{P}(t_k, x_k^p),\ k \geq 0$, is feasible (or, equivalently, if $x_k \in B_\rho$ for all $k \geq 0$) then the contractive MPC scheme is an exponentially stabilizing controller inside the reachable set $\mathcal{X}$. Moreover, we have shown that the commonly used quadratic objective function with finite prediction horizon is a Lyapunov function for the closed-loop system in the presence of the contractive constraint under extra, more conservative assumptions.

Now we will examine the stability properties of the closed-loop system subject to

Control Algorithm 2 but now under the conditions in **Problem 2**. Thus, our plant is now given by the following dynamic equation:

$$\dot{x}^p(t) = f(x^p(t), u(t)) + d(t) \tag{4.1}$$

where the additive disturbance $d(t)$ belongs to a compact, convex set $\mathcal{D}$ with $0 \in \mathcal{D}^\circ :=$ interior$(\mathcal{D})$ and is asymptotically decaying, i.e.:

$$d(t) \to 0 \text{ as } t \to \infty \tag{4.2}$$

And the model (used in the prediction step of the MPC scheme) is given by:

$$\dot{x}(t) = f(x(t), u(t)) \tag{4.3}$$

It is important to notice that even an exponentially decaying disturbance ($d(t) \leq ae^{-bt}$, where $a, b > 0$) can destabilize a nonlinear system, possibly resulting in finite escape time (as observed in [86]).

Thus, our main motivation for demonstrating perturbed stability for MPC is to show that a stable state estimator may be cascaded with a stabilizing controller with no risk of instability (given that certain conditions on the initial state estimate and on the nonlinear dynamics of the plant are satisfied). This has been done in the context of predictive control with linear models (see [93]). The result relies on exponential stability of the state estimator (usually a Kalman filter), asymptotic nominal stability of the system with state feedback and Lipschitz continuity of the control law.

In the nonlinear context, however, stable state estimators are difficult to formulate, let alone exponentially stable ones. Here we will show that this problem can be circumvented and our result is that any asymptotically stable nonlinear state estimator

may be cascaded with the proposed exponentially stabilizing nonlinear MPC controller to produce an asymptotically stable closed-loop response. This property has been previously demonstrated in [114] for discrete-time nonlinear systems of the kind $x_{k+1} = f(x_k, u_k) + d_k,\ k \in [0, \infty)$. In that work, the authors conclude that the closed-loop system generated by applying MPC with end equality constraint, $x_{k+P} = 0$, to a system subjected to an asymptotically decaying disturbance, i.e., $d_k \to 0$ as $k \to \infty$, is asymptotically stable. The authors suggest that this asymptotically decaying disturbance could originate from a state estimation procedure but they do not proceed to formulate a stable observer for the nonlinear system.

The formulation of stable nonlinear state estimators is an active area of research. An estimator based on minimization of a moving horizon cost function is presented in [100, 111]. Another variation of this technique is presented for continuous-time systems in [97].

The estimator proposed here is a recursive nonlinear dynamic observer based on a continuous-time system with discrete observations and we will provide sufficient conditions under which this estimator produces locally asymptotically convergent estimates.

But first let us show that **Control Algorithm 2** applied to a system of the form (4.1) subject to a disturbance of the kind (4.2) results in an asymptotically stable closed-loop system.

4.2 Stability of MPC under asymptotically decaying disturbances

4.2.1 Basic stability definitions

Consider a nonlinear system of the kind: $\dot{x}(t) = f(x(t))$ with initial condition x_0 at t_0 and $f : \Re^n \to \Re^n$ continuously differentiable.

Definition 4.1 *The equilibrium $x = 0$ is uniformly attractive if there exists a number $r > 0$ such that*

$$\| x_0 \|_p < r,\ t_0 \geq 0 \implies x(t, t_0, x_0) \to 0 \ \text{ as } \ t \to \infty, \quad \text{uniformly in } x_0, t_0 \tag{4.4}$$

or, equivalently, if for each $\epsilon > 0$ there exists a $T = T(\epsilon)$ such that

$$\| x_0 \|_p < r,\ \ t_0 \geq 0 \implies \| x(t, t_0, x_0) \|_p < \epsilon,\ \ \forall\, t \geq T(\epsilon) + t_0 \tag{4.5}$$

Definition 4.2 *The equilibrium $x = 0$ is uniformly stable if, for each $\epsilon > 0$, there exists a $\delta = \delta(\epsilon)$ such that*

$$\| x_0 \|_p < \delta(\epsilon),\ \ t_0 \geq 0 \implies \| x(t, t_0, x_0) \|_p < \epsilon,\ \ \forall t \geq t_0 \tag{4.6}$$

Definition 4.3 *The equilibrium $x = 0$ is asymptotically stable if it is stable and attractive. It is uniformly asymptotically stable if it is uniformly stable and uniformly attractive.*

These definitions hold for any $p-$norm (or Hölder norm), with $p \geq 1$.

4.2.2 Basic assumptions

Besides assumptions 3.1, 3.2, 3.3 and 3.4 in chapter 3, the following additional assumptions will be made in the derivation of the results in this chapter:

Assumption 4.1 *The disturbance satisfies the following boundedness condition:*

$$d_k(t) \in B_{\rho_k^d} := \{d \in \Re^n : \| d \|_{\hat{P}} \leq \rho_k^d\} \text{ for } \rho_k^d \in [0, \infty), \quad t \in [t_k, t_k + PT], \ \forall k \geq 0, \tag{4.7}$$

and the asymptotic properties of $d(t)$ are described as:

$$\begin{aligned} &\text{For any } \epsilon > 0, \exists \text{ a finite } \bar{k} := \bar{k}(\epsilon) \in N \text{ so that } \rho_k^d \leq \epsilon, \ \forall k \in [\bar{k}, \infty), \\ &\text{and } \bar{k}(\epsilon) \to \infty \text{ if } \epsilon \to 0 \end{aligned}$$

where N is the set of non-negative integers.

Assumption 4.2 *The function $f : \Re^n \times \Re^m \to \Re^n$ is Lipschitz continuous, i.e., there exists $L > 0$ such that*

$$\| f(x^p, u) - f(\bar{x}, u) \|_{\hat{P}} \leq L \ \| x^p - \bar{x} \|_{\hat{P}}, \quad x^p, \ \bar{x} \in \Re^n \text{ and } u \in \mathcal{U} \tag{4.8}$$

Remark 4.1 *Let the reachable set for the closed-loop system resulting from implementation of* **Control Algorithm 2** *to the plant (4.1), using the model (4.3) for prediction, be defined by:*

$$\begin{aligned} \mathcal{X} \ := \ &\{x^p(t), x(t) \text{ and } \bar{x}(t) \in \Re^n \mid x^p(t) = x^p(t, t_0, x_0^p, u, d), \ x(t) = x(t, t_0, x_0^p, u, 0) \\ &\text{and } \bar{x}(t) = \bar{x}(t, t_0, x_0^p, u, 0), \ t \in [t_0, \infty); x_0^p \in B_\rho, \ u \in \mathcal{U}, \ d \in \mathcal{D}\} \end{aligned} \tag{4.9}$$

Then, equation (4.8) only needs to be satisfied for x^p, $\bar{x} \in \mathcal{X}$. The reason why we do not state assumption 4.2 in this less conservative way is because the set $\mathcal{X}$ is not known a priori. Thus, in this form, condition (4.8) cannot be checked.

4.2.3 Stability analysis

Before the main result of this section is proven, we will prove the following lemma which will be very useful in our stability analysis of different variations of the contractive MPC controller throughout this thesis.

Lemma 4.1 *Consider the discrete linear system:*

$$z_{k+1} \leq a_k z_k + b_k, \quad k \in N \tag{4.10}$$

If $a_k \in [0,1)$ *and* $b_k \geq 0$, $\forall k \in N$, *then system (4.10) is stable in the practical sense, i.e.,*

1. $z_k < z_0 + \frac{b_{max}}{1-a_{max}}, \quad \forall k \in N$
2. $\lim_{k\to\infty} z_k \leq \frac{b_{max}}{1-a_{max}}$

where $a_{max} := \max_{k\in N} a_k$ *and* $b_{max} := \max_{k\in N} b_k$.

Proof: *From equation (4.10) it follows that:*

$$z_k \leq (\prod_{i=0}^{k-1} a_i) z_0 + \sum_{i=0}^{k-1} (\prod_{j=i+1}^{k-1} a_j) b_i \tag{4.11}$$

Therefore, we have:

$$z_k \leq a_{max}^k z_0 + b_{max} \sum_{i=1}^{k} a_{max}^{(i-1)} \tag{4.12}$$

Since $a_{max} \in [0,1)$, *we get:*

$$\lim_{k\to\infty} \sum_{i=1}^{k} a_{max}^{(i-1)} = \frac{1}{1-a_{max}} \tag{4.13}$$

Thus, from (4.12), it follows that:

$$z_k < a_{max}^k z_0 + \frac{b_{max}}{1 - a_{max}}, \qquad \forall k \in N \tag{4.14}$$

Since $a_{max} \in [0, 1)$, *we finally obtain:*

$$z_k < z_0 + \frac{b_{max}}{1 - a_{max}}, \qquad \forall k \in N \tag{4.15}$$

and

$$\lim_{k \to \infty} z_k \leq \frac{b_{max}}{1 - a_{max}} \tag{4.16}$$

□

Theorem 4.1 (Stabilizing properties of Control Algorithm 1 in the presence of asymptotically decaying disturbances) *Let* Assumptions 3.1, 3.2, 3.3, 3.4, 4.1 *and* 4.2 *be satisfied and let* x_k^p, $\bar{x} \in B_\rho$, $\forall k \geq 0$. *Then, the closed-loop system resulting from application of* Control Algorithm 1 *to system (4.1) is uniformly asymptotically stable (UAS).*

Proof:

The difference between the dynamics of the model and of the plant for $t \in [t_k^j, t_{k+1}^j]$, *is given by:*

$$\dot{x}_k^{p,j}(t) - \dot{x}_k^j(t) = f(x_k^{p,j}(t), u_k^j(t)) - f(x_k^j(t), u_k^j(t)) + d_k^j(t) \tag{4.17}$$

Then, since the states of the model are updated as the states of the plant at every t_k^j, $j = 0, \ldots, P-1$, $\forall k \geq 0$, *we can integrate (4.17) and obtain:*

$$x_k^{p,j}(t) - x_k^j(t) = \int_{t_k^j}^{t} [f(x_k^{p,j}(\tau), u_k^j(\tau)) - f(x_k^j(\tau), u_k^j(\tau))] d\tau + \int_{t_k^j}^{t} d_k^j(\tau) d\tau \qquad (4.18)$$

Therefore, using (4.7) and (4.8), we have:

$$\begin{aligned} \| x_k^{p,j}(t) - x_k^j(t) \|_{\hat{P}} &\leq \int_{t_k^j}^{t} \| f(x_k^{p,j}(\tau), u_k^j(\tau)) - f(x_k^j(\tau), u_k^j(\tau)) \|_{\hat{P}} \, d\tau + \\ &+ \int_{t_k^j}^{t} \| d_k^j(\tau) \|_{\hat{P}} \, d\tau \leq \\ &\leq L \int_{t_k^j}^{t} \| x_k^{p,j}(\tau) - x_k^j(\tau) \|_{\hat{P}} \, d\tau + \int_{t_k^j}^{t} \| d_k^j(\tau) \|_{\hat{P}} \, d\tau \leq \\ &\leq L \int_{t_k^j}^{t} \| x_k^{p,j}(\tau) - x_k^j(\tau) \|_{\hat{P}} \, d\tau + \rho_k^d (t - t_k^j) \qquad (4.19) \end{aligned}$$

Using the Bellman-Grownwall (BG) inequality and evaluating the right-hand-side of (4.19) at $t = t_k^{j+1}$ *, it results that:*

$$\| x_k^{p,j}(t) - x_k^j(t) \|_{\hat{P}} \leq \rho_k^d T e^{LT} \qquad (4.20)$$

Thus, for $j = P - 1$, *we have:*

$$\| x_{k+1}^p - x_{k+1} \|_{\hat{P}} \leq \rho_k^d T e^{LT} \qquad (4.21)$$

Since the trajectory $\bar{x}(t)$ *used to compute the contractive constraint is only updated with the states of the plant at every* t_k, *the following bound holds:*

$$\| x_k^p(t) - \bar{x}_k(t) \|_{\hat{P}} \leq \rho_k^d P T e^{LPT}, \quad \forall t \in [t_k, t_{k+1}] \qquad (4.22)$$

Due to the contractive constraint we know that $\| \bar{x}_{k+1} \|_{\hat{P}} \leq \alpha \| x_k^p \|_{\hat{P}}$, $\forall k \geq 0$. *Thus, using the triangle inequality we have:*

$$\| x_{k+1}^p \|_{\hat{P}} \leq \alpha \| x_k^p \|_{\hat{P}} + \rho_k^d PTe^{LPT} \tag{4.23}$$

Using assumption 4.1 and from equation (4.23), it follows that:

$$\| x_{k+1}^p \|_{\hat{P}} \leq \alpha \| x_k^p \|_{\hat{P}} + \epsilon PTe^{LPT}, \quad \forall k \in [\bar{k}, \infty) \tag{4.24}$$

Then, since $\alpha \in [0, 1)$ *we can use the results of lemma 4.1 and obtain:*

$$\| x_{\bar{k}(\epsilon)+l}^p \|_{\hat{P}} \leq \alpha^l \| x_{\bar{k}(\epsilon)}^p \|_{\hat{P}} + (\sum_{i=0}^{l-1} \alpha^i) \epsilon PTe^{LPT} < \alpha^l \| x_{\bar{k}(\epsilon)}^p \|_{\hat{P}} + \frac{\epsilon PTe^{LPT}}{1-\alpha}, \quad \forall l > 0 \tag{4.25}$$

Thus, by taking the limit as $\epsilon \to 0$, *we have:*

$$\lim_{\epsilon \to 0} \| x_{\bar{k}(\epsilon)+l}^p \|_{\hat{P}} < \alpha^l \lim_{\epsilon \to 0} \| x_{\bar{k}(\epsilon)}^p \|_{\hat{P}} \tag{4.26}$$

and if now we take the limit as $l \to \infty$ *knowing that* $\bar{k}(\epsilon) \to \infty$ *for* $\epsilon \to 0$ *and that* $\alpha^l \to 0$ *exponentially fast as* $l \to \infty$, *we finally obtain:*

$$\lim_{l \to \infty} [\lim_{\epsilon \to 0} \| x_{\bar{k}(\epsilon)+l}^p \|_{\hat{P}}] < (\lim_{l \to \infty} \alpha^l) [\lim_{\epsilon \to 0} \| x_{\bar{k}(\epsilon)}^p \|_{\hat{P}}] = 0 \tag{4.27}$$

or

$$\lim_{k \to \infty} \| x_k^p \|_{\hat{P}} = 0 \tag{4.28}$$

which means asymptotic convergence to the origin.

So, we have shown that as long as x_k^p, $x_k \in B_\rho$, *it follows that* $x_k^p \to 0$ *as* $k \to \infty$, *which means that the origin is an attractive equilibrium point.*

Let us now proceed to show that $(x, u) = (0, 0)$ *is actually uniformly attractive. Using (4.22), (4.24) and the triangle inequality, we get:*

$$\| x_k^p(t) \|_{\hat{P}} \leq \| \bar{x}_k(t) \|_{\hat{P}} + \epsilon PTe^{LPT}, \quad \forall t \geq t_{\bar{k}} := t_{\bar{k}(\epsilon)} \tag{4.29}$$

But we know from our transient state constraints that $\| \bar{x}_k(t) \|_{\hat{P}} \leq \beta \| x_k^p \|_{\hat{P}}$ *with* $x_k^p \in B_\rho$. *Thus, for each* $x_0^p \in B_\rho$, $t_0 > 0$, *we have:*

$$\| x^p(t, t_0, x_0^p, u) \|_{\hat{P}} \leq \beta\rho + \epsilon PTe^{LPT} =: \epsilon^*, \quad \forall t \geq t_{\bar{k}(\epsilon)} =: T(\epsilon^*) + t_0 \tag{4.30}$$

This means from definition 4.1 that the equilibrium $(x, u) = (0, 0)$ *is* <u>*uniformly attractive*</u>.

Let us now proceed to show that $(x, u) = (0, 0)$ *is also uniformly stable. Using (4.22) and the triangle inequality, we get:*

$$\| x_k^p(t) \|_{\hat{P}} \leq \| \bar{x}_k(t) \|_{\hat{P}} + \rho_k^d PTe^{LPT} \tag{4.31}$$

But we know that $\| \bar{x}_k(t) \|_{\hat{P}} \leq \beta \| x_k^p \|_{\hat{P}}$ *with* $x_k^p \in B_\rho$. *Thus, from (4.31) we have:*

$$\| x_k^p(t) \|_{\hat{P}} \leq \beta\rho + \rho^d PTe^{LPT} =: \bar{\epsilon} \tag{4.32}$$

where $\rho^d := \max_{k \in N} \{\rho_k^d\}$.

Therefore, from (4.32), it follows that $\rho = \frac{\bar{\epsilon} - \rho^d PTe^{LPT}}{\beta} =: \delta(\bar{\epsilon})$.

With these definitions, we finally have the following result. For

$$\| x_k^p \|_{\hat{P}} < \rho =: \delta(\bar{\epsilon}),\ t_k \geq 0 \implies \| x^p(t, t_k, x_k) \|_{\hat{P}} < \bar{\epsilon},\ \forall t \in [t_k, t_{k+1}],\ \forall k \geq 0 \quad (4.33)$$

From our definition of uniform stability 4.2 if follows that $(x, u) = (0, 0)$ *is an uniformly stable equilibrium point of the closed-loop system.*

Since we have shown that $(x, u) = (0, 0)$ *is both uniformly attractive and uniformly stable we finally conclude, from definition 4.3, that* $(0, 0)$ *is an uniformly asymptotically stable equilibrium point.*

□

We have shown so far that if **Control Algorithm 1** is well-defined, i.e., if x_k^p, $\bar{x}_k \in B_\rho$, $\forall k \geq 0$, the origin is a uniformly asymptotically stable equilibrium point of the closed-loop system which results from implementation of this control strategy on the plant (4.1).

We shall now proceed to derive a sufficient condition on the disturbance $d(t)$ under which the well-posedness condition is satisfied, i.e., a condition which guarantees that $x_k^p, \bar{x}_k$ stay inside B_ρ, the set of initial conditions for which $\mathcal{P}(t_k, x_k^p)$ is feasible for all $k \geq 0$.

Theorem 4.2 (Feasibility condition) *Using the Lipschitz assumption on the function* f, *4.2, and on the disturbance, 4.1, if* $\rho_d < \frac{\rho(1-\alpha)}{PTe^{LPT}}$, *then there exists* $\rho_0 \in (0, \rho]$ *such that for all* $x_0^p \in B_{\rho_0}$, *the sequences* $\{x_k^p\}_{k=0}^{\bar{k}}$ *and* $\{\bar{x}_k\}_{k=0}^{\bar{k}}$ *resulting from use of* **Control Algorithms 1** *or* **2** *are well-defined and stay inside the set* B_ρ.

Proof: *In the proof of theorem 4.1 we have derived that:*

$$\| x_{k+1}^p \|_{\hat{P}} \leq \alpha \| x_k^p \|_{\hat{P}} + \rho_k^d PTe^{LPT} \leq \alpha \| x_k^p \|_{\hat{P}} + \rho^d PTe^{LPT} \quad (4.34)$$

By defining $z_k := \| x_k^p \|_{\hat{P}}$, $a := \alpha$ *and* $b := \rho^d PTe^{LPT}$ *and using lemma 4.1 we have the following result:*

$$\| x_k^p \|_{\hat{P}} < \| x_0^p \|_{\hat{P}} + \frac{\rho^d PTe^{LPT}}{1-\alpha} \tag{4.35}$$

Now, if $x_0^p \in B_{\rho_0}$, *the application of* **Control Algorithm 1** *to system (4.1) assures that the states at the end of prediction horizons are bounded by:*

$$\| x_k^p \|_{\hat{P}} < \rho_0 + \frac{\rho^d PTe^{LPT}}{1-\alpha} \tag{4.36}$$

Therefore, a sufficient condition for the optimization problems $\mathcal{P}(t_k, x_k^p)$, $\forall k \geq 0$, *to be feasible, i. e.,* $\{x_k^p\}_{k=0}^{\infty} \in B_\rho$, *is given by:*

$$\rho > \rho_0 + \frac{\rho^d PTe^{LPT}}{1-\alpha} \tag{4.37}$$

or, equivalently,

$$\rho_0 < \rho - \frac{\rho^d PTe^{LPT}}{1-\alpha} \tag{4.38}$$

Thus, since $\rho_d < \frac{\rho(1-\alpha)}{PTe^{LPT}}$, *it follows that* $\rho_0 > 0$ *(or, equivalently,* B_{ρ_0} *is a non-empty set).*

So, we conclude that there exists $\rho_0 < \rho - \frac{\rho^d PTe^{LPT}}{1-\alpha}$ *(thus,* $\rho_0 < \rho$*) so that if* $x_0^p \in B_{\rho_0} \subset B_\rho$, *then* $x_k^p \in B_\rho$, *with* $\rho > \frac{\rho^d PTe^{LPT}}{1-\alpha}$, *and* $\mathcal{P}(t_k, x_k^p)$ *is well posed for all* $k \geq 0$.

Since from the contractive constraint we have $\| \bar{x}_{k+1} \|_{\hat{P}} \leq \alpha \| x_k^p \|_{\hat{P}}$ *and it has been shown that* $\exists\ \rho_0 > 0$ *such that for* $x_0^p \in B_{\rho_0}$, $x_k^p \in B_\rho$, $\forall k \geq 0$, *then* $\bar{x}_1 \in B_{\alpha\rho_0} \subset B_\rho$ *and* $\bar{x}_k \in B_{\alpha\rho} \subset B_\rho$, $\forall k > 1$.

Thus, we have proven that under the conditions of the theorem, the sequences $\{x_k^p\}_{k=0}^{\infty}$ *and* $\{\bar{x}_k\}_{k=0}^{\infty}$ *remain inside the set of feasible initial conditions,* B_ρ.

□

By now we have shown that **Control Algorithms 1** and **2** applied to the plant (4.1) are well-defined and that they produce an uniformly asymptotically stable closed-loop. Next we will show that this additive asymptotically decaying disturbance can be produced by introduction of an asymptotically convergent state estimator in the closed-loop system for estimation of the states of the nominal system (4.3). So our next step is to propose a recursive dynamic observer to estimate the states of the system (4.3) and study the conditions under which this nonlinear observer is asymptotically stable. Finally we will show that, under these conditions, the association of our exponentially stabilizing contractive MPC controller and the state estimator proposed in the next section, generates an asymptotically stable closed-loop.

Thus, we now address the following problem:

Problem 3 : *Output feedback with asymptotically convergent observer in the nominal case*

4.3 Dynamic observers for nonlinear systems

4.3.1 Observer design

Designing an observer for a nonlinear system is quite a challenge. In our design we follow guidelines similar to the ones used to derive the extended Kalman filter (EKF). The extended Kalman filter is a well-known standard linearization method for approximate nonlinear filtering. The available literature is vast and we refer the reader to [61, 76], and the references therein. In particular, in the context of param-

eter estimation for linear stochastic systems, a fairly systematic and comprehensive convergence analysis of the EKF is presented in [78].

Let us now consider a continuous-time dynamical system with discrete observations and nonlinear output map:

$$\begin{aligned} \dot{x}_k(t) &= F(x_k(t)), \quad x_k(t_k) =: x_k \\ y_k &= H(x_k) \end{aligned} \tag{4.39}$$

for $t \in [t_k, t_{k+1}]$ and $k \geq 0$.

Remark 4.2 *We will envision the system (4.39) as being resultant from implementation of* **Control Algorithm 1** *to the following original system:*

$$\begin{aligned} \dot{\psi}_{x,k}(t) &= f(\psi_{x,k}(t), u_k(t)) \\ \psi_{y,k} &= h(\psi_{x,k}, u_k) \end{aligned} \tag{4.40}$$

where we have made a distinction between the states $x(t)$ and $\psi_x(t)$ to allow for dynamic feedback (instead of restricting ourselves to static feedback).

We assume that $F : \Re^n \to \Re^n$ and $H : \Re^n \to \Re^p$ are smooth, at least twice differentiable, and therefore we define:

$$A(x) := DF(x) \quad \text{and} \quad C(x) := DH(x) \tag{4.41}$$

where $D(.) := \frac{d}{dx}(.)$ and A, C are the $n \times n$ and $p \times n$ matrices of first derivatives, respectively.

Motivated by the procedure commonly used for linear systems, we will construct an observer for system (4.39) as an approximation to the corresponding deterministic

estimator. Associate the following "noisy" system with (4.39):

$$\begin{aligned} \dot{z}_k(t) &= F(z_k(t)) + R_w w_k(t), \quad z_k(t_k) =: z_k, \quad t \in [t_k, t_{k+1}], \\ \zeta_k &= H(z_k) + R_v v_k, \quad \forall k \geq 0 \end{aligned} \tag{4.42}$$

As usual, we assume that $z_0, w(t)$ and $v(t)$ are jointly Gaussian and mutually independent. Furthermore $z_0 \sim \mathcal{N}(z_0, \bar{P}_0^{-1})$, $w(t) \sim \mathcal{N}(0, I_n)$ and $v(t) \sim \mathcal{N}(0, I_p)$. We also assume that the design variables R_w, R_v and $\bar{P}_0$ are always chosen such that R_w has rank n and R_v and $\bar{P}_0$ are positive definite.

Then let us propose the following structure for the nonlinear observer for the associated "noisy" system (4.42):

Estimation Procedure 1

$$\dot{\hat{x}}_k(t) = F(\hat{x}_k(t)) + \bar{P}_k(t)^{-1} C_k' (R_v R_v')^{-1} [\zeta_k - H(\hat{x}_k)], \quad \hat{x}_0(t_0) =: \hat{x}_0 \ \textit{(chosen)} \tag{4.43}$$

and $\bar{P}(t)$ satisfies the following differential Riccati equation:

$$\dot{\bar{P}}_k(t) = -\bar{P}_k(t) A(\hat{x}_k(t)) - A(\hat{x}_k(t))' \bar{P}_k(t) - \bar{P}_k(t) R_w R_w' \bar{P}_k(t) + Q_k' Q_k, \quad \bar{P}_0(t_0) =: \bar{P}_0 \tag{4.44}$$

where $C_k := C(\hat{x}_k)$ (analogous definition applies for A_k) and $Q_k := R_v^{-1} C_k$, for $t \in [t_k, t_{k+1}]$ and $\forall k \geq 0$.

Before we start our proof of asymptotic convergence of the estimator (4.43, 4.44) when applied to system (4.42), let us make some useful additional assumptions:

Assumption 4.3 *The linearized system determined by $(A_k(x), C_k)$ (where $A_k(x) := A(\hat{x}_k(t))$, $t \in [t_k, t_{k+1}]$), along the estimated trajectory of the observer (4.43, 4.44), is uniformly observable, that is, $(A_k(x), C_k)$ satisfies the uniform observability condition*

presented in [14, 38] for linear systems and in [118] for linear and nonlinear systems.

Assumption 4.4 *Let $A(z)$, $C(z)$ be as defined in (4.41) and $DA(z) := D^2F(z) \in L(\Re^n, L(\Re^n, \Re^n))$ and $DC(z) := D^2H(z) \in L(\Re^n, L(\Re^p, \Re^n))$. Then the following norms are bounded:*

$$\| A \| := \sup_{z \in \Re^n} \| A(z) \| \quad \text{and} \quad \| C \| := \sup_{z \in \Re^n} \| C(z) \| \tag{4.45}$$

$$\| \| D^2F \| \| := \sup_{z \in \Re^n} \| \| D^2F(z) \| \| \quad \text{and} \quad \| \| D^2H \| \| := \sup_{z \in \Re^n} \| \| D^2H(z) \| \| \tag{4.46}$$

Assumption 4.5 *Let $G(x, y) := H(x) - H(y) - C(y)(x - y)$, and suppose that there exists $G \in [0, \infty)$ such that $\| G(x, y) \| \leq G \ \| \| D^2H \| \| \ \| x - y \|^2$ for all $x, \ y \in \Re^n$.*

Remark 4.3 *From the mean value theorem and continuity of the function $G(x, y)$, we can always compute $G \in [0, \infty)$ such that assumption 4.5 is satisfied.*

Under assumptions 4.3, 4.4 it is possible to show that the error covariance $\bar{P}(t)^{-1}$ and its inverse $\bar{P}(t)$ are uniformly bounded (see [14] for derivation of these bounds). If assumption 4.3 holds then, since R_v is positive definite, we have that $(A_k(x), Q_k)$ is a uniformly observable pair, that is, there exists a bounded Borel matrix-valued function $\Lambda(x)$ such that

$$\nu'(A_k(x) + \Lambda(x)Q_k)\nu \leq -\alpha_0 \| \nu \|^2, \ \ \alpha_0 > 0, \ \ \forall x \in \Re^n \text{ and } k \geq 0. \tag{4.47}$$

In addition, we assume that the pair $(A_k(x), R_w)$ is uniformly controllable $\forall k \geq 0$, that is, there exists a bounded Borel function $\Gamma(x)$ such that

$$\mu'(A_k(x) + R_w\Gamma(x))\mu \leq \beta_0 \| \mu \|^2, \ \ \beta_0 > 0, \ \ \forall x \in \Re^n \text{ and } k \geq 0. \tag{4.48}$$

Then one can prove that the covariance matrices satisfy the following bounds:

$$\| \bar{P}(t)^{-1} \| \leq \| \bar{P}_0^{-1} \| + \frac{\| R_w \|^2 + \| \Lambda \|^2}{2\alpha_0} =: \bar{q} \tag{4.49}$$

$$\| \bar{P}(t) \| \leq \| \bar{P}_0 \| + \frac{\| Q \|^2 + \| \Gamma \|^2}{2\beta_0} =: \bar{p} \tag{4.50}$$

where $\| Q \| := \max_{k \in N} \| Q_k \|$, $\| \Gamma \| := \sup_{x \in \Re^n} \| \Gamma(x) \|$ and $\| \Lambda \| := \sup_{x \in \Re^n} \| \Lambda(x) \|$. Proof can be found in [14].

These bounds $\bar{p}$ and $\bar{q}$ are functions of the design parameters $\bar{P}_0, R_v$ and R_w and the given nonlinear functions F and H. Also, let R_w be such that $R_w R_w' \geq r I_n$ for some $r > 0$.

4.3.2 Asymptotic convergence

We wish to prove that the system (4.43, 4.44) is an observer for the nonlinear system (4.42). We will see that this is possible provided that we can bound the region where the initial condition lies and provided the second derivatives of F and H are not too large.

We should point out that the stability proof will be given for the noise-free case, that is, even though in equation (4.43) we have used the true measurements ζ_k, in the next theorem we will substitute this real measurements with the "noise-free measurements" y_k (as it is normally done for stability analysis purposes - see, e.g., [14, 118]).

Remark 4.4 *Proofs of asymptotic convergence of nonlinear observers applied to both continuous-time systems with continuous observations and linear output maps and discrete-time systems with discrete observations can be found in the literature [14, 118, 117] but here we are addressing the observer design problem for nonlinear continuous-time systems with discrete-observations and nonlinear output maps.*

The reason we choose a continuous-time representation for the nonlinear system is

that most systems are modeled by a set of differential/algebraic equations in continuous time and, in general, there is no closed-form discrete description for these systems. The discrete observations are also a much more reasonable assumption since, in reality, measurements are always taken at discrete periods of time, rarely continuously.

Theorem 4.3 (Stability region for the nonlinear observer) *Let* $t_0 = 0$ *and assume that*

$$\| x_0 - \hat{x}_0 \| \ \varphi(D^2F, D^2H, \bar{P}_0, R_v, R_w) \ < \ \frac{r}{\bar{p}^{\frac{1}{2}} \bar{q}^2 \| \bar{P}_0^{\frac{1}{2}} \|} \tag{4.51}$$

with the function φ *defined as:*

1. *Linear Output Map* ($y_k = Cz_k = H(z_k)$ *and, consequently,* $D^2H = 0$)

$$\varphi(D^2F, D^2H, \bar{P}_0, R_v, R_w) := \| \| D^2F \| \| \tag{4.52}$$

2. *Nonlinear Output Map*

$$\varphi(D^2F, D^2H, \bar{P}_0, R_v, R_w) := \| \| D^2F \| \| + 2(\frac{\bar{q}}{\bar{p}})^{\frac{1}{2}} \| C \| \ \kappa_v \ \| R_v R_v^{'} \|^{-1} \ G \| \| D^2H \| \| \tag{4.53}$$

where κ_v *is the condition number of the nonsingular symmetric matrix* $R_v R_v^{'}$.

Then the dynamical system (4.43, 4.44) is an asymptotically stable observer for the nonlinear system (4.39) provided that assumptions 4.3, 4.4, 4.5 hold. That is, there exists a constant $\delta > 0$ *such that*

$$V_{k+1} - V_k := V(t_{k+1}) - V(t_k) := \| \bar{P}_{k+1}^{\frac{1}{2}} e_{k+1} \|^2 - \| \bar{P}_k^{\frac{1}{2}} e_k \|^2 \leq -\delta, \quad \forall k \geq 0 \tag{4.54}$$

where $\bar{P}_k := \bar{P}_k(t_k)$, $t_{k+1} := t_k + T$ *(notice that the notation used in this theorem differs from the previous notation for* t_{k+1}, *where* $t_{k+1} := t_k + PT$*) and* $V(t) := \| \bar{P}(t)^{\frac{1}{2}} e(t) \|^2$ *will be shown to be a Lyapunov function for the closed-loop system which decreases discretely, at sampling times* t_k, $\forall k \geq 0$, *for all initial estimates satisfying (4.51).*

Proof: *Let* $e_k(t) := x_k(t) - \hat{x}_k(t)$ *be the estimation error at time* $t \in [t_k, t_{k+1}]$. *Then, from (4.43) and (4.39) we have:*

$$\dot{e}_k(t) = F(x_k(t)) - F(\hat{x}_k(t)) - \bar{P}_k(t)^{-1} C_k^{'} (R_v R_v^{'})^{-1} [H(x_k) - H(\hat{x}_k)] \tag{4.55}$$

Using assumption 4.5 we can rewrite (4.55) as:

$$\dot{e}_k(t) = F(x_k(t)) - F(\hat{x}_k(t)) - \bar{P}_k(t)^{-1} C_k^{'} (R_v R_v^{'})^{-1} [C_k e_k + G(x_k, \hat{x}_k)] \tag{4.56}$$

Thus,

$$\begin{aligned} \frac{d}{dt}(e_k(t)^{'} \bar{P}_k(t) e_k(t)) &= 2e_k(t)^{'} \bar{P}_k(t)[F(x_k(t)) - F(\hat{x}_k(t))] - 2e_k(t)^{'} Q_k^{'} Q_k e_k - \\ &- 2e_k(t)^{'} C_k^{'} (R_v R_v^{'})^{-1} G_k - e_k(t)^{'} [2\bar{P}_k(t) A(\hat{x}_k(t)) + \\ &+ \bar{P}_k(t) R_w R_w^{'} \bar{P}_k(t) - Q_k^{'} Q_k] e_k(t) \end{aligned} \tag{4.57}$$

where $G_k := G(x_k, \hat{x}_k)$.

The mean value theorem states that:

$$F(x(t)) - F(\hat{x}(t)) = \int_0^1 DF(sx(t) + (1-s)\hat{x}(t)) ds e(t) = \int_0^1 DF(\hat{x}(t) + se(t)) ds e(t) \tag{4.58}$$

Thus, by expanding the operator $DF(\hat{x}(t) + se(t))$ *around* $\hat{x}(t)$, *we can rewrite the*

preceding expression as:

$$F(x(t)) - F(\hat{x}(t)) - \frac{\partial F}{\partial x}(\hat{x}(t))e(t) \;=\; \int_0^1 \int_0^1 \sigma D^2 F(\hat{x}(t) + \sigma\varrho e(t))e(t)^2 d\sigma \, d\varrho \quad (4.59)$$

Using equation (4.59), we can rewrite (4.57) as:

$$\begin{aligned}
\frac{d}{dt}(e_k(t)^{'}\bar{P}_k(t)e_k(t)) &= 2e_k(t)^{'}\bar{P}_k(t) \int_0^1 \int_0^1 \sigma D^2 F(\hat{x}_k(t) + \sigma\varrho e_k(t))e_k(t)^2 d\sigma d\varrho - \\
&- e_k(t)^{'}\bar{P}_k(t)R_w R_w^{'}\bar{P}_k(t)e_k(t) + e_k(t)^{'}Q_k^{'}Q_k e_k(t) - \\
&- 2e_k(t)^{'}Q_k^{'}Q_k e_k - 2e_k(t)^{'}C_k^{'}(R_v R_v^{'})^{-1}G_k \leq \\
&\leq e_k(t)^{'}[\| \bar{P}_k(t)^{\frac{1}{2}}e_k(t) \| \bar{p}^{\frac{1}{2}} \| D^2 F \| - \frac{r}{\bar{q}^2}]e_k(t) + \\
&+ e_k(t)^{'}Q_k^{'}Q_k[e_k(t) - 2e_k] - 2e_k(t)^{'}C_k^{'}(R_v R_v^{'})^{-1}G_k \qquad (4.60)
\end{aligned}$$

Since we are only taking measurements at discrete sampling times t_k, $k \geq 0$, the most we can expect is that the state estimation error at sampling times, namely e_k, $k \geq 0$, converges to zero (but nothing can be said about $e_k(t)$, $t \in (t_k, t_{k+1})$, $\forall k \geq 0$). So, as we said before, we are looking for a Lyapunov function for the closed-loop system which decreases discretely rather than continuously.

Let us then evaluate (4.60) at time t_k:

$$\begin{aligned}
\frac{d}{dt}(e_k(t)^{'}\bar{P}_k(t)e_k(t)) \mid_{t=t_k} &\leq [\| \bar{P}_k^{\frac{1}{2}}e_k \| \bar{p}^{\frac{1}{2}} \| D^2 F \| - \frac{r}{\bar{q}^2}] \| e_k \|^2 - \\
&- 2e_k^{'}C_k^{'}(R_v R_v^{'})^{-1}G_k - \| Q_k e_k \|^2 \leq \\
&\leq [\, \| \bar{P}_k^{\frac{1}{2}}e_k \| \bar{p}^{\frac{1}{2}} \| D^2 F \| - \frac{r}{\bar{q}^2} + 2 \| e_k \| \| C_k \| \;\times \\
&\times \; \kappa_v \| R_v R_v^{'} \|^{-1} G \| D^2 H \|] \| e_k \|^2 \qquad (4.61)
\end{aligned}$$

Thus, if we have

$$\| \bar{P}_k^{\frac{1}{2}} e_k \| \bar{p}^{\frac{1}{2}} \| D^2 F \| + 2 \| e_k \| \| C_k \| \ \kappa_v \ \| R_v R_v^{'} \|^{-1} \ G \| D^2 H \| \leq \frac{r}{\bar{q}^2} - \gamma, \quad \gamma > 0 \tag{4.62}$$

$\forall k \geq 0$, *then, from (4.61), it follows that:*

$$\frac{d}{dt}(e_k(t)^{'} \bar{P}_k(t) e_k(t)) \ |_{t=t_k} \leq -\gamma \| e_k \|^2 \tag{4.63}$$

But from (4.50) we have that:

$$\| e_k \|^2 \geq \frac{\| \bar{P}_k^{\frac{1}{2}} e_k \|^2}{\bar{p}} \tag{4.64}$$

And thus, from (4.63) and (4.64) we obtain:

$$[\frac{d}{dt} \| \bar{P}_k(t)^{\frac{1}{2}} e_k(t) \| + \frac{\gamma}{\bar{p}} \| \bar{P}_k(t)^{\frac{1}{2}} e_k(t) \|] \ |_{t=t_k} \leq 0 \tag{4.65}$$

If $t_{k+1} - t_k = T$ *is sufficiently small, then inequality (4.65) will hold for all* $t \in [t_k, t_{k+1}]$ *and we can integrate (4.65) between* t_k *and* t_{k+1}

$$\int_{t_k}^{t_{k+1}} (\frac{d \| \bar{P}_k(t)^{\frac{1}{2}} e_k(t) \|}{\| \bar{P}_k(t)^{\frac{1}{2}} e_k(t) \|} + \frac{\gamma}{\bar{p}} dt) \ \leq \ 0 \tag{4.66}$$

which results in

$$\ln(\frac{\| \bar{P}_{k+1}^{\frac{1}{2}} e_{k+1} \|}{\| \bar{P}_k^{\frac{1}{2}} e_k \|}) + \frac{\gamma}{\bar{p}} T \leq 0 \tag{4.67}$$

Thus, it follows that:

$$\| \bar{P}_{k+1}^{\frac{1}{2}} e_{k+1} \| \leq \| \bar{P}_k^{\frac{1}{2}} e_k \| \ e^{-\frac{\gamma}{\bar{p}}T} \leq \| \bar{P}_k^{\frac{1}{2}} e_k \|, \quad \forall k \in N \tag{4.68}$$

Then, as a consequence of (4.68) we have that:

$$\| \bar{P}_0^{\frac{1}{2}} e_0 \| = \max_{k \in N} \| \bar{P}_k^{\frac{1}{2}} e_k \| \tag{4.69}$$

and

$$\| e_k \| \leq \bar{q}^{\frac{1}{2}} \| \bar{P}_0^{\frac{1}{2}} \| \| e_0 \| \tag{4.70}$$

Therefore, since $\bar{q}^{\frac{1}{2}} \geq \| \bar{P}_0^{\frac{1}{2}} \|^{-1}$, *a sufficient condition for (4.62) to be satisfied is given by:*

$$\| e_0 \| [\|\|D^2 F\|\| + 2(\frac{\bar{q}}{\bar{p}})^{\frac{1}{2}} \| C \| \ \kappa_v \ \| R_v R_v^{'} \|^{-1} \ G \ \|\|D^2 H\|\|] \leq \frac{1}{\bar{p}^{\frac{1}{2}} \| \bar{P}_0^{\frac{1}{2}} \|} (\frac{r}{\bar{q}^2} - \gamma) \tag{4.71}$$

It is straightforward to see that if the output map is linear (4.71) is reduced to:

$$\| e_0 \| \ \|\|D^2 F\|\| \leq \frac{1}{\bar{p}^{\frac{1}{2}} \| \bar{P}_0^{\frac{1}{2}} \|} (\frac{r}{\bar{q}^2} - \gamma), \quad \gamma > 0 \tag{4.72}$$

In conclusion, if (4.71) is satisfied then there exists $\delta > 0$ *such that*

$$V_{k+1} - V_k := \| \bar{P}_{k+1}^{\frac{1}{2}} e_{k+1} \| - \| \bar{P}_k^{\frac{1}{2}} e_k \| \leq -\delta, \quad \delta > 0 \tag{4.73}$$

which implies asymptotic convergence of the state estimation error.

□

Remark 4.5 *If the output map were continuous then, under condition (4.51) and using continuity arguments, the proposed nonlinear observer can be proven exponentially stable, i.e., there exist constants $\sigma, K > 0$, such that*

$$\| x(t) - \hat{x}(t) \| \leq K \| x_0 - \hat{x}_0 \| e^{-\sigma t}, \quad \forall t > 0 \tag{4.74}$$

Remark 4.6 *As pointed out in [118], if the output map is nonlinear it may be locally transformed via a coordinate change into a linear form provided the Jacobian of H has constant rank. In order to obtain this result rigorously the noisy system has to be constructed after the coordinate change since otherwise the noise terms become state dependent.*

Remark 4.7 *An alternative way of posing the observer problem when we have known controls is to replace $F(x_k(t))$ and $H(x_k)$ by $f(x_k(t), u_k(t))$ and $h(x_k, u_k)$ and assume that assumption 4.3 holds with the following bounds:*

$$\| A \| := \sup\{\| \frac{\partial f}{\partial x}(x, u) \| : \ x \in \Re^n, u \in \Re^m\}, \tag{4.75}$$

$$\| C \| := \sup\{\| \frac{\partial h}{\partial x}(x_k, u_k) \| : \ x_k \in \Re^n, u_k \in \Re^m, k \geq 0\}, \tag{4.76}$$

$$\| |D^2 F| \| := \sup\{\| \frac{\partial^2 f}{\partial x^2}(x, u) \| : \ x \in \Re^n, u \in \Re^m\}, \tag{4.77}$$

$$\| |D^2 H| \| := \sup\{\| \frac{\partial^2 h}{\partial x^2}(x_k, u_k) \| : \ x_k \in \Re^n, u_k \in \Re^m, k \geq 0\}, \tag{4.78}$$

$$\tag{4.79}$$

Then theorem 4.3 holds with the appropriate replacements. However, as we already mentioned, assumption 4.3 is closely tied with the observability properties of the system, which can be input dependent in the nonlinear case. Then, when known controls are considered the standard observability analysis is modified to "uniform observability" in the inputs (see [56]).

4.4 MPC algorithm with state estimation

In order to include state estimation, **Control Algorithm 1** has to be modified in the following way:

Control Algorithm 3

Data: *Initial Conditions:* t_0 *and* $\hat{x}_0$*; Controller Parameters:* $P, M, Q, R, S, \hat{P}, \alpha$, $T, u_{min}, u_{max}, \Delta u_{max}$*; Observer Parameters:* $\bar{P}_0, R_v, R_w$*; Output measurement at* t_0*:* y_0.

Step 0: *Set* $k = 0,\ j = 0$.

Step 1: *Solve the optimal control problem* $\mathcal{P}(t_k^j, \hat{x}_k^j)$ *specified by:*

$$\begin{aligned}
&\min_{u(kP+j|kP+j),\ldots,u(kP+j+M-1|kP+j)} \quad \int_{t_k^j}^{t_k^{j+P}} x_k^j(t)'\, Q\, x_k^j(t)\, dt + \\
&+ \sum_{i=0}^{P} u(kP+j+i|kP+j)'\, R\, u(kP+j+i|kP+j) + \\
&+ \sum_{i=0}^{M-1} \Delta u(kP+j+i|kP+j)'\, S\, \Delta u(kP+j+i|kP+j)
\end{aligned} \tag{4.80}$$

subject to:

$$\begin{cases}
\dot{x}_k^j(t) = f(x_k^j(t), u_k^j(t)), \quad x_k^j = \hat{x}_k^j := \text{ estimated states at } t_k^j \\
u_{min} \le u(kP+j+i|kP+j) \le u_{max}, \quad i \in [0, M-1] \\
|\Delta u(kP+j+i|kP+j)| \le \Delta u_{max}, \quad i \in [0, M-1] \\
\Delta u(kP+j+i|kP+j) = 0, \quad i \in [M, P] \\
\| \bar{x}_k^j(t_k^P) \|_{\hat{P}} \le \alpha \| \hat{x}_k \|_{\hat{P}}, \quad \alpha \in [0, 1)
\end{cases} \tag{4.81}$$

where

$$\dot{\bar{x}}_k^j(t) = f(\bar{x}_k^j(t), u_k^j(t)), \text{ with } \bar{x}_k^0 := \hat{x}_k \text{ and } \bar{x}_k^j = \bar{x}_k^{j-1}(t_k^j), \text{ for } j \ge 1 \tag{4.82}$$

is the trajectory of the model which is not updated with the estimated states of the plant at t_k^j for $j \in [1, P-1]$. The states $\bar{x}_k^j(t)$ are only updated with the states of the estimator at $t = t_k + PT =: t_k^P$, i.e., at intervals of one prediction horizon.

Step 2: *Apply the first control move, $u(kP+j|kP+j)$, to the real system for $t \in [t_k^j, t_k^{j+1}]$, measure the output at t_k^{j+1}, y_k^{j+1}, and estimate the states of the system at t_k^{j+1} (i.e., obtain $\hat{x}_k^{j+1}$) using the following equations with initial conditions $\hat{x}_k^j$ and $\bar{P}_k^j$:*

$$\begin{aligned} \dot{\hat{x}}_k^j(t) &= f(\hat{x}_k^j(t), u(kP+j|kP+j)) + \bar{P}_k^j(t)^{-1}(C_k^j)' \, (R_v R_v')^{-1} \times \\ &\times \; [y_k^j - H(\hat{x}_k^j, u(kP+j|kP+j))] \end{aligned} \tag{4.83}$$

with

$$\dot{\bar{P}}_k^j(t) = -\bar{P}_k^j(t)A(\hat{x}_k^j(t)) - A(\hat{x}_k^j(t))' \bar{P}_k^j(t) - \bar{P}_k^j(t) R_w R_w' \bar{P}_k^j(t) + (Q_k^j)' Q_k^j \tag{4.84}$$

where $t \in [t_k^j, t_k^{j+1}]$.

Result of the estimation: $\hat{x}_k^{j+1} := \hat{x}_k^j(t_k^{j+1})$ and $P_k^{j+1} := P_k^j(t_k^{j+1})$.

Step 3: *If $j < P-1$, set $j = j+1$ and go back to* **Step 1**. *If $j = P-1$ set $\hat{x}_{k+1}^0 =: \hat{x}_{k+1} = \hat{x}_k^P$, $t_{k+1}^0 = t_{k+1} = t_k^P$, $k = k+1$, $j = 0$ and go back to* **Step 1**.

where we have used the notation $x_k := x_k^0, y_k := y_k^0$ and $\bar{P}_0 := \bar{P}_0^0$.

4.5 Stability properties of contractive MPC + nonlinear observer

In section 4.2 we have shown that contractive MPC applied to a nonlinear plant subjected to an asymptotically decaying disturbance is uniformly asymptotically stabilizing. Then in section 4.3 we proposed a nonlinear state estimator and showed that if the initial estimation error and the nonlinearities are "small" then this estimator is asymptotically stable.

Now we will formally enunciate the main result of this chapter, that is, that **Control Algorithm 3** is uniformly asymptotically stabilizing for a set of initial estimates.

In the state feedback case, the state evolution of the model used in the prediction step of the contractive MPC algorithm at time step k is given by:

$$x_k(t) = x_k^p + \int_{t_k;\, x_k^p}^{t} f(x_k(\tau), u_k(\tau))\, d\tau, \quad \forall t \in [t_k, t_k + PT] \tag{4.85}$$

which makes it equal to the state evolution of the plant.

In the output feedback case, the trajectory of the model is given by:

$$x_k(t) = \hat{x}_k + \int_{t_k;\, \hat{x}_k}^{t} f(x_k(\tau), u_k(\tau))\, d\tau, \quad \forall t \in [t_k, t_k + PT] \tag{4.86}$$

The difference between the two model dynamics can be represented by an additive disturbance, i.e., the output feedback case is equivalent to the state feedback case modified to:

$$\dot{x}_k(t) = f(x_k(t), u_k(t)) + d_k(t) \;\text{ with }\; x_k(t_k) = x_k^p \tag{4.87}$$

If $d_k(t) = d_k$ = constant for $t \in [t_k, t_k + T]$, integration of (4.87) results in:

$$x_k(t) = x_k^p + \int_{t_k;\, x_k^p}^{t} f(x_k(\tau), u_k(\tau))\, d\tau \; + \; d_k(t - t_k) \tag{4.88}$$

Thus, we want to compute d_k so that it represents the difference in the dynamic behavior of the model caused by the estimation, i.e., the states in equation (4.88) have to be equal to the states in (4.86) for any $t \in [t_k, t_k + T]$. Thus, by subtracting equation (4.86) from equation (4.88) and evaluating at $t = t_k + T$, we have:

$$d_k T = \hat{x}_k - x_k^p + \int_{t_k;\, \hat{x}_k}^{t_k+T} f(x_k(\tau), u_k(\tau))\, d\tau - \int_{t_k;\, x_k^p}^{t_k+T} f(x_k(\tau), u_k(\tau))\, d\tau \tag{4.89}$$

Therefore, if $e_k := x_k^p - \hat{x}_k$ we obtain:

$$d_k = \frac{-e_k + \bar{F}(\hat{x}_k + e_k, u_k) - \bar{F}(\hat{x}_k, u_k)}{T} \tag{4.90}$$

where the function $\bar{F} : \Re^n \times \Re^m \to \Re^n$ is defined by:

$$\int_{t_1}^{t_2} f(x(\tau), u(\tau))\, d\tau = \bar{F}(x(t_2), u(t_2)) - \bar{F}(x(t_1), u(t_1)) \tag{4.91}$$

If $\bar{F}$ is Lipschitz continuous, i.e., if there exists $\tilde{L}_F \in [0, \infty)$ such that:

$$\| \bar{F}(x_1, u) - \bar{F}(x_2, u) \| \leq \tilde{L}_F \| x_1 - x_2 \|, \quad \forall x_1,\, x_2 \in \Re^n \text{ and } u \in \mathcal{U} \tag{4.92}$$

then, from equation (4.90), we have the following bound:

$$\| d_k \| \leq \hat{L}_F \| e_k \| \quad \text{with} \quad \hat{L}_F := \frac{\tilde{L}_F + 1}{T} \tag{4.93}$$

From the results of *Theorem 4.3*, we can then find $L_F \in [0, \infty)$ such that:

$$\| d_k \| \leq L_F \frac{\| \bar{P}_k^{\frac{1}{2}} e_k \|}{\bar{p}^{\frac{1}{2}}} \leq L_F \frac{\| \bar{P}_0^{\frac{1}{2}} \|}{\bar{p}^{\frac{1}{2}}} \| e_0 \| =: \rho^d, \quad \forall k \geq 0 \tag{4.94}$$

So, onto this chapter's main result:

Theorem 4.4 (Closed-loop stability with output feedback) *Let ρ_d, $\rho \in (0, \infty)$ be as defined in equation (4.94) and* Assumption 3.3, *respectively. Let x_k^p, $\hat{x}_k$, $\bar{x}_k \in B_\rho$, $\forall k \geq 0$, and $x_0^p \in B_{\rho_0}$, with $\rho_0 := \rho - \frac{\rho^d PTe^{LPT}}{1-\alpha}$, and let the initial estimate of the states $\hat{x}_0$ be such that e_0 and the functions F and H (i.e., the system dynamics after implementation of the control law - see equation (4.39)) satisfy condition (4.51) for the chosen observer parameters $\bar{P}_0, R_v, R_w$. Then, if $\rho^d < \frac{\rho(1-\alpha)}{PTe^{LPT}}$, the control problem is well-posed, the observer produces asymptotically convergent estimates and the resulting closed-loop system is uniformly asymptotically stable.*

Proof: *The proof follows straightforwardly from* Theorems 4.1, 4.2 *and* 4.3 *(and the assumptions made in their derivations) and equation (4.94).*

□

4.6 Example: van der Vusse Reactor

4.6.1 van der Vusse reactor dynamics

A benchmark problem for nonlinear control system design based on a continuous stirred tank reactor (CSTR) is described in [29, 43, 50]. The reactor is considered at an operating point where optimal yield with respect to the desired product is achieved. Operation at this point is very desirable for economic reasons but can considerably complicate the control system design. In particular, this benchmark problem is characterized by two interesting features:

- The steady state gain changes its sign at the operating point. Therefore, linear controllers will not be able to stabilize this reactor and accomplish satisfactory performance [98].
- The zero dynamics changes its stability properties at this operating point. Therefore, the qualitative behavior of the CSTR differs considerably for different setpoints and disturbances.

A more detailed discussion on the reasons and implications of these features can be found in [65].

The reactor under consideration is a continuous stirred tank reactor in which cyclopentenol is produced from cyclopentadiene by acid-catalyzed electrophylic hydration in aqueous solution. The description of the system used here is the same as in [64] with the only change being that the dynamics of the jacket used to cool the reactor are not taken into consideration (the fluid in the jacket is assumed to be at constant temperature). Details on the derivation of the chemical parameters and the chemical background can be found in [64].

Figure 4.1 shows a schematic diagram of the reactor. The main reaction is given by transformation of cyclopentadiene (substance A) into the product, cyclopentenol (substance B). The cyclopentadiene also reacts in an unwanted parallel reaction to originate the by-product dicyclopentadiene (substance D). Furthermore, cyclopentanediol (substance C) is formed in an unwanted decomposition of the product cyclopentenol. This so-called *van der Vusse* reaction is represented by the following reaction scheme:

$$\begin{aligned} A &\xrightarrow{k_1} B \xrightarrow{k_2} C \\ 2A &\xrightarrow{k_3} D \end{aligned} \tag{4.95}$$

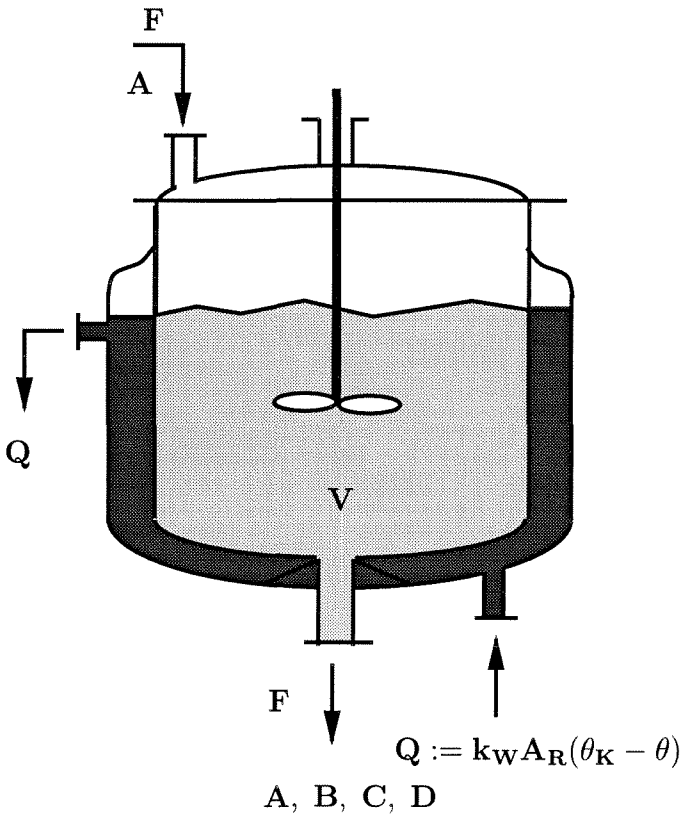

Figure 4.1: Schematic representation of the van der Vusse reactor.

The flow F fed to the reactor contains only cyclopentadiene (substance A) with concentration C_{A0} and temperature θ_0. The temperature of the fluid in the cooling jacket is equal to θ_K and is considered constant.

The dynamics of the reactor are described by the following nonlinear differential equations which are derived from mass balances for substances A and B and from energy balance for the reactor:

$$\dot{C}_A = -k_1(\theta)C_A - k_3(\theta)C_A^2 + \frac{F}{V}(C_{A0} - C_A), \qquad C_A \geq 0 \tag{4.96}$$

$$\dot{C}_B = k_1(\theta)C_A - k_2(\theta)C_B - \frac{F}{V}C_B, \qquad C_B \geq 0 \tag{4.97}$$

$$\dot{\theta} = -\frac{1}{\rho C_p}[\Delta H_{R_{AB}} k_1(\theta)C_A + \Delta H_{R_{BC}} k_2(\theta)C_B + \Delta H_{R_{AD}} k_3(\theta)C_A^2] + \\ + \frac{F}{V}(\theta_0 - \theta) + \frac{k_W A_R}{\rho C_p V}(\theta_K - \theta) \tag{4.98}$$

$$y = C_B \tag{4.99}$$

where C_A and C_B are the concentrations of A and B, respectively, θ is the temperature in the reactor, $u := \frac{F}{V}$ is the flow rate to the reactor and it is the manipulated variable for this system, $Q := k_W A_R\,(\theta - \theta_K)$ is the rate of heat exchanged between the reactor and the surroundings and C_{A0}, θ_0 are the concentration of A and the temperature in the feed stream, respectively. The reaction rates, k_i, $i = 1, 2, 3$, are assumed to depend on the temperature via the Arrhenius law:

$$k_i(\theta) := k_{i0}\, exp(\frac{E_i}{\theta(^0C) + 273.15}), \qquad i = 1, 2, 3 \tag{4.100}$$

where $\theta(^0C)$ means that the temperature θ should be expressed in Celsius degrees in this equation. E_i, $i = 1, 2, 3$, are the activation energies for the three different reactions occurring in the system.

Values for the physical and chemical parameters in the equations of this model are the following:

Parameters for the van der Vusse reactor	
$k_{10} = 1.287 \times 10^{12}\ \mathrm{h}^{-1}$	$k_{20} = 1.287 \times 10^{12}\ \mathrm{h}^{-1}$
$k_{30} = 9.043 \times 10^{9}\ \frac{1}{\mathrm{mol}_A . \mathrm{h}}$	$E_1 = 9758.3\ \mathrm{K}$
$E_2 = 9758.3\ \mathrm{K}$	$E_3 = 8560.0\ \mathrm{K}$
$\Delta H_{R_{AB}} = 4.2\ \frac{\mathrm{kJ}}{\mathrm{mol}_A}$	$\Delta H_{R_{BC}} = -11.0\ \frac{\mathrm{kJ}}{\mathrm{mol}_B}$
$\Delta H_{R_{AD}} = -41.85\ \frac{\mathrm{kJ}}{\mathrm{mol}_A}$	$\rho = 0.9342\ \mathrm{kg/l}$
$C_p = 3.01\ \frac{\mathrm{kJ}}{\mathrm{kg} . \mathrm{K}}$	$V = 0.01\ \mathrm{m}^3$
$k_W = 4032.0\ \frac{\mathrm{kJ}}{\mathrm{h} . \mathrm{K} . \mathrm{m}^2}$	$A_R = 0.215\ \mathrm{m}^2$
$C_{A0} = 5.10\ \mathrm{mol/l}$	$\theta_0 = 378.05\ \mathrm{K}$
$\theta_K = 386.05\ \mathrm{K}$	

4.6.2 Computation of steady states

We desire to operate the reactor at an equilibrium point where optimal yield with respect to product B is achieved. The yield Φ of product B is defined as the ratio between product concentration C_B at steady state (C_B^{ss}) and the concentration of reactant A in the feed, C_{A0}, i.e.,

$$\Phi = \frac{C_B^{ss}}{C_{A0}} \tag{4.101}$$

and is a measure of the effectiveness in the production of B. This optimal operating point is found by optimization of the steady state yield with respect to the steady state flow (a design variable), $u^{ss} := \frac{F}{V}^{ss}$. The coordinates of the optimal operating point are given by:

Steady state values for the van de Vusse reactor	
$u^{ss} = 14.19\ \mathrm{h}^{-1}$	$C_A^{ss} = 2.2291\ \mathrm{mol/l}$
$C_B^{ss} = 1.0887\ \mathrm{mol/l}$	$\theta^{ss} = 386.0518\ \mathrm{K}$

4.6.3 Simulation results

Here we will compare the nominal performance and stability properties of our contractive MPC (CNTMPC) scheme with those of a standard nonlinear MPC (SNLMPC) algorithm, when applied to the van der Vusse reactor, in three different situations (for both the unconstrained and constrained cases):

(1) No disturbances.

(2) Exponentially decaying additive disturbances.

(3) Output feedback case with use of an asymptotically convergent observer for computation of the state estimates.

The plotted variables for the van der Vusse reactor are the deviation variables with respect to the desired steady state (the point of maximum conversion).

In all the simulations for this example, the sampling time is equal to $T = 0.1$ h.

(1) No disturbances

Unconstrained case

Case 1

The results obtained for simulations with SNLMPC and CNTMPC for the following initial condition

Initial Condition		
$C_{A0} = 1$	$C_{B0} = 1$	$\theta_0 = 150$

are shown in figure 4.2.

The controller parameters used in **Case 1** are:

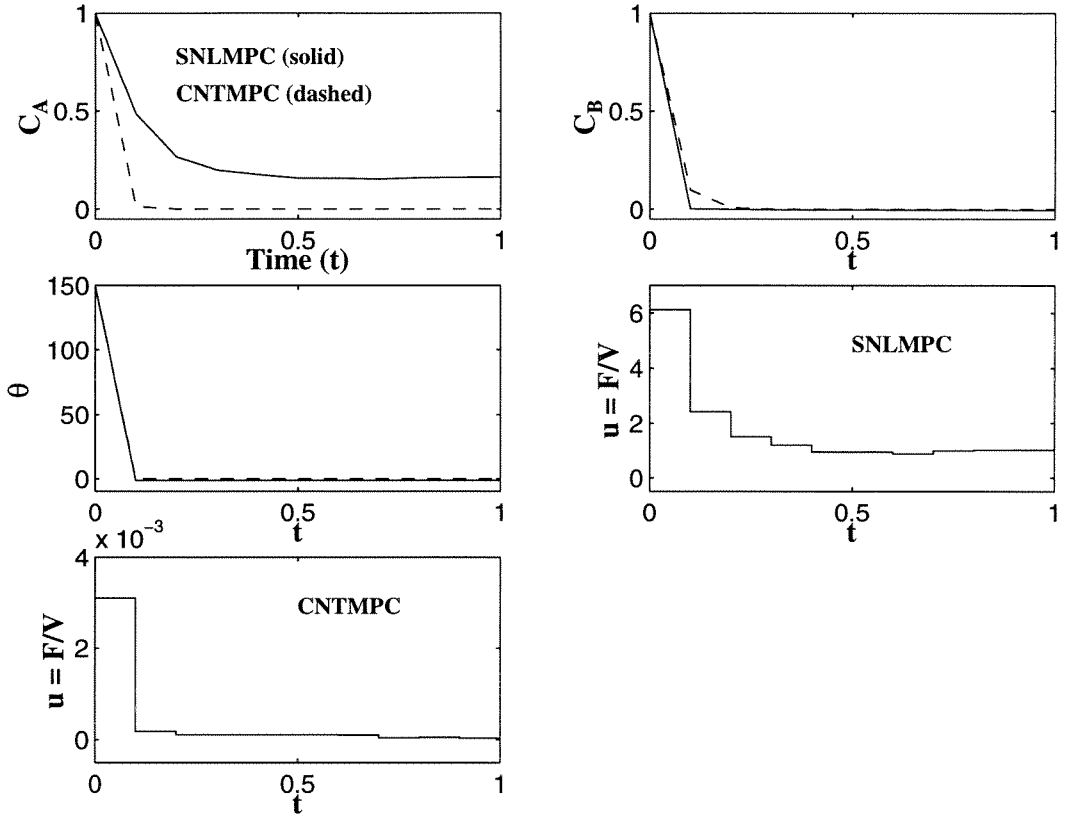

Figure 4.2: van der Vusse CSTR: State and control responses for SNLMPC and CNTMPC in the unconstrained **Case 1**.

Controller Parameters (figure 4.2)		
$Q = \text{diag}([0\ \ 1\ \ 0.5])$	$R = 0$	$S = 0$
$P = 4$	$M = 2$	$\alpha = 0.7$

We notice from figure 4.2 that the output response (C_B) for both controllers is very quick as the conversion of B can be brought to its maximum in about two sampling times. However, while C_A and θ are brought to zero in only one sampling time by the CNTMPC controller, they show large offsets when SNLMPC is used. The fact that C_A is not weighted in the objective function explains the large offset displayed by this variable.

The same explanation applies for the offset in the input variable. The presence of offset is mostly due to the fact that we have only one manipulated variable and three states, so there are insufficient degrees of freedom in

the SNLMPC formulation to bring all the states to the origin. Moreover, since we wish to operate the reactor near the point of maximum yield, additional difficulties (which we have discussed in section 4.6.1) contribute to the poor performance of SNLMPC.

The presence of the contractive constraint in the CNTMPC algorithm is what makes it possible to set all the states to zero in about the same time (it imposes an additional performance requirement which is not present in SNLMPC). Furthermore, we notice that the maximum control effort for the CNTMPC is equal to $u = 3.1 \times 10^{-3}$, while for the SNLMPC, it reaches a maximum higher than $u = 6.1$. In both cases, we have let the optimization routine find the initial guess for the input values so the poor performance of SNLMPC cannot be explained by inappropriate initialization.

Case 2

Since the control effort was rather small with the CNTMPC controller for the initial condition of **Case 1** (even though it represents a considerable deviation from the desired steady state), in the next simulations we will change the initial condition to:

Initial Condition		
$C_{A0} = -1$	$C_{B0} = 10$	$\theta_0 = -100$

The controller parameters used for simulations with this new initial condition are:

Controller Parameters (figure 4.3)		
$Q = \text{diag}([0\ \ 1\ \ 0.5])$	$R = 0$	$S = 0$
$P = 4$	$M = 2$	$\alpha = 0.6$

The simulation results are presented in figure 4.3.

From figure 4.3 it is clear that the SNLMPC scheme generates a response with offset in C_A and θ and for both controllers the output settles in

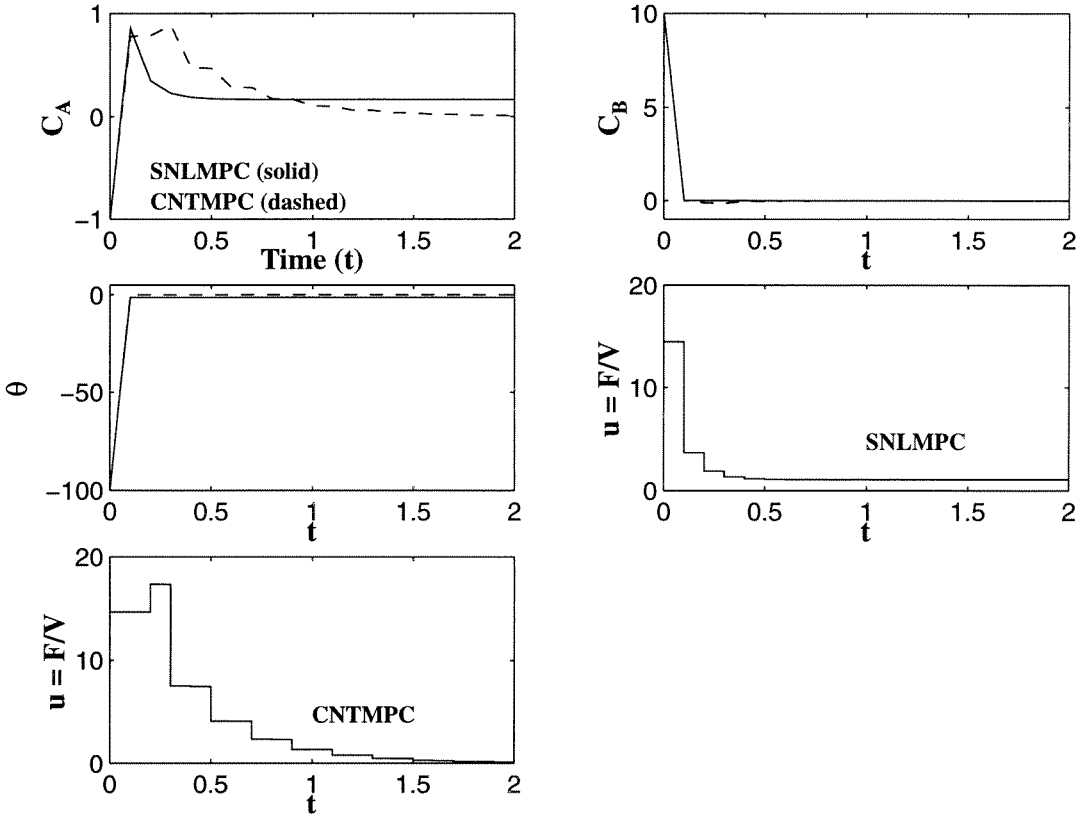

Figure 4.3: van der Vusse CSTR: State and control responses for SNLMPC and CNTMPC in the unconstrained **Case 2**.

approximately two sampling times for comparable control effort (slightly higher for CNTMPC).

Case 3

As we have seen, in **Case 1** and **Case 2** the responses of C_A, θ and $u = \frac{F}{V}$ obtained with SNLMPC show considerable offset while CNTMPC performs satisfactorily. In order to try to improve the performance obtained with SNLMPC and eliminate (or at least reduce) offset, we will choose a new set of controller parameters where the variables which have shown offset previously are now added more weight to in the objective function. The new set of controller parameters considered is the following:

Controller Parameters (figure 4.4)		
$Q = \text{diag}([0.5\ \ 1\ \ 1])$	$R = 0.1$	$S = 0$
$P = 4$	$M = 2$	$\alpha = 0.6$

The initial condition used in **Case 3** is the same one of **Case 2**.

The simulation results are shown in figure 4.4.

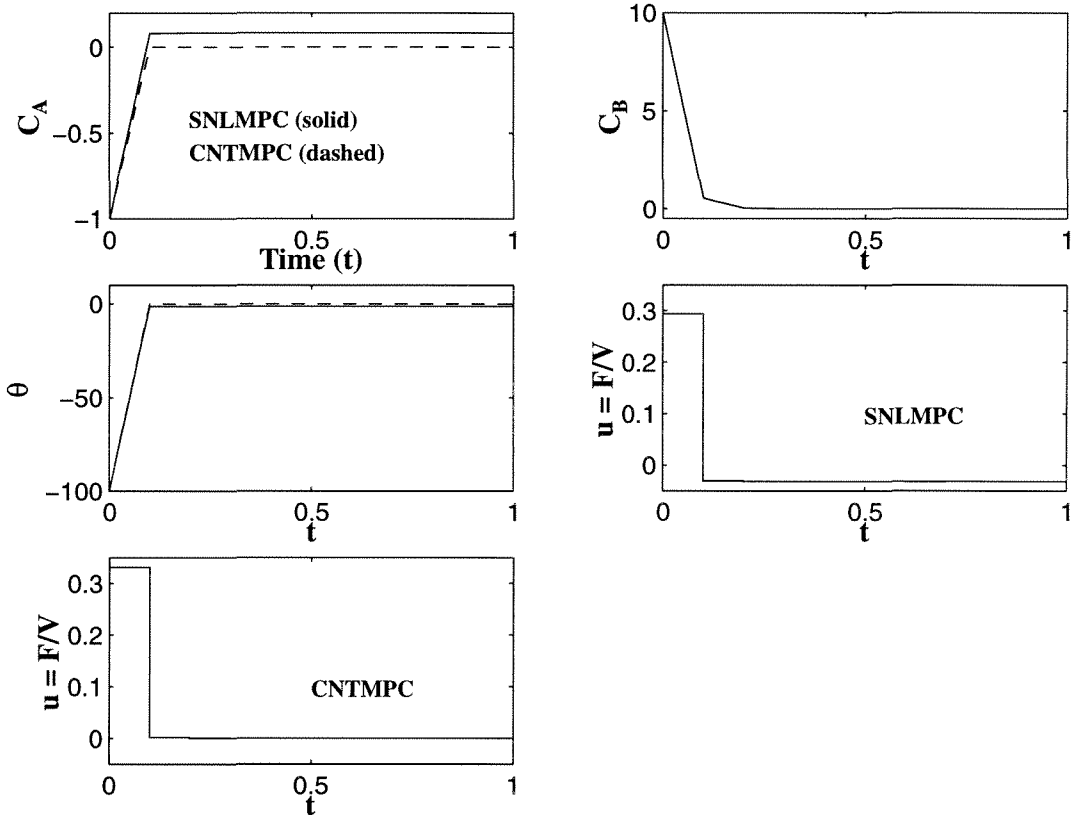

Figure 4.4: van der Vusse CSTR: State and control responses for SNLMPC and CNTMPC in the unconstrained **Case 3**.

From figure 4.4 we can see that in spite of the increased weights in the objective function, the simulations with SNLMPC still show offsets in C_A, θ and $u = \frac{F}{V}$. The offset in C_A decreased to about half its value in **Case 2** but the offset in θ remained the same. Different sets of weights and horizons have also been tried out but we did not succeed in improving the quality of the response obtained with SNLMPC. Regarding CNTMPC, we see that the new set of controller parameters reduces the control effort very

significantly compared to **Case 2** (compare figures 4.4 and 4.3) without compromising the response of the state variables.

So, as we see, it is very hard to adjust parameters in SNLMPC controllers in an ad hoc manner and predict the response. The contractive constraint takes away this guess work since, if the problem is feasible at the beginning of all prediction horizons, then exponential stability can be assured.

Constrained case

Since the performance displayed by SNLMPC in the unconstrained case was very poor and the presence of constraints will only deteriorate the response even further, here we will only show simulations obtained with CNTMPC.

The controller parameters used in these simulations are the following:

Controller Parameters (figure 4.5)		
$Q = \text{diag}([0\ \ 1\ \ 0.5])$	$R = 0$	$S = 0$
$P = 4$	$M = 2$	$\alpha = 0.6$
$u_{min} = 0$	$u_{max} = 1$	

The initial condition is the same used in the unconstrained **Case 2**. Thus, we have the same control problem as in the unconstrained **Case 2** but now the input variable is tightly constrained (since the maximum value of u in the unconstrained simulations was higher than 18, as we can see from figure 4.3).

The simulation results are found in figure 4.5.

By comparing figures 4.3 and 4.5 we can see that the presence of input constraints does not deteriorate the response of any of the states.

(2) Exponentially decaying additive disturbance

Here we will look at the responses of both SNLMPC and CNTMPC when an exponentially decaying additive disturbance acts on the system, i.e., given a nominal

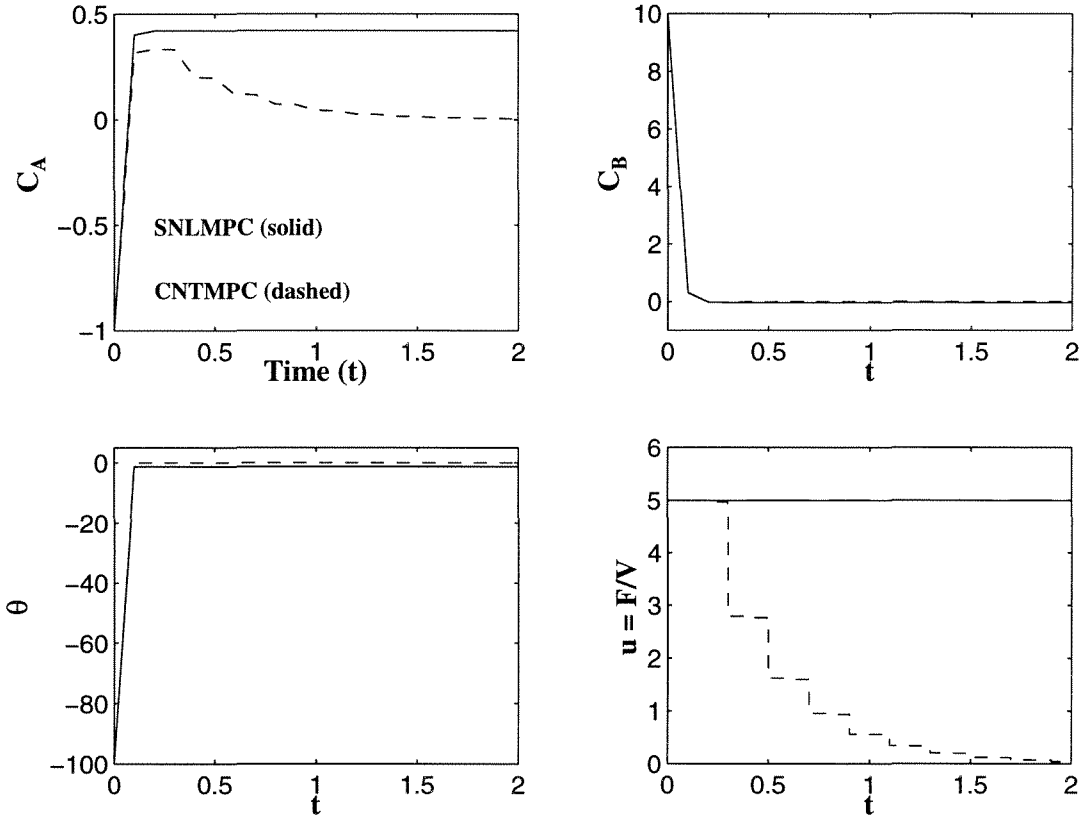

Figure 4.5: van der Vusse CSTR: State and control responses for CNTMPC in the constrained case.

system of the form

$$\dot{x}(t) = f(x(t), u(t)),$$

the "perturbed" system is given by:

$$\dot{x}^p(t) = f(x^p(t), u(t)) \; + \; d(t)$$

with $d(t)$ being an exponentially decaying deterministic disturbance.

The kind of disturbances which will be treated here are of the form:

$$d_i(t) \; = \; a_i \; e^{-b_i t}, \quad a_i, \; b_i > 0, \quad \text{for } i = 1, 2, \ldots$$

Thus, for different simulations, we will just use different values of a_i and b_i. a_i

determines an upper bound on the magnitude of the disturbance $d_i(t)$ (its initial value) and b_i its "duration" (the smaller b_i is, the longer the disturbance lasts).

We will examine unconstrained and constrained responses of both SNLMPC and CNTMPC to two different disturbances:

Disturbances	
d_1	d_2
$a_1 = 50$	$a_2 = 100$
$b_1 = 0.1$	$b_1 = 0.5$

Thus, disturbance d_1 has an upper bound which is half the size of the upper bound on d_2 but it has a longer duration.

Unconstrained case

The simulation results for d_1 and the disturbance itself are illustrated in figure 4.6. For d_2, the corresponding figure is 4.7.

The controller parameters and initial condition used in the simulations with disturbances d_1 and d_2 are given by:

Controller Parameters (figures 4.6 and 4.7)		
$Q = \text{diag}([0.5 \;\; 1 \;\; 0.1])$	$R = 0$	$S = 0$
$P = 4$	$M = 2$	$\alpha = 0.5$

Initial Condition		
$C_{A0} = -2$	$C_{B0} = 20$	$\theta_0 = -200$

From figures 4.3, 4.4, 4.6, 4.7 we notice that the disturbances have actually favored the asymptotic responses of C_A and θ in the case of the SLNMPC controller. The offsets, which we could not eliminate with various choices of

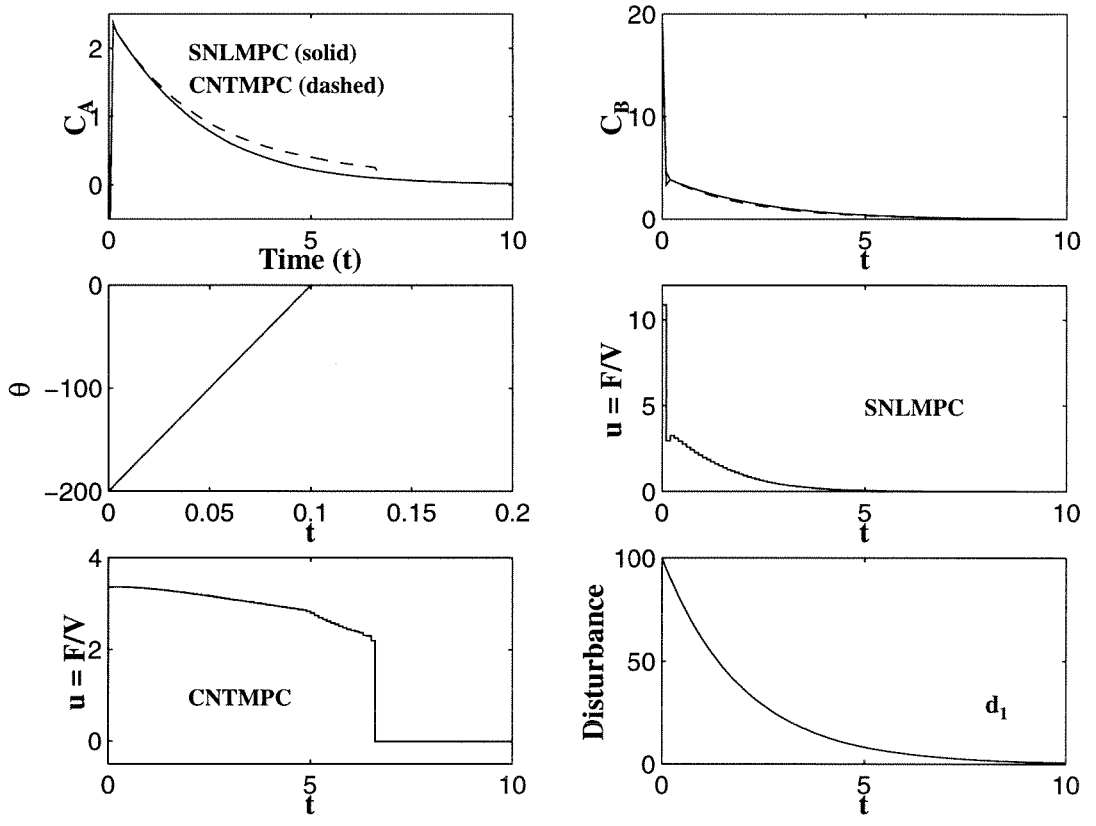

Figure 4.6: van der Vusse CSTR: State and control responses for SNLMPC and CNTMPC in the unconstrained case and under exponentially decaying disturbance d_1.

controller parameters in the absence of disturbances, are eliminated here due to the constant excitation that the exponentially decaying disturbance provokes on $\dot{C}_A$ and $\dot{\theta}$. For both controllers, θ settles to its steady state value in only one sampling time. However, the responses for C_A and C_B are slowed down very significantly (especially in the case of the longer lasting disturbance d_2).

For both disturbances, the SNLMPC and CNTMPC controllers originate very similar state responses but the initial control effort demonstrated by SNLMPC is always higher than the one needed by CNTMPC for virtually the same performance. Especially for d_1, which is a disturbance of large magnitude in the beginning, the CNTMPC controller has an initial control effort almost four times smaller than SNLMPC. In both cases, we have let the optimization routine find the initial guess for the input values so the higher initial control effort of

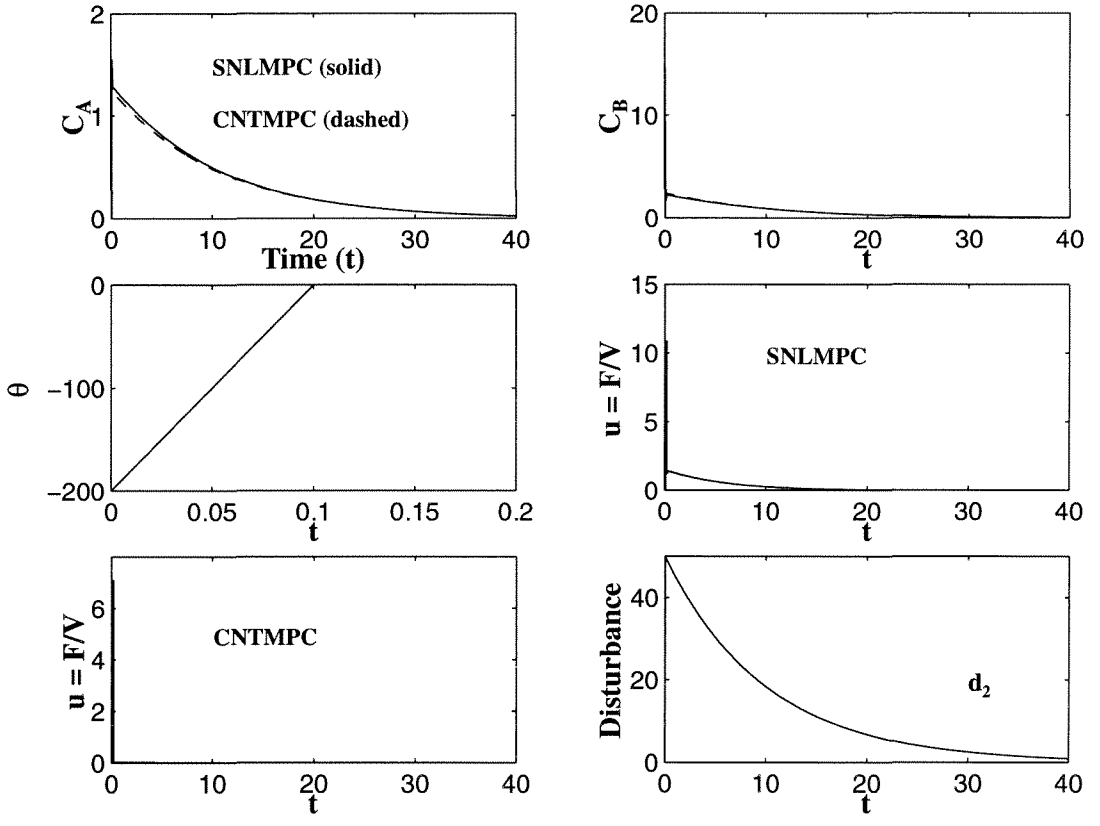

Figure 4.7: van der Vusse CSTR: State and control responses for SNLMPC and CNTMPC in the unconstrained case and under exponentially decaying disturbance d_2.

SNLMPC cannot be attributed to inappropriate initialization of this controller.

Constrained case

Since d_2 was a harder disturbance to eliminate in the unconstrained case, we will only look at constrained simulations with SNLMPC and CNTMPC under the influence of d_2.

The controller parameters used in these simulations are:

Controller Parameters (figure 4.8)		
$Q = \text{diag}([0.5 \;\; 1 \;\; 0.1])$	$R = 0$	$S = 0$
$P = 4$	$M = 2$	$\alpha = 0.5$
$u_{min} = 0$	$u_{max} = 1$	

The simulation results are illustrated in figure 4.8.

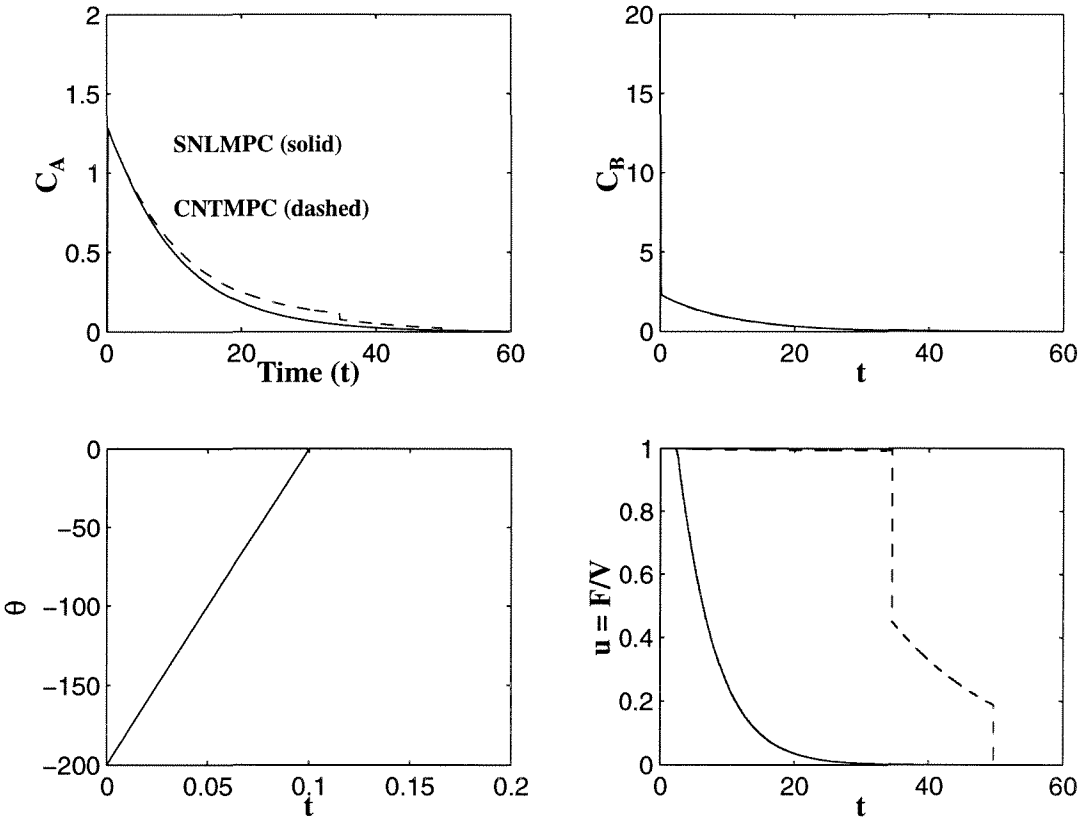

Figure 4.8: van der Vusse CSTR: State and control responses for SNLMPC and CNTMPC in the constrained case and under exponentially decaying disturbance d_2.

The results in figure 4.8 show that the two controllers perform equally well and that the presence of the constraints does not degrade the performance (compare with figure 4.7).

(3) Output feedback case with a nonlinear asymptotically convergent observer

Here we will study the output feedback case for both controllers, SNLMPC and CNTMPC. For state estimation, an asymptotically convergent observer will be used. In this chapter, we have proposed a formulation for such a nonlinear observer, designed for continuous-time systems with discrete observations. As we have seen, solving for

the current state estimates means that we have to find the solution of a differential Riccati equation. Since it is inconvenient to solve this kind of equation, we will use a discrete version of our proposed observer which involves the solution of a simple algebraic Riccati equation. This observer is a discrete extended Kalman filter and it has been proven exponentially stable for discrete-time systems, for initial conditions in a certain set and for systems which are not too strongly nonlinear (see [118]).

Let us consider a nonlinear system of the following form:

$$\dot{x}_k(t) = f(x_k(t), u_k(t)), \quad x_0 \text{ unknown}, \quad \text{for } t \in [t_k, t_{k+1}] \tag{4.102}$$

$$y_k = h(x_k, u_k), \quad \forall k \geq 0 \tag{4.103}$$

and its associated "noisy" system:

$$\dot{x}_k^p(t) = f(x_k^p(t), u_k(t)) + N_w \bar{w}_k \tag{4.104}$$

$$y_k^p = h(x_k^p, u_k) + R_\nu \bar{\nu}_k \tag{4.105}$$

Then, the extended Kalman filter for the associated system is given by the following equations:

Measurement update:

$$\hat{x}_k = \bar{x}_k + K_k \left[y_k^p - h(\bar{x}_k, u_k)\right], \tag{4.106}$$

$$P_k^{-1} = \bar{P}_k^{-1} + C_k^{'} \left(R_\nu R_\nu^{'}\right)^{-1} C_k \tag{4.107}$$

Time update:

$$\bar{x}_{k+1} = \hat{x}_k + \int_{t_k}^{t_{k+1}} f(\bar{x}_k(t), u_k(t))\, dt \tag{4.108}$$

$$\bar{P}_{k+1} = A_k P_k A_k^{'} + N_w N_w^{'} \tag{4.109}$$

where:

$$K_k := \bar{P}_k C_k' \left(C_k \bar{P}_k C_k' + R_\nu R_\nu'\right)^{-1} \tag{4.110}$$

$$A_k := \frac{\partial f}{\partial x}(\hat{x}_k) \tag{4.111}$$

$$C_k := \frac{\partial h}{\partial x}(\bar{x}_k) \tag{4.112}$$

As usual, x_0^p, $\bar{\nu}_k$, $\bar{w}_k$, are assumed jointly Gaussian and mutually independent. Furthermore, $x_0^p \sim \mathcal{N}(\bar{x}_0, \bar{P}_0)$, $w_k \sim \mathcal{N}(0, I_n)$ and $\nu_k \sim \mathcal{N}(0, I_p)$. N_m, R_ν and $\bar{P}_0$ are design variables and they should be chosen such that N_w has rank n and R_ν and $\bar{P}_0$ are positive definite.

Here we will define the "scaled" noises $w_k := N_w \bar{w}_k$ and $\nu_k := R_\nu \bar{\nu}_k$ and these are the noise variables which will be plotted.

Let us compare the responses obtained in the output feedback case for the SNLMPC and CNTMPC controllers. In our case, $C_k = [0 \quad 1 \quad 0]'$, i.e., C_B is our "noisy" measured output.

Unconstrained case

The simulations for this case are illustrated in figure 4.9. The dynamic and output noises, namely, w_k and ν_k, are also shown in figure 4.9.

The initial conditions for integration of the plant and for state estimation are chosen as:

Initial Conditions			
Plant:	$C_{A0} = -2$	$C_{B0} = 20$	$\theta_0 = -200$
Model/Observer:	$\bar{C}_{A0} = -1.5$	$\bar{C}_{B0} = 15$	$\bar{\theta}_0 = -150$

The controller and estimator parameters used in these simulations are given by:

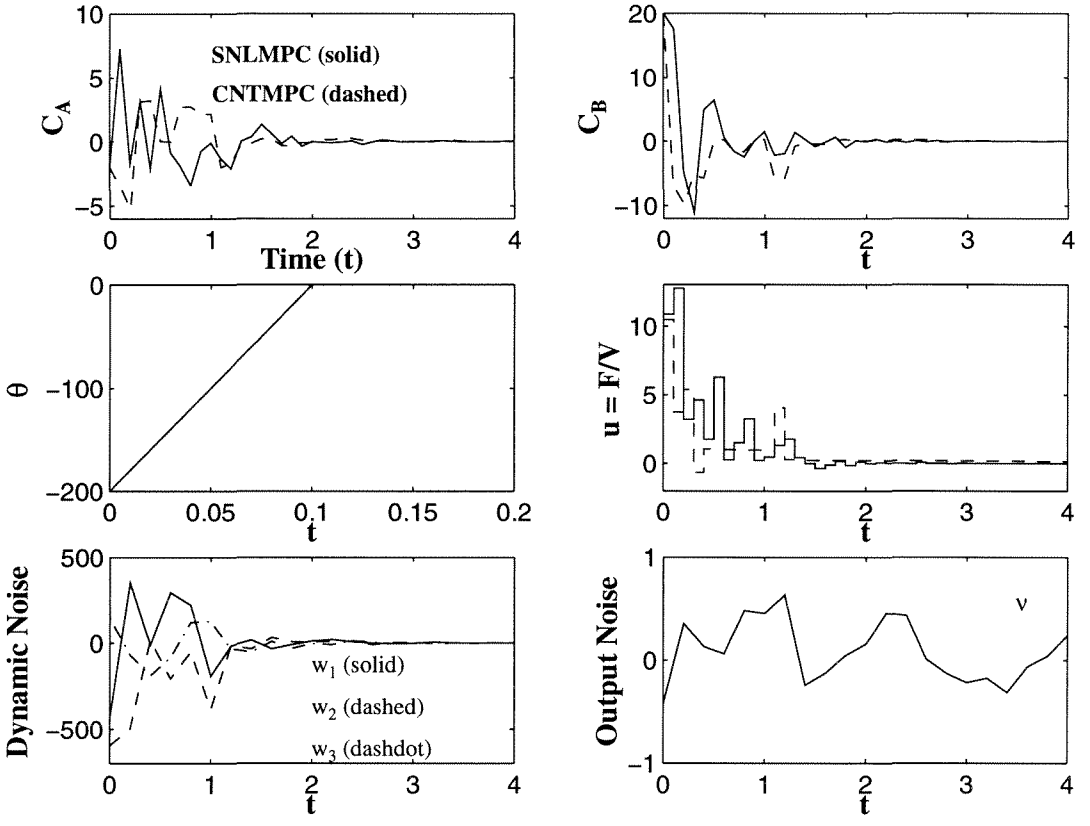

Figure 4.9: van der Vusse CSTR: State and control responses for SNLMPC and CNTMPC in the unconstrained output feedback case.

Controller and Estimator Parameters (figure 4.9)		
$Q = \text{diag}([0.5 \;\; 1 \;\; 0.1])$	$R = 0$	$S = 0$
$P = 4$	$M = 2$	$\alpha = 0.7$
		$\bar{P}_0 = I_n$

Our results show that, in spite of the initial state estimation error, θ responds in only one sampling interval. However, the responses of the other two variables are dramatically affected by the noise in the system. We also notice that the CNTMPC responses for C_A and C_B are much less oscillatory than the ones produced by SNLMPC. The same observation extends to the control profile which is not only less oscillatory in the CNTMPC case, but also displays a smaller control effort.

Constrained case

The simulations for the constrained case can be found in figure 4.10. The dynamic and output noises, namely, w_k and ν_k, are also shown in figure 4.10.

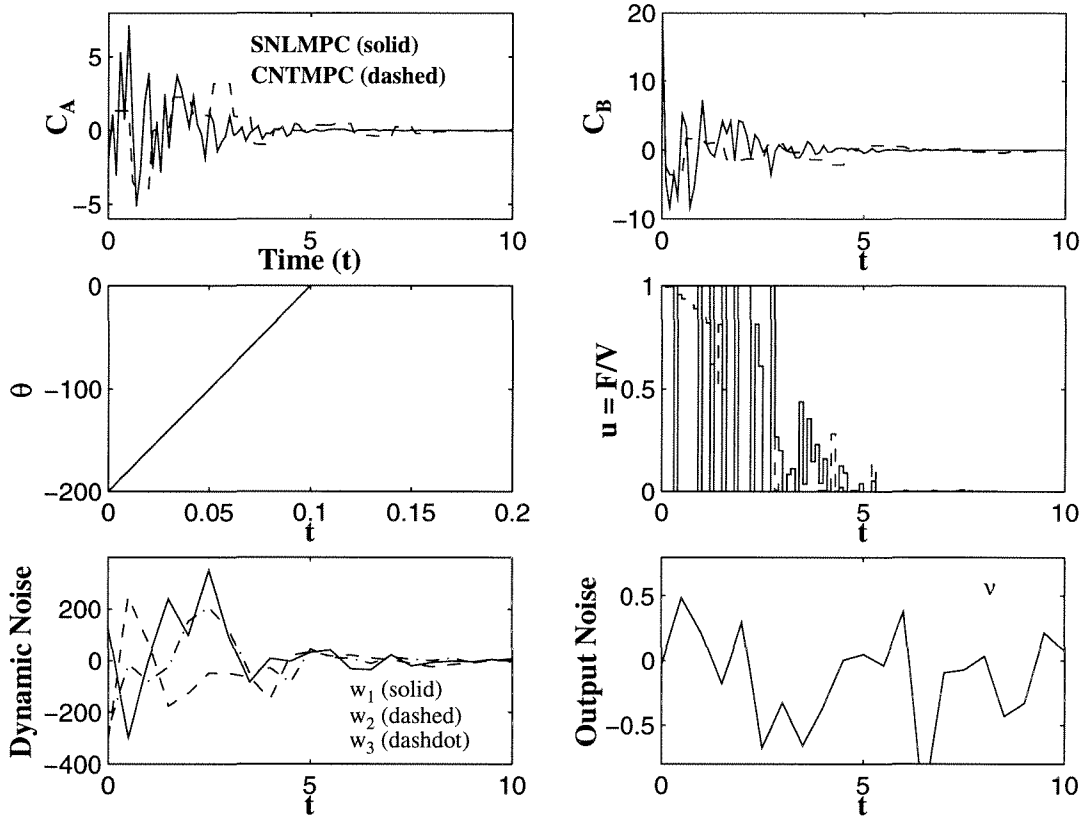

Figure 4.10: van der Vusse CSTR: State and control responses for SNLMPC and CNTMPC in the constrained output feedback case.

For the constrained responses we utilized the same initial conditions as in the unconstrained case and the following controller and estimator parameters:

Controller and Estimator Parameters (figure 4.10)		
$Q = \text{diag}([0.5 \;\; 1 \;\; 0.1])$	$R = 0$	$S = 0$
$P = 8$	$M = 5$	$\alpha = 0.9$
$u_{min} = 0$	$u_{max} = 1$	$\bar{P}_0 = I_n$

Notice that we needed to increase the prediction and control horizons, and the contractive parameter as well, in order to guarantee feasibility in the constrained case. Once again, θ responds in only one sampling time for both controllers.

As we can see from figures 4.9 and 4.10, even though the responses for CNTMPC and SNLMPC were very similar in the unconstrained case, the performance shown by CNTMPC in the presence of input constraints is much superior to that shown by SNLMPC. Even though the response speed is basically the same, C_A and C_B are much more affected by the noises when SNLMPC is used (which is revealed by their highly oscillatory behavior). Thus, in the presence of constraints, the beneficial effects of the introduction of the contractive constraint can be felt more strongly than in the unconstrained case.

Chapter 5 Robust Output Feedback Contractive NLMPC: Parameter Uncertainty

In this chapter we will be dealing with the following problem:

Problem 4 *: State feedback in the robust case (parameter uncertainty only)*

5.1 Introduction

In the previous chapter we looked into the stabilizing properties of **Control Algorithm 3** in the nominal case and when the states of the plant are not available for measurement and must therefore be estimated. We have shown that the output feedback case with use of an asymptotically convergent nonlinear observer is equivalent to the state feedback case when the plant is subjected to an asymptotically decaying additive disturbance which is not being estimated.

Since **Control Algorithms 1** and **2** were proven exponentially stabilizing in the nominal case and in the absence of disturbances, we could show in the previous chapter that the association of such a controller with **Estimation Procedure 1** (in the fashion shown in **Control Algorithm 3**) generates an asymptotically stable closed-loop system.

In this chapter we will explore the stabilizing properties of **Control Algorithm 1**

when the plant is subjected to a non-additive disturbance (a disturbance which is part of the nonlinear dynamics of the plant) which is not considered in the prediction step (i.e., the model used for prediction does not take into account the disturbance). The only assumption on the disturbance behavior is that it is bounded, i.e., it remains inside a convex and compact set containing the origin for all $t \geq 0$. From the controller design point of view, bounded, deterministic or stochastic, disturbances introduce a very different (and more complex) problem than asymptotically decaying disturbances. It is no longer possible to drive the states to the origin. If the disturbance is unknown but bounded (as in our assumption) then the best that can be hoped for is that the states are steered to a control invariant set and that is what will be shown here later.

A disturbance of this kind, which modifies the nonlinear dynamics of the plant, introduces a model/plant mismatch and makes it necessary for the designed controller to be *robust*. In the nonlinear context, there is no difference between this kind of disturbance and bounded parameter uncertainty.

After showing how the presence of this bounded disturbance affects the stabilizing properties of **Control Algorithm 1** under state feedback, we will then look into the output feedback case. This time we will use a least squares nonlinear state estimator to study the resulting stability properties of the closed-loop system.

First we will specialize the obtained results for the case where the dynamics of the plant is influenced by a set of *constant* unknown parameters which are not estimated. Then we will explore the case where the parameters can be time-varying and the estimation step is a combined nonlinear state/parameter least squares estimation procedure as proposed in [111].

5.2 Stability of contractive MPC in the presence of bounded disturbances

Let us now consider a nonlinear plant specified by the following set of equations:

$$\dot{x}^p(t) = f(x^p(t), u(t), d(t)) \tag{5.1}$$

with $f : \Re^n \times \Re^m \times \Re^q \to \Re^n$ continuously differentiable and where $d(t) \in \Re^q$ is an unknown bounded time-varying disturbance which belongs to a compact and convex set D for all $t \geq 0$, with $0 \in D^\circ$ (where $D^\circ :=$ interior(D)). More specifically, let $D := B_{\rho^d} := \{d \in \Re^q : \| d \| \leq \rho^d\}$.

Let the model used in the prediction step of our MPC algorithm be given by:

$$\dot{x}(t) = f(x(t), u(t), 0) \tag{5.2}$$

Thus, we are considering the case where no structural model/plant mismatch exists. The disturbance can also be seen as a set of unknown time-varying parameters and, in that case, we have a robust control problem at hand where the model error is due exclusively to parameter uncertainty.

5.2.1 Basic assumptions

The following assumptions are necessary in the derivation of the results in this section:

Assumption 5.1 $(x, u, d) \Longrightarrow f(x, u, d) : \Re^n \times \Re^m \times \Re^q \to \Re^n$ *is at least twice continuously differentiable and* $f(0, 0, 0) = 0$.

Our usual feasibility assumption:

Assumption 5.2 *We assume that there exists a* $\rho \in (0, \infty)$ *such that for all* $x_k \in B_\rho$, $\mathcal{P}(t_k, x_k)$ *is feasible. In other words, for all* $x_k \in B_\rho$, *we can find a contractive parameter* $\alpha \in [0, 1)$ *so that with the chosen finite horizon* P, *all the constraints on the inputs and states can be satisfied and the objective function is finite.*

Assumption 5.3 *The continuous function* f *is locally Lipschitz continuous, i.e, there exists a finite constant* $L > 0$ *such that:*

$$\begin{aligned} \| f(x_1, u_1, d_1) - f(x_2, u_2, d_2) \|_{\hat{P}} \;\leq\; & L \, [\, \| x_1 - x_2 \|_{\hat{P}} + \| u_1 - u_2 \| + \| d_1 - d_2 \| \,], \\ & \forall x_1, x_2 \in \Re^n, \; u_1, u_2 \in \mathcal{U}, \; d_1, d_2 \in B_{\rho^d} \end{aligned} \tag{5.3}$$

with $\mathcal{U}$ *defined, as usual, by:*

$$u(t) \in \mathcal{U} := \{ u \in \Re^m : u_{min} \leq u \leq u_{max} \}, \;\; \forall t \in [0, \infty) \tag{5.4}$$

Remark 5.1 *Strictly speaking, assumption 5.3 only needs to be satisfied for* $x_1, \; x_2 \in \mathcal{X}$, *where* $\mathcal{X}$ *is the reachable set defined in this case by:*

$$\begin{aligned} \mathcal{X} \;:=\; & \{ x^p(t) = x^p(t, t_0, x_0^p, u, d) \text{ or } x(t) = x(t, t_0, x_0^p, u, 0), \; t \in [t_0, \infty); \\ & x_0^p \; \in B_\rho, \; u \in \mathcal{U}, \; d \in B_{\rho^d} \} \end{aligned} \tag{5.5}$$

Since this condition cannot be checked a priori (given that $x^p(t)$, $x(t)$ *are trajectories generated through application of the controller), we require the Lipschitz condition on* f *to be valid everywhere in the state space.*

5.2.2 Stability analysis of Control Algorithm 1

Under the previously established assumptions, the following result can be derived:

Theorem 5.1 (Bound on the difference between model and plant states in the presence of parameter uncertainty: state feedback case) *Let* $\rho \in (0, \infty)$ *and* $L \in [0, \infty)$ *satisfy assumptions 5.2 and 5.3, respectively. Then if* $x_k^p, x_k \in B_\rho$, $\forall k \geq 0$, *there exist* λ, $\bar{\lambda} \in [0, \infty)$ *such that:*

$$\| x_k^p - x_k \|_{\hat{P}} \leq \lambda, \tag{5.6}$$

$$\| x_k^p - \bar{x}_k \|_{\hat{P}} \leq \bar{\lambda}, \quad \forall k > 0 \tag{5.7}$$

with λ, $\bar{\lambda} \to 0$ *as* $\rho^d \to 0$.

Proof: *Using the notation in* **Control Algorithm 1**, *the difference between the dynamics of the plant (5.1) and that of the model (5.2) for a fixed* k, $k \geq 0$, *is given by:*

$$\dot{x}_k^{p,j}(t) - \dot{x}_k^j(t) = f(x_k^{p,j}(t), u_k^j(t), d_k^j(t)) - f(x_k^j(t), u_k^j(t), 0), \quad t \in [t_k^j, t_k^{j+1}] \tag{5.8}$$

where $j = 0, \ldots, P-1$.

By integrating (5.8), knowing that x_k^j *is set to* $x_k^{p,j}$, *we get:*

$$x_k^{p,j}(t) - x_k^j(t) = \int_{t_k^j}^{t} [f(x_k^{p,j}(\tau), u_k^j(\tau), d_k^j(\tau)) - f(x_k^j(\tau), u_k^j(\tau), 0)]\, d\tau \tag{5.9}$$

Then, it follows that:

$$\begin{aligned} \| x_k^{p,j}(t) - x_k^j(t) \|_{\hat{P}} &\leq \int_{t_k^j}^{t} \| f(x_k^{p,j}(\tau), u_k^j(\tau), d_k^j(\tau)) - f(x_k^j(\tau), u_k^j(\tau), 0) \|_{\hat{P}} \, d\tau \leq \\ &\leq L \int_{t_k^j}^{t} [\| x_k^{p,j}(\tau) - x_k^j(\tau) \|_{\hat{P}} + \| d_k^j(\tau) \|] d\tau \end{aligned} \tag{5.10}$$

Using the BG inequality and the fact that $\| d_k^j(t) \| \leq \rho^d$, $j \in [0, P-1]$, $\forall k \geq 0$, *and making* $t = t_k^{j+1}$, *it results that:*

$$\| x_k^{p,(j+1)} - x_k^{j+1} \|_{\hat{P}} \leq \rho^d L T e^{LT} \tag{5.11}$$

In particular, if $j = P - 1$, *we have:*

$$\| x_{k+1}^p - x_{k+1} \|_{\hat{P}} := \| x_k^{p,P} - x_k^P \|_{\hat{P}} \leq \rho^d L T e^{LT} =: \lambda, \qquad \forall k \geq 0 \tag{5.12}$$

Since the trajectory $\bar{x}(t)$ *is only updated with the states of the plant at the end of prediction horizons, the integration of (5.8) is carried out from* t_k *to* t_{k+1} *and the following bound is obtained:*

$$\| x_{k+1}^p - \bar{x}_{k+1} \|_{\hat{P}} \leq \rho^d L P T e^{LPT} =: \bar{\lambda} \tag{5.13}$$

Thus, λ, $\bar{\lambda} \to 0$ *as* $\rho^d \to 0$, *which is the result we wanted to prove.*

□

Theorem 5.2 (Stabilizing properties of the state feedback controller in the presence of parameter uncertainty) *Under our assumptions and if* $x_k^p, x_k \in B_\rho$, $\forall k \geq 0$, *then it follows that:*

$$\| x_k^p \|_{\hat{P}} < \| x_0^p \|_{\hat{P}} + \gamma \tag{5.14}$$

and

$$\lim_{k \to \infty} \| x_k^p \|_{\hat{P}} < \gamma \tag{5.15}$$

with $\gamma \to 0$ *as* $\rho^d \to 0$. *Thus, since we have a bounded disturbance which does not necessarily decay to zero asymptotically, the states converge to the interior of a control invariant set* $B_\gamma := \{x \in \Re^n \mid \| x \|_{\hat{P}} \leq \gamma\}$.

Proof: *Since the contractive constraint imposes* $\| \bar{x}_{k+1} \|_{\hat{P}} \leq \alpha \| x_k^p \|_{\hat{P}}$, *then using the triangle inequality and equation (5.11) it results that:*

$$\| x_{k+1}^p \|_{\hat{P}} \leq \| \bar{x}_{k+1} \|_{\hat{P}} + \rho^d LPTe^{LPT} \leq \alpha \| x_k^p \|_{\hat{P}} + \rho^d LPTe^{LPT} \tag{5.16}$$

Then, using lemma 4.1, we arrive at the following bounds:

$$\| x_k^p \|_{\hat{P}} < \| x_0^p \|_{\hat{P}} + \frac{\rho^d LPTe^{LPT}}{1 - \alpha} \tag{5.17}$$

and

$$\lim_{k \to \infty} \| x_k^p \|_{\hat{P}} < \frac{\rho^d LPTe^{LPT}}{1 - \alpha} =: \gamma \tag{5.18}$$

So, $\gamma \to 0$ *as* $\rho^d \to 0$, *which is the result we wanted to prove.*

□

Theorem 5.3 (Feasibility condition) *Under the previously established assumptions on the function f and on the disturbance d, if $\gamma < \rho$, then there exists $\rho_0 \in (0, \rho]$ such that for all $x_0^p \in B_{\rho_0}$, the sequences $\{x_k^p\}_{k=0}^{\infty}$ and $\{x_k\}_{k=0}^{\infty}$ resulting from use of* **Control Algorithm 1** *are well-defined and stay inside the set B_ρ.*

Proof: *Due to our Lipschitz continuity assumption on f, the proof is very similar to the one presented in the previous chapter for additive disturbances and will be omitted here for that reason.*

□

Remark 5.2 *If instead of a bounded time-varying disturbance we have a constant unknown parameter $p \in \Re^q$, i.e., the dynamics of the plant is given by:*

$$\dot{x}^p(t) = f(x^p(t), u(t), p) \tag{5.19}$$

and the model used in the prediction is:

$$\dot{x}(t) = f(x(t), u(t), \bar{p}) \tag{5.20}$$

where $\bar{p} \in \Re^q$ is the nominal parameter value, then in the state feedback case, the states converge asymptotically to a control invariant set $B_{\bar{\gamma}}$, i.e., $\lim_{k\to\infty} \| x_k^p \|_{\hat{P}} < \bar{\gamma}$, with $\bar{\gamma}$ given by:

$$\bar{\gamma} := \frac{LPTe^{LPT}}{1-\alpha} \| p - \bar{p} \| \tag{5.21}$$

i.e., ρ^d is replaced by the weighed norm of the difference between true and nominal parameter values. Naturally, $\bar{\gamma} = 0$ if $p = \bar{p}$.

In the following section we will address the following problem:

Problem 5 : *Output feedback in the robust case (parameter uncertainty only)*

5.3 Stability of MPC + state estimation scheme in the presence of parameter uncertainty

In the previous section we have analyzed the stability of **Control Algorithm 1** when unknown bounded disturbances or unknown constant parameters affect the dynamics of the system. We saw that in the case of parameter uncertainty, the states of the plant converge asymptotically to a control invariant set whose size is proportional to the weighted norm of the difference between true and nominal parameter values, i.e.,

$$\lim_{k\to\infty} \| x_k^p \|_{\hat{P}} < \bar{\gamma} \sim \| p - \bar{p} \| \tag{5.22}$$

where the symbol $\sim$ means proportionality.

Now we want to study how this result is modified in the output feedback case when a nonlinear least squares procedure for state estimation is used in combination with **Control Algorithm 1**. The state estimation procedure used here is a moving horizon-based approach for least squares estimation which has been proposed by Robertson et al. in [111].

The dynamics of model and plant considered in this section are given by:

Plant:

$$\dot{x}^p(t) = f(x^p(t), u(t), p) \tag{5.23}$$

$$y_k^p = g(x_k^p, p) \tag{5.24}$$

Model:

$$\dot{x}(t) = f(x(t), u(t), \bar{p}) \tag{5.25}$$

$$y_k = g(x_k, \bar{p}) \tag{5.26}$$

where $x_k^p := x^p(t_k)$ and $x_k := x(t_k)$, with $t_k := t_1 + kT$, $k \geq 0$, t_1 is the initial time for computations and $p, \bar{p} \in \Re^q$ are the true and nominal parameter values, respectively.

5.3.1 Moving horizon formulation of the least squares estimation (LSE) procedure

The objective of batch state estimation at time t_k can be stated as:

> Given an initial estimate x_1 at t_1, the measurement sequence $\{y_1, \ldots, y_k\}$, and the model (5.25),(5.26), estimate the error in the initial estimate $x^e(1|k) := x(1|k) - x_1$.

Once estimates of the unknown states, $x(1|k)$, have been determined, the current state estimate, $x(k|k)$, is obtained via the model equations.

The size of the estimation problem posed in this way increases linearly with the number of measurements. For an estimation technique to be computationally feasible, we must be able to bound the number of variables to be estimated. The batch estimation problem can be modified to employ a fixed-size moving window in which

the number of measurements that we base our estimate on (and hence the size of the optimization) remains constant. The moving horizon state estimation problem at time t_k with horizon size of $m-1$ (here the horizon size is equal to the number of measurements used minus one) is formulated as follows:

Estimation Procedure 2

$$\min_{x^e(k-m+1|k)} \quad J(\bar{p}, x(k-m+1|k)) := \tfrac{1}{2}[(x^e(k-m+1|k))' P(k-m+1|k-1) \times \\ \times x^e(k-m+1|k) \; + \; \textstyle\sum_{l=k-m+1}^{k} \nu(l|k)' \bar{R}^{-1} \nu(l|k)] \qquad (5.27)$$

subject to:

$$\nu(l|k) \;=\; y_l^p - g(x(l|k), \bar{p}), \;\; l = k-m+1, \ldots, k \qquad (5.28)$$

$$\dot{x}(t|k) \;=\; f(x(t|k), u_{l-1}, \bar{p}), \; t \in [t_{l-1}, t_l], \;\; l = k-m+1, \ldots, k \qquad (5.29)$$

where $x^e(k-m+1|k) := x(k-m+1|k) - x(k-m+1|k-1)$, $x(l|k) := x(t_l|k)$ *and* $u(t)$ *is constant for* $t \in [t_{l-1}, t_l]$ *and equal to* u_{l-1}, *for all* $l \in [k-m+1, k]$.

$x(k-m+1|k-1)$ *represents the least squares estimate of* $x(k-m+1|k)$ *at* $t = t_{k-m+1}$ *obtained at time* t_{k-1} *and* $P(k-m+1|k-1)$ *is the weighting matrix expressing the confidence in the estimate (e.g., inverse of the conditional covariance of* $x(k-m+1|k)$ *at time* t_{k-1}*). At the beginning of the estimation, the number of measurements is allowed to grow until it reaches the size of the horizon (i.e., from* t_1 *to* t_m*). At the next time step the initial estimate* $x(1|m-1)$ *is replaced by* $x(2|m)$ *and the weighting matrix* $P(1|m-1)$ *is replaced by* $P(2|m)$*. The first measurement* y_1 *is discarded as the current measurement* y_{m+1} *is made available. This procedure is repeated at each time step, and the optimization remains at constant size for all future times. Given the probabilistic interpretation of* $P^{-1}(k-m+1|k-1)$ *as the covariance of*

$x(k-m+1|k) - x(k-m+1|k-1)$, we can calculate $P^{-1}(k-m+2|k)$ from $P^{-1}(k-m+1|k-1)$, $\forall k \geq m$, using linear filtering theory:

$$P^{-1}(k-m+1|k) = P^{-1}(k-m+1|k-1) - P^{-1}(k-m+1|k-1)\Xi' \times$$
$$\times[\Xi P^{-1}(k-m+1|k-1)\Xi' + \bar{R}]^{-1}\Xi P^{-1}(k-m+1|k-1) \quad (5.30)$$
$$P^{-1}(k-m+2|k) = \Phi P^{-1}(k-m+1|k)\Phi' \quad (5.31)$$

where $\Phi := \frac{\partial f}{\partial x}(x(k-m+1|k), u_{k-m+1}, \bar{p})$, $\Xi := \frac{\partial g}{\partial x}(x(k-m+1|k-1), \bar{p})$ and $\bar{R}^{-1}$ represents a quantitative measure of our confidence in the output model.

In [111], Robertson et al. have shown the equivalence between the well-known extended Kalman filter (EKF) technique and the moving horizon least squares algorithm when a linearized output model is used and $m = 1$. When $m = 1$ the state equations do not appear in the formulation and the problem becomes a *linear* least squares problem. The obtained solution corresponds to the measurement correction step of the EKF. Thus, the EKF-based moving horizon estimator is equivalent to the EKF when $m = 1$. Furthermore, the horizon size is the only additional tuning parameter other than the ones used in the EKF formulation.

The effect of increasing the horizon size is that the moving horizon estimator retains all of the most recent information and is more efficient than the EKF at summarizing past information (because it uses $m + 2$ instead of only three statistics as the EKF does). None of the information contained in the last m measurements is lost, and the estimation is based on the nonlinear model over this measurement horizon. When the system is linear, these two procedures are equivalent independent of the size of the horizon. However, when the system is nonlinear, the conditional density is non-Gaussian and use of the EKF means that some information will be lost.

5.3.2 Basic assumptions

Assumption 5.4 *We assume that for any* $p \in \Re^q$, $(x,u) = (0,0)$ *is an equilibrium point of the system (5.19), i.e.,* $f(0,0,p) = 0$ *and* $g(0,p) = 0$.

Assumption 5.5 *The feasibility assumption for the control problem* $\mathcal{P}(t_{m+nP}, x(m+nP|m+nP)), n \geq 0$,*is slightly altered in this case due to the fact that the contractive constraint will be imposed with respect to a state estimate* $2P$ *steps behind,* $x(m+(n-1)P|m+nP)$ *(instead of* P *steps behind as in the state feedback case), as we will see later. Also, since the contractive constraint is not changed for the period of one horizon, if* $\mathcal{P}(t_{m+nP}, x(m+nP|m+nP))$ *is feasible for a particular* $n \geq 0$, *then the subsequent* $P-1$ *control problems,* $\mathcal{P}(t_k, x(k|k))$, $k = m+nP+1, \ldots, m+(n+1)P-1$ *will be feasible as well.*

Thus, we will assume that there exists $\rho > 0$ *such that* $\mathcal{P}(t_k, x(k|k)), k \geq m$, *is feasible for all* $x(m+(n-1)P|m+nP)$, $x^p_{m+(n-1)P} \in B_\rho$, $\forall n \geq 0$.

The following assumptions hold for all $x_1, x_2 \in \Re^n$, $u_1, u_2 \in \mathcal{U}$, and arbitrary parameters p_1, p_2:

1. Assumptions on $f : \Re^n \times \Re^m \times \Re^q \to \Re^n$

   Assumption 5.6

   $$\| f(x_1,u_1,p_1) - f(x_2,u_2,p_1) \| \leq L_f(p_1) \, [\| x_1 - x_2 \| + \| u_1 - u_2 \|] \qquad (5.32)$$

   Then, if $u_2 = u_1$, *we have:*

   $$\| f(x_1,u_1,p_1) - f(x_2,u_1,p_1) \| \leq L_f(p_1) \; \| x_1 - x_2 \| \qquad (5.33)$$

   which implies that

$$\| \frac{\partial f}{\partial x}(x, u, p_1) \| \leq L_f(p_1) =: L_f \tag{5.34}$$

Assumption 5.7 *Growth condition on f:*

$$\| f(x_1, u_1, p_1) \| \leq \eta_f(p_1)[1 + \| x_1 \| + \| u_1 \|] =: \eta_f[1 + \| x_1 \| + \| u_1 \|] \tag{5.35}$$

Assumption 5.8

$$\| f(x_1, u_1, p_1) - f(x_1, u_1, p_2) \| \leq \gamma_f \| p_1 - p_2 \| \ [\| x_1 \| + \| u_1 \|] \tag{5.36}$$

Assumption 5.9 *From assumptions 5.6 and 5.8, we have:*

$$\begin{aligned} \| f(x_1, u_1, p_1) \ - \ & f(x_2, u_2, p_2) \| \leq L_f[\| x_1 - x_2 \| + \| u_1 - u_2 \|] + \\ + \ & \gamma_f \| p_1 - p_2 \| [\| x_1 \| + \| u_1 \|] \end{aligned} \tag{5.37}$$

2. Assumptions on $g : \Re^n \times \Re^q \to \Re^p$

Assumption 5.10

$$\| g(x_1, p_1) - g(x_2, p_1) \| \leq L_g(p_1) \| x_1 - x_2 \| \tag{5.38}$$

from which, it follows that:

$$\| \frac{\partial g}{\partial x}(x, p_1) \| \leq L_g(p_1) =: L_g \tag{5.39}$$

Assumption 5.11

$$\| g(x_1, p_1) - g(x_1, p_2) \| \leq \gamma_g \| p_1 - p_2 \| \| x_1 \| \tag{5.40}$$

Assumption 5.12 *From assumptions 5.10 and 5.11, it follows that:*

$$\| g(x_1, p_1) - g(x_2, p_2) \| \leq L_g \| x_1 - x_2 \| + \gamma_g \| p_1 - p_2 \| \| x_1 \| \tag{5.41}$$

Remark 5.3 *Assumptions 5.6, 5.7, 5.8, 5.9, 5.10, 5.11, 5.12 only need to be satisfied for x_1, x_2 inside the reachable set.*

With control computations starting at $t = t_m$ (after m measurements, $\{y_1, \ldots, y_m\}$, have been obtained), with the estimate for the unknown states of the plant, x_m^p, being denoted by $x(m|m)$, our reachable set, $\mathcal{X}$, for any values of p and $\bar{p}$, is defined as:

$$\begin{aligned} \mathcal{X} \;:=\; & \{x^p(t) = x^p(t, t_m, x_m^p, u, p) \text{ or } x(t) = x(t, t_m, x(m|m), u, \bar{p}),\ t \in [t_m, \infty); \\ & x_1^p,\ x(1|m) \in B_\rho,\ u \in \mathcal{U}\} \end{aligned} \tag{5.42}$$

Assumption 5.13 *Let $m\ p := m\ dim(y) \geq n := dim(x)$ and let $\hat{\mathcal{P}}(x(k - m + 1|k), \bar{p})$ denote the optimal estimation problem to be solved at time $t = t_k$ with $P(k - m + 1|k - 1) = 0,\ \forall k \geq m$, and $\bar{R} = I_p$ (i.e., the objective function is*

reduced to the sum of the output errors from $k-m+1$ to k) and in the absence of measurement noise, being $x(k-m+1|k)$ and $\bar{p}$ the decision variables and parameter values, respectively. Then, if $p=\bar{p}$ (no parameter uncertainty), $\hat{\mathcal{P}}(x(k-m+1|k),p)$ admits a unique optimal solution $x^*(k-m+1|k)$ which is equal to the states of the plant at t_{k-m+1}, i.e., $x^*(k-m+1|k)=x^p_{k-m+1}$.

Remark 5.4 *Since the objective function is quadratic in the output error, $\nu(l|k)$, $l=k-m+1,\ldots,k$, and in the decision variable $x^e(k-m+1|k)$, if both f and g (which represent the state and output model, respectively) are convex functions of $x(k-m+1|k)$, then the optimal estimation problem is convex. In this case, every local solution $x^*(k-m+1|k)$ is a global solution, and the set of global solutions is convex (see [46]). Furthermore, if f and g are such that $J(\bar{p},x^e(k-m+1|k))$ is strictly convex, then any global solution is also unique. 5.13.*

5.3.3 MPC with state estimation: implementation

In order to include the moving horizon least squares state estimation procedure, **Control Algorithm 1** has to be modified in the following way:

Control Algorithm 4

Data: *Initial Conditions: t_1 and x_1; Controller Parameters: P,M,Q,R,S, $\hat{P}$, α, $T,u_{min},u_{max},\Delta u_{max}$; Observer Parameters: $m-1=P$ (i.e., choose prediction horizon equal to estimation horizon), $P_1,\bar{R}$; Output measurement at t_1: y_1.*

Step 0: *Set $t=t_1$.*

Step 1: *Solve the optimal control problem $\mathcal{P}(t_1,x_1)$ (assuming that it is feasible for the chosen initial estimate x_1).*

Result: *Optimal (or feasible) control sequence* $\{u(1|1), \ldots, u(P|1)\}$ *with* $u(i|1) = u(M|1)$ *for* $i \in [M+1, P]$.

Step 2: *Apply the whole sequence of control moves* $\{u(1|1), \ldots, u(P|1)\}$ *to the plant, measuring the output at every sampling time. Thus, at* t_m *we have the sequence of* m *outputs* $\{y_1, \ldots, y_m\}$.

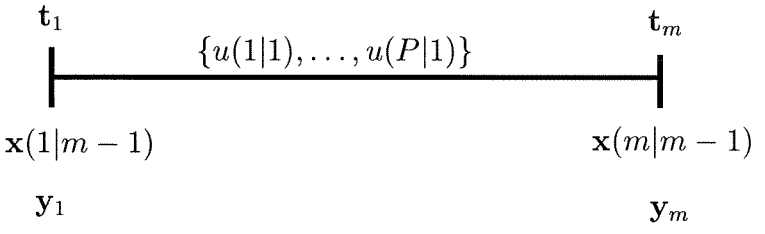

Step 3: *Set* $k = m$, $P(1|m-1) := P_1$ *and* $x(1|m-1) := x_1$.

Step 4: *With* $x(k-m+1|k-1), P(k-m+1|k-1)$, $\{y_{k-m+1}, \ldots, y_k\}$ *and the* $m-1$ *control moves most recently applied to the plant, calculate* $x(k-m+1|k)$ *by solving* $\hat{\mathcal{P}}(x(k-m+1|k), \bar{p})$.

Step 5: *Compute* $x(k|k)$ *by integrating the model equations (5.20) with the* $m-1$ *control moves most recently applied to the plant.*

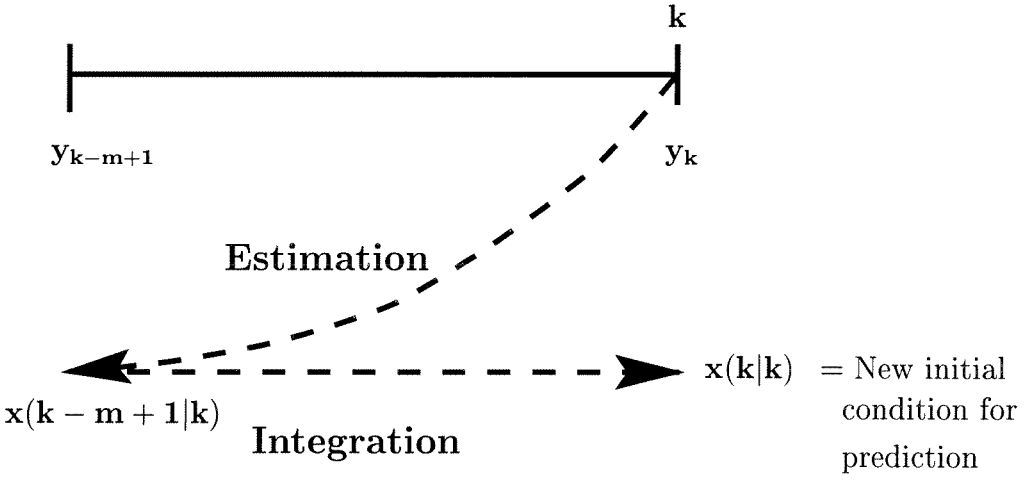

Step 6: *Solve the optimal control problem* $\mathcal{P}(t_k, x(k|k))$.

Result: $\{u(k|k), \ldots, u(k+M-1|k)\}$.

Step 7: *Apply* $u(k|k)$ *to the plant and measure the output at* t_{k+1}, y_{k+1}.

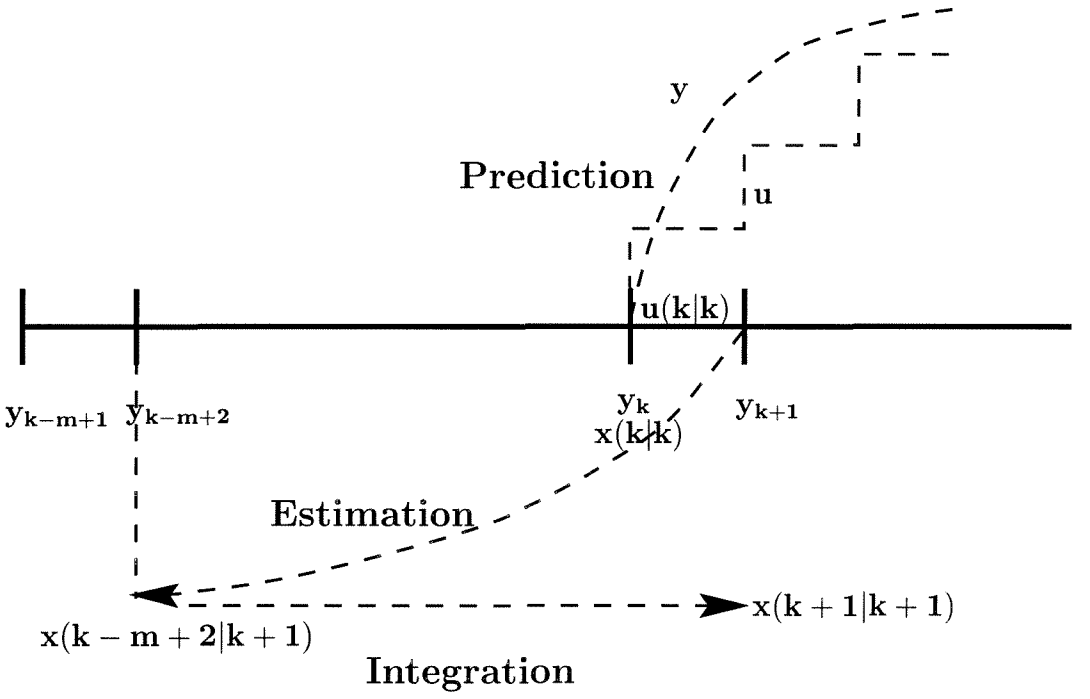

Step 8: *Set* $k = k+1$.

Step 9: *Compute* $P^{-1}(k-m+1|k-1)$ *from* $P^{-1}(k-m|k-2)$ *using equations (5.30) and (5.31) and go to* **Step 4**.

Remark 5.5 *For* $k \geq 2m-1$, *the* $m-1$ *control moves most recently applied to the plant are* $\{u(k-m+1|k-m+1), \ldots, u(k-1|k-1)\}$.

Remark 5.6 *It is important to notice that we can accept feasible solutions (instead of optimal solutions) of the control problem without interfering with the stability properties of the closed-loop. However, for the estimator, it is important that an optimal solution be found. This will be clear later in our stability analysis but it is important to call attention to this property of the algorithm at this point.*

Remark 5.7 *Here we will not address the issue of feasibility of the optimal estimation problem. We are assuming that $\hat{\mathcal{P}}(x(k-m+1|k), \bar{p})$ is feasible for all $k \geq m$ and that an optimal solution can always be found.*

Remark 5.8 *The optimal control problems $\mathcal{P}(t_1, x(1|m-1))$ and $\mathcal{P}(t_k, x(k|k))$, $k \geq m$, are formulated as in* **Control Algorithm 3** *with the only exception being the contractive constraint which is here given by:*

1. *Contractive constraint for $\mathcal{P}(t_1, x(1|m-1))$:*

$$\| x(m|m-1) \|_{\hat{P}} \leq \alpha \| x(1|m-1) \|_{\hat{P}} \tag{5.43}$$

2. *Contractive constraint for $\mathcal{P}(t_j, x(j|j))$ with $j = k-P, \ldots, k-1$ and $k = m + iP$, $i = 1, \ldots, \infty$:*

$$\| \bar{x}(k|j) \|_{\hat{P}} \leq \alpha \ \| x(k-2P|k-P) \|_{\hat{P}} =: \alpha \ \| x_{k-2P} \|_{\hat{P}} \tag{5.44}$$

Let us remember that the states $\bar{x}(t)$ are only updated with the estimated states at every t_{m+iP}, $i > 0$. The contractive constraint is only satisfied by the states of the model (i.e., not the predicted states) at $j = k-1$. Thus, we have:

$$\| \bar{x}(k|k-1) \|_{\hat{P}} \leq \alpha \| x_{k-2P} \|_{\hat{P}} \tag{5.45}$$

where $\bar{x}(k|k-1)$ are the states of the model used for computation of the contractive constraint at t_k and x_{k-2P} are the estimated states at $t_k - 2PT$.

Remark 5.9 *Note that the horizon for imposing the contractive constraint is now equal to $2P$ (instead of P, as in our previous algorithms). This is due to the association of the contractive MPC controller with the moving horizon least squares estimation scheme which has an estimation window equal to $m-1 = P$.*

Remark 5.10 *Our combined MPC + estimation procedure generates the following trajectories for the interval of* $2P$*:*

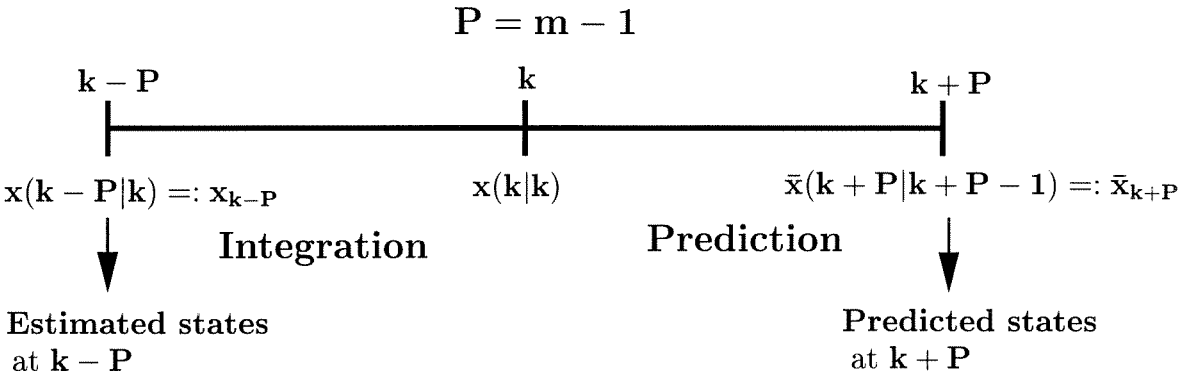

Contractive Constraint: $\| \bar{\mathbf{x}}_{\mathbf{k+P}} \|_{\hat{\mathbf{P}}} \leq \alpha \| \mathbf{x}_{\mathbf{k-P}} \|_{\hat{\mathbf{P}}}$

5.3.4 Stability analysis of Control Algorithm 4

The generalization of the classical implicit function theorem can be fruitfully used in various branches of mathematical analysis. Here we will enunciate the existence theorem for an implicit function and the classical implicit function theorem which we will then use as tools in the stability analysis of **Control Algorithm 4**.

Theorem 5.4 (Existence theorem for an implicit function) *Let* X *be a topological space, let* Y *and* Z *be Banach spaces, let* W *be a neighborhood of a point* (x_0, y_0) *in* $X \times Y$*, let* Ψ *be a mapping from* W *into* Z*, and let* $\Psi(x_0, y_0) = z_0$*.*

If

1. *the mapping* $x \to \Psi(x, y_0)$ *is continuous at the point* x_0*;*

2. *there exists a continuous linear operator* $\Lambda : Y \to Z$ *such that, given any* $\epsilon > 0$*, there exists a number* $\delta > 0$ *and a neighborhood* Ξ *of the point* x_0 *possessing*

the property that the condition $x \in \Xi$ *and the inequalities* $\| y' - y_0 \| < \delta$ *and* $\| y'' - y_0 \| < \delta$ *imply the inequality*

$$\| \Psi(x, y') - \Psi(x, y'') - \Lambda(y' - y'') \| < \epsilon \| y' - y'' \|; \tag{5.46}$$

3. $\Lambda Y = Z$;

then there exists a number $K > 0$, *a neighborhood* Υ *of the point* (x_0, y_0) *in* $X \times Z$ *and a mapping* $\varphi : \Upsilon \to Y$ *such that:*

- $\Psi(x, \varphi(x, z)) = z$;

  and

- $\| \varphi(x, z) - y_0 \| \leq K \ \| \Psi(x, y_0) - z \|$.

Theorem 5.5 (Classical implicit function theorem) *Let* X, Y *and* Z *be Banach spaces, let* W *be a neighborhood in* $X \times Y$, *and let* $\Psi : W \to Z$ *be a mapping of class* $C^1(W)$. *If*

1. $\Psi(x_0, y_0) = 0$,
2. *there exists the inverse operator* $[\Psi_y(x_0, y_0)]^{-1} \in \mathcal{L}(Z, Y)$,

then there exist $\epsilon > 0$, $\delta > 0$ *and a mapping* $\varphi : B^\circ(x_0, \delta) \to Y$ *(with* $B(x, r) := \{y \in \Re^{dim(x)} \mid \| y - x \| \leq r\}$ *and* $B^\circ(x, r) :=$ *interior*$(B(x, r))$*) of class* $C^1(B^\circ(x_0, \delta))$ *such that:*

- $\varphi(x_0) = y_0$;
- $\| x - x_0 \| < \delta \implies \| \varphi(x) - y_0 \| < \epsilon$ *and* $\Psi(x, \varphi(x)) = 0$;

- *the equality* $\Psi(x, y) = 0$ *is possible in the "rectangle"* $B^\circ(x_0, \delta) \times B^\circ(y_0, \epsilon)$ *only for* $y = \varphi(x)$;
- $\varphi'(x) = -[\Psi_y(x, \varphi(x))]^{-1}\Psi_x(x, \varphi(x))$.

Proof: *Proof of both theorems can be found in many books which address geometric differential methods. A good reference is [4].*

Now, let the operator Ψ be the gradient of the objective function (5.27) of the estimation problem. Then, since x^p_{k-m+1} is the unique solution of the estimation problem $\hat{\mathcal{P}}(x_{k-m+1}, p)$, where $x_{k-m+1} := x(k-m+1|k)$, we have:

$$\frac{\partial J}{\partial x_{k-m+1}}(p, x^p_{k-m+1}) = 0 \tag{5.47}$$

Then, let $x_0 = p$, $y_0 = x^p_{k-m+1}$, $X = \Re^q$, $Y = \Re^n$, $Z = \Re$ and W a neighborhood in $\Re^q \times \Re^n$. If the Hessian matrix $\frac{\partial^2 J}{\partial x^2_{k-m+1}}(p, x_{k-m+1})$ is invertible in $\mathcal{L}(\Re, \Re^n)$, then there exist $\rho_x > 0$, $\rho_p > 0$ and a mapping $\varphi : B^\circ(p, \rho_p) \to \Re^n$ of class $C^1(B^\circ(p, \rho_p))$ such that:

- $\varphi(p) = x^p_{k-m+1}$;
- $\| \bar{p} - p \| < \rho_p \Rightarrow \| \varphi(\bar{p}) - x^p_{k-m+1} \| < \rho_x$ and $\frac{\partial J}{\partial \varphi}(\bar{p}, \varphi(\bar{p})) = 0$;
- the equality $\frac{\partial J}{\partial x_{k-m+1}}(\bar{p}, x_{k-m+1}) = 0$ is possible in the "rectangle" $B^\circ(p, \rho_p) \times B^\circ(x^p_{k-m+1}, \rho_x)$ only for $x_{k-m+1} = \varphi(\bar{p})$.

Now, if the conditions of theorem 5.4 are satisfied, with Ψ, x_0, y_0 defined as above, it follows that $z_0 = 0$ and there exists $K > 0$ such that:

$$\| \varphi(\bar{p}) - x^p_{k-m+1} \| =: \| x_{k-m+1} - x^p_{k-m+1} \| \leq K \ \| \frac{\partial J}{\partial x_{k-m+1}}(\bar{p}, x^p_{k-m+1}) \| \tag{5.48}$$

Thus, if we find an upper bound for $\| \frac{\partial J}{\partial x_{k-m+1}}(\bar{p}, x_{k-m+1}) \|$ evaluated at $(\bar{p}, x^p_{k-m+1})$ we immediately obtain a bound on the state estimation error at t_{k-m+1}.

Our task is then to find an upper bound for $\| \frac{\partial J}{\partial x_{k-m+1}}(\bar{p}, x^p_{k-m+1}) \|$.

Theorem 5.6 (Bound on the difference between true and estimated states in the presence of parameter uncertainty) *Under assumptions 5.6, 5.7, 5.8, 5.9, 5.10, 5.11, 5.12 and 5.13, let* x_{k-m+1} *and* x^p_{k-m+1} *denote the solutions of the estimation problems* $\hat{\mathcal{P}}(\bar{p}, x_{k-m+1})$ *and* $\hat{\mathcal{P}}(p, x_{k-m+1})$*, respectively. Then, there exists* $\bar{K} \in [0, \infty)$ *such that*

$$\begin{aligned} \| x_{k-m+1} - x^p_{k-m+1} \|_{\hat{P}} &\leq K \, \lambda_{max}(\hat{P})^{\frac{1}{2}} \, \| \frac{\partial J}{\partial x_{k-m+1}}(\bar{p}, x^p_{k-m+1}) \| \leq \\ &\leq \bar{K} \, \| \bar{p} - p \| \leq \bar{K} \rho_p \end{aligned} \tag{5.49}$$

for all nominal parameter values $\bar{p} \in B^\circ(p, \rho_p)$.

Proof: *We begin by evaluating* $\frac{\partial J}{\partial x_{k-m+1}}(\bar{p}, x_{k-m+1})$ *with* $P(k-m+1|k-1) = 0, \ \forall k \geq m$, *and* $\bar{R} = I_p$ *(so that assumption 5.13 can be satisfied):*

$$\frac{\partial J}{\partial x_{k-m+1}}(\bar{p}, x_{k-m+1}) = \sum_{l=k-m+1}^{k} \nu_l' \frac{\partial \nu_l}{\partial x_{k-m+1}} \tag{5.50}$$

But, from (5.28), we have:

$$\frac{\partial \nu_l}{\partial x_{k-m+1}} = -\frac{\partial g(x_l, \bar{p})}{\partial x_{k-m+1}} = -\frac{\partial g(x_l, \bar{p})}{\partial x_l} \frac{\partial x_l}{\partial x_{k-m+1}}; \ \ l = k-m+1, \ldots, k \tag{5.51}$$

From (5.50) and (5.51), it follows that:

$$\| \frac{\partial J}{\partial x_{k-m+1}}(\bar{p}, x_{k-m+1}) \| \leq \sum_{l=k-m+1}^{k} \| \nu_l \| \, \| \frac{\partial g}{\partial x_l}(x_l, \bar{p}) \| \, \| \frac{\partial x_l}{\partial x_{k-m+1}} \| \tag{5.52}$$

Using assumption 5.10 we have:

$$\| \frac{\partial J}{\partial x_{k-m+1}}(\bar{p}, x_{k-m+1}) \| \leq L_g \sum_{l=k-m+1}^{k} \| \nu_l \| \| \frac{\partial x_l}{\partial x_{k-m+1}} \| \tag{5.53}$$

Then, from the equations of the model (5.25), we obtain:

$$x(t) = x_{k-m+1} + \int_{t_{k-m+1}}^{t} f(x(\tau), u(\tau), \bar{p})\, d\tau \tag{5.54}$$

Thus, by differentiating with respect to x_{k-m+1} and taking the $2-$norm we get:

$$\| \frac{\partial x(t)}{\partial x_{k-m+1}} \| \leq 1 + \int_{t_{k-m+1}}^{t} \| \frac{\partial f}{\partial x}(x(\tau), u(\tau), \bar{p}) \| \| \frac{\partial x(\tau)}{\partial x_{k-m+1}} \|\, d\tau \tag{5.55}$$

Using assumption 5.6 and the BG inequality, it follows that:

$$\| \frac{\partial x(l|k)}{\partial x_{k-m+1}} \| \leq e^{L_f(t_l - t_{k-m+1})}, \quad l = k-m+1, \ldots, k \tag{5.56}$$

which means that

$$\| \frac{\partial x(l|k)}{\partial x_{k-m+1}} \| \leq e^{L_f(m-1)T}, \quad \forall l \in [k-m+1, k] \tag{5.57}$$

Now that we have obtained a bound for $\| \frac{\partial x(l|k)}{\partial x_{k-m+1}} \|$, all that is left to do is to find a bound on $\| \nu_l \| := \| g(x_l^p, p) - g(x(l|k), \bar{p}) \|$ (note that ν_l is being evaluated in the noise-free case). From assumption 5.12, in order to find a bound for $\| \nu_l \|$, it is necessary to find bounds for $\| x_l^p \|$ and $\| x_l^p - x(l|k) \|$, which is what we will proceed to do next.

1. *Upper bound on* $\| x_l^p \|$:

From the equations which govern the dynamics of the plant, (5.23), we get:

$$\| x^p(t) \| \leq \| x^p_{k-m+1} \| + \int_{t_{k-m+1}}^{t} \| f(x^p(\tau), u(\tau), p) \| \, d\tau \tag{5.58}$$

Using the growth condition on f*, (5.7), it results that:*

$$\| x^p(t) \| \leq \| x^p_{k-m+1} \| + \eta_f(1+\bar{u})(m-1)T + \eta_f \int_{t_{k-m+1}}^{t} \| x^p(\tau) \| \, d\tau \tag{5.59}$$

where $\bar{u} := \max\{\| u_{min} \|, \| u_{max} \|\}$.

Thus, by applying the BG inequality, we obtain:

$$\| x^p(t) \| \leq [\| x^p_{k-m+1} \| + \eta_f(1+\bar{u})(m-1)T] \, e^{\eta_f(t-t_{k-m+1})} \tag{5.60}$$

And at $t = t_l$,

$$\| x_l^p \| \leq [\| x^p_{k-m+1} \| + \eta_f(1+\bar{u})(m-1)T] e^{\eta_f(t_l - t_{k-m+1})}, \quad l = k-m+1, \ldots, k \tag{5.61}$$

2. *Upper bound on* $\| x_l^p - x_l \|$:

Subtracting (5.25) from (5.23), taking the $2-$*norm and using assumption 5.9, we get:*

$$\begin{aligned} \| x^p(t) - x(t) \| \leq \| x^p_{k-m+1} - x_{k-m+1} \| + \gamma_f \bar{u}(m-1)T \| p - \bar{p} \| + \\ + \gamma_f \| p - \bar{p} \| \int_{t_{k-m+1}}^{t} \| x^p(\tau) \| \, d\tau + L_f \int_{t_{k-m+1}}^{t} \| x^p(\tau) - x(\tau) \| \, d\tau \end{aligned} \tag{5.62}$$

But, by integrating (5.59), we know that:

$$\int_{t_{k-m+1}}^{t} \| x^p(\tau) \| d\tau \leq [\frac{\| x^p_{k-m+1} \|}{\eta_f} + (1+\bar{u})(m-1)T](e^{\eta_f[t-t_{k-m+1}]} - 1) \quad (5.63)$$

Thus, by substituting (5.63) into (5.62) and evaluating the resulting inequality at $t = t_l$, $l \in [k-m+1, k]$, *we obtain:*

$$\begin{aligned} \| x^p_l \; - \; x_l \| \leq \{\gamma_f \| p - \bar{p} \| \; [\bar{u}(m-1)T + (\frac{\| x^p_{k-m+1} \|}{\eta_f} + (1+\bar{u})(m-1)T) \times \\ \times \; (e^{\eta_f(m-1)T} - 1)] + \| x^p_{k-m+1} - x_{k-m+1} \| \} e^{L_f[t_l - t_{k-m+1}]} \end{aligned} \quad (5.64)$$

where $x_l := x(l|k)$.

Then, by using (5.61) and (5.64) we obtain the following bound on $\| \nu_l \|$, $\forall l \in [k-m+1, k]$*:*

$$\begin{aligned} \| \nu_l \| \; \leq \; & L_g\{\gamma_f \| p - \bar{p} \| \; [\bar{u}(m-1)T + (\frac{\| x^p_{k-m+1} \|}{\eta_f} + (1+\bar{u})(m-1)T) \times \\ & \times \; (e^{\eta_f(m-1)T} - 1)] + \| x^p_{k-m+1} - x_{k-m+1} \| \} e^{L_f[t_l - t_{k-m+1}]} + \\ & + \; \gamma_g \| p - \bar{p} \| \; [\, \| x^p_{k-m+1} \| + \eta_f(1+\bar{u})(m-1)T] e^{\eta_f[t_l - t_{k-m+1}]} \end{aligned} \quad (5.65)$$

Finally, we are able to derive an upper bound for $\| \frac{\partial J}{\partial x_{k-m+1}}(\bar{p}, x_{k-m+1}) \|$*:*

$$\| \frac{\partial J}{\partial x_{k-m+1}}(\bar{p}, x_{k-m+1}) \| \leq \; \mu_1 \| x^p_{k-m+1} - x_{k-m+1} \| + \mu_2 \| p - \bar{p} \| \quad (5.66)$$

with

$$\mu_1 := L_g^2 \sum_{l=k-m+1}^{k} e^{2L_f[t_l - t_{k-m+1}]} \tag{5.67}$$

$$\begin{aligned}\mu_2 := & L_g \sum_{l=k-m+1}^{k} e^{L_f[t_l - t_{k-m+1}]}\{L_g\gamma_f\ [\ \bar{u}(m-1)T + \\ & + \ (\frac{\parallel x^p_{k-m+1} \parallel}{\eta_f} + (1+\bar{u})(m-1)T)(e^{\eta_f(m-1)T} - 1)\ ]\ e^{L_f[t_l - t_{k-m+1}]} + \\ & + \ \gamma_g\ [\ \parallel x^p_{k-m+1} \parallel + \eta_f(1+\bar{u})(m-1)T\ ]\ e^{\eta_f[t_l - t_{k-m+1}]}\},\end{aligned} \tag{5.68}$$

where we could replace $t_l - t_{k-m+1}$ *by* $(l-k+m-1)T$.

From (5.49), we see that in order to obtain an upper bound on the estimation error at time t_{k-m+1}, *we need to evaluate the inequality (5.66) at* $x_{k-m+1} = x^p_{k-m+1}$. *Then, it is clear from (5.66) that the first term of the right side of the inequality vanishes and all we are left with is:*

$$\parallel \frac{\partial J}{\partial x_{k-m+1}}(\bar{p}, x^p_{k-m+1}) \parallel \leq \ \mu_2 \parallel p - \bar{p} \parallel \tag{5.69}$$

Thus, from (5.49), we end up with:

$$\begin{aligned}\parallel x^p_{k-m+1} \ - \ x_{k-m+1} \parallel_{\hat{P}} & \leq K\lambda_{max}(\hat{P})^{\frac{1}{2}} \parallel \frac{\partial J}{\partial x_{k-m+1}}(\bar{p}, x^p_{k-m+1}) \parallel \ \leq \\ & \leq \ K\lambda_{max}(\hat{P})^{\frac{1}{2}}\mu_2 \ \parallel p - \bar{p} \parallel =: \ \bar{K} \parallel p - \bar{p} \parallel \leq \ \bar{K}\rho_p\end{aligned} \tag{5.70}$$

And we have finally concluded our proof.

□

Theorem 5.7 (Stabilizing properties of Control Algorithm 4 in the presence of parameter uncertainty) *Under assumptions 5.4, 5.5, 5.6, 5.7, 5.8, 5.9, 5.10, 5.11, 5.12 and 5.13, and given that the contractive constraint in the control*

problem $\mathcal{P}(t_{k+P-1}, x(k+P-1|k+P-1))$, $k \geq m$, *is given by:*

$$\| \bar{x}_{k+P} \|_{\hat{P}} := \| \bar{x}(k+P|k+P-1) \|_{\hat{P}} \leq \alpha \| x_{k-P} \|_{\hat{P}} \tag{5.71}$$

if $x(m+(n-1)P|m+nP)$, $x^p_{m+(n-1)P} \in B_\rho$, $\forall n \geq 0$, *the control problems* $\mathcal{P}(t_k, x(k|k))$ *are well-defined (according to assumption 5.5) and it follows that there exists* $\hat{\rho} > 0$ *such that:*

$$\| x^p_{m+(n-1)P} \|_{\hat{P}} < \max\{\| x^p_1 \|_{\hat{P}}, \| x^p_m \|_{\hat{P}}\} + \hat{\rho}, \qquad \forall n \geq 0 \tag{5.72}$$

and

$$\lim_{n\to\infty} \| x^p_{m+nP} \|_{\hat{P}} < \hat{\rho} \tag{5.73}$$

i.e., under the constant parameter deviation, $\| p - \bar{p} \|$, *the best that we can be assured to achieve is that the states will be driven to a neighborhood of the origin* $B_{\hat{\rho}}$ *(a control invariant set) whose size is determined by this deviation between nominal and true parameter values, with* $\hat{\rho} = 0$ *if* $\bar{p} = p$.

Proof: *Subtracting the equations of the model used in the computation of the contractive constraint from the equations of the plant we get:*

$$\dot{x}^p(t) - \dot{\bar{x}}(t) = f(x^p(t), u(t), p) - f(\bar{x}(t), u(t), \bar{p}) \tag{5.74}$$

We know that the optimal control problem $\mathcal{P}(t_k, x(k|k))$ *is solved after* $x(k|k)$ *is obtained by integration of the model equations with initial condition* x_{k-m+1} *at* t_{k-m+1}. *Thus, we can integrate (5.74) from* $t_{k-m+1} = t_{k-P} = t_k - PT$ *to any* $t \in [t_k - PT, t_k + PT]$ *(i.e., within an interval of* $2P$*) and obtain:*

$$\begin{aligned} \| x^p(t) - \bar{x}(t) \| \;\leq\; & \{\gamma_f \| p - \bar{p} \| \; [2\bar{u}PT + (\frac{\| x^p_{k-P} \|}{\eta_f} + 2(1+\bar{u})PT)(e^{2\eta_f PT} - 1)] + \\ + \;\; & \| x^p_{k-P} - x_{k-P} \|\} e^{L_f[t - t_{k-m+1}]} \end{aligned} \tag{5.75}$$

Then, at $t_{k+P} = t_k + PT$, using inequality (5.70) and the fact that:

$$\lambda_{min}(\hat{P})^{\frac{1}{2}} \; \| \, . \, \| \leq \| \, . \, \|_{\hat{P}} \leq \; \lambda_{max}(\hat{P})^{\frac{1}{2}} \; \| \, . \, \| \tag{5.76}$$

we have:

$$\| x^p_{k+P} - \bar{x}_{k+P} \|_{\hat{P}} \leq \bar{\delta}_1 \; \| x^p_{k-P} \|_{\hat{P}} + \bar{\delta}_2 \tag{5.77}$$

where:

$$\begin{aligned} \bar{\delta}_1 &:= \; \lambda_{max}(\hat{P})^{\frac{1}{2}} \frac{\lambda_f}{\eta_f}(e^{2\eta_f PT} - 1)e^{2L_f PT} \; \rho_p \\ \bar{\delta}_2 &:= \; \lambda_{max}(\hat{P})^{\frac{1}{2}}\{\gamma_f[2\bar{u}PT + 2(1+\bar{u})PT(e^{2\eta_f PT} - 1)] + \frac{\bar{K}}{\lambda_{min}(\hat{P})}\} e^{2L_f PT} \rho_p \end{aligned} \tag{5.78}$$

Notice that $\bar{\delta}_1, \; \bar{\delta}_2 = 0$ if there is no parameter uncertainty, i.e., $\rho_p = 0$.

Using our contractive constraint and the triangle inequality we get:

$$\| x^p_{k+P} \|_{\hat{P}} \leq \; \alpha \; \| x_{k-P} \|_{\hat{P}} + \bar{\delta}_1 \; \| x^p_{k-P} \|_{\hat{P}} + \bar{\delta}_2, \;\; k \geq m \tag{5.79}$$

Then, from (5.70), it follows that:

$$\| x^p_{k+P} \|_{\hat{P}} \leq (\alpha + \bar{\delta}_1) \| x^p_{k-P} \|_{\hat{P}} + \bar{\delta}_2 + \alpha \bar{K} \rho_p =: \delta_1 \| x^p_{k-P} \|_{\hat{P}} + \delta_2 \tag{5.80}$$

Thus, we have an inequality of the kind:

$$\| x^p_{m+(n+1)P} \|_{\hat{P}} \leq \delta_1 \| x^p_{m+(n-1)P} \|_{\hat{P}} + \delta_2, \quad n \geq 0 \tag{5.81}$$

So, x^p_{m+P} is related to $x^p_{m-P} = x^p_1$ via (5.81), x^p_{m+2P} is related to x^p_m, x^p_{m+3P} is related to x^p_{m+P} and so on.

Thus, we have an inequality of the kind:

$$z_{n+1} \leq a\, z_{n-1} + b, \quad \forall n \geq 0 \tag{5.82}$$

where $z_n := \| x^p_{m+nP} \|_{\hat{P}}$.

This is slightly different from what we had in lemma 4.1 since there z_{n+1} was related to z_n directly. In this case, following the same procedure used to prove lemma 4.1, we get:

$$z_{2n-1} \leq a^n z_{-1} + b \left(\sum_{i=0}^{n-1} a^i\right), \quad n \geq 1 \tag{5.83}$$

and

$$z_{2n} \leq a^n z_0 + b \left(\sum_{i=0}^{n-1} a^i\right), \quad n \geq 1 \tag{5.84}$$

Thus, for any $n \geq 1$, if

$$a := \delta_1 < 1 \tag{5.85}$$

we have:

$$z_n \leq a^{n^*} \max\{z_{-1}, z_0\} + b\,(\sum_{i=0}^{n^*-1} a^i); \quad n \geq 1 \tag{5.86}$$

where $n^* := int(\frac{n+1}{2})$ *and* $int(r)$ *denotes the integer part of* r, $\forall r \in \Re$.

Therefore, the following bounds can be obtained:

$$z_n < \max\{z_{-1}, z_0\} + \frac{b}{1-a} \tag{5.87}$$

and

$$\lim_{n\to\infty} z_n < \frac{b}{1-a} \tag{5.88}$$

or, in our original notation,

$$\| x^p_{m+(n-1)P} \|_{\hat{P}} < \max\{\| x^p_1 \|_{\hat{P}}, \| x^p_m \|_{\hat{P}}\} + \frac{\delta_2}{1-\delta_1}, \quad n \geq 0 \tag{5.89}$$

and

$$\lim_{n\to\infty} \| x^p_{m+nP} \|_{\hat{P}} < \frac{\delta_2}{1-\delta_1} =: \hat{\rho} \tag{5.90}$$

Since $\delta_2 = 0$ *if* $\bar{p} = p$ *then it follows that* $\hat{\rho} = 0$ *if* $\bar{p} = p$ *and* $B_{\hat{\rho}}$ *is a control invariant set to which the states of the plant (5.23) converge asymptotically when* **Control Algorithm 4** *is used for output feedback control.*

□

Theorem 5.8 (Feasibility condition) *Let* $x^p_1,\ x^p_m \in B_{\rho_0}$. *Then, if* $\rho_0 < \rho - (\hat{\rho} + \bar{K}\ \rho_p)$ *(notice that the set* B_{ρ_0}, *with* ρ_0 *satisfying this inequality, is non-empty if and only if* $\hat{\rho} + \bar{K}\ \rho_p < \rho$*) it follows that* $x^p_{m+(n-1)P},\ x_{m+(n-1)P} \in B_\rho$, $\forall n \geq 0$, *and therefore*

the control problems $\mathcal{P}(t_k, x(k|k))$, $\forall k \geq m$, are well-posed.

Proof: *In theorem 5.7 we have shown that the contractive MPC controller associated with the least squares estimator produces real states which satisfy:*

$$\| x^p_{m+(n-1)P} \|_{\hat{P}} < \max\{\| x^p_1 \|_{\hat{P}}, \| x^p_m \|_{\hat{P}}\} + \hat{\rho}, \quad \forall n \geq 0 \tag{5.91}$$

Thus, if x^p_1, $x^p_m \in B_{\rho_0}$, we have:

$$\| x^p_{m+(n-1)P} \|_{\hat{P}} < \rho_0 + \hat{\rho} \tag{5.92}$$

Now, from equation (5.70) we know that:

$$\begin{aligned} \| x^p_{m+(n-1)P} - x_{m+(n-1)P} \|_{\hat{P}} &:= \| x^p_{m+(n-1)P} - x(m+(n-1)P|m+nP) \|_{\hat{P}} \leq \\ &\leq \bar{K} \| p - \bar{p} \| \leq \bar{K}\rho_p \end{aligned} \tag{5.93}$$

Then, using the triangle inequality, we have:

$$\| x_{m+(n-1)P} \|_{\hat{P}} \leq \| x^p_{m+(n-1)P} \|_{\hat{P}} + \bar{K} \rho_p \tag{5.94}$$

Taking inequality (5.92) into consideration, it results that:

$$\| x_{m+(n-1)P} \|_{\hat{P}} \leq \rho_0 + \hat{\rho} + \bar{K} \rho_p, \quad \forall n \geq 0 \tag{5.95}$$

If ρ_0 satisfies:

$$\rho_0 < \rho - (\hat{\rho} + \bar{K}\ \rho_p) \tag{5.96}$$

with the parameter uncertainty being such that:

$$\hat{\rho} + \bar{K}\ \rho_p\ <\ \rho \tag{5.97}$$

so that $\rho_0 > 0$ *and* $\rho_0 = \rho$ *if* $\| p - \bar{p} \| = \rho_p = 0$, *we have* $x^p_{m+(n-1)P}$, $x_{m+(n-1)P} \in B_\rho$, $\forall n \geq 0$, *and, according to assumption 5.5, the control problems* $\mathcal{P}(t_k, x(k|k))$ *are well-posed (feasible) for all* $k \geq m$.

□

5.4 Mixed state/parameter LSE problem

We have so far studied the state estimation problem in the presence of parameter uncertainty (constant parameters), examined its implementation together with the contractive MPC controller and analyzed the stability properties of the closed-loop system originated by this combination. In that case, we were using in both the estimation and prediction steps a model with constant parameter deviation from the plant. Our stability analysis shows that this uncertainty only allows us to drive the states of the plant asymptotically to a control invariant set whose size depends on the parameter error. Now, we are prepared to study the properties of the mixed state/parameter estimation problem when there is no structural mismatch between the model used in the estimation and the real plant. Then, by combining this estimator with contractive MPC we can see how the obtained stability results compare with the ones we got previously. We will see that even though the analysis is slightly more complicated the results are highly intuitive. Since the analysis will follow a similar reasoning to what has been already presented, we will not go into as much detail as we did in the previous sections.

The moving horizon-based least squares state/parameter estimation problem is posed as:

Estimation Procedure 3

$$\begin{aligned}\min_{X^e(k-m+1|k),\,\{\bar{w}(k-m+1|k),\ldots,\bar{w}(k|k)\}} & J(\{\bar{w}(l|k)\}_{l=k-m+1}^{k},\ X(k-m+1|k)) \ := \\ := \tfrac{1}{2}\{(X^e(k-m+1|k))' & P(k-m+1|k-1)X^e(k-m+1|k) \ + \\ + \textstyle\sum_{l=k-m+1}^{k} & [\nu(l|k)'\bar{R}^{-1}\nu(l|k) + \bar{w}(l|k)'\bar{Q}^{-1}\bar{w}(l|k)]\}\end{aligned} \tag{5.98}$$

subject to:

$$\nu(l|k) = \ y_l^p - g(X(l|k)), \qquad l = k-m+1,\ldots,k \tag{5.99}$$

$$\dot{X}(t|k) = \ f(X(t|k), u_{l-1}) + \bar{w}(t|k),\ t \in [t_{l-1}, t_l],\ l \in [k-m+1, k] \tag{5.100}$$

where $X(l|k) := X(t_l|k) := [x(t_l|k)^T \quad \bar{p}(t_l|k)^T]^T \in \Re^{n+q}$ *is the "augmented" state vector, containing the* n *model states and the* q *parameters to be estimated. Moreover, we are adopting the following notation:* $\bar{w}(l|k) := \bar{w}(t_l|k) \in \Re^{n+q}$ *is the dynamic disturbance vector,* $\nu(l|k) := \nu(t_l|k) \in \Re^p$ *is the vector of output errors,* $X^e(k-m+1|k) := X(k-m+1|k) - X(k-m+1|k-1)$ *is the state/parameter estimation error of the estimates at time* t_{k-m+1} *computed at time step* $k-1$ *relatively to the newly computed estimates at time step* k *and* $u(t)$ *is constant for* $t \in [t_{l-1}, t_l]$ *and equal to* u_{l-1} *for all* $l = k-m+1,\ldots,k$.

Remark 5.11 *When the dynamics of the parameters to be estimated is unknown, the most common model to use in the estimation procedure is a continuous (discrete) random walk process where* $\bar{w}^p(t)$ *(*$\bar{w}_k^p$*) is a zero-mean, uncorrelated random trajectory (sequence). In this case, the combined output/state/parameter model is given by:*

$$\begin{aligned}
\nu(l|k) = &\quad y_l^p - g(x(l|k), \bar{p}(l|k)), && l = k-m+1, \ldots, k \\
\dot{x}(t|k) = &\quad f(x(t|k), u_{l-1}, \bar{p}(t|k)) + \bar{w}^x(t|k),\ t \in [t_{l-1}, t_l],\ l \in [k-m+1, k] \\
\dot{\bar{p}}(t|k) = &\quad \bar{w}^p(t|k), && t \in [t_{k-m+1}, t_k] \quad (5.101)
\end{aligned}$$

Similarly to what we had before, $P^{-1}(k-m+1|k-1)$ *is interpreted as the covariance of* $X(k-m+1|k)$ *computed at time* t_{k-1} *and can be calculated using linear filtering theory:*

$$\begin{aligned}
P^{-1}(k-m+1|k) = P^{-1}(k-m+1|k-1) - P^{-1}(k-m+1|k-1)\Xi' \times \\
\times[\Xi P^{-1}(k-m+1|k-1)\Xi' + \bar{R}]^{-1}\Xi P^{-1}(k-m+1|k-1) \quad (5.102) \\
P^{-1}(k-m+2|k) = \Phi P^{-1}(k-m+1|k)\Phi' + \bar{Q} \quad (5.103)
\end{aligned}$$

where $\Phi := \frac{\partial f}{\partial X}(X(k-m+1|k), u_{k-m+1})$, $\Xi = \frac{\partial g}{\partial X}(X(k-m+1|k-1))$ *and* $\bar{Q}^{-1}$, $\bar{R}^{-1}$ *represent a quantitative measure of our confidence in the state/parameter and output models, respectively.*

5.4.1 Basic assumptions

Assumption 5.14 *Lipschitz assumption on* $f : \Re^{n+q} \times \Re^m \to \Re^{n+q}$

$$\| f(X_1, u_1) - f(X_2, u_2) \| \leq L_f \left[\| X_1 - X_2 \| + \| u_1 - u_2 \| \right] \quad (5.104)$$

which implies that

$$\| \frac{\partial f}{\partial X}(X,u) \| \leq L_f \tag{5.105}$$

Assumption 5.15 *Lipschitz assumption on* $g : \Re^{n+q} \rightarrow \Re^p$

$$\| g(X_1) - g(X_2) \| \leq L_g \| X_1 - X_2 \| \tag{5.106}$$

from which, it follows that:

$$\| \frac{\partial g}{\partial X}(X) \| \leq L_g \tag{5.107}$$

Assumption 5.16 *The unknown disturbances are norm bounded, i.e., there exists a constant* $w_{max} \in (0, \infty)$*, such that:*

$$w(t) \in \mathcal{W} := \{w \in L_2^{(n+q)}[0,\infty) \mid w \in B_{w_{max}}\}, \quad \forall t \in [0,\infty) \tag{5.108}$$

where w *denotes the disturbances in the real system and* $B_{w_{max}} := \{w \in \Re^{n+q} \mid \| w \| \leq w_{max}\}$.

Assumption 5.17 *Let the output measurement at time step* l*,* y_l*, be given by:*

$$y_l = g(X_l^p) + R_v \, v_l \tag{5.109}$$

where $v_l \sim \mathcal{N}(0, I_p)$*,* $\forall l \geq 0$*, is a discrete Gaussian sequence and* R_v *is a positive-definite matrix (a design parameter).*

Assumption 5.18 *Let $m\ p := m\ dim(y) \geq n+q := dim(X)$ and let $\hat{\mathcal{P}}(\{\bar{w}(l|k)\}_{l=k-m+1}^{k}, X(k-m+1|k))$ denote the optimal estimation problem to be solved at time $t = t_k$ with $P(k-m+1|k-1) = 0,\ \forall k \geq m$, and in the absence of measurement noise, being $X(k-m+1|k)$ and $\{\bar{w}(k-m+1|k), \ldots, \bar{w}(k|k)\}$ the decision variables (all independent). Then, if the estimated sequence of disturbances $\{\bar{w}(l|k)\}_{l=k-m+1}^{k}$ is equal to the sequence of disturbances which affect the real system, $\{w_l\}_{l=k-m+1}^{k}$ (where $w_l := w(t_l)$), the estimate of the augmented states at time t_{k-m+1} computed at time step k is $X(k-m+1|k) = X_{k-m+1}^{p}$. Moreover, we assume that the solution corresponding to $\bar{w}(l|k) = w_l,\ \forall l \in [k-m+1, k]$, is unique.*

5.4.2 Properties of Estimation Procedure 3

Theorem 5.9 (Bound on the difference between true and estimated augmented states) *Under assumptions 5.14, 5.15, 5.17 and 5.18, let X_{k-m+1} and X_{k-m+1}^{p} denote the solutions of the estimation problems $\hat{\mathcal{P}}(\{\bar{w}(l|k)\}_{l=k-m+1}^{k}, X(k-m+1|k))$ and $\hat{\mathcal{P}}(\{w_l\}_{l=k-m+1}^{k}, X(k-m+1|k))$, respectively. Then, there exists a quadratic function of its arguments, $\Psi(\rho_w, w_{max}, \rho_v)$, such that*

$$\| X_{k-m+1}^{p} - X_{k-m+1} \|_{\hat{P}} \leq \Psi(\rho_w, w_{max}, \rho_v)^{\frac{1}{2}} \tag{5.110}$$

where $\rho_v := \| R_v \|$.

In other words, the difference between true and estimated augmented states (which includes estimated states and parameters) is bounded by a function of the uncertainty on the disturbance values, the magnitude of the real disturbances and of the measurement noise.

Proof: *Any (local or global) optimal solution $\{\{\bar{w}^*(l|k)\}_{l=k-m+1}^{k}, X^*(k-m+1|k)\}$*

satisfies the following set of equations:

$$\frac{\partial J}{\partial \Lambda}(\{\bar{w}^*(l|k)\}_{l=k-m+1}^{k}, X^*(k-m+1|k)) = 0 \tag{5.111}$$

where $\Lambda := [\ \bar{w}(k-m+1|k)^T, \ldots, \bar{w}(k|k)^T\ X(k-m+1|k)^T\ ]^T$.

As a consequence of assumption 5.18, we have:

$$\frac{\partial J}{\partial \Lambda}(\{w_l\}_{l=k-m+1}^{k}, X_{k-m+1}^{p}) = 0 \tag{5.112}$$

Thus, if $(\frac{\partial}{\partial X_{k-m+1}}(\frac{\partial J}{\partial \Lambda}))^{-1}$ *exists, as a consequence of the classical implicit function theorem 5.5 and of the uniqueness assumption 5.18, there exist* $\rho_w,\ \rho_X > 0$ *and a mapping* $\varphi : B^\circ(w, \rho_w) \rightarrow \Re^{n+q}$ *of class* $C^1(B^\circ(w, \rho_w))$ *(where* w *represents* $w(t),\ \forall t \geq 0$*) such that:*

- $\varphi(w_{k-m+1}, \ldots, w_k) = X_{k-m+1}^{p}$.
- $\max_{t\in[t_{k-m+1},t_k]} \parallel w(t) - \bar{w}(t|k) \parallel < \rho_w \implies \parallel \varphi(\{\bar{w}(l|k)\}_{l=k-m+1}^{k}) - X_{k-m+1}^{p} \parallel < \rho_X$ *and* $\frac{\partial J}{\partial \Lambda}(\{\bar{w}(l|k)\}_{l=k-m+1}^{k}, \varphi(\{\bar{w}(l|k)\}_{l=k-m+1}^{k})) = 0$ *with* $\Lambda = [\ \bar{w}(k-m+1|k)^T \ldots \bar{w}(k|k)^T\ \varphi(\bar{w}(k-m+1|k), \ldots, \bar{w}(k|k))^T\ ]^T$.
- *the equality* $\frac{\partial J}{\partial \Lambda}(\{\bar{w}(l|k)\}_{l=k-m+1}^{k}, X(k-m+1|k)) = 0$ *is possible in the "rectangle"* $B^\circ(w, \rho_w) \times B^\circ(X_{k-m+1}^{p}, \rho_X)$ *only for* $X(k-m+1|k) = \varphi(\{\bar{w}(l|k)\}_{l=k-m+1}^{k})$.

So, as a consequence of the implicit function theorem, there exists $\rho_w > 0$ *such that for* $\bar{w}(t|k) \in B^\circ(w, \rho_w),\ \forall t \in [t_{k-m+1}, t_k]$, *it follows that* $\{\ \{\bar{w}(l|k)\}_{l=k-m+1}^{k}, X(k-m+1|k))\ \}$ *with* $X(k-m+1|k) = \varphi(\{\bar{w}(l|k)\}_{l=k-m+1}^{k}) \in B^\circ(X_{k-m+1}^{p}, \rho_X)$, *is an optimal solution of the optimization problem at time step* k.

Thus, since there exists such $\rho_w > 0$ *and from assumption 5.16, it follows that:*

$$\| \bar{w}(t|k) \| < \| w(t) \| + \rho_w \leq w_{max} + \rho_w =: \bar{w}_{max} \tag{5.113}$$

for all $t \in [t_{k-m+1}, t_k]$, $k \geq m$.

As a consequence of the existence theorem for an implicit function 5.4, there exists $K > 0$ *such that:*

$$\begin{aligned} \| X^p_{k-m+1} - X_{k-m+1} \| &:= \| X^p_{k-m+1} - X(k-m+1|k) \| \leq \\ &\leq K \| \frac{\partial J}{\partial \Lambda}(\{\bar{w}(l|k)\}^k_{l=k-m+1}, X^p_{k-m+1}) \| \end{aligned} \tag{5.114}$$

Thus, in order to find an upper bound for $\| X^p_{k-m+1} - X_{k-m+1} \|$, *once again we need to find an upper bound for the gradient of the objective function* J *with respect to the decision variables in* Λ *evaluated at* X^p_{k-m+1}, *i.e.:*

$$\Lambda := [\ \bar{w}(k-m+1|k)^T \ \ldots\ \bar{w}(k|k)^T\ (X^p_{k-m+1})^T\ ]^T \tag{5.115}$$

The $2-$*norm of the gradient of* J *with respect to* Λ *is then given by:*

$$\| \frac{\partial J}{\partial \Lambda} \|^2 = \| \frac{\partial J}{\partial X^p_{k-m+1}} \|^2 + \sum_{i=k-m+1}^{k} \| \frac{\partial J}{\partial \bar{w}_i} \|^2 \tag{5.116}$$

where we have omitted the arguments of J *to shorten the notation.*

Thus, we will proceed to find upper bounds for the individual gradients:

$$\begin{aligned} &\textbf{1.}\quad \frac{\partial J}{\partial X^p_{k-m+1}} = \sum_{l=k-m+1}^{k} \nu(l|k)^T \bar{R}^{-1} \frac{\partial \nu(l|k)}{\partial X^p_{k-m+1}} \\ &\textbf{2.}\quad \frac{\partial J}{\partial \bar{w}_i} = \sum_{l=k-m+1}^{k} [\nu(l|k)^T \bar{R}^{-1} \frac{\partial \nu(l|k)}{\partial \bar{w}_i} + \bar{w}(l|k)^T \bar{Q}^{-1} \frac{\partial \bar{w}(l|k)}{\partial \bar{w}_i}] \end{aligned} \tag{5.117}$$

Since $\frac{\partial \bar{w}(l|k)}{\partial \bar{w}_i} = \delta_{li}$, *where* $\delta_{li} = 1$ *if* $l = i$ *and* $\delta_{li} = 0$ *if* $l \neq i$, *we have:*

$$\begin{aligned} &\textbf{1.} \quad \| \frac{\partial J}{\partial X^p_{k-m+1}} \| \leq \sum_{l=k-m+1}^{k} \| \nu(l|k) \| \| \bar{R}^{-1} \| \| \frac{\partial \nu(l|k)}{\partial X^p_{k-m+1}} \| \\ &\textbf{2.} \quad \| \frac{\partial J}{\partial \bar{w}_i} \| \leq \| \bar{Q}^{-1} \| \| \bar{w}(i|k) \| + \sum_{l=k-m+1}^{k} \| \nu(l|k) \| \| \bar{R}^{-1} \| \| \frac{\partial \nu(l|k)}{\partial \bar{w}_i} \| \end{aligned} \tag{5.118}$$

So, let us find upper bounds for the $2-$*norm of the derivatives of* $\nu(l|k)$ *with respect to* Λ*:*

$$\textbf{1.} \quad \| \frac{\partial \nu(l|k)}{\partial \bar{w}_i} \| \leq \| \frac{\partial g(X(l|k))}{\partial X_l} \| \| \frac{\partial X(l|k)}{\partial \bar{w}_i} \| \tag{5.119}$$

$$\textbf{2.} \quad \| \frac{\partial \nu(l|k)}{\partial X^p_{k-m+1}} \| \leq \| \frac{\partial g(X(l|k))}{\partial X_l} \| \| \frac{\partial X(l|k)}{\partial X^p_{k-m+1}} \| \tag{5.120}$$

We will not go into a lot of details in the derivation of these upper bounds because the procedure is similar to what we did before in the state estimation case only.

- *Upper bound on* $\| \frac{\partial \nu(l|k)}{\partial \bar{w}_i} \|$, $\forall i = k - m + 1, \ldots, k$*:*

  From equation (5.119) and assumption 5.15, we have:

$$\| \frac{\partial \nu(l|k)}{\partial \bar{w}_i} \| \leq L_g \| \frac{\partial X(l|k)}{\partial \bar{w}_i} \| \tag{5.121}$$

  Since

$$X(t|k) = X^p_{k-m+1} + \int_{t_{k-m+1}}^{t} f(X(\tau|k), u(\tau))d\tau + \int_{t_{k-m+1}}^{t} \bar{w}(\tau)d\tau, \tag{5.122}$$

  the decision variables are mutually independent and assumption 5.14 is used, we have:

$$\| \frac{\partial X(t|k)}{\partial \bar{w}_i} \| \leq L_f \int_{t_{k-m+1}}^{t} \| \frac{\partial X(\tau|k)}{\partial \bar{w}_i} \| d\tau + \int_{t_{k-m+1}}^{t} \| \frac{\partial \bar{w}(\tau|k)}{\partial \bar{w}_i} \| d\tau \qquad (5.123)$$

Then, using the BG inequality and the fact that $\frac{\partial \bar{w}(t|k)}{\partial \bar{w}_i} = 1$ *it* $t \geq t_i$ *and* $\frac{\partial \bar{w}(t|k)}{\partial \bar{w}_i} = 0$ *if* $t < t_i$*, it follows that:*

$$\| \frac{\partial X(l|k)}{\partial \bar{w}_i} \| \leq (m-1)Te^{L_f(t_l - t_{k-m+1})} \quad if \quad t_l \geq t_i \qquad (5.124)$$

$$\| \frac{\partial X(l|k)}{\partial \bar{w}_i} \| = 0 \quad if \quad t_l < t_i \qquad (5.125)$$

Thus, using assumption 5.15, we finally get:

$$\| \frac{\partial \nu(l|k)}{\partial \bar{w}_i} \| \leq L_g(m-1)Te^{L_f(t_l - t_{k-m+1})} \quad if \quad t_l \geq t_i \qquad (5.126)$$

$$\| \frac{\partial \nu(l|k)}{\partial \bar{w}_i} \| = 0 \quad if \quad t_l < t_i \qquad (5.127)$$

- *Upper bound on* $\| \frac{\partial \nu(l|k)}{\partial X^p_{k-m+1}} \|$*:*

  Using equation (5.120) and assumption 5.15, we have:

$$\| \frac{\partial \nu(l|k)}{\partial X^p_{k-m+1}} \| \leq L_g \| \frac{\partial X(l|k)}{\partial X^p_{k-m+1}} \| \qquad (5.128)$$

Taking the derivative of equation (5.122) with respect to X^p_{k-m+1}*, applying the* $2-$*norm and using the BG inequality, it results that:*

$$\| \frac{\partial X(t|k)}{\partial X^p_{k-m+1}} \| \leq e^{L_f(t - t_{k-m+1})} \qquad (5.129)$$

By substituting this expression into (5.128), we get:

$$\| \frac{\partial \nu(l|k)}{\partial X^p_{k-m+1}} \| \leq L_g \, e^{L_f(t_l - t_{k-m+1})}, \quad l = k-m+1, \ldots, k \qquad (5.130)$$

Now, in order to compute the gradient of J with respect to the decision variables we still need to compute an upper bound for $\| \nu(l|k) \|$. Using assumptions 5.15 and 5.17, it results that:

$$\| \nu(l|k) \| = \| g(X_l^p) - g(X(l|k)) + R_v \, v_l \| \leq L_g \| X_l^p - X(l|k) \| + \| R_v \| \quad (5.131)$$

So, let us evaluate $X^p(t) - X(t|k)$, $\forall t \in [t_{k-m+1}, t_k]$:

$$\begin{aligned} X^p(t) - X(t|k) &= \int_{t_{k-m+1}}^{t} [f(X^p(\tau), u(\tau)) - f(X(\tau|k), u(\tau))] \, d\tau + \\ &+ \int_{t_{k-m+1}}^{t} [w(\tau) - \bar{w}(\tau|k)] \, d\tau \end{aligned} \quad (5.132)$$

Using assumption 5.14, the fact that $\bar{w}(t|k) \in B^\circ(w, \rho_w)$, $\forall t \in [t_{k-m+1}, t_k]$, and the BG inequality, we obtain:

$$\| X_l^p - X(l|k) \| \leq \rho_w (m-1) T \, e^{L_f (t_l - t_{k-m+1})} \quad (5.133)$$

And, by substituting this expression into (5.131), we finally get the desired bound on $\| \nu(l|k) \|$:

$$\| \nu(l|k) \| \leq L_g \, (m-1) T \, e^{L_f (t_l - t_{k-m+1})} \, \rho_w + \| R_v \| =: \delta_l \rho_w + \rho_v \quad (5.134)$$

Thus, from (5.118) and the previous upper bound computations, it follows that there exist constants $\sigma_1, \bar{\sigma}_1, \sigma_2, \bar{\sigma}_2 \in (0, \infty)$, such that:

$$\begin{aligned} &\mathbf{1.} \quad \| \tfrac{\partial J}{\partial X^p_{k-m+1}} \| \leq \sigma_1 \, \rho_w + \bar{\sigma}_1 \, \rho_v \\ &\mathbf{2.} \quad \| \tfrac{\partial J}{\partial \bar{w}_i} \| \leq \| \bar{Q}^{-1} \| \; w_{max} + \sigma_2 \rho_w + \bar{\sigma}_2 \rho_v \end{aligned} \tag{5.135}$$

and, from (5.116), it results that there exists a quadratic function of its arguments, $\bar{\Psi}(x, y, z)$*, such that:*

$$\| \tfrac{\partial J}{\partial \Lambda}(\{\bar{w}(l|k)\}^k_{l=k-m+1}, X^p_{k-m+1}) \| \leq \bar{\Psi}(\rho_w, w_{max}, \rho_v)^{\frac{1}{2}} \tag{5.136}$$

which, from (5.114), means that:

$$\| X^p_{k-m+1} - X_{k-m+1} \| \leq \Psi(\rho_w, w_{max}, \rho_v)^{\frac{1}{2}} \tag{5.137}$$

where $\Psi := K\bar{\Psi}$.

Thus, a sufficient condition for obtaining error-free estimates, i.e., $X_{k-m+1} = X^p_{k-m+1}$*, is given by* $\rho_w = 0$, $w_{max} = 0$ *and* $\rho_v = 0$. *If these three conditions are satisfied simultaneously, it means that there are no disturbances* ($w(t) = \bar{w}(t|k) = 0, \; \forall t \in [t_{k-m+1}, t_k], \; k \geq m$) *and no measurement noise* ($v_l = 0, \; \forall l \in [k-m+1, k], \; k \geq m$). □

Thus, the stability analysis follows in the same way as for the state estimation problem with parameter uncertainty with the only differences being that the term $K \; \rho_p$ is replaced by $\Psi(\rho_w, w_{max}, \rho_v)^{\frac{1}{2}}$ in the results previously derived, and the contractive constraint is now imposed on the augmented states X (assuming that the same nonlinear state/parameter model is used in the prediction and estimation steps).

5.5 Example: Biochemical Reactor

5.5.1 Biochemical reactor dynamics

The chemical engineering example adopted here is a continuous bioreactor with substrate inhibition. Figure 5.1 is a schematic representation of this CSTR system.

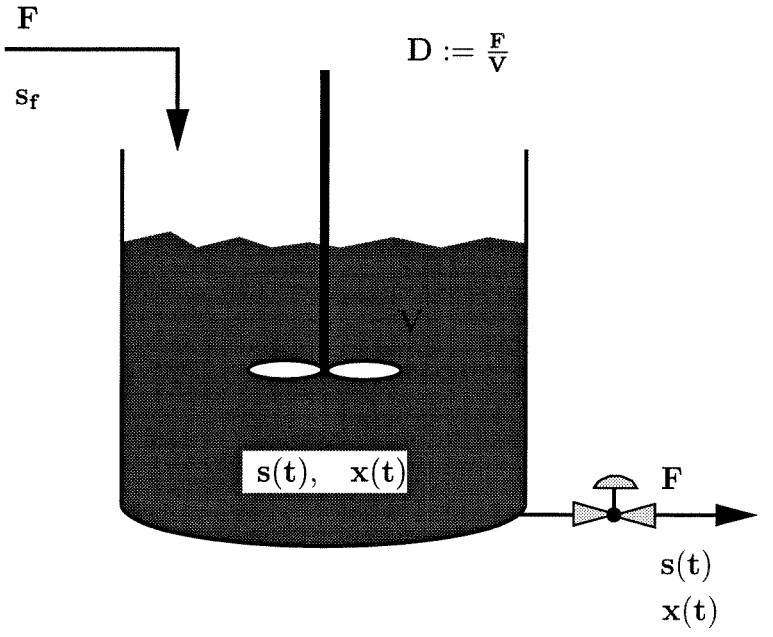

Figure 5.1: Schematic representation of a continuous bioreactor with substrate inhibition.

For some regions of the parameter and input variable space, this system exhibits multiple and saddle type of steady state behavior. The state equations are:

$$\dot{x}(t) = [\mu(t) - D(t)]\, x(t) \tag{5.138}$$

$$\dot{s}(t) = [s_f(t) - s(t)]\, D(t) - \frac{\mu(t)x(t)}{y(t)} \tag{5.139}$$

where

$$\mu(t) = \frac{\mu_{max}(t)s(t)}{k_m(t) + s(t) + k_1(t)s^2(t)}$$

The dilution rate, D, is manipulated to control the cell mass concentration, x. The other state and parameters are the substrate concentration, s, the specific growth rate, μ, the yield of cell mass, y, and the substrate concentration in the feed stream, s_f.

Eaton and Rawlings [40] apply a classical nonlinear model predictive control strategy to this example and they show that for a step in the setpoint from a stable to a saddle point, if some of the parameters of the plant differ slightly from their nominal values, the system will not be stable unless frequent measurements from the plant are taken into consideration in the control computations.

The performance objective in this example is to obtain specific cell mass and substrate concentrations without large control efforts.

According to our notation, we have:

$$x^p(t) \hat{=} [x_1^p(t) \;\; x_2^p(t)]^T \quad \text{with} \quad x_1^p(t) \hat{=} x(t) - x_{ss} \quad \text{and} \quad x_2^p(t) \hat{=} s(t) - s_{ss}$$

$$u(t) \hat{=} D(t) - D_{ss}$$

$$d(t) \hat{=} s_f(t) - s_{f,ss}$$

$$p(t) \hat{=} [p_1(t) \; p_2(t) \; p_3(t) \; p_4(t)]^T \text{ with } p_1(t) \hat{=} \mu_{max}(t) - \mu_{max,ss}, \; p_2(t) \hat{=} k_m(t) - k_{m,ss},$$
$$p_3(t) \hat{=} k_1(t) - k_{1,ss}, \quad p_4(t) \hat{=} y(t) - y_{ss}$$

where $\mu_{max,ss}$, $k_{m,ss}$, $k_{1,ss}$, y_{ss} are the nominal values of the parameters, $s_{f,ss}$ is the nominal value of the input variable and x_{ss}, s_{ss}, u_{ss} represent the desired steady state values of the two states and manipulated variables, respectively.

Naturally, since cell and substrate concentrations and the dilution rate are all positive quantities, the physical constraints on the state space and control variables are:

$$x_1^p(t) \geq -x_{ss}, \;\; x_2^p(t) \geq -s_{ss}, \;\; u(t) \geq -D_{ss}, \quad \forall t \in [0, \infty)$$

5.5.2 Computation of steady states

With u_{ss}, d_{ss} and p_{ss} representing the steady state values of the manipulated variable, input variable and parameters, respectively, we have:

1. if $(u_{ss} - p_{1,ss})^2 > 4u_{ss}^2 p_{2,ss} p_{3,ss}$ the system presents three distinct steady states given by $(0, d_{ss})$, $(p_{4,ss}(d_{ss} - x_{2,ss}^-), x_{2,ss}^-)$ and $(p_{4,ss}(d_{ss} - x_{2,ss}^+), x_{2,ss}^+)$, where:

$$x_{2,ss}^- = \frac{p_{1,ss} - u_{ss} - [(u_{ss} - p_{1,ss})^2 - 4u_{ss}^2 p_{2,ss} p_{3,ss}]^{\frac{1}{2}}}{2p_{3,ss} u_{ss}} \tag{5.140}$$

$$x_{2,ss}^+ = \frac{p_{1,ss} - u_{ss} + [(u_{ss} - p_{1,ss})^2 - 4u_{ss}^2 p_{2,ss} p_{3,ss}]^{\frac{1}{2}}}{2p_{3,ss} u_{ss}} \tag{5.141}$$

2. if $(u_{ss} - p_{1,ss})^2 = 4u_{ss}^2 p_{2,ss} p_{3,ss}$ the system presents two distinct steady states given by $(0, d_{ss})$, $(p_{4,ss}(d_{ss} - x_{2,ss}), x_{2,ss})$, where:

$$x_{2,ss} = (\frac{p_{2,ss}}{p_{3,ss}})^{\frac{1}{2}} \tag{5.142}$$

3. if $(u_{ss} - p_{1,ss})^2 < 4u_{ss}^2 p_{2,ss} p_{3,ss}$ the system presents only one steady state given by $(0, d_{ss})$.

The stability properties of these equilibrium points are:

First Equilibrium Point: $(0, d_{ss})$

1. if $u_{ss} = \frac{p_{1,ss}}{1+2(p_{2,ss}p_{3,ss})^{\frac{1}{2}}}$ then:

   (1.1) if $d_{ss} \neq (\frac{p_{2,ss}}{p_{3,ss}})^{\frac{1}{2}}$ the equilibrium point is a **sink**.

   (1.2) if $d_{ss} = (\frac{p_{2,ss}}{p_{3,ss}})^{\frac{1}{2}}$ the equilibrium point is a **center** (here we denote by center stationary points at which the linearization has one or more eigenvalues on the imaginary axis; the stability characteristics of these points cannot be determined by this first order analysis).

2. if $p_{2,ss}p_{3,ss} \geq \frac{1}{4}$ and $u_{ss} > \frac{p_{1,ss}}{1+2(p_{2,ss}p_{3,ss})^{\frac{1}{2}}}$ the equilibrium point is a **sink**.

3. if $u_{ss} \in [0, \frac{p_{1,ss}}{1+2(p_{2,ss}p_{3,ss})^{\frac{1}{2}}})$ then:

   (3.1) if $u_{ss} = 0$ the equilibrium point is a **center**.

   (3.2) if $u_{ss} \in (0, \frac{p_{1,ss}}{1+2(p_{2,ss}p_{3,ss})^{\frac{1}{2}}})$ we have:

   (3.2.1) if $d_{ss} = d_{ss}^{-}$ or $d_{ss} = d_{ss}^{+}$, where

$$d_{ss}^{-} = \frac{p_{1,ss} - u_{ss} - [(u_{ss} - p_{1,ss})^2 - 4u_{ss}^2 p_{2,ss}p_{3,ss}]^{\frac{1}{2}}}{2p_{3,ss}u_{ss}} \tag{5.143}$$

$$d_{ss}^{+} = \frac{p_{1,ss} - u_{ss} + [(u_{ss} - p_{1,ss})^2 - 4u_{ss}^2 p_{2,ss}p_{3,ss}]^{\frac{1}{2}}}{2p_{3,ss}u_{ss}} \tag{5.144}$$

   the equilibrium point is a **center**.

   (3.2.2) if $d_{ss} \in (d_{ss}^{-}, d_{ss}^{+})$ the equilibrium point is a **saddle**.

   (3.2.3) if $d_{ss} \in [0, d_{ss}^{-})$ or $d_{ss} > d_{ss}^{+}$ the equilibrium point is a **sink**.

4. if $p_{2,ss}p_{3,ss} < \frac{1}{4}$ and $u_{ss} \in (\frac{p_{1,ss}}{1+2(p_{2,ss}p_{3,ss})^{\frac{1}{2}}}, \frac{p_{1,ss}}{1-2(p_{2,ss}p_{3,ss})^{\frac{1}{2}}})$ the equilibrium point is a **sink**.

5. if $p_{2,ss}p_{3,ss} < \frac{1}{4}$ and $u_{ss} > \frac{p_{1,ss}}{1-2(p_{2,ss}p_{3,ss})^{\frac{1}{2}}}$ we have:

   (5.1) if $d_{ss} = d_{ss}^{-}$ or $d_{ss} = d_{ss}^{+}$ the equilibrium point is a **center**.

   (5.2) if $d_{ss} \in [0, d_{ss}^{-})$ or $d_{ss} > d_{ss}^{+}$ the equilibrium point is a **sink**.

   (5.3) if $d_{ss} \in (d_{ss}^{-}, d_{ss}^{+})$ the equilibrium point is a **saddle**.

Second Equilibrium Point: $(p_{4,ss}(d_{ss} - x_{2,ss}^{-}), x_{2,ss}^{-})$

1. if $u_{ss} = 0$ and $d_{ss} \geq x_{2,ss}^{-}$ the equilibrium point is a **center**.

2. if $u_{ss} \in (0, \frac{p_{1,ss}}{1+2(p_{2,ss}p_{3,ss})^{\frac{1}{2}}})$ and $d_{ss} > x_{2,ss}^{-}$ the equilibrium point is a **sink**.

3. if $u_{ss} \in (0, \frac{p_{1,ss}}{1+2(p_{2,ss}p_{3,ss})^{\frac{1}{2}}})$ and $d_{ss} = x_{2,ss}^{-}$ the equilibrium point is a **center**.

Third Equilibrium Point: $(p_{4,ss}(d_{ss} - x^+_{2,ss}), x^+_{2,ss})$

1. if $u_{ss} = 0$ and $d_{ss} \geq x^+_{2,ss} = 0$ the equilibrium point is a **center**.
2. if $u_{ss} \in (0, \frac{p_{1,ss}}{1+2(p_{2,ss}p_{3,ss})^{\frac{1}{2}}})$ and $d_{ss} > x^+_{2,ss}$ the equilibrium point is a **saddle**.
3. if $u_{ss} \in (0, \frac{p_{1,ss}}{1+2(p_{2,ss}p_{3,ss})^{\frac{1}{2}}})$ and $d_{ss} = x^+_{2,ss}$ the equilibrium point is a **center**.

In the case where $u_{ss} = \frac{p_{1,ss}}{1+2(p_{2,ss}p_{3,ss})^{\frac{1}{2}}}$ the two last equilibrium points coincide into one and this point is a **center**.

This local stability analysis allows us to better interpret the results obtained from simulations of the closed-loop system.

5.5.3 Simulation results

The nominal values of the parameters, disturbance and input variable used in the simulations performed here are:

Nominal parameter and disturbance values for the bioreactor	
$\mu_{max} = 0.53$	$k_m = 0.12$
$k_1 = 0.4545$	$y = 0.4$
$d := s_f = 4.0$	

The steady state coordinates for these parameter and disturbance steady state values for both the open-loop stable and unstable equilibria are:

Steady state values for the biochemical reactor		
Variables	**Unstable (1)**	**Stable (2)**
$u := D$	0.3	0.3
x	0.9951	1.5302
s	1.5122	0.1746

We will use the biochemical CSTR to demonstrate how contractive MPC handles both time-variant and time-invariant parameter uncertainty in the model used for prediction, in both state and output feedback case.

A variety of situations for two main cases will be considered here:

Transition 1: Step change from steady state (**1**) to steady state (**2**),

Transition 2: Step change from steady state (**2**) to steady state (**1**).

Naturally, the step change proposed in **Transition 2** is more challenging than the one in **Transition 1** due to the unstable characteristics of the steady state around which we wish to operate the plant. For each of these transitions we will consider six different scenarios in our simulations:

Case 1: State Feedback

Case 1.1 Nominal case, no disturbances.

Case 1.2 Constant parameter deviation between model and plant.

Case 1.3 Non-additive, bounded, exponentially decaying disturbance which converges to a non-zero value.

Case 1.4 Non-additive, bounded, exponentially decaying disturbance which converges to zero.

Case 2: Output Feedback under constant parameter deviation between plant and model

Case 2.1 Using the state estimator (the extended Kalman filter) in chapter 4.

Case 2.2 Using a least-squares moving horizon-based estimation (LSE) algorithm as proposed in this chapter.

In all of these cases we will examine the unconstrained and constrained responses obtained with our contractive MPC algorithm (which is modified to deal with **Case 2.2** and assumes the form of **Control Algorithm 4**).

The input and state variables which will be plotted for the bioreactor example are the deviation variables with respect to the desired steady state values.

Transition 1

Case 1.1

This is a very simple case since there is no model/plant mismatch and the targeted steady state is open-loop stable. The simulations for the unconstrained and constrained cases are shown in figure 5.2.

The controller parameters used in **Case 1.1** are given by:

Controller Parameters (figure 5.2)		
$Q = \text{diag}([1 \quad 0.1])$	$R = 0$	$S = 0$
$P = 4$	$M = 2$	$\alpha = 0.6$
$u_{min} = -1$	$u_{max} = 0$	

Unless otherwise indicated, the hard control constraints for the simulations of **Transition 1** will be the same as the ones used here in the nominal case.

As we can see from figure 5.2, the response in the unconstrained case occurs in approximately two sampling times. The effect of tight input constraints (more than four times smaller than the maximum control effort in the unconstrained case) is to delay the response by a few samples.

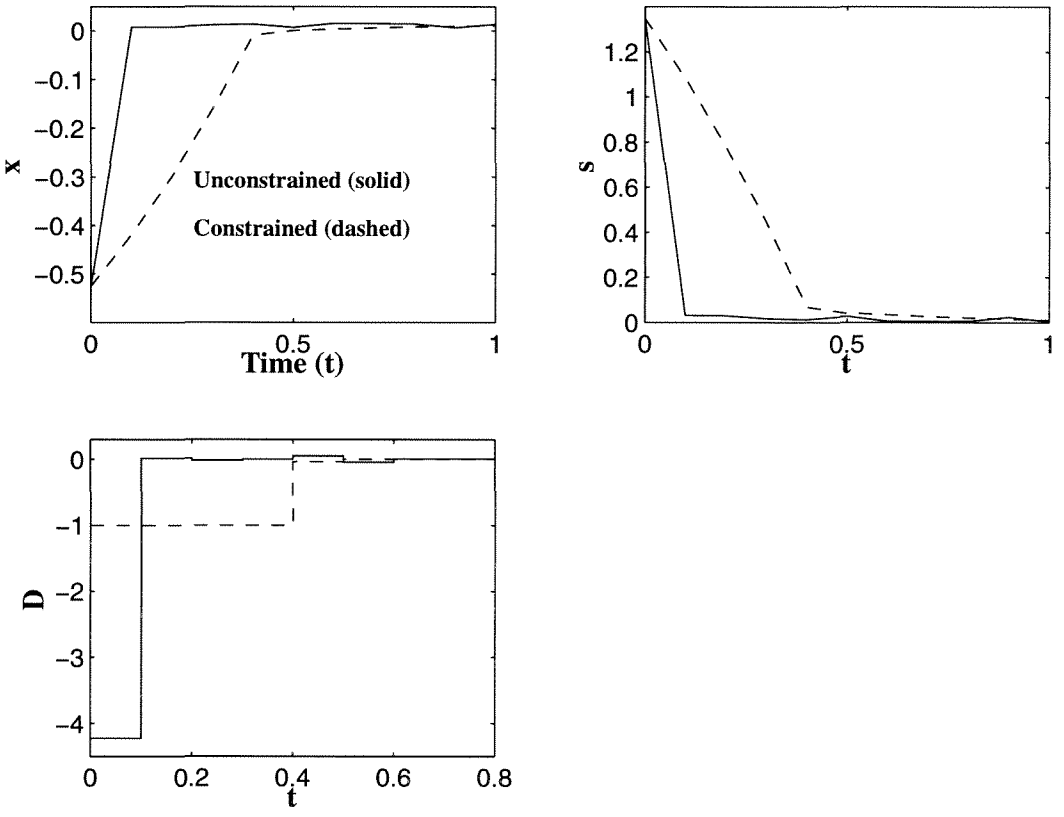

Figure 5.2: Bioreactor: State and control responses in **Case 1.1** (**Transition 1**).

Case 1.2

In this case, the parameters of the model and the plant are constant and different. As discussed earlier in this chapter, asymptotic stability cannot be guaranteed in this case any longer. Due to the stabilizing effects of the contractive constraint, we can assure that the states will converge asymptotically to a control invariant set whose size depends on the constant parameter deviation. Moreover, if integral action is introduced, we can eliminate offset in as many states as there are inputs (in this case, one) at the expense of perhaps introducing larger offsets in the responses of the other states.

The simulation results for the unconstrained and constrained cases are depicted in figure 5.3.

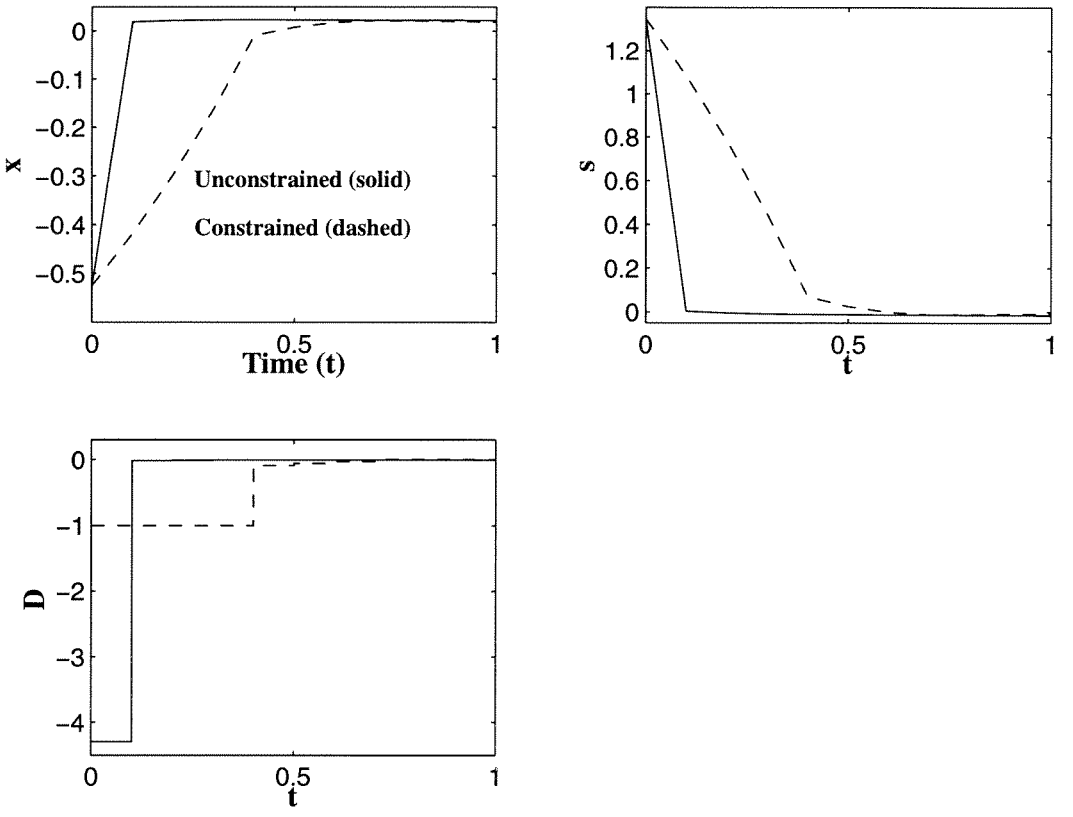

Figure 5.3: Bioreactor: State and control responses in **Case 1.2** (**Transition 1**).

The controller and model/plant parameters used in **Case 1.2** are:

Controller Parameters (figure 5.3)		
$Q = \text{diag}([1 \quad 0.1])$	$R = 0$	$S = 0$
$P = 4$	$M = 2$	$\alpha = 0.9$

Model/Plant Parameters		
Parameters	**Plant**	**Model**
μ_{max}	0.53	0.424
k_m	0.12	0.108
k_1	0.4545	0.409
y	0.4	0.32

As we can see from figure 5.3, C_A shows a small offset, i.e., due to the parameter uncertainty, exponential (or even asymptotic) stability to the origin cannot be achieved for both states since we have only one manipulated variable. We call this convergence to a small control invariant set containing the origin "practical stability". Once again, the effect of the input constraints is to delay the state response by a few samples.

Case 1.3

In this case, the variable s_f (the substrate concentration in the feed), which is commonly seen as a non-manipulated input variable, will work as a disturbance acting on the system. We will simulate s_f as an exponentially decaying disturbance which starts at $t = 0$ at its nominal value $s_{f,ss} = 4.0$ and converges to a value 5% smaller. Thus, $s_f(t)$ is given by:

$$s_f(t) = 3.8 \; + \; 0.2 \, e^{-\frac{t}{2}}$$

In the beginning, since the disturbance is near its nominal value, we expect that the response will not be very different from the one obtained in the nominal case. Thus, the important consideration in this simulation is the asymptotic behavior of the closed-loop, when the disturbance settles to a value different from the value it should have at steady state.

The expected results are that the states can be taken to a control invariant set containing the origin and be kept there. Asymptotic stability cannot be expected since this is a persistent disturbance.

The unconstrained and constrained simulations taking into account this disturbance in s_f are illustrated in figure 5.4. The disturbance behavior is also depicted in figure 5.4.

The controller parameters used in **Case 1.3** are the following:

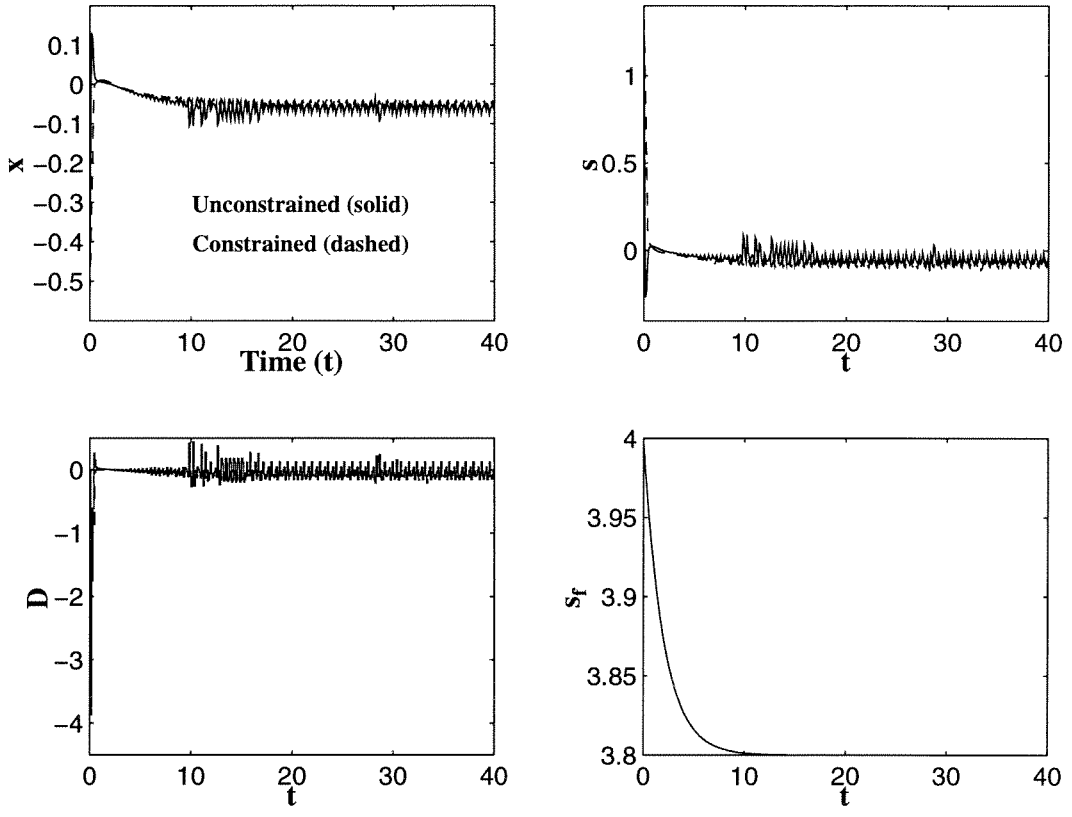

Figure 5.4: Bioreactor: State and control responses in **Case 1.3** (**Transition 1**).

Controller Parameters (figure 5.4)		
$Q = \text{diag}([1 \quad 0.1])$	$R = 0$	$S = 0$
$P = 6$	$M = 4$	$\alpha = 0.9$

As we notice from figure 5.4, this level of asymptotic disturbance deviation from its nominal value and the persistence of such disturbance do not allow the states to be brought to the origin.

Some of the oscillation obtained in the response as t increases is due to numerical instabilities which we could not eliminate completely with our adjustments of tolerance parameters in both the optimization and integration routines.

In spite of the numerical problems which we were not able to avoid, we can see that our theoretical prediction of the closed-loop response was correct and the

states can indeed be brought to the interior of a control invariant set and be kept there as $t \rightarrow \infty$. In order to keep the states inside this neighborhood of the origin, the control variable does not settle to the origin either but stays in a close vicinity of it.

The effect of the input constraints is to reduce the controller's power of action in the beginning and, therefore, delay the response. The constraints do not have any effect on the asymptotic response since they are no longer active at that stage.

Case 1.4

Here we want to study the transient effect of a disturbance which converges exponentially to its nominal value. Once again, the disturbance is introduced in the substrate concentration in the feed, s_f. Contrary to what we experienced in **Case 1.3**, we expect that the initial response will be largely perturbed but the states should still be able to reach the origin asymptotically.

The time-varying behavior of $s_f(t)$ is modeled in the following manner:

$$s_f(t) \;=\; 4.0 \;+\; 2.0\, e^{-\frac{t}{2}}$$

The responses for the unconstrained and constrained simulations can be found in figure 5.5. The disturbance behavior is also illustrated in this figure.

The controller parameters used in **Case 1.4** are as follows:

Controller Parameters (figure 5.5)		
$Q = \text{diag}([1 \quad 0.1])$	$R = 0$	$S = 0$
$P = 6$	$M = 4$	$\alpha = 0.9$

The obtained results are as expected from our theoretical investigations for this class of disturbances and they also show that the influence of the input constraints is not strongly felt in this case.

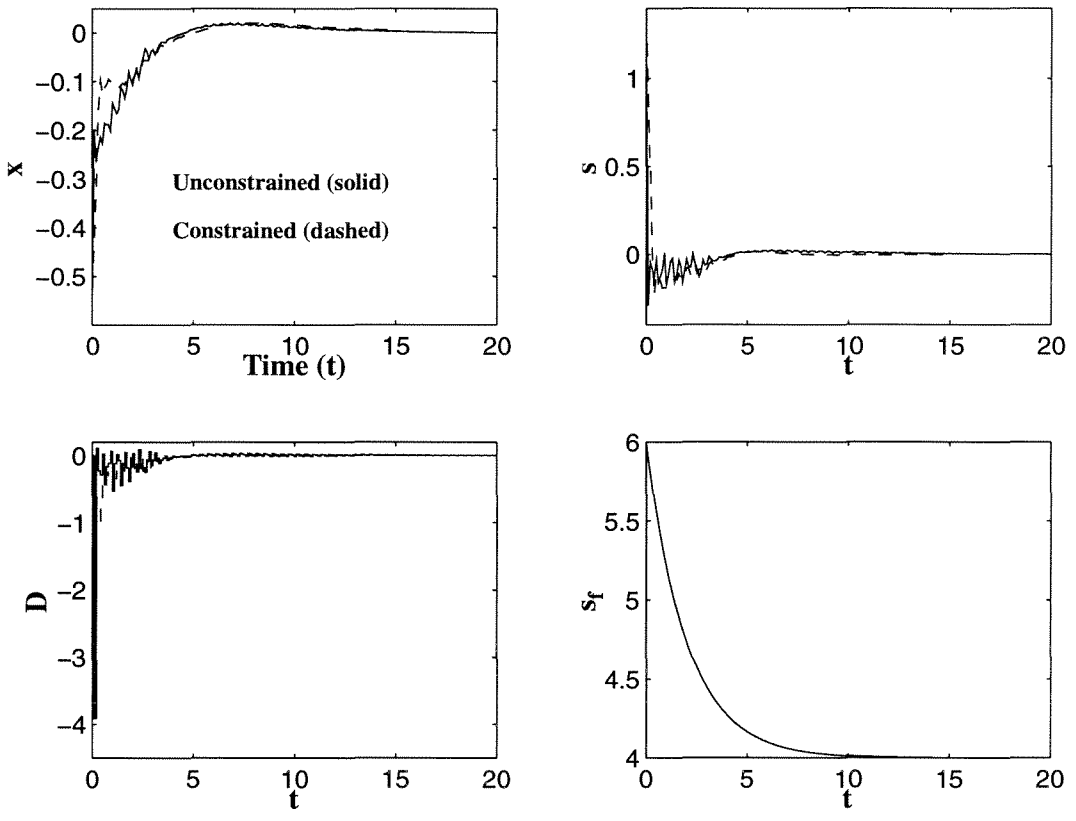

Figure 5.5: Bioreactor: State and control responses in **Case 1.4** (**Transition 1**).

Case 2.1

In this case, the parameters of the plant and the model used in the prediction step of the contractive MPC algorithm are different and constant and only one of the states (the cell concentration in the reactor, x) is available for measurement. The measurement is corrupted by noise and the plant is also simulated with the influence of additive dynamic random noise.

The state estimator used here is the discrete version of the asymptotically stable continuous-time filter introduced in chapter 4.

Our objective is to compare the closed-loop responses obtained with state estimation to the ones previously presented for the state feedback case (**Case 1.2**).

The simulation results for the constrained case are depicted in figure 5.6. The behavior of the dynamic and output noises is also shown in this figure.

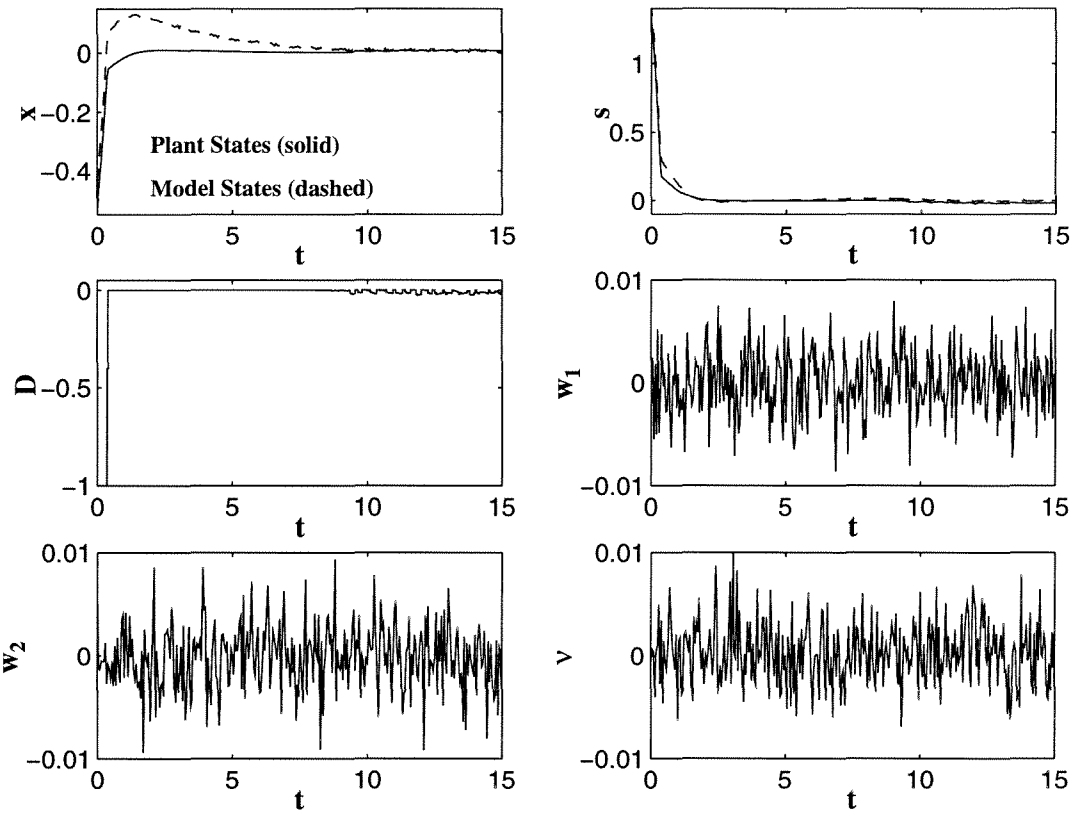

Figure 5.6: Bioreactor: State and control responses in the constrained **Case 2.1** (**Transition 1**).

The control and estimation parameters and initial conditions for the plant and estimator/model used in **Case 2.1** are given by:

Controller and Estimator Parameters (figure 5.6)		
$Q = \text{diag}([1 \quad 0.1])$	$R = 0$	$S = 0$
$P = 5$	$M = 3$	$\alpha = 0.9$
$u_{min} = -1$	$u_{max} = 0$	$\bar{P}_0 = I_n$

Initial Conditions		
Plant:	$x_0 = -0.5351$	$s_0 = 1.3376$
Model/Observer:	$\bar{x}_0 = -0.4351$	$\bar{s}_0 = 1.4376$

Model/Plant Parameters		
Parameters	**Plant**	**Model**
μ_{max}	0.53	0.424
k_m	0.12	0.108
k_1	0.4545	0.409
y	0.4	0.32

As we can see from figure 5.6, the extended Kalman filter provides estimates which converge asymptotically to the states of the model with nominal parameter values (thus, showing offset with respect to the states of the plant) and the contractive MPC controller is able to drive the states of the plant to a control invariant set containing the origin and keep them there.

Because of the imposed input constraints, the control action cannot change its sign ($u_{max} = 0$) and the system is left open-loop after a few initial samples. Since the target steady state is open-loop stable, the system evolves towards it in spite of the constraints.

Case 2.2

Here we applied the combined control/state estimation procedure proposed in this chapter (**Control Algorithm 4**) to the biochemical reactor, under the same constant parameter deviation used in the state feedback case (**Case 1.2**) and when an extended Kalman filter is the state estimator (**Case 2.1**).

The unconstrained and constrained responses are illustrated in figure 5.7.

The dynamic and output noises used in the present simulations are of much higher magnitude than the noises used in the case of state estimation with the

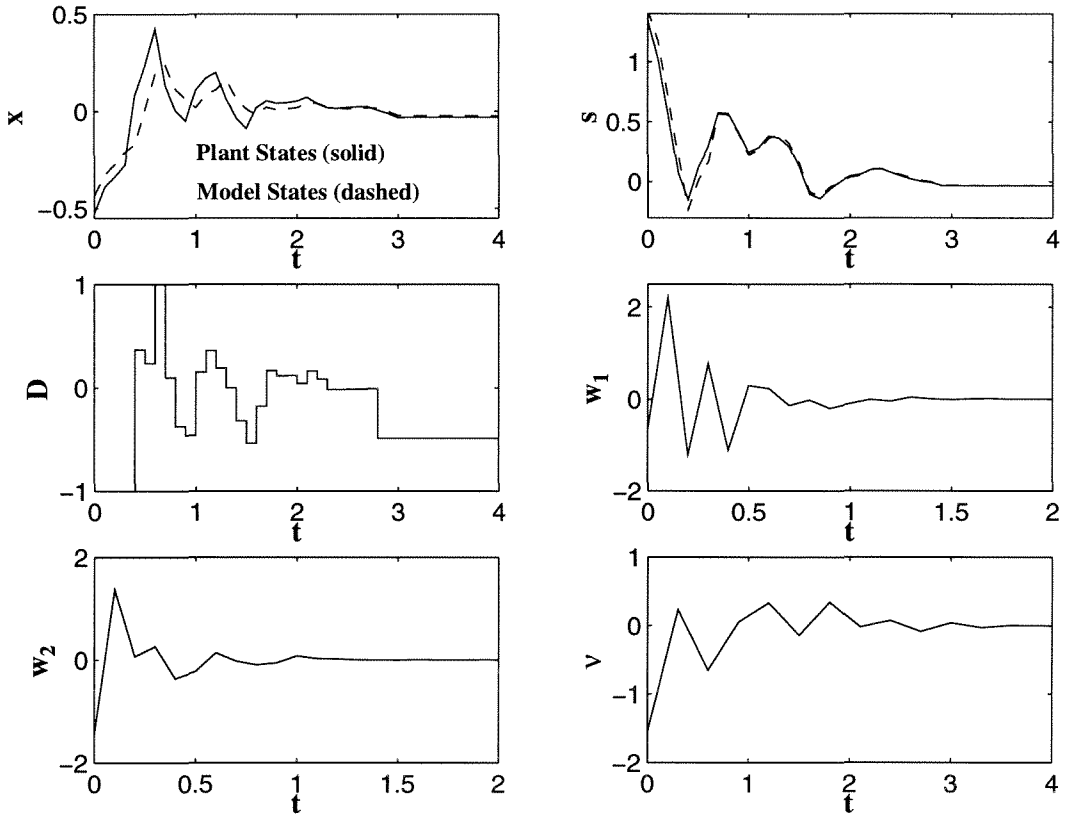

Figure 5.7: Bioreactor: State and control responses in the constrained **Case 2.2** (**Transition 1**).

EKF but they are not persistent (the scaling factors for the noises, i.e., the matrices N_w and R_v are of asymptotically decaying magnitude). This was done here so that we could examine the effect of larger noises in the transient behavior of the closed-loop system. The behavior of the simulated random noises is also illustrated in figure 5.7.

The control and estimation parameters and initial conditions for the plant and estimator/model used in **Case 2.2** are given by:

Controller and Estimator Parameters (figure 5.7)		
$Q = \text{diag}([1 \quad 0.1])$	$R = 0$	$S = 0$
$P = 5$	$M = 3$	$\alpha = 0.9$
$u_{min} = -1$	$u_{max} = 1$	
$m = 6$	$P_1 = 0.01\ I_n$	$\bar{R}^{-1} = 10\ I_p$

Initial Conditions		
Plant:	$x_0 = -0.5351$	$s_0 = 1.3376$
Model/Observer:	$\bar{x}_0 = -0.4351$	$\bar{s}_0 = 1.4376$

Model/Plant Parameters		
Parameters	**Plant**	**Model**
μ_{max}	0.53	0.424
k_m	0.12	0.108
k_1	0.4545	0.409
y	0.4	0.32

As we notice from figure 5.7, the states of the plant still converge to a small control invariant set around the origin. Notice also the offset in $u = D$.

The transient behavior of the closed-loop for the implementation with the LSE scheme is worse than in **Case 2.1** (estimation with EKF) due to the noise being of initial magnitude 20 times higher than the noise used there.

Transition 2

Case 1.1

The unconstrained and constrained simulations with the plant being the same as the model and in the absence of disturbances are shown in figure 5.8.

The controller parameters used in **Case 1.1** are given by:

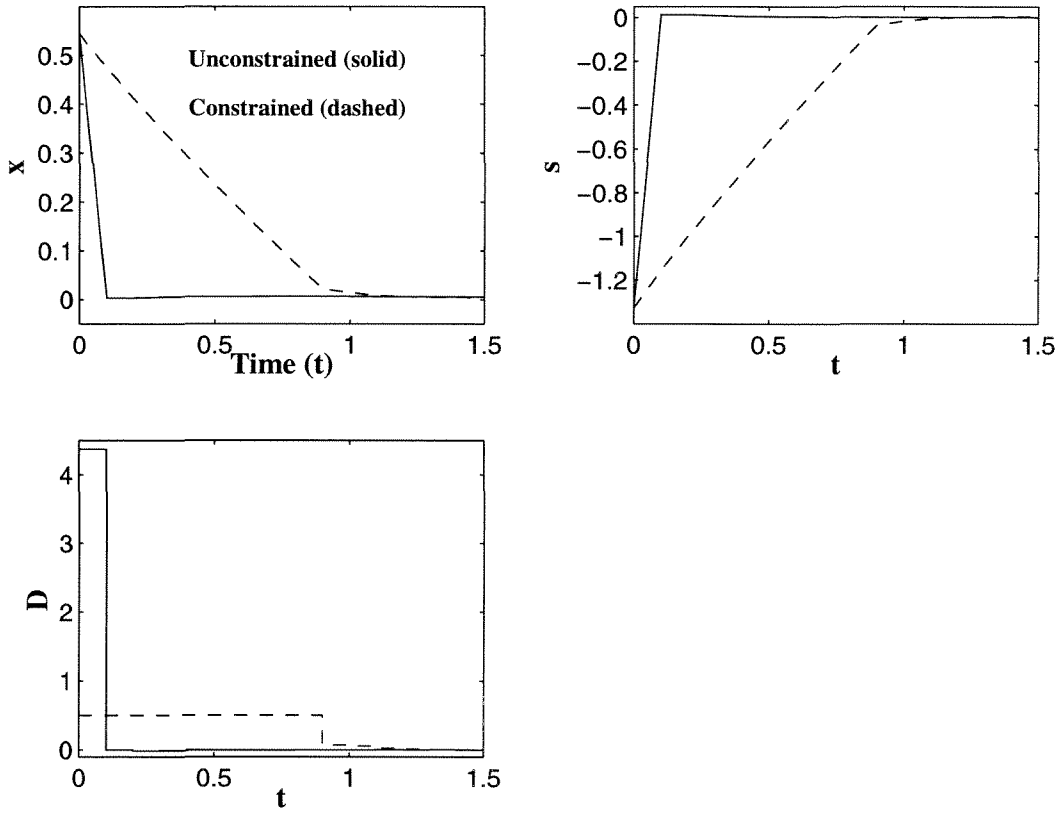

Figure 5.8: Bioreactor: State and control responses in **Case 1.1** (**Transition 2**).

Controller Parameters (figure 5.8)		
$Q = \text{diag}([1 \quad 0.1])$	$R = 0$	$S = 0$
$P = 4$	$M = 2$	$\alpha = 0.6$
$u_{min} = 0$	$u_{max} = 0.5$	

Unless otherwise indicated, the hard control constraints used in the simulations of the step change from steady state (**2**) to (**1**) will be the same as the ones used here in the nominal case.

As we can see from figure 5.8, the response in the unconstrained case occurs in only one sampling time. The effect of tight input constraints (approximately nine times smaller than the maximum control effort in the unconstrained case) is to delay the response which now occurs only after thirteen samples.

Case 1.2

The simulation results for the unconstrained and constrained cases are depicted in figure 5.9.

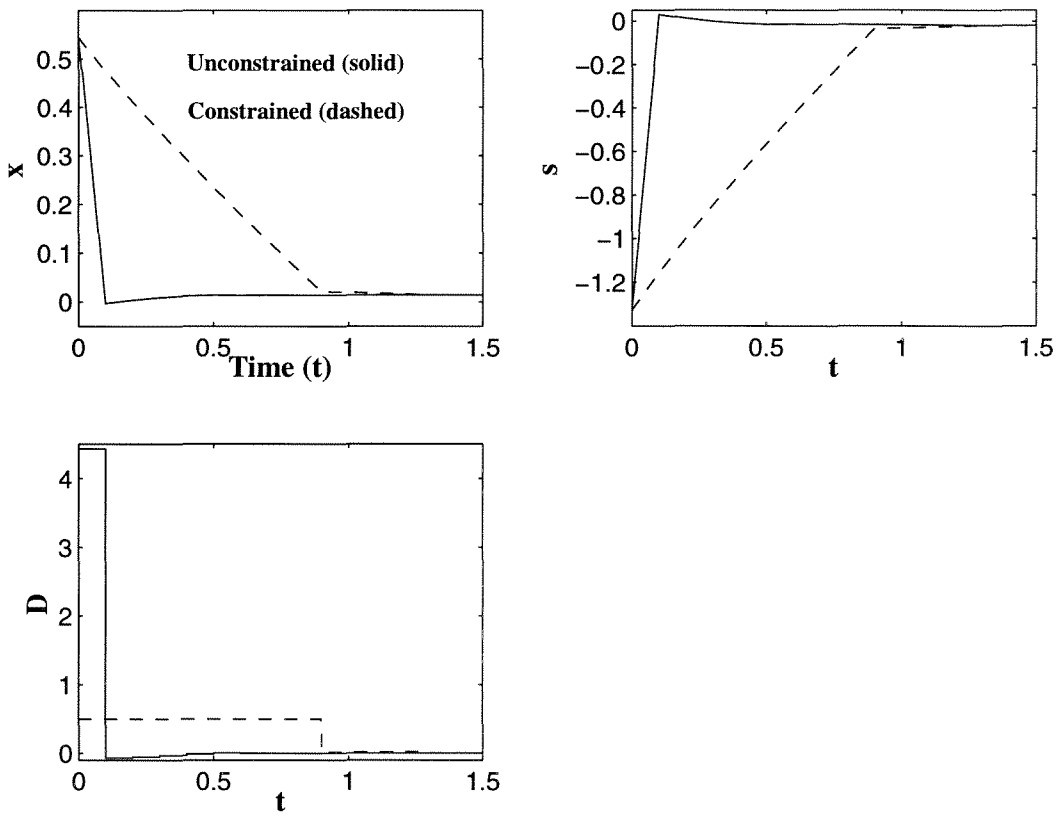

Figure 5.9: Bioreactor: State and control responses in **Case 1.2** (**Transition 2**).

The controller and model/plant parameters used in **Case 1.2** are:

Controller Parameters (figure 5.9)		
$Q = \text{diag}([1 \quad 0.1])$	$R = 0$	$S = 0$
$P = 4$	$M = 2$	$\alpha = 0.9$

Model/Plant Parameters		
Parameters	**Plant**	**Model**
μ_{max}	0.53	0.424
k_m	0.12	0.12
k_1	0.4545	0.4545
y	0.4	0.32

As we can see from figure 5.9, the states show a small offset, i.e., due to the parameter uncertainty, exponential (or even asymptotic) stability to the origin cannot be achieved. Once again, the effect of the input constraints is to delay the state response by a few samples (approximately nine, in this case).

Case 1.3

The disturbance in s_f considered here has the behavior shown in figure 5.4, i.e., it decays exponentially to a value 5% below its value at steady state.

The same observations which we made regarding the stability properties of the closed-loop under this kind of disturbance for **Transition 1** hold for **Transition 2**.

The unconstrained and constrained simulations taking into account this disturbance in s_f are illustrated in figure 5.10.

The controller parameters used in **Case 1.3** are the following:

Controller Parameters (figure 5.10)		
$Q = \text{diag}([1 \quad 0.1])$	$R = 0$	$S = 0$
$P = 8$	$M = 4$	$\alpha = 0.9$

As we notice from figure 5.10, this level of asymptotic disturbance deviation from its nominal value and the persistence of such disturbance do not allow the states to be brought to the origin.

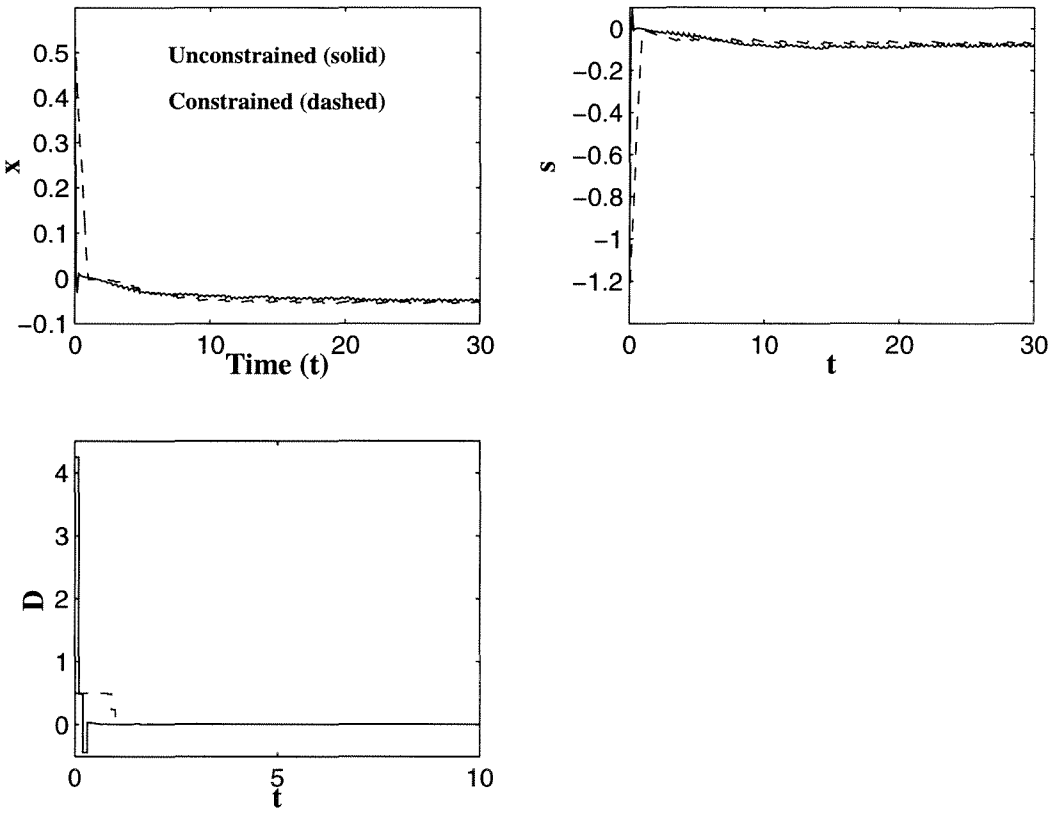

Figure 5.10: Bioreactor: State and control responses in **Case 1.3** (**Transition 2**).

As in the simulations for the previous step change, some of the oscillation obtained in the response as t increases is due to numerical instabilities which we were not able to eliminate completely with our adjustments of tolerance parameters in both the optimization and integration routines.

Even in the unstable operating region and in spite of the numerical problems which we could not avoid through change of tolerance parameters for both the optimization and integration routines, we can see that our theoretical prediction of the closed-loop response was correct and the states can indeed be brought to the interior of a control invariant set and be kept there as $t \to \infty$.

As in most cases, the effect of the input constraints is to delay the response. The constraints do not have any effect on the asymptotic response since they are no longer active at that stage.

Case 1.4

The responses for the unconstrained and constrained simulations can be found in figure 5.11. The disturbance behavior is also shown in this figure.

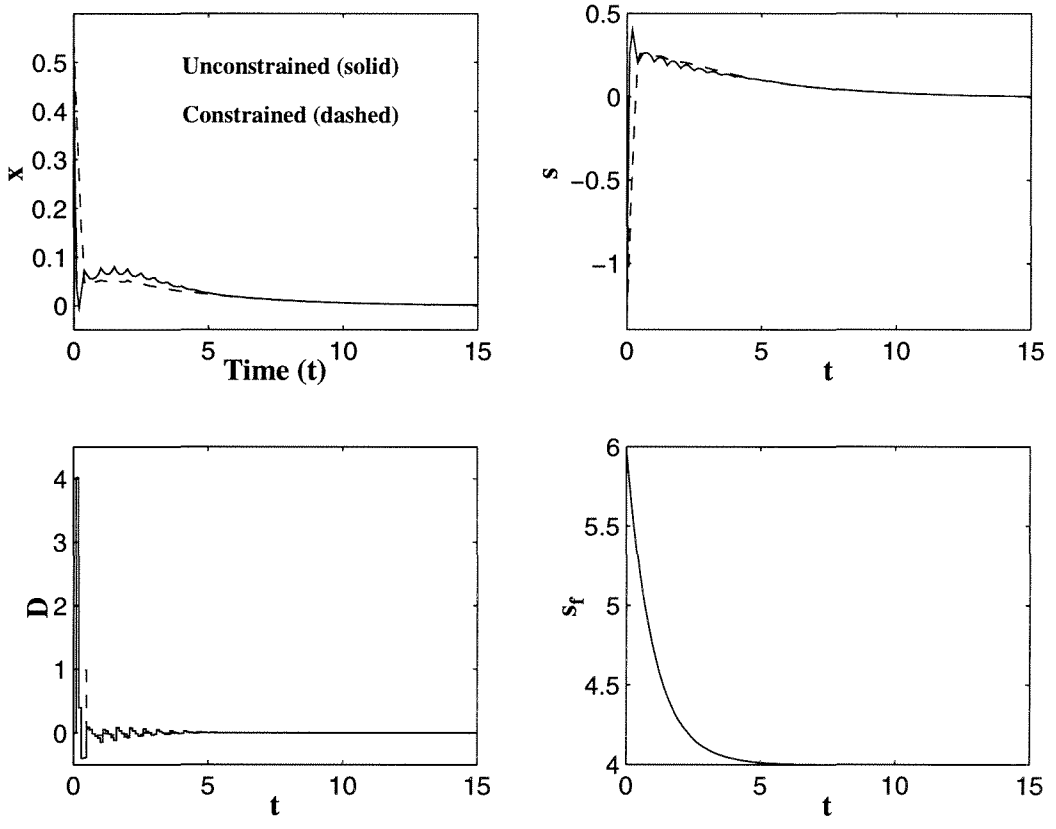

Figure 5.11: Bioreactor: State and control responses in **Case 1.4** (**Transition 2**).

The controller parameters used in **Case 1.4** are as follows:

Controller Parameters (figure 5.11)		
$Q = \text{diag}([1 \quad 0.1])$	$R = 0$	$S = 0$
$P = 8$	$M = 5$	$\alpha = 0.9$
$u_{min} = -0.05$	$u_{max} = 1$	

The obtained results are as expected from our theoretical investigations of this class of disturbances and they also show that the influences of the input con-

straints and of the open-loop instability of the final steady state are not felt strongly in this case.

Case 2.1

As we have noticed from the previous simulations, controlling the operation around the unstable point with contractive MPC in the state feedback case, has not presented much more of a challenge than in the case of operation in the stable region.

The following simulation results will tell a different story for the output feedback case. The introduction of an initial estimation error and of measurement and dynamic noises in the simulations near the unstable operating point causes many more difficulties for the EKF to provide asymptotically convergent estimates than in the step change to the stable steady state (especially if there are active input constraints). The fact that the linearization of the system near the operating point is open-loop unstable has made the filter (which utilizes this linearization for update of the state estimates and covariance matrices) more sensitive to the effects of noise and initial estimation error.

Since the introduction of parameter uncertainty represents an additional difficulty, we have simulated the output feedback response for reasonably small initial state deviations but in the presence of a considerable amount of noise and the closed-loop is shown to be asymptotically stable in figure 5.12. The output and dynamic random noises are also plotted in this figure.

The control/estimator parameters and initial conditions for these simulations are:

Controller and Estimator Parameters (figure 5.12)		
$Q = \text{diag}([1 \quad 0.1])$	$R = 0$	$S = 0$
$P = 8$	$M = 5$	$\alpha = 0.9$
		$\bar{P}_0 = I_n$

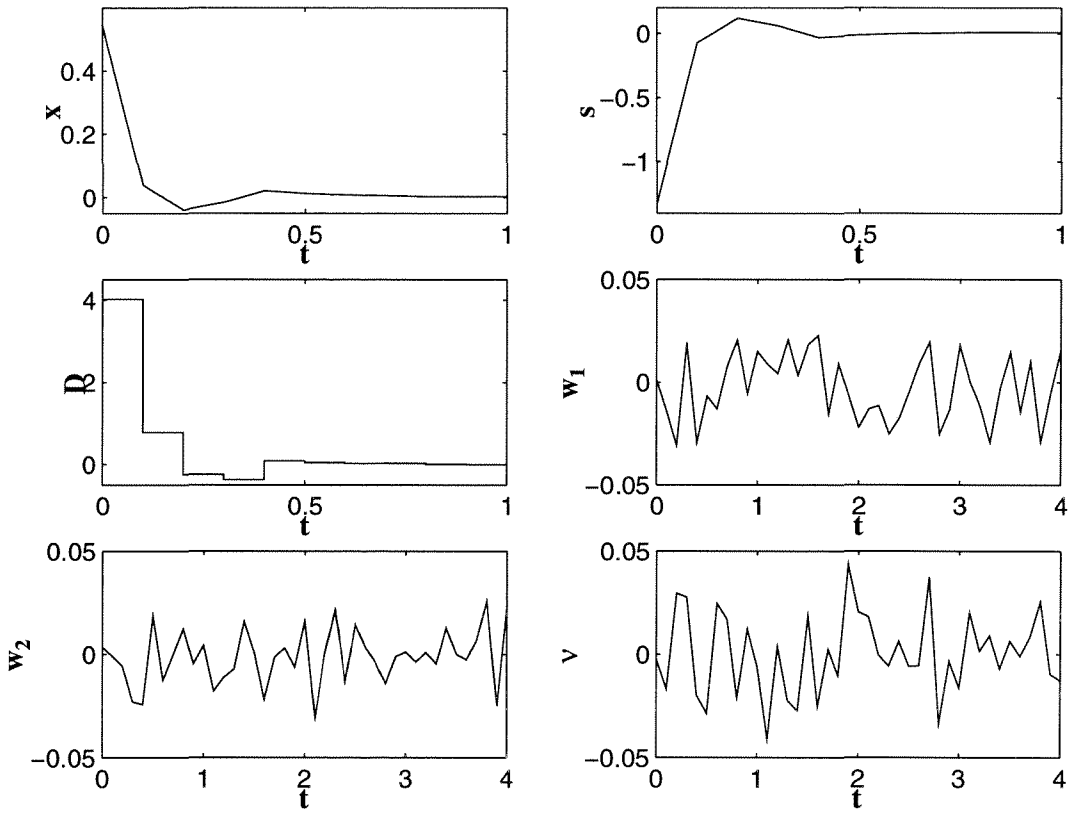

Figure 5.12: Bioreactor: State and control responses in the unconstrained output feedback nominal case using EKF (**Transition 2**).

Initial Conditions		
Plant:	$x_0 = -0.5351$	$s_0 = 1.3376$
Model/Observer:	$\bar{x}_0 = -0.52$	$\bar{s}_0 = 1.31$

Contrary to what happens in the stable operating regime, the EKF provides estimates which completely diverge from the states of the plant in the presence of parameter uncertainty and, since the contractive constraint is imposed on the states of the model (which are obtained by integration of the model equations with the estimated states as initial condition at each sampling time), the closed-loop response is unstable as we can see in figure 5.13.

The level of noise used here is the same as in the output feedback simulation of the nominal case (figure 5.12).

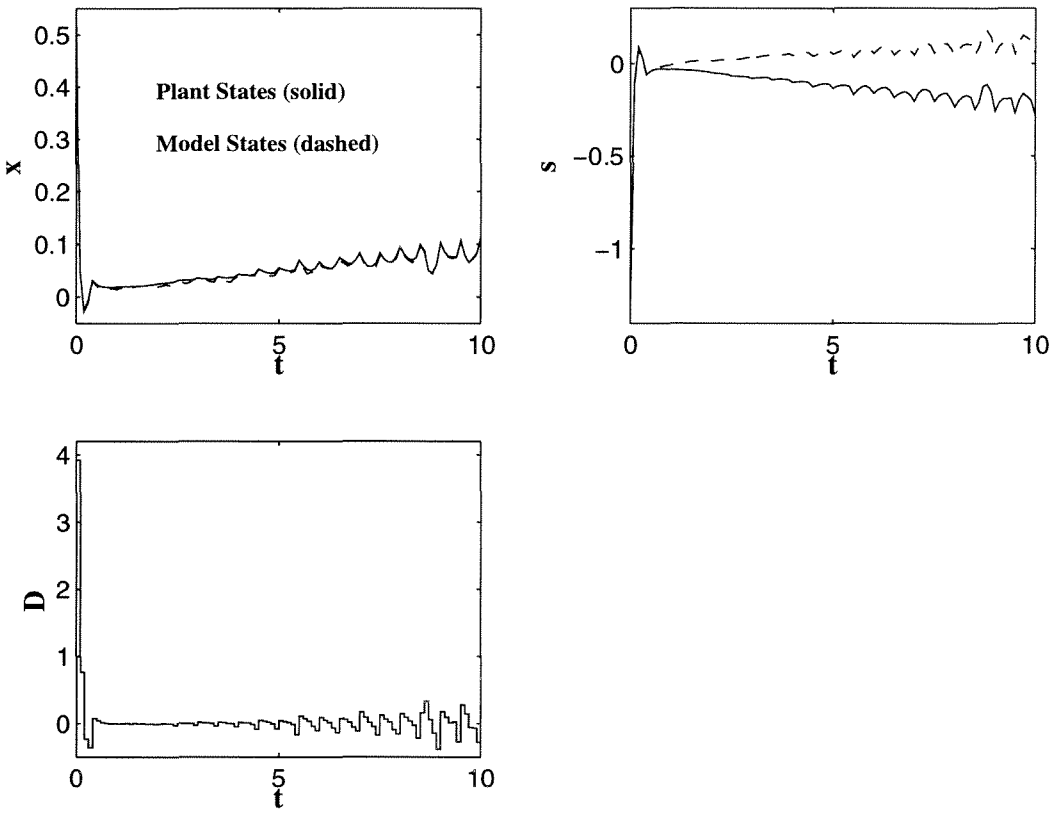

Figure 5.13: Bioreactor: State and control responses in the unconstrained output feedback robust case using EKF (**Transition 2**).

The model/plant, controller and estimator parameters in **Case 2.1** are given by:

Controller and Estimator Parameters (figure 5.13)		
$Q = \text{diag}([1 \quad 0.1])$	$R = 0$	$S = 0$
$P = 8$	$M = 5$	$\alpha = 0.9$
		$\bar{P}_0 = I_n$

Model/Plant Parameters		
Parameters	**Plant**	**Model**
μ_{max}	0.53	0.424
k_m	0.12	0.108
k_1	0.4545	0.409
y	0.4	0.32

The initial conditions are:

Initial Conditions		
Plant:	$x_0 = 0.5351$	$s_0 = -1.3376$
Model/Observer:	$\bar{x}_0 = 0.5$	$\bar{s}_0 = -1.2$

As we can see from figure 5.13, due to the relatively small level of noise, and because the measured output is the concentration of cells in the reactor, x, the estimates of x provided by the EKF converge to the true cell concentration (as they should). However, since the estimates of s (the substrate concentration in the reactor) diverge completely, the closed-loop becomes unstable even in the absence of input constraints.

Case 2.2

We will see here that the LSE procedure does not suffer from the same drawbacks that we pointed out for the EKF in **Transition 2** (**Case 2.1**). LSE is able to provide better estimates in this case because it uses the nonlinear system model (as explained earlier in this chapter) in the optimal estimation procedure and not the unstable linear approximation. Moreover, the estimates are computed using $m = P + 1$ previous measurements and not only the most recent one as with the Kalman filter.

The results show that the LSE provides as good estimates as it did in **Transition 1**.

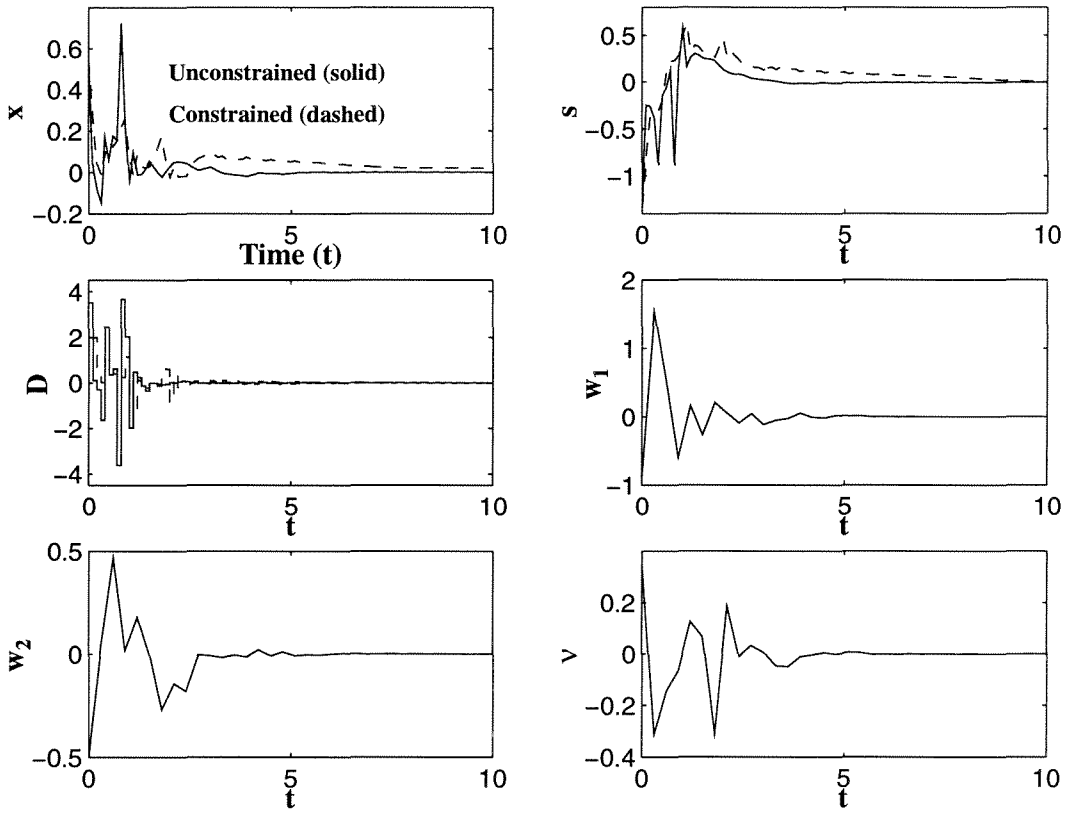

Figure 5.14: Bioreactor: State and control responses in the output feedback robust case using LSE (**Transition 2**).

The unconstrained and constrained responses are illustrated in figure 5.14.

Also here, the dynamic and output noises used in the present simulations are of much higher magnitude than the noises used in the case of state estimation with the EKF but they are not persistent. The behavior of the simulated random noises is also illustrated in figure 5.14.

The controller/estimator parameters and initial conditions for the plant and model/observer used in **Case 2.2** are given by:

Controller and Estimator Parameters (figure 5.14)		
$Q = \text{diag}([1 \quad 0])$	$R = 0$	$S = 0$
$P = 5$	$M = 3$	$\alpha = 0.9$
$u_{min} = -2$	$u_{max} = 2$	$\bar{P}_0 = I_n$
$m = 6$	$P_1^{-1} = I_n$	$\bar{R} = 0$

Model/Plant Parameters		
Parameters	**Plant**	**Model**
μ_{max}	0.53	0.424
k_m	0.12	0.108
k_1	0.4545	0.409
y	0.4	0.32

Initial Conditions		
Plant:	$x_0 = -0.5351$	$s_0 = 1.3376$
Model/Observer:	$\bar{x}_0 = 0.5$	$\bar{s}_0 = -1.3$

The transient behavior of the closed-loop is poor due to the high levels of process noise up to time $t = 5$.

Chapter 6 Contractive NLMPC reformulated as a Quadratic Programming (QP) Problem

In this chapter we will be dealing with the following problem:

Problem 6 : *Stability and computational properties of contractive MPC when the model used for prediction is a linearization of the nonlinear plant about the predicted trajectory*

6.1 Introduction

In the previous chapters we have shown how the contractive constraint exponentially stabilizes the closed-loop system when no model uncertainty or disturbances are present. Then, we demonstrated that the closed-loop becomes uniformly asymptotically stable if asymptotically decaying disturbances affect the system. We have also shown that this kind of disturbance could be caused by introduction of an asymptotically convergent observer into the closed-loop for state estimation. We derived sufficient conditions under which the association of an exponentially stable controller (such as contractive MPC) with an asymptotically convergent observer generates an asymptotically stable closed-loop system. Furthermore, we have designed such an observer for a continuous-time system with discrete observations.

In the last chapter, we have first looked into the state feedback control problem when persistent, bounded and non-additive disturbances affect the nonlinear dynamics of the system. In the nonlinear context, the problem posed by disturbances of this kind is equivalent to having parameter uncertainty only (i.e., model and plant are matched in the nonlinear structure, only some - or all - parameters are unknown). We have demonstrated that the most which can be guaranteed under non-additive bounded disturbances or parameter mismatch, is that the states are driven to a control invariant set whose size is proportional to the "size" of the disturbances or parameter deviation. Then, we examined how these results change when the states are also unknown (output feedback case) if the parameters are unknown but constant. We have used a moving horizon-based estimator as proposed in [111] for state estimation. Finally, we studied how the results are modified if both states and parameters are unknown, the parameters are time-varying, the system is subject to additive disturbances and the estimation procedure seeks to estimate states, disturbances and parameters.

All the previously proposed MPC schemes involve the solution of a nonlinear programming problem at each time step to find the optimal (or, at least, feasible) control sequence. Nonlinear programming is the general case in which both the objective and constraint functions may be nonlinear, and is the most difficult of the smooth optimization problems. Indeed there is no general agreement on the best approach to be used for its solution and much research is still to be done. Penalty and barrier functions constitute a global approach to nonlinear programming but they suffer from well-known computational deficiencies and are not entirely efficient. An alternative way to proceed is to consider local methods which perform well in a neighborhood of the solution as described, e.g., in [45, 46, 72]. Some well-known local methods are Newton's method (applied to the first-order conditions that arise in the method of Lagrange multipliers). It can be shown that this method generalizes to give the *sequential quadratic programming (SQP) method.* This method converges locally at second order and has the same standing for nonlinear programming as Newton's

method does for unconstrained minimization. Another idea which has attracted a lot of attention is that of a *feasible direction method* which generalizes the active set type of method for linear constraints and aims to avoid the use of a penalty function. Although software is available for this type of method, there are nonetheless difficulties in determining a fully reliable algorithm.

Due to the difficulties inherent to solving nonlinear programming problems and since MPC requires the optimal (feasible) solution to be computed on-line, it is important that an alternative implementation be found which guarantees that the problem can be solved in a finite number of steps. It is well-known that both linear and quadratic programming (QP) problems satisfy this requirement. A QP problem is an optimization problem in which the objective function is quadratic and the constraint functions are linear. Thus the problem is to find a solution z^* to

$$\begin{aligned} \text{minimize} \quad & J(z) := \tfrac{1}{2} z' H z + h' z \\ \text{subject to} \quad & a_i' z = b_i, \quad i \in E, \\ & a_i' z \geq b_i, \quad i \in I \end{aligned} \tag{6.1}$$

where z are the decision variables, $J(z)$ is the performance criterion, H is a symmetric positive (semi-)definite matrix, E and I are the sets of equality and inequality constraints, respectively, and the matrix A and vector b define the linear equality and inequality constraints on the optimization variable z. As in linear programming, the problem may be infeasible or the solution may be unbounded; however, these possibilities are readily detected in the standard algorithms, so for the most part it is assumed that a solution z^* exists. If the Hessian matrix H is positive semi-definite, z^* is a global solution, and if H is positive definite, z^* is also unique. These results follow from the (strict) convexity of $J(z)$, so that (6.1) is a convex programming problem. Thus, results which apply to convex optimization automatically apply for QPs. When the Hessian H is indefinite then local solutions which are not global can occur, and the computation of any such local solution is of interest.

In [48] one can find for the first time an implementation of MPC to nonlinear systems where the model used for prediction is a linearization of the original nonlinear dynamics around the states at the current time step. Combining that with a quadratic objective function and linear constraints on the control variables, the MPC problem is formulated as a QP to be solved at each time step. The resulting MPC strategy is known as quadratic dynamic matrix control (QDMC). This is a very simple and effective alternative implementation of MPC from a computational point of view but the resulting closed-loop may be unstable. In the present chapter, we will look into how to combine the attractive computational features of Garcia's method in [48], and subsequently used by Ricker and Lee in [74, 110] (by linearizing the nonlinear system about the predicted trajectory) with the stability guarantees which we obtained through the use of the contractive constraint. We will see that even though the contractive constraint is a quadratic constraint (and not a linear one as required for the problem to be posed as a QP), there are ways to incorporate this constraint into the optimization in combination with a quadratic objective function, a linear prediction model and other additional linear constraints, and still obtain a QP.

Since the model used for prediction is a linear approximation of the original nonlinear dynamics, this linearization procedure which makes the algorithm much simpler from a computational point of view, makes the stability analysis much more complex because of the model/plant mismatch caused by the linear approximation. It is no longer possible to guarantee exponential or even asymptotic stability of the closed-loop system to the origin. We will show that the states can be steered to a neighborhood of the origin whose size is proportional to the mismatch between the nonlinear system and its linear approximation. We know that the dynamics of a nonlinear model and that of its linearization about an equilibrium point converge locally, i.e., in a small neighborhood of the considered equilibrium point (see [121]). Indeed, even though we are performing linearization at transient points (and not equilibrium points), the state trajectories of the nonlinear plant and that of the linear model are very close to one another if the sampling time is small.

6.2 Contractive MPC posed as a QP

6.2.1 Description of the system

The nonlinear systems considered in this chapter are described by the following equations:

$$\dot{\bar{x}}(t) = \bar{f}(\bar{x}(t), \bar{u}(t), \bar{p}(t), \bar{d}(t)) \tag{6.2}$$

where $\bar{x}(t) \in \Re^n$ is the vector of state variables, $\bar{u}(t) \in \Re^m$ are the manipulated variables, $\bar{p}(t) \in \Re^s$ is the vector of unknown time-varying parameters, $\bar{d}(t) \in \Re^d$ are the unknown time-varying disturbances which affect the system and $\bar{f} : \Re^n \times \Re^m \times \Re^s \times \Re^d \rightarrow \Re^n$ represents the function that models the uncertainties and nonlinearities in the plant. $\bar{f}$ is assumed to be a continuously differentiable function.

Now, let $(\bar{x}, \bar{u}, \bar{p}, \bar{d}) = (x^*, u^*, p^*, d^*)$ be the equilibrium point at which one desires to operate the system. p^* and d^* denote the nominal values of the parameters and disturbance variables, respectively.

So let the following deviation variables be defined:

$$\begin{aligned} x^p(t) &:= \bar{x}(t) - x^* \\ u(t) &:= \bar{u}(t) - u^* \\ p(t) &:= \bar{p}(t) - p^* \\ d(t) &:= \bar{d}(t) - d^* \end{aligned}$$

Under this change of variables, the original system (6.2) is expressed as:

$$\dot{x}^p(t) = f(x^p(t), u(t), p(t), d(t)) \tag{6.3}$$

where the definition of the continuously differentiable function f follows straightforwardly from equation (6.2).

It is assumed that $d(t) \in \mathcal{D}$ and $p(t) \in \mathcal{P}, \forall t \in [0, \infty)$, where the sets $\mathcal{D}$ and $\mathcal{P}$ are defined by:

$$\mathcal{D} := \{ d(t) \in \Re^d \mid \| d(t) \| \leq \epsilon_d, \ \ \forall t \in [0, \infty) \} \tag{6.4}$$

$$\mathcal{P} := \{ p(t) \in \Re^s \mid \| p(t) \| \leq \epsilon_p, \ \ \forall t \in [0, \infty) \} \tag{6.5}$$

where $\epsilon_d, \ \epsilon_p \in [0, \infty)$ are known constant values.

Besides, the hard constraints on the manipulated variables, $u(t)$, will be expressed in the usual manner:

$$u(t) \in \mathcal{U} := \{u \in \Re^m : u_{min} \leq u \leq u_{max}\}, \ \ \forall t \in [0, \infty) \tag{6.6}$$

where $u_{min}, \ u_{max} \in \Re^m$ are known constant vectors.

Linear constraints on the rates of change of the manipulated variables are also commonly present, as we have pointed out in chapter 2 (see equations 2.26 and 2.27).

6.2.2 State feedback contractive MPC algorithm with linear approximation

Control Algorithm 5

Data: *Initial Conditions:* t_0 *and* $x_0^p := x^p(t_0)$*; Controller Parameters: horizons* P, M*, weights* $Q, R, S, \hat{P} > 0$*, contractive parameter* $\alpha \in [0, 1)$*, sampling time* T *and control constraints* $u_{min}, u_{max}, \Delta u_{max}$.

Step 0: *Set* $k = 0,\ j = 0$.

Step 1: *Assuming that the optimal control problem* $\mathcal{P}(t_k^j, x_k^{p,j})$ *is feasible for the chosen set of parameters, then at* $t = t_k^j$ *solve* $\mathcal{P}(t_k^j, x_k^{p,j})$ *which is specified by:*

$$\begin{aligned}\min_{u(kP+j|kP+j),\ldots,u(kP+j+M-1|kP+j)}\ J_k^j\ &:= \sum_{i=1}^{P}\ \| x(kP+j+i|kP+j) \|_Q^2 \\ &+ \sum_{i=0}^{M-1}[\ \| u(kP+j+i|kP+j) \|_R^2 + \| \Delta u(kP+j+i|kP+j) \|_S^2\ ] \quad (6.7)\end{aligned}$$

subject to:

$$\begin{cases} \dot{x}_k^j(t) = C_k^j + A_k^j x_k^j(t) + B_k^j u_k^j(t),\ \ x_k^j := \text{ measured states at } t_k^j \quad (x_k^{p,j}) \\ u_{min} \le u(kP+j+i|kP+j) \le u_{max},\ \ i \in [0, M-1] \\ |\Delta u(kP+j+i|kP+j)| \le \Delta u_{max},\ \ i \in [0, M-1] \\ \Delta u(kP+j+i|kP+j) = 0,\ \ i \in [M, P-1] \\ \| \bar{x}_k^j(t_k^P) \|_{\hat{P}} \le \alpha \| x_k^p \|_{\hat{P}},\ \ \alpha \in [0,1) \end{cases} \quad (6.8)$$

where $x(kP+j+i|kP+j)$ *are the predicted states at time* t_k^{j+i} *computed with information up to time* t_k^j, *i.e.,* $x(kP+j+i|kP+j) := x_k^j(t_k^{j+i})$ *and*

$$\dot{\bar{x}}_k^j(t) = C_k^0 + A_k^0 \bar{x}_k^j(t) + B_k^0 u_k^j(t),\ \text{with } \bar{x}_k^0 := x_k^p := x^p(t_k) \text{ and } \bar{x}_k^j = \bar{x}_k^{j-1}(t_k^j), \quad (6.9)$$

for $j \ge 1$, *is the trajectory of the linearized model which is not updated with the states of the plant at* t_k^j *for* $j \in [1, P-1]$. *The states* $\bar{x}_k^j(t)$ *are only updated with the states of the plant at* $t = t_k + PT =: t_k^P$, *i.e., at intervals of one prediction horizon. Moreover, the nonlinear system is not re-linearized at every sampling time for computation of the states* $\bar{x}(t)$ *as it is for computation of the predicted states* $x(t)$. *In other words, while the matrices* A, B, C *are re-calculated at every* $t_k^j,\ j = 0, \ldots, P-1$, *for computation of the predicted trajectories, they are only re-calculated at the beginning of prediction horizons for purpose of computation of the contractive constraint.*

The result of this step is an optimal sequence of control moves $\{u(kP+j|kP+j), \ldots, u(kP+j+M-1|kP+j)\}$.

Step 2: *Apply the first control move, $u(kP+j|kP+j)$, to the plant (6.3) for $t \in [t_k^j, t_k^{j+1}]$ and measure the states at t_k^{j+1}. Set x_k^{j+1} equal to the measured states, $x_k^{p,j+1} := x^p(t_k^{j+1})$, and $\bar{x}_k^{j+1} = \bar{x}_k^j(t_k^{j+1})$, $j \geq 0$.*

Step 3: *If $j < P-1$, set $j = j+1$ and go back to* **Step 1**. *If $j = P-1$ set $x_{k+1}^0 =: x_{k+1} = x_{k+1}^p$, $t_{k+1}^0 = t_{k+1} = t_k^P$, $k = k+1$, $j = 0$, and go back to* **Step 1**.

Remark 6.1 *Notice that in* **Problem 6** *the states $x(t)$ and $\bar{x}(t)$ are computed using linear approximations of the original nonlinear system (6.3). The matrices A_k^j, B_k^j, C_k^j are given by:*

$$A_k^j := \frac{\partial f}{\partial x}(x_k^j, u_k^j, 0, 0) \tag{6.10}$$

$$B_k^j := \frac{\partial f}{\partial u}(x_k^j, u_k^j, 0, 0) \tag{6.11}$$

$$C_k^j := f(x_k^j, u_k^j, 0, 0) - A_k^j x_k^j - B_k^j u_k^j \tag{6.12}$$

i.e., these matrices are computed at nominal values of disturbances and parameters, d^*, p^*, respectively. Thus, the linear approximation of the nonlinear system (6.3) is simply obtained by expanding the nonlinear dynamics in a Taylor series expansion and neglecting second and higher order terms.

Remark 6.2 *The optimization step formulated as in* **Control Algorithm 5** *is a convex programming problem in the control variables (and no longer a general nonlinear programming problem, as we had in the previous chapters). The convexity of the optimization is due to the fact that the objective function is quadratic in the decision variables Δu, the trajectory and input constraints are linear and the contractive constraint is quadratic and convex (since the matrix $\hat{H}$ in the term $(\Delta u)' \hat{H} \Delta u$, which results from writing the contractive constraint as a function of the decision variables, is positive definite - this is easy to verify since the contractive constraint is derived in the same way as the objective function which is convex, the only difference being the independent terms in the former).*

The problem of minimizing a convex function on a convex set $\mathcal{K}$ is what we call a convex programming problem. These problems have the following structure:

$$\begin{aligned} &\textit{minimize} && J(z) \\ &\textit{subject to} && c_i(z) \geq 0, \quad i = 1, \ldots, nc \end{aligned} \tag{6.13}$$

where nc is the number of constraints, $J(z)$ is a convex function on $\mathcal{K}$ and the functions $c_i(z)$, $i = 1, \ldots, nc$, are concave on $\Re^n$.

It is a well-known result that every local solution z^* to a convex programming problem (6.13) is a global solution, and the set of global solutions is convex. Furthermore, if $J(z)$ is strictly convex on $\mathcal{K}$ then any global solution is unique.

Thus, just by using linear models for prediction and computation of constraints, we have reduced a potentially complex nonlinear programming problem into a very tractable convex problem. Well-established constrained optimization algorithms such as the sequential quadratic programming (SQP) method (also known as Lagrange-Newton method), feasible direction method, etc., are known to perform quite well with convex problems.

Even though, posed as it is, **Control Algorithm 5** is much simpler than **Control Algorithm 1** from a computational point of view, further improvement can still be achieved. In fact, since the prediction model is linear and the constraints on the control variable are also linear, the optimization would be a quadratic programming (QP) problem in the absence of the state constraints (which are quadratic in the control variables). There are, however, alternative ways to implement these quadratic state constraints into the optimization step such that the optimization can still be posed as a QP. We will examine these alternatives in the next section.

6.2.3 Transforming the optimization into a QP

We have identified three different ways to incorporate the contractive constraint into the optimization step of our contractive MPC scheme in order to pose it as a QP:

Procedure 1: Approximate it by a set of $2n + 1$ (where n is the dimension of the state vector) linear constraints.

Procedure 2: Add it to the objective function, pre-multiplied by a chosen scalar weight $\gamma \geq 0$, and remove it from the list of constraints. This leads to an iterative procedure on the weight γ which is carried out until the contractive constraint is satisfied (this is known as a *penalty function approach*).

Procedure 3: Re-write it as:

$$\| \bar{x}_k^j(t_k^P) \|_1 \leq \alpha \, \delta_k^j \, \| x_k^p \|_{\hat{P}} \tag{6.14}$$

where $\delta_k^j := \frac{\|\bar{x}_k^j(t_k^P)\|_1}{\|\bar{x}_k^j(t_k^P)\|_{\hat{P}}}$, with $\bar{x}_k^j(t)$ being the trajectory used in the computation of the contractive constraint at $j = 0, \ldots, P-1$ for a given k.

The modified contractive constraint (6.14), can then be written as a set of $2n+1$ linear constraints in the control variables (this will be shown when we explain procedure 1 in more details).

The purpose is then to find, at time t_k^j, $\delta_k^j > 0$ such that $\delta_k^j = \frac{\|\bar{x}_k^j(t_k^P)\|_1}{\|\bar{x}_k^j(t_k^P)\|_{\hat{P}}}$ for the chosen control parameters. Thus, we have an optimization problem (a QP) whose solution depends now on the parameter δ_k^j. The computation of this parameter value is done through a uni-directional search resulting from a first-order sensitivity analysis of the optimality conditions of the QP with respect to this parameter.

Unlike the penalty function approach, the QP needs to be solved only once at each time step. Then, a linear system is solved and a uni-directional search

is performed on the parameter δ_k^j until the desired equality, $\delta_k^j = \frac{\|\bar{x}_k^j(t_k^P)\|_1}{\|\bar{x}_k^j(t_k^P)\|_{\hat{P}}}$, is obtained [21].

Now we will go into a more detailed description of the three previous approaches to transforming the optimization problem into a QP:

Procedure 1 (approximate or conservative approach)

Since $\| \cdot \|_1 \geq \| \cdot \|_2 \geq \frac{1}{\lambda_{max}^{\frac{1}{2}}(\hat{P})} \| \cdot \|_{\hat{P}}$, we have that if

$$\| \bar{x}_k^j(t_k^P) \|_1 \leq \frac{\alpha}{\lambda_{max}^{\frac{1}{2}}(\hat{P})} \| x_k^p \|_{\hat{P}} \tag{6.15}$$

then the original contractive constraint is automatically satisfied. In other words, equation (6.15) is a sufficient condition for satisfaction of the contractive constraint.

It is well-known that 1−norm constraints can be re-written as a set of linear constraints adding new decision variables to the optimization problem.

To illustrate the procedure, let us consider the constraint:

$$\| b \|_1 \leq a \tag{6.16}$$

with $b \in \Re^n$ and $a > 0$ a scalar. Then, we can re-write constraint (6.16) componentwise, i.e.,

$$\begin{aligned} b_i &\leq c_i, \quad i = 1, \ldots, n \\ -b_i &\leq c_i, \quad i = 1, \ldots, n \\ \sum_{i=1}^{n} c_i &\leq a \end{aligned} \tag{6.17}$$

where the vector c (vector whose components are c_i, $i = 1, \ldots, n$) constitutes a set of n new optimization variables. Thus, this procedure increases the size of the

optimization by n and the number of constraints by $2n$.

The new objective function at step k, j for the problem with modified constraints is given by:

$$\bar{J}_k^j \;:=\; J_k^j + (c_k^j)' c_k^j \tag{6.18}$$

i.e., the objective function is now minimized with respect to the newly introduced variables, c_k^j, as well.

Since the contractive constraint is here approximated by conservative linear constraints, if an optimal solution is found under the new constraints, it means that we may be "over-satisfying" the contractive constraint.

Procedure 2 (penalty function approach)

In this approach, the objective function is modified to:

$$\bar{J}_k^j \;:=\; J_k^j + \gamma \;\| \bar{x}_k^j(t_k^P) \|_P^2, \quad \gamma \geq 0 \tag{6.19}$$

i.e., the contractive constraint is added as a penalty to the original objective function. Simultaneously, the contractive constraint is removed from the list of constraints to which the minimization is subjected. Thus, we still have a quadratic objective function on the control variables and all the constraints are linear.

It is easy to see that by solving this new optimization problem (a QP) for an arbitrary value of the weight $\gamma \geq 0$ does not necessarily imply satisfaction of the contractive constraint. Thus, the QP problem has to be solved iteratively on γ until it is large enough so that the contractive constraint is satisfied. Naturally, we do not want to start by choosing a large value of γ because we are then giving less importance to the minimization of the chosen performance criterion J_k^j. This means that although stability will be assured, the resulting performance can become rather poor. Furthermore, we do not want to "over-satisfy" the contractive constraint by choosing a larger

γ than necessary.

If the optimization problem is well-posed and feasible for an $\alpha \in [0,1)$, then the existence of a finite γ for which the corresponding optimal solution satisfies the contractive constraint is guaranteed.

A major disadvantage of this procedure is that several QPs (for different values of γ) may have to be solved at the beginning of prediction horizons. Because the $P-1$ subsequent control problems are feasible if the optimization at the beginning of the horizon is feasible, these optimizations are solved with the same γ computed then. Still, this procedure can become very expensive computationally.

Procedure 3 (sensitivity analysis approach)

Here we will show a procedure for a very simple first-order sensitivity analysis of QPs . For an important reference on sensitivity and stability analysis in nonlinear programming the reader is referred to [44].

As previously described, this procedure consists in trying to find, at time t_k^j, a parameter $\delta_k^j = \frac{\|\bar{x}_k^j(t_k^P)\|_1}{\|\bar{x}_k^j(t_k^P)\|_{\hat{P}}}$ or, alternatively, to satisfy the constraint:

$$\| \bar{x}_k^j(t_k^P) \|_1 \leq \alpha \, \delta_k^j \, \| x_k^p \|_{\hat{P}} \tag{6.20}$$

As we saw in procedure 1, this constraint can be re-written as $2n+1$ linear constraints with the introduction of n additional optimization variables. Notice that only the last constraint in (6.17) is directly dependent on the parameter δ_k^j.

The quadratic programming problem to be solved at time t_k^j, has the following format:

$$\text{minimize} \qquad J(z) := \tfrac{1}{2} z' H z + h' z$$

$$\text{subject to} \quad \begin{bmatrix} G & 0 \\ 0 & a \end{bmatrix} z \geq \begin{bmatrix} b \\ c\,\delta \end{bmatrix} \tag{6.21}$$

where $a := -1_n$ (with 1_n being a row vector of n ones) and $c := \alpha \parallel x_k^p \parallel_{\hat{P}}$, as it should be clear from (6.17). For simplicity of notation, we have written (and will write from this point on) δ in (6.21) instead of δ_k^j but it should not be forgotten that this parameter will be re-computed at sampling times.

In our problem, the decision variable z has dimension $mM + n$ (number of control moves multiplied by the size of the control vector plus a number of "dummy" variables introduced to re-define the contractive constraint as $2n + 1$ linear constraints).

The computation of the Hessian matrix H, the gradient vector h, the constraint matrix G and the lower bound vector b will be demonstrated in the following section. The dimensions of these matrices and vectors are $H \in \Re^{(mM+n)\times(mM+n)}$, $h \in \Re^{mM+n}$, $G \in \Re^{(4mM+2n)\times mM}$ and $b \in \Re^{4mM+2n}$.

Thus, at time step k (i.e., at the beginning of horizons) we need an initial guess for the parameter value δ so as to solve our QP with. Let us make $\delta^{(0)} := \frac{1}{\lambda_{max}(\hat{P})^{\frac{1}{2}}}$ to be our initial guess. This choice of δ makes us solve the same QP as if we were using procedure 1, i.e., we are solving the QP to satisfy a constraint which is a sufficient condition for satisfaction of the original contractive constraint. Therefore, if the contractive constraint is feasible so will be our modified constraint with $\delta^{(0)}$.

Assuming that the contractive constraint is feasible, we then solve our QP for $\delta^{(0)}$ and find the optimal solution $z^{(0)}$.

This optimal solution obviously satisfies the optimality conditions for the QP problem which are given, for a general nonlinear programming (NLP) problem, by the Kuhn-Tucker (KT) conditions [67]. It is worth just mentioning these Kuhn-Tucker conditions which are first-order necessary conditions for optimality of an NLP.

Given a general NLP problem represented by

$$\begin{aligned} \text{minimize} \quad & J(z) \\ \text{subject to} \quad & c_i(z) = 0, \quad i \in E \\ & c_i(z) \geq 0, \quad i \in I, \end{aligned} \tag{6.22}$$

the following theorem holds:

Theorem 6.1 (First-order necessary conditions or KT conditions) *If z^* is a local minimizer of problem (6.22) and if certain regularity assumptions (see [46] for these assumptions) hold at z^*, then there exist Lagrange multipliers λ^* such that z^*, λ^* satisfy the following system of equations:*

$$\begin{aligned} \nabla_z \mathcal{L}(z, \lambda) &= 0 \\ c_i(z) &= 0, \quad i \in E \\ c_i(z) &\geq 0, \quad i \in I \\ \lambda_i &\geq 0 \\ \lambda_i c_i(z) &= 0, \quad \forall i \end{aligned} \tag{6.23}$$

with

$$\mathcal{L}(z, \lambda) := J(z) - \sum_i \lambda_i c_i(z) \tag{6.24}$$

The point z^* which satisfies equations (6.24) is often known as a *KT point.* $\mathcal{L}(z, \lambda)$ is called a *Lagrangian function.*

The final condition $\lambda_i^* c_i^* = 0$ is referred to as the *complementarity condition* and states that both λ_i^* and c_i^* cannot be non-zero, or equivalently that inactive constraints have a zero multiplier. If there is no i such that $\lambda_i^* = c_i^* = 0$, then *strict complementarity* is said to hold. The case $\lambda_i^* = c_i^* = 0$ is an intermediate state between a constraint being strongly active and being inactive.

Returning to our QP problem, there are two distinct possibilities when it comes to our modified contractive constraint (6.20):

- For the chosen $\delta^{(0)}$ the constraint (6.20) is *active* (which means that the contractive constraint is active).
- For the chosen $\delta^{(0)}$ the constraint (6.20) is *inactive* (which means that the contractive constraint may or may not be active).

If $\delta^{(0)} = \frac{\|\bar{x}_k^{(0)}(t_k^P)\|_1}{\|\bar{x}_k^{(0)}(t_k^P)\|_{\hat{P}}}$ where $\bar{x}_k^{(0)}(t)$ is the optimal linear trajectory obtained by solving the QP with $\delta = \delta^{(0)}$, then we are done and the sensitivity analysis is not necessary. If not, we should proceed as explained below.

Let us examine the KT conditions which originate when constraint (6.20) is active and inactive.

(1) KT conditions for constraint (6.20) *active*:

The Lagrangian function in this case is represented by:

$$\mathcal{L} := \frac{1}{2} z' H z + h' z - \lambda' \left\{ \begin{bmatrix} \bar{G} & 0 \\ 0 & a \end{bmatrix} z - \begin{bmatrix} \bar{b} \\ c\,\delta \end{bmatrix} \right\} \tag{6.25}$$

Thus, according to (6.23), the KT conditions are:

$$\begin{aligned} \tfrac{\partial \mathcal{L}}{\partial z} &= Hz + h - \begin{bmatrix} \bar{G} & 0 \\ 0 & a \end{bmatrix}' \lambda = 0 \\ \begin{bmatrix} \bar{G} & 0 \\ 0 & a \end{bmatrix} z &= \begin{bmatrix} \bar{b} \\ c\,\delta \end{bmatrix} \\ \lambda &\geq 0 \end{aligned} \tag{6.26}$$

where $\bar{G}$ and $\bar{b}$ represent the set of active constraints. The dimension of the Lagrange multiplier vector is $\lambda \in \Re^{4mM+2n+1}$.

(2) KT conditions for constraint (6.20) *inactive*:

The Lagrangian function in this case is represented by:

$$\mathcal{L} := \frac{1}{2} z' H z + h' z - \lambda' \{ [\bar{G} \quad 0] \, z - \bar{b} \} \tag{6.27}$$

Therefore, according to (6.23), the KT conditions are:

$$\begin{array}{rl} \frac{\partial \mathcal{L}}{\partial z} & = Hz + h - [\bar{G} \quad 0]' \, \lambda = 0 \\ [\bar{G} \quad 0] \, z & = \bar{b} \\ \lambda & \geq 0 \end{array} \tag{6.28}$$

Thus, $\lambda \in \Re^{4mM+2n}$.

In order to perform our first-order sensitivity analysis of these optimality conditions, we need to compute the gradients of z and λ with respect to the parameter δ. Let us denote these gradients $\nabla_\delta z$ and $\nabla_\delta \lambda$, respectively.

Using our KT conditions (6.26) and (6.28), let us then examine how these gradient computations are performed in the case of (6.20) being active and inactive.

(1) Gradient computations when constraint (6.20) is *active*:

These gradients are computed by differentiating the equality KT conditions in (6.26) with respect to δ. The resulting linear system in $\nabla_\delta z$ and $\nabla_\delta \lambda$ is given by:

$$\begin{bmatrix} \bar{G} & 0 \\ 0 & a \end{bmatrix} \nabla_\delta z = \begin{bmatrix} 0 \\ c \end{bmatrix} \tag{6.29}$$

$$\begin{bmatrix} \bar{G} & 0 \\ 0 & a \end{bmatrix}' \nabla_\delta \lambda = H \, \nabla_\delta z \tag{6.30}$$

Notice that $\nabla_\delta z$ can be computed from (6.29) first and then substituted in (6.30) for computation of $\nabla_\delta \lambda$.

(2) Gradient computations when constraint (6.20) is *inactive*:

These gradients are computed by differentiating the equality KT conditions in (6.28) with respect to δ. The resulting linear system in $\nabla_\delta z$ and $\nabla_\delta \lambda$ is given by:

$$[\bar{G} \;\; 0]\, \nabla_\delta z \;=\; 0 \;\;\Longrightarrow\;\; \nabla_\delta z \in \mathrm{Ker}(G^*), \text{ with } G^* := [\bar{G} \;\; 0] \tag{6.31}$$

$$(G^*)'\, \nabla_\delta \lambda \;=\; H \nabla_\delta z \tag{6.32}$$

It is easy to show that as a consequence of equations (6.31), (6.32) and the fact that H is positive definite and, therefore, invertible, it follows that $\nabla_\delta \lambda = 0$. If (6.32) is pre-multiplied by H^{-1} and then by G^* we obtain:

$$G^*\, H^{-1}\, (G^*)'\, \nabla_\delta \lambda \;=\; G^*\, \nabla_\delta z \;=\; 0 \tag{6.33}$$

Since $G^*\, H^{-1}\, (G^*)'$ is a positive definite matrix, it follows that $\nabla_\delta \lambda = 0$.

Once a new value for δ is chosen, the *exact* optimal solution of the QP for this δ can be computed from the previous one through the following equations:

$$\begin{aligned} z^{(i+1)} &= z^{(i)} + (\nabla_\delta z)^{(i)}\; \Delta\delta^{(i+1)} \\ \lambda^{(i+1)} &= \lambda^{(i)} + (\nabla_\delta \lambda)^{(i)}\; \Delta\delta^{(i+1)} \end{aligned} \tag{6.34}$$

where $\Delta\delta^{(i+1)} := \delta^{(i+1)} - \delta^{(i)}$, $\forall i \geq 0$, and $(\nabla_\delta z)^{(i)}$, $(\nabla_\delta \lambda)^{(i)}$ are the gradients computed through equations (6.29), (6.30) (if constraint (6.20) is active) or (6.31), (6.32) (if constraint (6.20) is inactive) with $\bar{G}_{(i)}$, $\bar{b}_{(i)}$ being the active constraint sets used in these gradient computations.

Thus, once the QP is solved for $\delta = \delta^{(0)}$ (i.e., the optimal solution $z^{(0)}$ is obtained) and if $\delta^{(0)} \neq \frac{\|\bar{x}_k^{(0)}(t_k^P)\|_1}{\|\bar{x}_k^{(0)}(t_k^P)\|_{\hat{P}}}$, the exact optimal solutions for different values of δ can be

obtained from (6.34) until $\delta^{(i)} = \frac{\|\bar{x}_k^{(i)}(t_k^P)\|_1}{\|\bar{x}_k^{(i)}(t_k^P)\|_{\hat{P}}}$ for some $i \in (0, \infty)$.

The methodology used to update δ is a separate issue. If we choose $\delta^{(i+1)} = \frac{\|\bar{x}_k^{(i)}(t_k^P)\|_1}{\|\bar{x}_k^{(i)}(t_k^P)\|_{\hat{P}}}$ in order to compute $z^{(i+1)}$ we will be off again unless $(\nabla_\delta z)^{(i)} = 0$, i.e., $\delta^{(i+1)} \neq \frac{\|\bar{x}_k^{(i+1)}(t_k^P)\|_1}{\|\bar{x}_k^{(i+1)}(t_k^P)\|_{\hat{P}}}$ for $(\nabla_\delta z)^{(i)} \neq 0$.

Since $F(\delta_k^0) := \delta_k^0 - \frac{\|\bar{x}_k^0(t_k^P)\|_1}{\|\bar{x}_k^0(t_k^P)\|_{\hat{P}}}$ is a monotonic function in δ (if we increase δ it becomes easier to satisfy constraint (6.20) and if we decrease it we make this constraint tighter or even infeasible) and we want to find δ so that $F(\delta) = 0$, a good strategy is to use a bisection algorithm to find this value of δ. Suppose that we start with a large δ so that $F(\delta) > 0$, then we can decrease it until $F(\delta) < 0$. Since we know that the δ we search for lies in the interval between the last δ for which $F(\delta) > 0$ and the first δ for which $F(\delta) < 0$ ($F(\delta)$ is monotonic) we can then perform a bisection in this interval to find our solution. An analogous procedure applies if we start with a value of δ for which $F(\delta) < 0$.

However, we cannot change the values of δ and recompute the optimal solutions (6.34) without checking if the configuration of the active and inactive sets of constraints has changed. If it has, we must re-compute the gradients using (6.29) and (6.30) (or (6.31) and (6.32), depending on constraint (6.20) being active or inactive) and update our optimal solutions accordingly.

The equations used to check if our choice of $\delta^{(i)}$, $i > 0$, preserves the inactive constraint set (which, if the problem is feasible, means that the active set has also remained unchanged) are:

$$(\hat{G}^*_{(i-1)} z^{(i)} - \hat{b}_{(i-1)}) + \hat{G}^*_{(i-1)} (\nabla_\delta z)^{(i-1)} \Delta\delta^{(i)} > 0 \tag{6.35}$$

$$\lambda^{(i)} + (\nabla_\delta \lambda)^{(i-1)} \Delta\delta^{(i)} \geq 0 \tag{6.36}$$

where $\hat{G}^*_{(i-1)}$, $\hat{b}_{(i-1)}$ represent the inactive constraint sets computed at iteration i, with $i > 0$, in the iterative procedure of computing δ. $z^{(i)}$, $\lambda^{(i)}$ is the optimal solution

computed via (6.34) once $\delta^{(i)}$ is selected.

In order to check if the contractive constraint has become inactive, we must check if:

$$a^* \, z^{(i)} - c \;\; \delta^{(i)} \;\; > \;\; 0 \tag{6.37}$$

where $a^* := [a \quad 0]$ and $(a^*)' \in \Re^{mM+n}$.

Once this checking has been done for the chosen value of $\delta^{(i)}$, if the constraint sets have changed (i.e., if some of the inactive constraints have now become active due to the choice of δ), new constraint sets need to be computed. This is a straightforward procedure given the optimal solution $z^{(i)}$. All we need to do is to check which inequality constraints have now become equalities (active constraints) and shift this once inactive constraints into the set $\bar{G}_{(i)}$, $\bar{b}_{(i)}$ of active constraints.

With these newly computed active constraint sets we can re-compute the gradients, i.e., obtain $(\nabla_\delta z)^{(i)}$, $(\nabla_\delta \lambda)^{(i)}$; update the optimal solution with these gradients and the new value of δ, $\delta^{(i+1)}$; check if $\delta^{(i+1)} = \frac{\|\bar{x}_k^{(i+1)}(t_k^P)\|_1}{\|\bar{x}_k^{(i+1)}(t_k^P)\|_{\hat{P}}}$. If the equality is not satisfied, check if the constraint sets have been preserved and repeat the whole procedure; if the equality is indeed satisfied, we are done and the optimal solution of the QP is given by $z^{(i+1)}$, $\lambda^{(i+1)}$.

We have explained so far how to compute δ_k^0, i.e., the parameter δ at the beginning of prediction horizons. However, at each $j = 1, \ldots, P-1$, for a fixed $k \geq 0$, we need to calculate a new parameter δ_k^j which satisfies $\delta_k^j = \frac{\|\bar{x}_k^j(t_k^P)\|_1}{\|\bar{x}_k^j(t_k^P)\|_{\hat{P}}}$ using the same technique discussed for computation of δ_k^0. However, to repeat the sensitivity analysis at each sampling time can become computationally expensive. Once we have found $\delta_k^0 = \frac{\|\bar{x}_k^0(t_k^P)\|_1}{\|\bar{x}_k^0(t_k^P)\|_{\hat{P}}}$, we know that there exists a control sequence at each $j = 1, \ldots, P-1$ such that the constraints

$$\| \, \bar{x}_k^j(t_k^P) \, \|_1 \;\; \leq \;\; \alpha \delta_k^0 \, \| \, x_k^p \, \|_{\hat{P}} \tag{6.38}$$

are feasible. Thus, at time t_k^j, $\forall j \in [1, P-1]$, we should solve the QP with

$\delta = \delta_k^0$. Then, with the obtained trajectory $x_k^j(t), \quad t \in [t_k^j, t_k^{j+P}]$, we can check if the contractive constraint at t_k^j is satisfied, i.e., if

$$\| \bar{x}_k^j(t_k^P) \|_{\hat{P}} \leq \alpha \| x_k^p \|_{\hat{P}} \tag{6.39}$$

If yes, we accept the computed control sequence $u(kP+j|kP+j), \ldots, u(kP+j+M-1|kP+j)$. If not, rigorously, we should have to solve for $\delta_k^j = \frac{\|\bar{x}_k^j(t_k^P)\|_1}{\|\bar{x}_k^j(t_k^P)\|_{\hat{P}}}$ using sensitivity analysis of the QP problem at time t_k^j. However, since we only need to have the contractive constraint satisfied at $j = P-1$ for stability purposes, we can solve the optimization problems at $j = 1, \ldots, P-2$ with $\delta = \delta_k^0$ (which are feasible if the problem at t_k with δ_k^0 is feasible), and only check for satisfaction of the contractive constraint at t_k^{P-1}. In case it is not satisfied by using the control sequence computed with $\delta = \delta_k^0$ (which implies that $\delta_k^{P-1} := \frac{\|\bar{x}_k^{P-1}(t_k^P)\|_1}{\|\bar{x}_k^{P-1}(t_k^P)\|_{\hat{P}}} < \delta_k^0$), then we should use the search procedure, described previously for computation of δ_k^0, in order to calculate δ_k^{P-1}. In this case, the computation of δ using sensitivity analysis of the QP would be repeated only twice for a whole prediction horizon and stability would still be assured.

All along we have been saying that the updated solutions given by equations (6.34) are *exact* optimal solutions of the QP for the new parameter value even if the active constraint set changes. We must emphasize that this is the case because our optimization is a QP. For a general nonlinear programming problem this does not hold true, i.e., an update given by (6.34) is only a first-order approximation of the exact solution and does not have much significance. The only reason why this first-order update is optimal is due to the fact that the Kuhn-Tucker conditions for a QP are linear. It is very straightforward to prove that the solutions are indeed optimal, all we need to do is to replace the updated solution into the optimality conditions for the previous solution (with an updated active constraint set, if it has changed) and we will verify that they satisfy these conditions as a result of the way in which the gradients are computed. Thus, if the optimality conditions are satisfied by the first-order update, this is indeed an optimal solution.

6.2.4 QP format

Here we will illustrate how the optimization problem in **Control Algorithm 5** can be re-written in QP format (as in (6.1)) for each of the three procedures proposed for implementation of the contractive constraint.

The Hessian matrix H and the gradient vector h' are basically the same (with minor modifications, which we will point out) for the three methods. The main change occurs in the definition of the constraint matrices because of the different ways of implementing the contractive constraint.

In the optimization step in **Control Algorithm 5**, the objective function is defined in terms of states x, control moves u and rates of change of the control variables Δu. Let us then adopt Δu to be our decision variables and in order to write the problem at time step k, j in QP format, we need to express x and u as functions of the M optimization variables $\Delta u(kP+j|kP+j), \ldots, \Delta u(kP+j+M-1|kP+j)$, $j \in [0, P-1]$, $k \geq 0$.

Our continuous-time linear approximation of the nonlinear dynamics of the model used in the prediction step can be put into discrete form with discretization time equal to the sampling time T. The discrete state trajectory is then given by:

$$x(kP+j+i+1|kP+j) = (\Phi_k^j)^{(i+1)} x(kP+j|kP+j) + \sum_{l=0}^{i} (\Phi_k^j)^l [\Gamma_k^j u(kP+j+l|kP+j) + \eta_k^j] \tag{6.40}$$

for $i = 0, \ldots, P-1$, $\forall j = 0, \ldots, P-1$, for each $k \geq 0$ and $x(kP+j|kP+j)$ set equal to the states of the plant measured at time t_k^j, $x_k^{p,j}$. The matrices Φ_k^j, Γ_k^j, η_k^j are defined by:

$$\begin{aligned} \Phi_k^j &:= e^{A_k^j T} \\ \Gamma_k^j &:= \int_0^T e^{A_k^j (T-t)} B_k^j dt \\ \eta_k^j &:= \int_0^T e^{A_k^j (T-t)} C_k^j dt \end{aligned} \tag{6.41}$$

Φ_k^j is known as the state transition matrix computed at time t_k^j.

Moreover, from the definition of $\Delta u(kP+j+i|kP+j)$ it is easy to see that:

$$u(kP+j+i+1|kP+j) = u(kP+j-1|kP+j-1)+\sum_{l=0}^{i+1} \Delta u(kP+j+l|kP+j) \quad (6.42)$$

for $i = 0,\ldots,M-1,\ \ \forall j = 1,\ldots,P-1$, and

$$u(kP+i|kP) = u((k-1)P+P-1|(k-1)P+P-1)+\sum_{l=0}^{i} \Delta u(kP+l|kP),\ \ i = 0,\ldots,P-1 \quad (6.43)$$

By substituting (6.43) and (6.42) into (6.40) we have:

$$\begin{aligned} x(kP+j+i+1|kP+j) &= (\Phi_k^j)^{(i+1)}\ x(kP+j|kP+j) + \\ &+ \sum_{l=0}^{i} (\Phi_k^j)^l\ [\Gamma_k^j\ u(kP+j-1|kP+j-1)+\eta_k^j] + \\ &+ \sum_{l=0}^{i}(\Phi_k^j)^l\ \Gamma_k^j[\sum_{n=j}^{i-l} \Delta u(kP+j+n|kP+j)] \end{aligned} \quad (6.44)$$

for $i = 0,\ldots,P-1,\ \forall j = 1,\ldots,P-1$, and

$$\begin{aligned} x(kP+i+1|kP) &= (\Phi_k^0)^{(i+1)}\ x(kP|kP) + \\ &+ \sum_{l=0}^{i} (\Phi_k^0)^l\ [\Gamma_k^0 u((k-1)P+P-1|(k-1)P+P-1)+\eta_k^0] + \\ &+ \sum_{l=0}^{i}(\Phi_k^0)^l\ \Gamma_k^0\ [\sum_{n=0}^{i-l} \Delta u(kP+n|kP)],\quad i = 0,\ldots,P-1 \end{aligned} \quad (6.45)$$

By substituting equations (6.42), (6.43), (6.44), (6.45) into the expression for the objective function (6.7) and through a rather cumbersome process of collecting all the linear and quadratic terms in $\Delta u(kP+j|kP+j),\ldots,\Delta u(kP+j+M-1|kP+j)$ (a process which we will omit here because it has been described in detail for models

in step response format in [99]), we obtain:

$$J_k^j \;=:\; \Delta u^j(k)' \; H_k^j \; \Delta u^j(k) \;+\; (h_k^j)' \; \Delta u^j(k) \tag{6.46}$$

where $\Delta u^j(k) := [\Delta u(kP+j|kP+j)' \;\; \ldots \;\; \Delta u(kP+j+M-1|kP+j)']'$ and the matrix H_k^j and vector h_k^j are defined by:

Hessian matrix

"Block" diagonal elements H_{ll}, $l = 1, \ldots, M$:

$$H_{ll} := \Gamma'\{\sum_{i=0}^{P-l}[\sum_{q=0}^{i}(\Phi')^q]Q[\sum_{q=0}^{i}\Phi^q]\}\Gamma + S + [M-(l-1)]R \tag{6.47}$$

Lower "block" diagonal elements H_{lp}, $l = p, \ldots, M$, $\forall p = 1, \ldots, M-1$:

$$H_{lp} := \Gamma'\{\sum_{i=l-1}^{P-1}[\sum_{q=0}^{i-(l-1)}(\Phi')^q]Q[\sum_{q=0}^{i-(p-1)}\Phi^q]\}\Gamma + [M-(l-1)]R \tag{6.48}$$

For simplicity of notation, we have here omitted the subscripts and superscripts on the matrices H, Φ, Γ, but it should be clear that in order to compute H_k^j we should use Φ_k^j, Γ_k^j.

Since H is symmetric, the upper diagonal elements are given by $H_{lp} = H_{pl}'$, $\forall l < p$. Each "block" element H_{lp}; $l, p = 1, \ldots, M$; is an $m \times m$ matrix.

Elements of the gradient vector h_l', $l = 1, \ldots, M$

$$\begin{aligned}\frac{h_l'}{2} \;&:=\; [M-(l-1)](u^*)'R + [(u^*)'\Gamma' + \eta'] \sum_{i=l-1}^{P-1}\{[\sum_{q=0}^{i}(\Phi')^q]Q[\sum_{q=0}^{i-(l-1)}\Phi^q]\}\Gamma + \\ &+\; (x^*)'\{\sum_{i=l-1}^{P-1}(\Phi^{(i+1)})'Q[\sum_{q=0}^{i-(l-1)}\Phi^q]\}\Gamma\end{aligned} \tag{6.49}$$

Each "element" $h_l^{'}$, $l = 1, \ldots, M$, is a row vector of dimension m. u^* is equal to $u(kP+j-1|kP+j-1)$, $\forall j = 1, \ldots, P-1$, for the problem at iteration j, being k fixed. u^* is equal to $u((k-1)P+P-1|(k-1)P+P-1)$ for $j = 0$. x^* is equal to $x(kP+j|kP+j) = x_k^{p,j}$ for the problem at time step k, j.

The constraints on the control moves and rate of change of these control moves, keeping in mind that $\Delta u^j(k)$ are our decision variables, can be expressed as:

$$G \begin{bmatrix} \Delta u(kP+j|kP+j) \\ \Delta u(kP+j+1|kP+j) \\ \vdots \\ \Delta u(kP+j+M-1|kP+j) \end{bmatrix} \geq b_k^j \tag{6.50}$$

with G and b given by:

$$G := \begin{bmatrix} I_m & 0_m & \ldots & 0_m & 0_m \\ 0_m & I_m & 0_m & \ldots & 0_m \\ \vdots & \vdots & \vdots & & \vdots \\ 0_m & 0_m & \ldots & 0_m & I_m \\ -I_m & 0_m & \ldots & 0_m & 0_m \\ 0_m & -I_m & 0_m & \ldots & 0_m \\ \vdots & \vdots & \vdots & & \vdots \\ 0_m & 0_m & \ldots & 0_m & -I_m \\ I_m & 0_m & \ldots & 0_m & 0_m \\ I_m & I_m & 0_m & \ldots & 0_m \\ \vdots & \vdots & \vdots & & \vdots \\ I_m & I_m & \ldots & I_m & I_m \\ -I_m & 0_m & \ldots & 0_m & 0_m \\ -I_m & -I_m & 0_m & \ldots & 0_m \\ \vdots & \vdots & \vdots & & \vdots \\ -I_m & -I_m & \ldots & -I_m & -I_m \end{bmatrix} \tag{6.51}$$

where I_m, 0_m are the identity and zero matrices of dimension m, respectively,

and

$$b_k^j := \begin{bmatrix} -\Delta u_{max}(0) \\ -\Delta u_{max}(1) \\ \vdots \\ -\Delta u_{max}(M-1) \\ -\Delta u_{max}(0) \\ -\Delta u_{max}(1) \\ \vdots \\ -\Delta u_{max}(M-1) \\ u_{min}(0) - u^* \\ u_{min}(1) - u^* \\ \vdots \\ u_{min}(M-1) - u^* \\ -u_{max}(0) + u^* \\ -u_{max}(1) + u^* \\ \vdots \\ -u_{max}(M-1) + u^* \end{bmatrix} \tag{6.52}$$

with u^* as previously defined.

Notice that we are allowing for different lower and upper bounds on the control moves and rate of change of the control moves predicted at different time steps.

Now we will examine how the matrices H_k^j, G and vectors $(h_k^j)'$ and b_k^j are augmented in each of the three different procedures proposed for implementation of the contractive constraint.

Procedure 1 (approximate or conservative approach)

In this case, the number of decision variables is increased by n as previously discussed and the objective function at time step k, j is re-defined as:

$$J_k^j =: [\Delta u^j(k)' \quad (c_k^j)'] \; (H^*)_k^j \begin{bmatrix} \Delta u^j(k) \\ c_k^j \end{bmatrix} + [(h_k^j)' \quad 0] \begin{bmatrix} \Delta u^j(k) \\ c_k^j \end{bmatrix} \tag{6.53}$$

where c_k^j are the new optimization variables introduced in the implementation of the contractive constraint and $(H^*)_k^j$ is defined by:

$$(H^*)_k^j := \begin{bmatrix} H_k^j & 0_{mM\times n} \\ 0_{n\times mM} & I_n \end{bmatrix} \tag{6.54}$$

where $0_{mM\times n}$ is a zero matrix with mM rows and n columns.

So, all we did was to augment H_k^j in order to include the new decision variables in the objective function.

The constraint matrix G and vector b must also be augmented in order to include the $2n+1$ state constraints. Thus, our constraints are now defined as:

$$(G^*)_k^j \begin{bmatrix} \Delta u(kP+j|kP+j) \\ \Delta u(kP+j+1|kP+j) \\ \vdots \\ \Delta u(kP+j+M-1|kP+j) \\ (c_1)_k^j \\ \vdots \\ (c_n)_k^j \end{bmatrix} \geq (b^*)_k^j \tag{6.55}$$

with G^*, b^* (notice that we have dropped the subscripts and superscripts to simplify

the notation) are given by:

$$G^* := \begin{bmatrix} G & 0_{4mM\times n} \\ -\Upsilon^* & I_n \\ \Upsilon^* & I_n \\ 0_{1\times mM} & -1_n \end{bmatrix} \tag{6.56}$$

where:

$$\Upsilon^* := \begin{bmatrix} \Upsilon & 0_{n\times(M-p)m} \end{bmatrix} \tag{6.57}$$

with

$$\Upsilon := \begin{bmatrix} \sum_{i=0}^{p-1}\phi_1^i\Gamma & \sum_{i=1}^{p-1}\phi_1^i\Gamma & \dots & \phi_1^{p-1}\Gamma \\ \sum_{i=0}^{p-1}\phi_2^i\Gamma & \sum_{i=1}^{p-1}\phi_2^i\Gamma & \dots & \phi_2^{p-1}\Gamma \\ \vdots & \vdots & & \vdots \\ \sum_{i=0}^{p-1}\phi_n^i\Gamma & \sum_{i=1}^{p-1}\phi_n^i\Gamma & \dots & \phi_n^{p-1}\Gamma \end{bmatrix} \tag{6.58}$$

and

$$b^* := \begin{bmatrix} b \\ \begin{bmatrix} \sum_{i=0}^{p-1}\phi_1^i \\ \vdots \\ \sum_{i=0}^{p-1}\phi_n^i \end{bmatrix} (\Gamma u^* + \eta) + \Phi^p x^* \\ -\begin{bmatrix} \sum_{i=0}^{p-1}\phi_1^i \\ \vdots \\ \sum_{i=0}^{p-1}\phi_n^i \end{bmatrix} (\Gamma u^* + \eta) - \Phi^p x^* \\ -\frac{1}{\lambda_{max}^{\frac{1}{2}}(\hat{P})}\,\alpha \parallel x_k^p \parallel_{\hat{P}} \end{bmatrix} \tag{6.59}$$

where ϕ_l^i, $l = 1, \dots, n$, represents the l^{th} row of the matrix Φ^i and $p := P - j$, $j = 0, \dots, P-1$, represents the number of steps the initial condition for the prediction at time t_k^j, namely $x(kP+j|kP+j)$, lies behind the point where the contractive constraint is imposed, i.e., t_k^P. Here, the matrices Φ, Γ, η are actually $\Phi_k^0, \Gamma_k^0, \eta_k^0$, since the linearization of the plant used in the computation of the contractive constraint is only updated at the beginning of horizons.

Procedure 2 (penalty function approach)

In this case, the objective function J_k^j has to be modified to have the term $\gamma \parallel \bar{x}_k(t_k^P) \parallel_{\hat{P}}$ added to it as previously explained.

The new objective function at time t_k^j is specified by the following Hessian matrix $(H^*)_k^j$ and gradient vector $(h^*)_k^j$:

Hessian matrix

"Block" diagonal elements H_{ll}^*, $l = 1, \ldots, M$:

$$H_{ll}^* := H_{ll} + \gamma\, \Gamma' \,[\sum_{q=0}^{P-j-1} (\Phi')^q] Q [\sum_{q=0}^{P-j-1} \Phi^q] \Gamma \tag{6.60}$$

Lower "block" diagonal elements H_{lp}^*, $l = p, \ldots, M$, $\forall p = 1, \ldots, M-1$:

$$H_{lp}^* := H_{lp} + \gamma\, \Gamma' \,[\sum_{q=0}^{P-j-l} (\Phi')^q] Q [\sum_{q=0}^{P-j-p} \Phi^q] \Gamma \tag{6.61}$$

For simplicity of notation, we have here omitted the subscripts and superscripts on the matrices H^*, H, Φ, Γ.

Elements of the gradient vector h_l', $l = 1, \ldots, M$

$$(h_l^*)' := h_l' + 2\gamma \,\{[(u^*)'\Gamma' + \eta'] \,[(\sum_{q=0}^{P-j-1} (\Phi')^q) Q (\sum_{q=0}^{P-j-l} \Phi^q)] \Gamma + (x^*)' \,(\Phi^{(P-j)})' Q [\sum_{q=0}^{P-j-l} \Phi^q] \Gamma\} \tag{6.62}$$

The constraint matrix G and vector b are not changed since in this formulation there are no explicit state constraints but only control constraints.

Procedure 3 (sensitivity analysis approach)

Here H, $h^{'}$ and G are augmented in the same way as in procedure 1. The vector b is the only one to be changed to depict the modified contractive constraint (6.20), i.e.,

$$b^* := \begin{bmatrix} b \\ \begin{bmatrix} \sum_{i=0}^{p-1} \phi_1^i \\ \vdots \\ \sum_{i=0}^{p-1} \phi_n^i \end{bmatrix} (\Gamma u^* + \eta) + \Phi^p x^* \\ -\begin{bmatrix} \sum_{i=0}^{p-1} \phi_1^i \\ \vdots \\ \sum_{i=0}^{p-1} \phi_n^i \end{bmatrix} (\Gamma u^* + \eta) - \Phi^p x^* \\ -\delta_k^j \ \alpha \ \| \ x_k^p \ \|_{\hat{P}} \end{bmatrix} \tag{6.63}$$

The only difference with respect to procedure 1 is that the factor $\frac{1}{\sqrt{\lambda_{max}(\hat{P})}}$ in the last element of b^* is now replaced by the parameter δ_k^j which is iterated upon until the original quadratic contractive constraint is satisfied.

6.2.5 Basic philosophy of the controller design

Figures 6.1 and 6.2 illustrate the behavior of the contractive MPC controller in **Control Algorithm 5** when there is structural/parameter mismatch between the model used in the computation of the contractive constraint (which is linear in **Problem 6**) and the nonlinear plant.

In these figures we have:

- $x(kP|kP) := x_k^p := x^p(t_k), \ \forall k \geq 0$ in the state feedback case
- $x(kP|kP) := \hat{x}_k := \hat{x}(t_k), \ \forall k \geq 0$ in the output feedback case

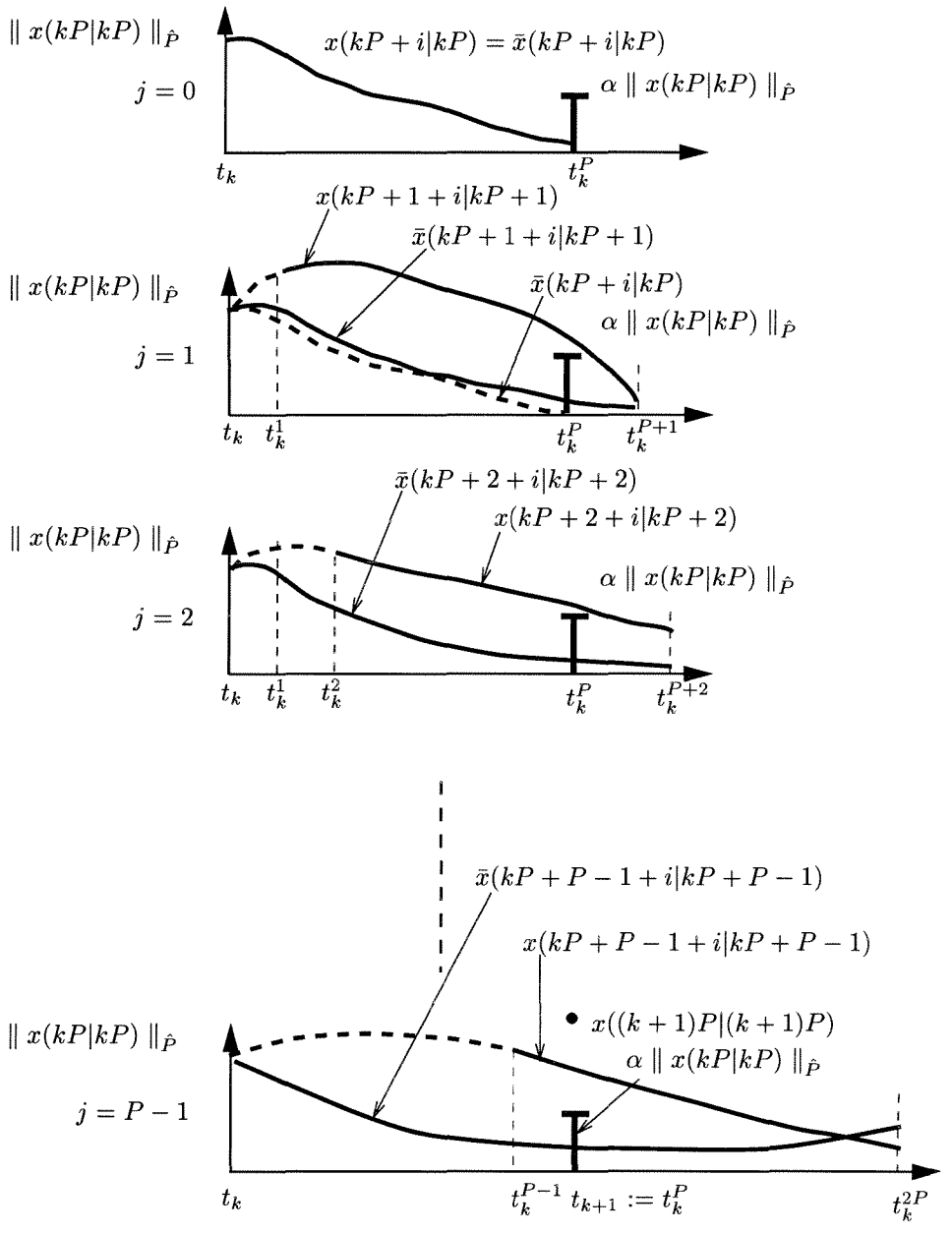

Figure 6.1: P control problems for a fixed k. Predicted trajectories generated by the robust contractive MPC scheme for a fixed k and j varying in the interval $j = 0, \ldots, P-1$.

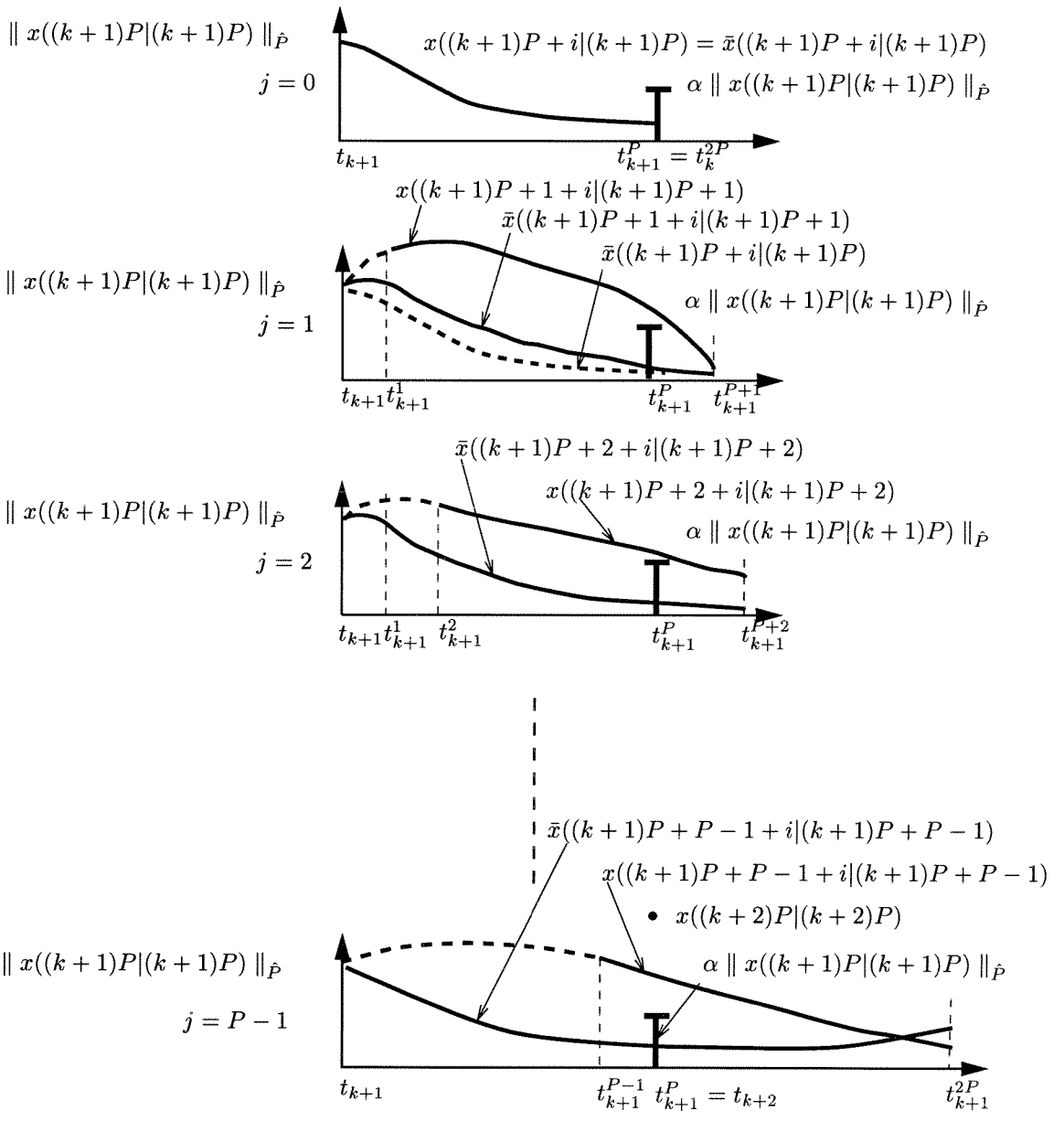

Figure 6.2: Next P control problems at $k+1$. Predicted trajectories generated by the robust contractive MPC scheme at $k+1$ and j varying in the interval $j = 0, \ldots, P-1$.

Thus, while the optimization problem remains solved over P time steps for different values of j and for a constant k, the number of steps between the beginning of the prediction and the location of the contractive constraint is equal to $P-j$ and therefore decreases as j increases, as we can clearly see in figures 6.1 and 6.2.

Let us consider, for generalization purposes, the output feedback problem. Let $\mathcal{X}$ be the reachable set and B_ρ the set of initial conditions for which the optimization problem at time step k, $k \geq 0$, is feasible. Then the trajectories of the linear model used for computation of the contractive constraint, the nonlinear plant and the observer are illustrated in figure 6.3.

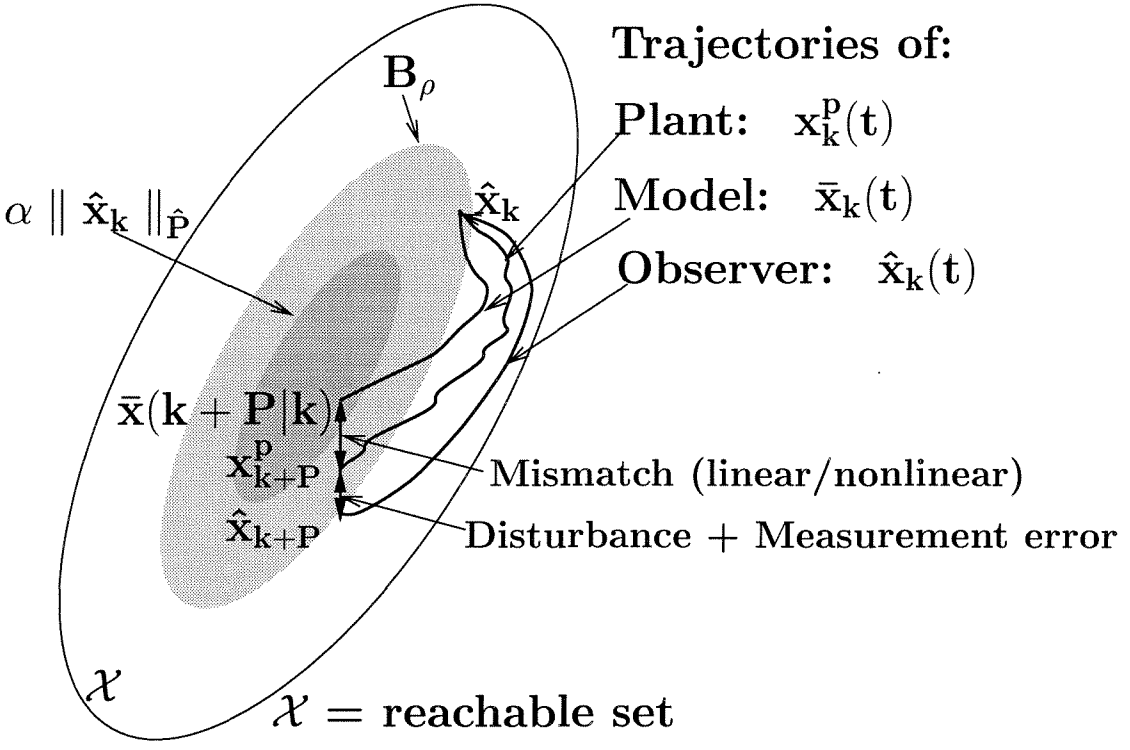

Figure 6.3: State trajectories generated by the contractive MPC scheme.

6.3 Stability analysis of Control Algorithm 5

In this section we will examine how the results obtained in chapter 3, when the models used in the prediction and in the computation of the contractive constraint exactly match the nonlinear dynamics of the plant, are modified by use of a linear approximation of the nonlinear system in the control computations. As previously pointed out, this procedure, which simplifies the controller from a computational point of view, introduces a model/plant mismatch which needs to be quantified and dealt with by the controller.

Finding appropriate uncertainty descriptions for nonlinear systems is an area only quite recently explored and much remains to be done. In [15, 34, 47, 77], e.g., in order to achieve either stabilization or tracking, some assumptions were introduced regarding the structure of the uncertainties and are often referred to as matching condition, a rather restrictive assumption. Recently, [18] brings up the so-called generalized matching condition for a class of nonlinear systems and [16, 30, 119, 115, 126] conduct the robustness analysis of uncertain dynamical systems for mismatched uncertainties.

Here we will express our linear/nonlinear mismatch through a conic sector bound. This description of the mismatch is appropriate in this set up because it is well-known that a nonlinear model and its linearization behave very similarly in a close neighborhood of the point where the linearization is performed. Thus, as long as our sampling time is reasonably small, the difference between the dynamics of the linear model and that of the nonlinear plant should lie within a conic sector bound. In other words, this bound assumes that in a close vicinity of the point of linearization, the second and higher order terms of the dynamics of the nonlinear system are "small" in magnitude when compared to the linear ones.

Through this description of the linear/nonlinear mismatch and other assumptions which we will soon consider, our stability analysis will reveal that the states of the

closed-loop system can be driven to a control invariant set as long as the contractive parameter α stays within certain lower and upper bounds in the interval $[0, 1)$.

6.3.1 Basic assumptions for the state feedback controller

Assumption 6.1 *It is assumed that there exists a constant $\rho \in (0, \infty)$ such that for all x_k^p, $\bar{x}_k \in B_\rho$, the QP problem to be solved in the prediction step of our contractive MPC controller at time step k, $k \geq 0$, is feasible. Since the contractive constraint does not change for the subsequent $P-1$ time steps, if $\mathcal{P}(t_k, x_k^p)$ is feasible then $\mathcal{P}(t_k^j, x_k^{p,j})$ is also feasible for all $j = 1, \ldots, P-1$. Moreover, the properly restricted optimal solution of $\mathcal{P}(t_k, x_k^p)$ is a feasible solution of the following $P-1$ control problems.*

The basic assumptions on the nonlinear system are:

Assumption 6.2 *We assume that if x_k^p, $\bar{x}_k \in B_\rho$, $\forall k \geq 0$ (with $\rho \in (0, \infty)$ defined in assumption 6.1), then there exists a constant $\beta \in (0, \infty)$ so that the transient states of the model used in the computation of the contractive constraint remain inside the set $B_{\beta \| x_k \|_{\hat{P}}}$, i.e., $\| \bar{x}_k^j(t) \|_{\hat{P}} \leq \beta \| x_k \|_{\hat{P}} \leq \beta\rho$, $\forall j = 0, \ldots, P-1$, $k \geq 0$.*

Assumption 6.3 *The linearization of the plant characterized by the pair $(A, B) := (\frac{\partial f}{\partial x}(x^*, u^*, 0, 0), \frac{\partial f}{\partial u}(x^*, u^*), 0, 0)$ is stabilizable for all points $(x^*, u^*) \in \Re^n \times \Re^m$ around which the linearization is performed.*

It is assumed that there exists a Lipschitz constant $L \in [0, \infty)$ and a so-called modeling bound $\gamma \in [0, \infty)$ such that for all x^p, $\bar{x} \in \Re^n$; $u \in \mathcal{U}$; $d \in \mathcal{D}$ and $p \in \mathcal{P}$, the following bounds hold:

Assumption 6.4

$$\| C + A\bar{x} + Bu \|_{\hat{P}} \leq L \left[\| \bar{x} \|_{\hat{P}} + \| u \| \right] \tag{6.64}$$

where $A := \frac{\partial f}{\partial x}(x^*, u^*, 0, 0)$, $B := \frac{\partial f}{\partial u}(x^*, u^*, 0, 0)$, $C := f(x^*, u^*, 0, 0) - Ax^* - Bu^*$ *with* $(x^*, u^*, 0, 0)$ *being the point around which the linearization is performed.*

Assumption 6.5

$$\| f(x^p, u, p, d) - f(\bar{x}, u, 0, 0) \|_{\hat{P}} =: \| f(x^p, u, p, d) - C - A\bar{x} - Bu - F(\bar{x}, u, 0, 0) \|_{\hat{P}} \leq L[\| x^p - \bar{x} \|_{\hat{P}} + \| p \| + \| d \|] \tag{6.65}$$

$F(\bar{x}, u, 0, 0)$ *represents the second and higher order terms of the Taylor series expansion of* $f(\bar{x}, u, 0, 0)$ *around the point* $(x^*, u^*, 0, 0)$.

Assumption 6.6 *Growth condition on* F*:*

$$\| F(\bar{x}, u, 0, 0) \|_{\hat{P}} \leq \gamma \ [\| \bar{x} \|_{\hat{P}} + \| u \|] \tag{6.66}$$

Remark 6.3 *Let the reachable set of states* $\mathcal{X}$ *be defined by:*

$$\begin{aligned}
&\mathcal{X} := \{x_k^{p,j}(t), x_k^j(t) \text{ and } \bar{x}_k^j(t) \in \Re^n \mid x_k^{p,j}(t) := x_k^{p,j}(t, t_k^j, x_k^{p,j}, u_k^j(t), p_k^j(t), d_k^j(t)), \\
&x_k^j(t) := x_k^j(t, t_k^j, x_k^{p,j}, u_k^j(t), 0, 0) \text{ and } \bar{x}_k^j(t) := \bar{x}_k^j(t, t_k^j, \bar{x}_k^{j-1}(t_k^j), u_k^j(t), 0, 0), \\
&t \in [t_k^j, t_k^{j+1}], x_k^p, \bar{x}_k \in B_\rho, u_k^j(t) \in \mathcal{U}, p_k^j(t) \in \mathcal{P}, d_k^j(t) \in \mathcal{D}; \\
&j = 0, \ldots, P-1, \forall k \geq 0\}
\end{aligned} \tag{6.67}$$

Then, it is only necessary to satisfy assumptions 6.4, 6.5 and 6.6 along the trajectories generated by the contractive MPC algorithm, i.e., $x_k^{p,j}(t)$ *and* $\bar{x}_k^j(t) \in \mathcal{X}$ *for all* $j = 0, \ldots, P-1$ *and* $\forall\ k \geq 0$. *Because this is difficult to check beforehand (since we*

do not know a priori which control moves will be computed by the contractive MPC controller and, consequently, which trajectories will be generated), we have posed the assumptions in a more conservative way, as valid for all x^p, $\bar{x} \in \Re^n$.

6.3.2 Stability results for the state feedback MPC controller

Theorem 6.2 (Bound on the difference between model and plant states at $\mathbf{t_k}$, $\forall \mathbf{k} \geq \mathbf{1}$**)** *Let* $\rho \in (0, \infty)$ *and* $L, \gamma \in [0, \infty)$ *satisfy assumptions 6.1, 6.4 and 6.5, 6.6, respectively. Then if* x_k^p, $\bar{x}_k \in B_\rho, \forall k \geq 0$, *there exist* λ_1, $\lambda_2 \in [0, \infty)$ *so that*

$$\| x_{k+1}^p - \bar{x}_{k+1} \|_{\hat{P}} \leq \lambda_1 \| x_k^p \|_{\hat{P}} + \lambda_2, \quad \forall k \geq 0 \tag{6.68}$$

with $\lambda_1 \to 0$ *as* $\gamma \to 0$ *and* $\lambda_2 \to 0$ *as* γ, ϵ_p, $\epsilon_d \to 0$.

Proof: *First note that the optimal control problem* $\mathcal{P}(t_k, x_k^p)$ *has a solution for all* $k \geq 0$ *since we assume that* x_k^p, $\bar{x}_k \in B_\rho$. *As a result, the state trajectory* $x^p(t, t_0, x_0^p, u(t))$ *is well-defined.*

Given x_k^p, $\bar{x}_k \in B_\rho$ *and* $u_k(t) \in \mathcal{U}$, *for* $t \in [t_k, t_{k+1} := t_k^P]$, *obtained by solving* $\mathcal{P}(t_k, x_k^p)$, *let* $x_k^p(t)$ *and* $\bar{x}_k(t)$ *be the state trajectories of the plant and of its linear approximation computed for* $t \in [t_k, t_{k+1}]$, $\forall k \geq 0$, *respectively.*

Then since the states $\bar{x}(t)$ *are set to* x_k^p *at* $t = t_k$ *and using the assumptions in the previous section, we have that for all* $t \in [t_k, t_{k+1}]$, *the following inequality holds:*

$$\begin{aligned}
&\| x_k^p(t) - \bar{x}_k(t) \|_{\hat{P}} \leq \int_{t_k}^t \| f(x_k^p(\tau), u_k(\tau), p_k(\tau), d_k(\tau)) - C_k - A_k \bar{x}_k(\tau) - \\
&- B_k u_k(\tau) \|_{\hat{P}} \, d\tau \leq \int_{t_k}^t \| f(x_k^p(\tau), u_k(\tau), p_k(\tau), d_k(\tau)) - C_k - A_k \bar{x}_k(\tau) - \\
&- B_k u_k(\tau) - F(\bar{x}_k(\tau), u_k(\tau), 0, 0) \|_{\hat{P}} \, d\tau + \int_{t_k}^t \| F(\bar{x}_k(\tau), u_k(\tau), 0, 0) \|_{\hat{P}} \, d\tau \leq \\
&\leq L\epsilon PT + L \int_{t_k}^t \| x_k^p(\tau) - \bar{x}_k(\tau) \|_{\hat{P}} \, d\tau + \gamma \bar{u} PT + \gamma \int_{t_k}^t \| \bar{x}_k(\tau) \|_{\hat{P}} \, d\tau
\end{aligned} \tag{6.69}$$

where $\epsilon := \epsilon_d + \epsilon_p$ *and* $\bar{u} := \max\{\| u_{min} \|, \| u_{max} \|\}$.

Besides, for all $t \in [t_k, t_{k+1}]$, *we have:*

$$\begin{aligned} \| \bar{x}_k(t) \|_{\hat{P}} &\leq \| x_k^p \|_{\hat{P}} + \int_{t_k}^{t} \| C_k + A_k \bar{x}_k(\tau) + B_k u_k(\tau) \|_{\hat{P}} \, d\tau \leq \\ &\leq \| x_k^p \|_{\hat{P}} + L\bar{u}PT + L \int_{t_k}^{t} \| \bar{x}_k(\tau) \|_{\hat{P}} \, d\tau \end{aligned} \tag{6.70}$$

Now, using the Bellman-Grownwall (BG) inequality, we get:

$$\| \bar{x}_k(t) \|_{\hat{P}} \leq [\| x_k^p \|_{\hat{P}} + L\bar{u}PT] \, e^{L(t-t_k)} \tag{6.71}$$

By integrating both sides of inequality (6.71), we obtain:

$$\int_{t_k}^{t} \| \bar{x}_k(\tau) \|_{\hat{P}} \, d\tau \leq \frac{[\| x_k^p \|_{\hat{P}} + L\bar{u}PT]}{L} (e^{LPT} - 1) \tag{6.72}$$

By substituting (6.72) into (6.69), it results that:

$$\begin{aligned} \| x_k^p(t) - \bar{x}_k(t) \|_{\hat{P}} &\leq L\epsilon PT + \gamma PT\bar{u}e^{LPT} + \frac{\gamma}{L}(e^{LPT} - 1) \| x_k^p \|_{\hat{P}} + \\ &+ L \int_{t_k}^{t} \| x_k^p(\tau) - \bar{x}_k(\tau) \|_{\hat{P}} \, d\tau \end{aligned} \tag{6.73}$$

Finally, using the BG inequality once more and setting $t = t_{k+1}$, *we get:*

$$\begin{aligned} \| x_{k+1}^p - \bar{x}_{k+1} \|_{\hat{P}} &\leq \frac{\gamma}{L} e^{LPT}(e^{LPT} - 1) \| x_k^p \|_{\hat{P}} + L\epsilon PT e^{LPT} + \gamma PT\bar{u}e^{2LPT} =: \\ &=: \lambda_1 \| x_k^p \|_{\hat{P}} + \lambda_2 \end{aligned} \tag{6.74}$$

Thus, λ_1, λ_2 are given by:

$$\lambda_1 := \frac{\gamma}{L} e^{LPT} (e^{LPT} - 1) \tag{6.75}$$

$$\lambda_2 := [\, \gamma \bar{u} e^{LPT} + L\epsilon \,] PTe^{LPT} \tag{6.76}$$

From these definitions we clearly see that $\lambda_1 \to 0$ as $\gamma \to 0$ and $\lambda_2 \to 0$ as γ, ϵ_d, $\epsilon_p \to 0$. Moreover, both λ_1 and λ_2 increase as L and γ increase, which is natural since these constants "quantify" the strength of the nonlinearities in the system.

□

Since we have established in assumption 6.1 that there exists a non-empty set of initial conditions B_ρ for which feasibility of the successive optimal control problems is guaranteed, we must now establish conditions on the controller and plant parameters under which the state trajectory $\{x_k^p\}_{k=0}^{\infty}$, $\{\bar{x}\}_{k=0}^{\infty}$ remains inside this set. In the next theorem we will compute bounds on the contractive parameter α so that stability and feasibility are guaranteed within these bounds.

Theorem 6.3 (Feasibility condition) *Let the constants α, L, γ, ϵ_p, ϵ_d and ρ be as previously postulated. Then, there exists $\bar{\alpha} \in [0, \infty)$ such that if $\alpha < \bar{\alpha}$ the closed-loop system is stable and the states of the plant can be steered to a control invariant set $B_{\hat{\rho}}$ where $\hat{\rho}$ is a function of α, γ, L, ρ, ϵ_p, ϵ_d and $\hat{\rho} \to 0$ as γ, ϵ_p, $\epsilon_d \to 0$.*

Proof: *The proof is constructive, i.e., we calculate $\bar{\alpha}$ so that the statement of the theorem holds.*

From the triangle inequality it follows that:

$$\| x_{k+1}^p \|_{\hat{P}} \leq \| x_{k+1}^p - \bar{x}_{k+1} \|_{\hat{P}} + \| \bar{x}_{k+1} \|_{\hat{P}} \tag{6.77}$$

Now, using the contractive constraint, i.e., $\| \bar{x}_{k+1} \|_{\hat{P}} \leq \alpha \| x_k^p \|_{\hat{P}}$, $\forall k \geq 0$, *we get:*

$$\| x_{k+1}^p \|_{\hat{P}} \leq \| x_{k+1}^p - \bar{x}_{k+1} \|_{\hat{P}} + \alpha \| x_k^p \|_{\hat{P}} \tag{6.78}$$

Then by substituting (6.74) into (6.78), we obtain:

$$\| x_{k+1}^p \|_{\hat{P}} \leq (\lambda_1 + \alpha) \| x_k^p \|_{\hat{P}} + \lambda_2 =: \alpha^* \| x_k^p \|_{\hat{P}} + \lambda_2 \tag{6.79}$$

Using the Contraction Mapping Principle we conclude that stability will hold if $\alpha^* = \alpha + \lambda_1 < 1$, *which implies that:*

$$\alpha < 1 - \frac{\gamma \, e^{LPT} \, (e^{LPT} - 1)}{L} \quad =: \quad \bar{\alpha}^{(1)} \tag{6.80}$$

Naturally, since $\alpha \geq 0$ *a necessary condition on the nonlinearities of the system so that* $\bar{\alpha}^{(1)}$ *exists is that:*

$$\gamma < \frac{L}{e^{LPT}(e^{LPT} - 1)} \tag{6.81}$$

Now, applying the results of lemma 4.1, we get:

1.

$$\| x_k^p \|_{\hat{P}} < \| x_0^p \|_{\hat{P}} + \frac{\lambda_2}{1 - \alpha^*} \leq \rho_0 + \frac{\lambda_2}{1 - \alpha^*} \tag{6.82}$$

for all initial conditions $x_0^p \in B_{\rho_0}$.

2.

$$\lim_{k \to \infty} \| x_k^p \|_{\hat{P}} \leq \frac{\lambda_2}{1 - \alpha^*} \quad =: \quad \hat{\rho} \tag{6.83}$$

Thus, $\hat{\rho}$ *is given by:*

$$\hat{\rho} := \frac{LPTe^{LPT}[\gamma\bar{u}e^{LPT} + L\epsilon]}{L(1-\alpha) + \gamma e^{LPT}(e^{LPT} - 1)} \tag{6.84}$$

Using equations (6.84) and (6.83), we conclude that:

$$\lim_{\gamma,\epsilon_p,\epsilon_d \to 0} \hat{\rho} = \lim_{\gamma,\epsilon_p,\epsilon_d \to 0} [\lim_{k \to \infty} \| x_k^p \|_{\hat{P}}] = 0 \tag{6.85}$$

Therefore, the states are driven by **Control Algorithm 5** *to the interior of the control invariant set $B_{\hat{\rho}}$ asymptotically and the size of this set decreases the less disturbances and parameter uncertainty there exist and the weaker the nonlinearities of the system are. Also, notice that $\hat{\rho}$ decreases for smaller values of α. This makes sense since we should be able to drive the states of the plant to a smaller control invariant set by requiring a stronger contraction of the model states. $\hat{\rho}$ increases as γ increases for $\alpha < 1 - \frac{\epsilon}{\bar{u}}(e^{LPT} - 1)$ (we can see that by examining $\frac{\partial\hat{\rho}}{\partial\gamma}$). Thus, if $\epsilon = 0$, $\hat{\rho}$ increases as γ increases for any chosen α. Moreover, $\hat{\rho}$ always increases as ϵ increases.*

Our next step is to establish conditions which guarantee that x_k^p, $\bar{x}_k \in B_\rho$, $\forall k \geq 0$. Using inequality (6.82), a sufficient condition on the control and plant parameters so that x_k^p remains inside B_ρ for all $k \geq 0$ is given by:

$$0 \; < \; \rho_0 + \hat{\rho} \; < \; \rho \tag{6.86}$$

Since $\| \bar{x}_{k+1} \|_{\hat{P}} \leq \alpha \| x_k^p \|_{\hat{P}}$, if inequality (6.86) is satisfied then the states $\bar{x}_k$ also remain inside B_ρ for all $k \geq 0$ (since $\bar{x}_0$ is set to $x_0^p \in B_{\rho_0}$).

A necessary condition on the nonlinearities, disturbances and parameter mismatch, given the chosen controller parameters α, P, T, for $B_{\rho_0} \subset B_\rho$ with ρ_0 satisfying inequality (6.86) not to be an empty set is obviously that:

$$\frac{LPTe^{LPT}[\gamma\bar{u}e^{LPT}+L\epsilon]}{L(1-\alpha)+\gamma e^{LPT}(e^{LPT}-1)} \;<\; \rho \tag{6.87}$$

Or, expressed in terms of the contractive parameter α, we have:

$$\alpha \;<\; 1-\frac{\gamma}{L}e^{LPT}(e^{LPT}-1)-\frac{[\gamma\bar{u}e^{LPT}+L\epsilon]PTe^{LPT}}{\rho} \;=:\; \bar{\alpha}^{(2)} \tag{6.88}$$

Since $\bar{\alpha}^{(2)} < \bar{\alpha}^{(1)}$ for all $\rho \in [0,\infty)$ and $\bar{\alpha}^{(2)} \to \bar{\alpha}^{(1)}$ if $\rho \to \infty$ (i.e., if the optimization problems $\mathcal{P}(t_k, x_k^p)$ are feasible for all initial conditions $x_k^p \in \Re^n$, then the bound on the contractive parameter α is dictated only by the stability requirement as in (6.80)) then we have that $\bar{\alpha}$ is defined by:

$$\alpha \;<\; \bar{\alpha} \;:=\; 1-\frac{\gamma}{L}e^{LPT}(e^{LPT}-1)-\frac{[\gamma\bar{u}e^{LPT}+L\epsilon]PTe^{LPT}}{\rho} \tag{6.89}$$

Naturally, since $\alpha > 0$, a necessary condition on the combined effect of disturbances, parameter uncertainty and linear/nonlinear mismatch so that $\bar{\alpha}$ is meaningful is given by:

$$\frac{\gamma}{L}e^{LPT}(e^{LPT}-1)+\frac{[\gamma\bar{u}e^{LPT}+L\epsilon]PTe^{LPT}}{\rho} < 1 \tag{6.90}$$

Then, for $\alpha < \bar{\alpha}$ both feasibility and asymptotic stability to the control invariant set $B_{\hat{\rho}}$ are guaranteed.

□

Theorem 6.4 (Well-posedness of the controller) *Let $\bar{\alpha}$ and ρ_0 be as defined in theorem 6.3 and $\beta \in (0,\infty)$ be as in assumption 6.2. Then,*

1. *there exists a $\Delta_1 \in (0,\infty)$ such that for any $x_0^p \in B_{\rho_0}$, it follows that $\| x_k^p(t, t_k, x_k^p, u_k(t), p_k(t), d_k(t)) \|_{\hat{P}} \leq \Delta_1$, $t \in [t_k, t_{k+1}]$, $\forall k \geq 0$, and*

2. *there exists a* $\Delta_2 \in (0, \infty)$, *depending on* γ *and* ϵ, *such that* $\Delta_2 \to 0$ *as* $\gamma,\ \epsilon \to 0$ *and for any* $x_0^p \in B_{\rho_0}$, *the trajectory* $x^p(t, t_0, x_0^p, u(t), p(t), d(t)), t \in [t_0, \infty)$, *satisfies the inequality* $\lim_{t\to\infty} \| x^p(t, t_0, x_0, u(t), p(t), d(t)) \|_{\hat{P}} \leq \Delta_2$.

Proof: *We want to prove that for any* $x_0^p \in B_{\rho_0}$, *we have* $\| x_k^p(t) \|_{\hat{P}} := \| x_k^p(t, t_k, x_k^p, u_k(t), p_k(t), d_k(t)) \|_{\hat{P}}$ *bounded for all* $t \in [t_k, t_{k+1}]$ *and* $k \geq 0$. *We know that:*

$$\| x^p(t) \|_{\hat{P}} \leq \| x^p(t) - \bar{x}(t) \|_{\hat{P}} + \| \bar{x}(t) \|_{\hat{P}}, \qquad \forall t \in [t_k, t_{k+1}] \tag{6.91}$$

with $\bar{x}_k(t) := \bar{x}(t, t_k, x_k^p, u_k(t), 0, 0)$.

Besides, the transient states $\bar{x}_k(t)$ *satisfy the inequality:*

$$\| \bar{x}_k(t) \|_{\hat{P}} \leq \beta \| x_k^p \|_{\hat{P}}, \qquad \beta \in (0, \infty), \quad t \in [t_k, t_{k+1}], \quad \forall k \geq 0 \tag{6.92}$$

We also know from theorem 6.2 that:

$$\| x_k^p(t) - \bar{x}_k(t) \|_{\hat{P}} \leq \lambda_1 \| x_k^p \|_{\hat{P}} + \lambda_2 \tag{6.93}$$

Thus, by substituting (6.92) and (6.93) into equation (6.91), we obtain:

$$\| x_k^p(t) \|_{\hat{P}} \leq (\beta + \lambda_1) \| x_k^p \|_{\hat{P}} + \lambda_2 \leq (\beta + \lambda_1)\rho + \lambda_2 =: \Delta_1 \tag{6.94}$$

Therefore, we conclude that:

$$\| x_k^p(t) \|_{\hat{P}} \leq \Delta_1 < \infty, \quad t \in [t_k, t_{k+1}], \quad \forall k \geq 0 \tag{6.95}$$

Next, it follows from the proof of theorem 6.3 that $\lim_{k\to\infty} \| x_k^p \|_{\hat{P}} < \hat{\rho}$. *Hence, from (6.94) we have:*

$$\lim_{k\to\infty} \| x_k^p(t) \|_{\hat{P}} \leq (\beta + \lambda_1)[\lim_{k\to\infty} \| x_k^p \|_{\hat{P}}] + \lambda_2 < (\beta + \lambda_1)\hat{\rho} + \lambda_2 =: \Delta_2 \qquad (6.96)$$

So, we have proven that:

$$\lim_{k\to\infty} \| x_k^p(t) \|_{\hat{P}} \leq \Delta_2 < \infty, \quad t \in [t_k, t_{k+1}], \quad \forall k \in N \qquad (6.97)$$

Since $\hat{\rho},\ \lambda_2 \to 0$ *as* $\gamma, \epsilon_p, \epsilon_d \to 0$ *it follows from (6.96) that* $\Delta_2 \to 0$ *as* $\gamma,\ \epsilon_p,\ \epsilon_d \to 0$. □

The results derived in theorems 6.2, 6.3, 6.4 were based on the assumption that there exists a non-empty set B_ρ of initial conditions for which feasibility of the optimization step in **Control Algorithm 5** is guaranteed. This is the same assumption which we have used in previous chapters when the optimization problem in our contractive MPC scheme was a general NLP.

Here, we will take advantage of the fact that the model used in the computation of the contractive constraint is linear to derive a lower bound $\underline{\alpha}$ on $\alpha \in [0, 1)$ which establishes a sufficient condition for feasibility. This lower bound can only be derived under a more restrictive assumption than assumption 6.3, namely that:

Assumption 6.7 $A := \frac{\partial f}{\partial x}(x^*, u^*, 0, 0)$ *is stable (i.e., it has all eigenvalues located in the left half plane) for all points* $(x^*, u^*) \in \Re^n \times \Re^m$ *around which the linearization is performed.*

Theorem 6.5 (Feasibility conditions for systems satisfying assumption 6.7) *If assumption 6.7 is satisfied, then there exists* $\underline{\alpha} > 0$ *such that if* $\alpha \geq \underline{\alpha}$ *then the*

optimization at time step k in the prediction step of **Control Algorithm 5** *is feasible for all* $k \geq 0$.

Proof: *From (6.40) it is clear that:*

$$\begin{aligned} \bar{x}(kP+j+i+1|kP+j) &= (\Phi_k^0)^{(i+1)}\ \bar{x}(kP+j|kP+j) + \\ &+ \sum_{l=0}^{i} (\Phi_k^0)^l\ [\Gamma_k^0 u(kP+j+l|kP+j) + \eta_k^0] \end{aligned} \quad (6.98)$$

for all $i = 0, \ldots, P-1$ *and* $j = 0, \ldots, P-1$. $\bar{x}(kP+j|kP+j) = \bar{x}(kP+j|kP+j-1)$ *for* $j = 1, \ldots, P-1$ *and* $\bar{x}(kP|kP) = x_k^p$.

Because the local linearization is assumed stable, the worst case scenario in terms of trying to satisfy the contractive constraint is if the applied control action is such that $B_k u_k^j(t) = -C_k$ *for all* $t \in [t_k^j, t_k^{j+P}]$ *and* $j = 0, \ldots, P-1$ *(i.e., there are no driving terms in the system). Obviously, we are not considering the case when one may be trying to drive the states of the system away from the origin.*

In this case, we have:

$$\bar{x}(kP+j+i+1|kP+j) = (\Phi_k^0)^{(i+1)}\ \bar{x}(kP+j|kP+j) \quad (6.99)$$

Since the trajectories $\bar{x}_k^j(t)$ *do not differ for different values of* j *if* $B_k u_k^j(t)$ *lies in the range of* C_k*, then we can drop the superscript* j *and by applying the* $\hat{P}-$*norm we have:*

$$\| \bar{x}(kP+i+1|kP) \|_{\hat{P}} \leq \sqrt{\lambda_{max}(\hat{P}^{\frac{1}{2}}\ \Phi_k^{(i+1)}\ \hat{P}^{-\frac{1}{2}})}\ \ \| x_k^p \|_{\hat{P}}, \quad i = 0, \ldots, P-1 \quad (6.100)$$

where Φ_k *represents* $\Phi_k^0 := e^{A_k^0 PT}$, *i.e., the state transition matrix computed at time* t_k.

For $i = P - 1$, *we have:*

$$\begin{aligned} \| \bar{x}((k+1)P|kP) \|_{\hat{P}} \leq \sqrt{\lambda_{max}(\hat{P}^{\frac{1}{2}} \Phi_k^P \hat{P}^{-\frac{1}{2}})} \quad \| x_k^p \|_{\hat{P}} := \\ := \sqrt{\lambda_{max}(\hat{P}^{\frac{1}{2}} e^{A_k PT} \hat{P}^{-\frac{1}{2}})} \quad \| x_k^p \|_{\hat{P}} =: \underline{\alpha}_k \quad \| x_k^p \|_{\hat{P}} \end{aligned} \tag{6.101}$$

with A_k *representing* A_k^0.

Since our contractive constraint is given by:

$$\| \bar{x}((k+1)P|kP) \|_{\hat{P}} \leq \alpha \quad \| x_k^p \|_{\hat{P}} \tag{6.102}$$

Then, if

$$\alpha \geq \underline{\alpha} := \sup_{k \geq 0} \sqrt{\lambda_{max}(\hat{P}^{\frac{1}{2}} e^{A_k PT} \hat{P}^{-\frac{1}{2}})} =: \sqrt{\lambda_{max}(\hat{P}^{\frac{1}{2}} e^{APT} \hat{P}^{-\frac{1}{2}})}, \tag{6.103}$$

the QP is feasible at time step k, $\forall k \geq 0$. *Thus, since we have assumed that* A_k *is stable for all* $k \geq 0$, *there always exists a finite prediction horizon* P *long enough (since* e^{APT} *decreases the larger* P *is for* A *stable) such that* $\underline{\alpha} \in [0, 1)$.

□

Remark 6.4 *Thus, according to the results in* **Theorems 6.3** *and* **6.5** *and in the absence of disturbances, if* **Assumption 6.7** *is satisfied and if* α *is such that* $\underline{\alpha} \leq \alpha < \bar{\alpha}$ *with* $\bar{\alpha} := 1 - \frac{\gamma e^{LPT}(e^{LPT}-1)}{L}$ *and* $\underline{\alpha} := \sqrt{\lambda_{max}(\hat{P}^{\frac{1}{2}} e^{APT} \hat{P}^{-\frac{1}{2}})}$, *then feasibility and asymptotic stability to the control invariant set* $B_{\hat{\rho}}$, *with* $\hat{\rho}$ *given by*

$$\hat{\rho} := \frac{LPT\ \gamma\bar{u}\ e^{2LPT}}{L(1-\alpha)+\gamma e^{LPT}(e^{LPT}-1)} \tag{6.104}$$

are guaranteed.

Notice that the inequality $\underline{\alpha} \leq \alpha < \bar{\alpha}$ *only has meaning if the nonlinearity "strength" (expressed in the magnitude of* γ*) is such that* $0 \leq \underline{\alpha} < \bar{\alpha} < 1$*, i.e.,*

$$\gamma < \frac{L\ (1-\sqrt{\lambda_{max}(\hat{P}^{\frac{1}{2}}\ e^{APT}\ \hat{P}^{-\frac{1}{2}})})}{e^{LPT}\ (e^{LPT}-1)} \tag{6.105}$$

6.3.3 Output feedback contractive MPC algorithm with linear approximation

We have seen in chapter 4 that, in the nominal case, the exponentially stabilizing contractive MPC, when associated with an asymptotically convergent state estimator, originates a uniformly asymptotically stable closed-loop. In the previous section of this chapter, we have derived stability results for the contractive MPC controller in the case where the models used for prediction and computation of the contractive constraint are linear. We have seen that this mismatch between the real nonlinear plant and its linear approximation used in the optimization step of **Control Algorithm 5** (quantified in assumption 6.6 through a linear growth condition on the nonlinearities) weakens the stability results. The exponential stability properties of the nominal case are now lost and, instead, we can only guarantee to steer the states to the interior of a control invariant set whose size is proportional to this linear/nonlinear mismatch.

Now we want to combine these results in chapter 4 with the results in the previous section of this chapter to analyze the closed-loop response in the output feedback case when the model used by the contractive MPC controller is a linear approximation of the nonlinear plant and the nonlinear state estimator produces asymptotically

convergent estimates in the absence of disturbances and parameter uncertainty (as, e.g., the nonlinear **Estimation Procedure 1** derived in chapter 4).

In the state feedback case, the states of the model used in the computation of the contractive constraint at step k after one sampling time are given by:

$$\bar{x}_k(t_k + T) = \Phi_k x_k^p + \Psi_k[B_k^0 u_k + C_k^0] \tag{6.106}$$

where the matrices Φ_k, Ψ_k are defined as:

$$\Phi_k := e^{A_k^0 T} \qquad \text{and} \qquad \Psi_k := \int_0^T e^{A_k^0 (T-t)} dt \tag{6.107}$$

In the output feedback case, these model states are given by:

$$\bar{x}_k(t_k + T) = \Phi_k \hat{x}_k + \Psi_k[B_k^0 u_k + C_k^0] \tag{6.108}$$

The difference between the two model dynamics can be represented by an additive disturbance, i.e., the state evolution of the model in the output feedback case is equivalent to the state feedback case modified to:

$$\dot{\bar{x}}_k(t) = A_k^0 \bar{x}_k(t) + B_k^0 u_k(t) + C_k^0 + \tilde{d}_k(t) \;\text{ with }\; \bar{x}_k(t_k) = x_k^p \tag{6.109}$$

If $\tilde{d}_k(t) = \tilde{d}_k$ = constant for $t \in [t_k, t_k + T]$, integration of (6.109) results in:

$$\bar{x}_k(t_k + T) = \Phi_k x_k^p + \Psi_k[B_k^0 u_k + C_k^0 + \tilde{d}_k] \tag{6.110}$$

Thus, we want to compute $\tilde{d}_k$ so that it represents the difference in the dynamic behavior of the model caused by the estimation, i.e., the states in equation (6.110)

have to be equal to the states in (6.108). Thus, by subtracting equation (6.108) from (6.110), we have:

$$\tilde{d}_k = \Psi_k^{-1}\ \Phi_k\ e_k = -[e^{-A_k^0 T} - I_n]^{-1}\ A_k^0\ e_k \tag{6.111}$$

where I_n is the identity matrix of dimension n and e_k is the estimation error defined as $e_k := \hat{x}_k - x_k^p$.

Applying the $\hat{P}-$norm to equation (6.111), we get:

$$\| \tilde{d}_k \|_{\hat{P}} \leq \| [e^{-A_k^0 T} - I_n]^{-1}\ A_k^0 \|_{\hat{P}} \| e_k \|_{\hat{P}} =: \phi_k \| e_k \|_{\hat{P}} =: \rho_k^d \tag{6.112}$$

Thus, the additive disturbance is proportional to the estimation error. In [37] the author proposes a nonlinear observer for continuous-time systems with discrete observations which produces asymptotically convergent estimates if the initial estimation error is not very large and the nonlinearities are reasonably weak (the exact sufficient conditions can be found in that reference). In this case, there exists $K \in [0, \infty)$ such that the estimation error at any sampling time t_k satisfies the following inequality:

$$\| e_k \|_{\hat{P}} \leq K \| e_0 \|_{\hat{P}}, \quad \forall k \geq 0 \tag{6.113}$$

From equations (6.112) and (6.113) we obviously have:

$$\| \tilde{d}_k \|_{\hat{P}} \leq \phi_k\ K \| e_0 \|_{\hat{P}} \leq \phi K \| e_0 \|_{\hat{P}} =: \rho^d \tag{6.114}$$

where $\phi := \max_{k \geq 0}\ \phi_k$.

Thus, if an asymptotically stable nonlinear observer is used (such as the one proposed

in [37]) then its effect is to introduce an additive asymptotically decaying disturbance into the dynamics of the models used in the prediction and in the computation of the contractive constraint.

Assumption 6.8 *Let the asymptotically decaying properties of the discrete disturbance sequence* $\{\tilde{d}_k\}_{k\geq 0}$ *introduced by the observer be expressed as:*

$$\begin{aligned}&\textit{For any } \tilde{\epsilon} > 0, \exists \textit{ a finite } \bar{k} := \bar{k}(\tilde{\epsilon}) \in \mathcal{N} \textit{ so that } \rho_k^d \leq \tilde{\epsilon}, \ \forall k \in [\bar{k}, \infty),\\ &\textit{and } \bar{k}(\tilde{\epsilon}) \to \infty \textit{ if } \tilde{\epsilon} \to 0\end{aligned}$$

Our stability results in the output feedback case will reveal that we can still drive the states of the plant to the same control invariant set $B_{\hat{\rho}}$ to which they could be driven in the state feedback case. This result is proven in the following theorem.

Theorem 6.6 (Stability and feasibility properties of the output feedback scheme) *Let* ρ, L, γ, $\rho^d \in (0, \infty)$ *be as defined in* **Assumptions 6.1, 6.4** *and* **6.5, 6.6** *and equation (6.114), respectively, and let the state estimator be asymptotically stable (such that* **Assumption 6.8** *holds). Then, if the norm of the additive disturbance caused by introduction of the observer into the closed-loop is bounded by,*

$$\| \tilde{d}_k \|_{\hat{P}} \leq \rho^d < \frac{[L(1-\alpha) - \gamma e^{LPT}(e^{LPT} - 1)]}{LPT\, e^{LPT}} [\rho - K \| e_0 \|_{\hat{P}}] - \gamma \bar{u} e^{LPT}, \quad \forall k \geq 0 \tag{6.115}$$

the output feedback control problem is well-posed (since x_k^p, $\bar{x}_k$, $\hat{x}_k \in B_\rho$, $\forall k \geq 0$, *and* $x_0^p \in B_{\rho_0}$ *which is a non-empty set) and the states of the resulting closed-loop system converge asymptotically to* $B_{\hat{\rho}}$ *with* $\hat{\rho}$ *given by:*

$$\hat{\rho} := \frac{\gamma \bar{u} LPT e^{2LPT}}{L(1-\alpha) + \gamma e^{LPT}(e^{LPT}-1)} \tag{6.116}$$

which means that the states converge to the same control invariant set $B_{\hat{\rho}}$ as in the state feedback case (compare with equation (6.84)).

Proof: *Following the same procedure used to prove* **Theorem 6.2**, *if the model used in the computation of the contractive constraint is now given by (6.109) due to the state estimation error, we obtain:*

$$\| x^p_{k+1} - \bar{x}_{k+1} \|_{\hat{P}} \leq \frac{\gamma}{L} e^{LPT}(e^{LPT}-1) \| x^p_k \|_{\hat{P}} + [\gamma \bar{u} e^{LPT} + \rho^d_k] PT e^{LPT} =: \lambda_1 \| x^p_k \|_{\hat{P}} + \lambda_{2,k} \tag{6.117}$$

where (6.117) follows directly from (6.74) by making $\epsilon_d = 0$ and by adding the term resulting from integration of the additive discrete disturbance sequence $\tilde{d}_k, \ldots \tilde{d}_{k+P-1}$ (which satisfies equation (6.112)).

Using the contractive constraint and the triangle inequality in equation (6.117), we have:

$$\| x^p_{k+1} \|_{\hat{P}} \leq (\alpha + \lambda_1) \| x^p_k \|_{\hat{P}} + \lambda_{2,k} \tag{6.118}$$

Since the state estimation error is such that for any $\tilde{\epsilon} > 0$, $\exists\ \bar{k} := \bar{k}(\tilde{\epsilon}) \in \mathcal{N}$ large enough so that $\rho^d_k \leq \tilde{\epsilon}$ for $k \in [\bar{k}, \infty)$, then from (6.118) it follows that:

$$\| x^p_{k+1} \|_{\hat{P}} \leq (\alpha + \lambda_1) \| x^p_k \|_{\hat{P}} + [\gamma \bar{u}\, e^{LPT} + \tilde{\epsilon}] PT\, e^{LPT}, \quad \forall k \in [\bar{k}, \infty) \tag{6.119}$$

Then, if $\alpha + \lambda_1 =: \alpha^* \in [0, 1)$, we can use the results of **Lemma 4.1** *to obtain:*

$$\| x^p_{\bar{k}(\tilde{\epsilon})+l} \|_{\hat{P}} \leq (\alpha^*)^l \| x^p_{\bar{k}(\tilde{\epsilon})} \|_{\hat{P}} + [\sum_{i=0}^{l-1} (\alpha^*)^i][\gamma \bar{u} e^{LPT} + \tilde{\epsilon}] PTe^{LPT} <$$

$$< (\alpha^*)^l \| x^p_{\bar{k}(\tilde{\epsilon})} \|_{\hat{P}} + \frac{[\gamma \bar{u} e^{LPT} + \tilde{\epsilon}] PTe^{LPT}}{1 - \alpha^*}, \qquad \forall l > 0 \quad (6.120)$$

Thus, by taking the limit as $\tilde{\epsilon} \to 0$, *we have:*

$$\lim_{\tilde{\epsilon} \to 0} \| x^p_{\bar{k}(\tilde{\epsilon})+l} \|_{\hat{P}} < (\alpha^*)^l \left[\lim_{\tilde{\epsilon} \to 0} \| x^p_{\bar{k}(\tilde{\epsilon})} \|_{\hat{P}}\right] + \frac{\gamma \bar{u} PT\, e^{2LPT}}{1 - \alpha^*} =$$

$$= (\alpha^*)^l [\lim_{\tilde{\epsilon} \to 0} \| x^p_{\bar{k}(\tilde{\epsilon})} \|_{\hat{P}}] + \frac{\gamma \bar{u} LPT e^{2LPT}}{L(1-\alpha) + \gamma e^{LPT}(e^{LPT} - 1)} =:$$

$$=: (\alpha^*)^l \left[\lim_{\tilde{\epsilon} \to 0} \| x^p_{\bar{k}(\tilde{\epsilon})} \|_{\hat{P}}\right] + \hat{\rho} \quad (6.121)$$

and if now we take the limit as $l \to \infty$ *knowing that* $\bar{k}(\tilde{\epsilon}) \to \infty$ *for* $\tilde{\epsilon} \to 0$ *and that* $\alpha^l \to 0$ *exponentially fast as* $l \to \infty$, *we finally obtain:*

$$\lim_{l \to \infty} [\lim_{\tilde{\epsilon} \to 0} \| x^p_{\bar{k}(\tilde{\epsilon})+l} \|_{\hat{P}}] < (\lim_{l \to \infty} \alpha^l)[\lim_{\tilde{\epsilon} \to 0} \| x^p_{\bar{k}(\tilde{\epsilon})} \|_{\hat{P}}] + \hat{\rho} = \hat{\rho} \quad (6.122)$$

or

$$\lim_{k \to \infty} \| x^p_k \|_{\hat{P}} < \hat{\rho} \quad (6.123)$$

which means asymptotic convergence of the plant states to the control invariant set $B_{\hat{\rho}}$.

Now, it remains to be shown that x^p_k, $\bar{x}_k$, $\hat{x}_k \in B_\rho$, $\forall k \geq 0$. *From equation (6.117) and the definition of* ρ^d, *we have:*

$$\| x^p_{k+1} - \bar{x}_{k+1} \|_{\hat{P}} \leq \frac{\gamma}{L} e^{LPT}(e^{LPT} - 1) \| x^p_k \|_{\hat{P}} + [\gamma \bar{u} e^{LPT} + \rho^d] PTe^{LPT} =: \lambda_1 \| x^p_k \|_{\hat{P}} + \lambda_2 \quad (6.124)$$

Thus, using the contractive constraint and the results of **Lemma 4.1**, *we obtain:*

$$\| x_k^p \|_{\hat{P}} < \| x_0^p \|_{\hat{P}} + \frac{\lambda_2}{1-\alpha^*} \leq \rho_0 + \frac{\lambda_2}{1-\alpha^*} = \rho_0 + \frac{[\gamma \bar{u} e^{LPT} + \rho^d] LPT\, e^{LPT}}{L(1-\alpha) - \gamma e^{LPT}(e^{LPT}-1)}, \tag{6.125}$$

$\forall k > 0$ *and* $x_0^p \in B_{\rho_0}$.

We have then found an upper bound on the states of the plant at the end of horizons. Since the estimated states are given by $\hat{x}_k = x_k^p + e_k$ *and the estimation error satisfies equation (6.113), we have the following bound on the estimated states:*

$$\| \hat{x}_k \|_{\hat{P}} < \rho_0 + \frac{[\gamma \bar{u} e^{LPT} + \rho^d] LPT\, e^{LPT}}{L(1-\alpha) - \gamma e^{LPT}(e^{LPT}-1)} + K \| e_0 \|_{\hat{P}}, \quad \forall k > 0 \text{ and } x_0^p \in B_{\rho_0} \tag{6.126}$$

Thus, if $\rho_0 := \rho - K \| e_0 \|_{\hat{P}} - \frac{[\gamma \bar{u} e^{LPT} + \rho^d] LPT\, e^{LPT}}{L(1-\alpha) - \gamma e^{LPT}(e^{LPT}-1)}$ *and the disturbance* $\{\tilde{d}_k\}_{k \geq 0}$ *satisfies (6.115), it follows that* $\rho_0 > 0$, $\{x_k^p\}_{k=0}^{\infty}$, $\{\hat{x}_k\}_{k=0}^{\infty} \in B_\rho$ *and, due to the contractive constraint, we also have* $\{\bar{x}_k\}_{k=0}^{\infty} \in B_\rho$, *which means that the control problem* $\mathcal{P}(t_k, \hat{x}_k)$ *is feasible and well-defined for all* $k \geq 0$.

□

6.4 Examples

The examples examined here have been previously introduced in chapters 3 and 4, where closed-loop simulations of the systems using contractive MPC and standard nonlinear finite horizon MPC were performed using the exact nonlinear model of the system as the prediction model and in the computation of the contractive constraint. In some cases, we addressed the effect of parameter uncertainty, bounded, additive and non-additive, persistent and non-persistent disturbances and state estimation with different nonlinear observers, using different levels of noise and initial state estimation error.

Here we will perform simulations of the same examples but by applying the computationally simpler and more efficient implementation of contractive MPC proposed in the present chapter. The optimization problem to be solved at each time step is now a QP and, therefore, the simulations run at a much faster speed, allowing, e.g., the exploration of longer prediction and control horizons without making the computation time unacceptable.

The contractive constraint is implemented as suggested in procedure 3, i.e., by solving the QP using a linear version of the constraint, while iterating on the parameter δ, until the original quadratic contractive constraint is satisfied. The QP is solved only once at each sampling time.

Exponential stability can no longer be guaranteed for all controller parameter choices which render the optimization feasible at every sample (i.e., feasibility does not imply exponential stability even in the absence of disturbances and parameter mismatch). The reason for this weakening of the closed-loop stability properties is that the model used in the prediction is a local linearization of the original nonlinear system and this linear/nonlinear mismatch makes it necessary for the controller to be robust. In mathematical terms, this robustness condition translates into an upper bound on α above which stability cannot be assured and below which, convergence of the states to a control invariant set containing the origin is guaranteed. The size of this control invariant set depends on the chosen controller parameters and on the linear/nonlinear mismatch (i.e., on the "strength" of the nonlinearities neglected in the prediction step of the MPC controller).

In the simulations which follow, we will plot the state responses for the original nonlinear system and for the linear approximation used in the computation of the contractive constraint (which is only updated with the states of the plant at the end of prediction horizons).

6.4.1 Example 1: A Nonholonomic System (Car)

Computation of upper bound on the contractive parameter

Due to the simplicity of the model dynamics for this example, it is possible to calculate an upper bound on the contractive parameter α, $\bar{\alpha} \leq 1$, such that the optimization problem is feasible for $\alpha \in [0, \bar{\alpha})$ and, therefore, the closed-loop response is stable. As we saw in chapter 3, for this example, we have:

State Vector X:

$$X := \begin{bmatrix} x \\ y \\ \theta \end{bmatrix}$$

Input Vector u:

$$u := \begin{bmatrix} v \\ w \end{bmatrix}$$

Nonlinear Dynamics $f(X, u)$:

$$f(X, u) := \begin{bmatrix} cos(\theta)\ v \\ sin(\theta)\ v \\ w \end{bmatrix}$$

Linearization at an arbitrary point (X^*, u^*):

$$A^*X + B^*u + C^* := \begin{bmatrix} -sin(\theta^*)v^*(\theta - \theta^*) + cos(\theta^*)(v - v^*) + cos(\theta^*)v^* \\ cos(\theta^*)v^*(\theta - \theta^*) + sin(\theta^*)(v - v^*) + sin(\theta^*)v^* \\ w \end{bmatrix}$$

Thus, for any X, $\bar{X} \in \Re^n$ and $u \in \Re^m$, it follows that:

$$\| f(X,u) - f(\bar{X},u) \| \leq 2\,|v| \tag{6.127}$$

which shows that $f(X,u)$ does not satisfy Lipschitz condition (6.65). Moreover,

$$\| F(X,u) \| := \| f(X,u) - A^*X - B^*u - C^* \| \leq \gamma\,(|\theta - \theta^*| + |v|) \tag{6.128}$$

with $\gamma := \max\{2,\ |v^*|,\ \sqrt{|v^*|}\}$.

If the control constraints are such that $|v| \leq v_{max}$ for a chosen $v_{max} > 0$, inequality (6.128) is satisfied for any point (X^*, u^*) around which the linearization is performed if $\gamma := \max\{2,\ |v_{max}|,\ \sqrt{|v_{max}|}\}$.

Therefore, using equation (6.69), we get the following bound on the difference between the states of the nonlinear system and the linearization performed at (X_k, u_k) at time t_k, for $t \in [t_k, t_{k+1}]$, $\forall k \geq 0$:

$$\| X_k^p(t) - \bar{X}_k(t) \| \leq 2\int_{t_k}^{t} |v_k(\tau)|d\tau + \gamma \int_{t_k}^{t} (|\theta_k(\tau) - \theta_k| + |v_k(\tau)|)d\tau \tag{6.129}$$

$|v|$ is bounded given the input constraint $|v| \leq v_{max}$ and from the dynamic equation on θ we get:

$$\theta_k(t) - \theta_k = \int_{t_k}^{t} w_k(\tau)d\tau \tag{6.130}$$

Therefore, given the constraint on w, $|w| \leq w_{max}$, it results that:

$$|\theta_k(t) - \theta_k| \leq w_{max}(t - t_k) \tag{6.131}$$

Using these bounds in equation (6.129), we obtain:

$$\| X_{k+1}^p - \bar{X}_{k+1} \| \leq PT \left[v_{max}(2+\gamma) + \frac{\gamma w_{max} PT}{2} \right] \tag{6.132}$$

Since the contractive constraint imposes that $\| \bar{X}_{k+1} \| \leq \alpha \| X_k^p \|$ (where we have adopted $\hat{P} = I_n$, for simplicity), we have:

$$\| X_{k+1}^p \| \leq \alpha \| X_k^p \| + PT \left[v_{max}(2+\gamma) + \frac{\gamma w_{max} PT}{2} \right] \tag{6.133}$$

Given that $\alpha \in [0, 1)$ by definition, we can apply lemma 4.1 to show that:

$$\| X_k^p \| < \| X_0 \| + \frac{PT \left[v_{max}(2+\gamma) + \frac{\gamma w_{max} PT}{2} \right]}{1-\alpha}, \quad \forall k \geq 0 \tag{6.134}$$

and

$$\lim_{k \to \infty} \| X_k^p \| \leq \frac{PT \left[v_{max}(2+\gamma) + \frac{\gamma w_{max} PT}{2} \right]}{1-\alpha} =: \hat{\rho} \tag{6.135}$$

From equation (6.134), a sufficient condition for $X_k^p \in B_\rho$ (which translates into feasibility of the control problem, as stated in assumption 6.1) is given by:

$$\rho > \rho_0 + \frac{PT \left[v_{max}(2+\gamma) + \frac{\gamma w_{max} PT}{2} \right]}{1-\alpha} \tag{6.136}$$

This inequality re-written as a condition on α, gives us the upper bound $\bar{\alpha}$ which we wanted to derive:

$$\alpha < \bar{\alpha} := 1 - \frac{PT}{\rho - \rho_0} \left[v_{max}(2+\gamma) + \frac{\gamma w_{max} PT}{2} \right] \tag{6.137}$$

Naturally, this bound only has significance only if $\frac{PT}{\rho-\rho_0}\left[v_{max}(2+\gamma)+\frac{\gamma w_{max} PT}{2}\right] < 1$. Notice that ρ increases as $\bar{\alpha}$ increases, i.e., the larger we allow α to be, the larger the set of initial conditions for which the optimization problem is feasible. Thus, if we re-write equation (6.137) to express ρ as a function of $\bar{\alpha}$ we can easily verify that $\lim_{\bar{\alpha}\to 1}\ \rho \to \infty$. However, as we have previously discussed, determining ρ is not a trivial task and that is the main obstacle in actually computing numerical values of $\bar{\alpha}$ so that stability and feasibility are guaranteed for $\alpha \in [0, \bar{\alpha})$.

It is also interesting to notice that even though $f(X,u)$ does not satisfy a Lipschitz condition in $\Re^n \times \Re^m$, it was possible to derive an upper bound on α in the same fashion used in theorems 6.2 and 6.3. However, because f is not Lipschitz continuous, this bound does not possess the same properties of that derived in theorem 6.3, namely that $\bar{\alpha} = 1$ if $\gamma = 0$ (this bound meaning that in the absence of model/plant mismatch we are allowed to choose α as near to one as desired; see equation (6.89)).

Thus, in the simulations which follow, we will not test if this bound is satisfied. Since the bound is derived from a sufficient condition to guarantee feasibility and stability, if the control problems in our simulations are feasible at successive time steps, then α may or may not satisfy the bound. All that matters for simulation purposes is that we choose the control parameters P and α in a way that feasibility is obtained at all time steps. If the result is an unstable closed-loop, we know that for the given P, we must reduce α or, if feasibility can no longer be guaranteed for this smaller value of α, we should increase the horizon and search for a new α small enough to provide stability and large enough to ensure feasibility.

6.4.2 Comparison between contractive MPC with local linearization and Astolfi's discontinuous controller (unconstrained case)

Contractive MPC with local linearization

Figure 6.4 shows the resulting paths in the $xy-$plane of the controlled car using our contractive MPC scheme with local linearization in the absence of input constraints.

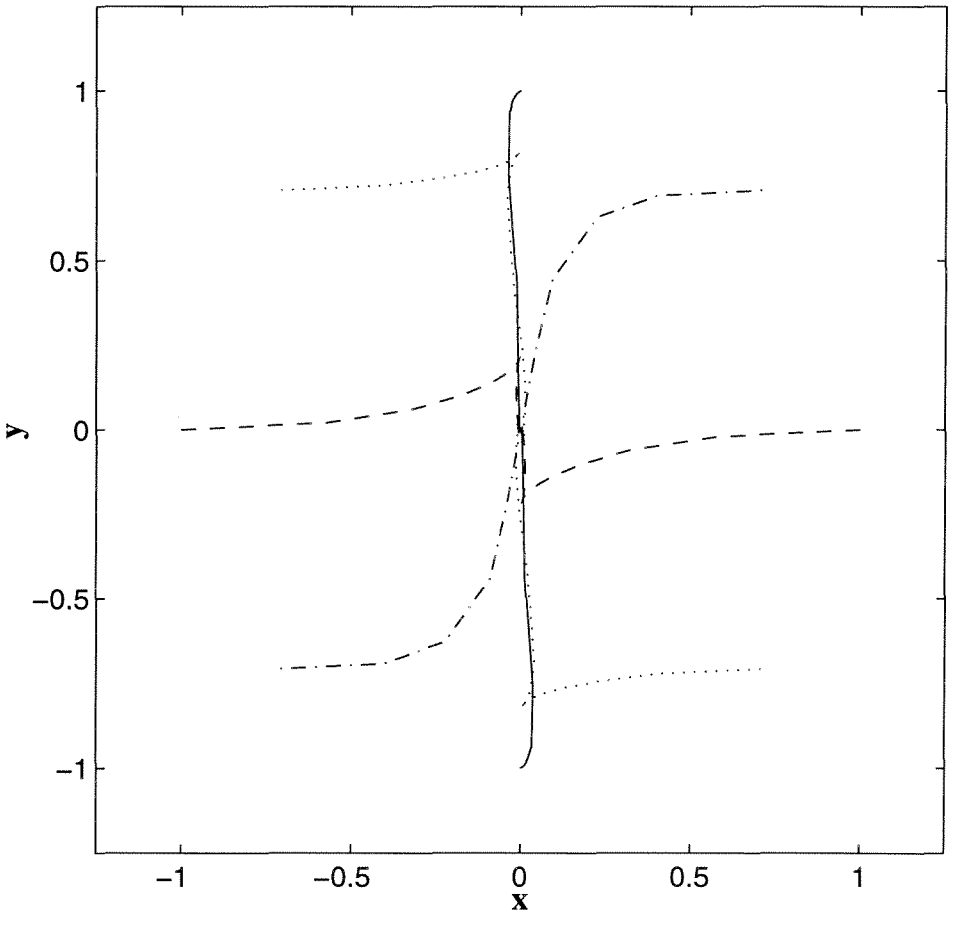

Figure 6.4: Resulting paths in the $xy-$plane using contractive MPC with local linearization when the car is initially on the unit circle and parallel to the $x-$axis.

The controller parameters used in these simulations are given by:

Controller Parameters (figure 6.4)		
$Q = \text{diag}([50\ \ 1\ \ 0])$	$R = 0$	$S = 0$
$P = 3$	$M = 1$	$\alpha = 0.8$

Better trajectories are obtained in figure 6.5 where the controller is finely retuned for each initial condition.

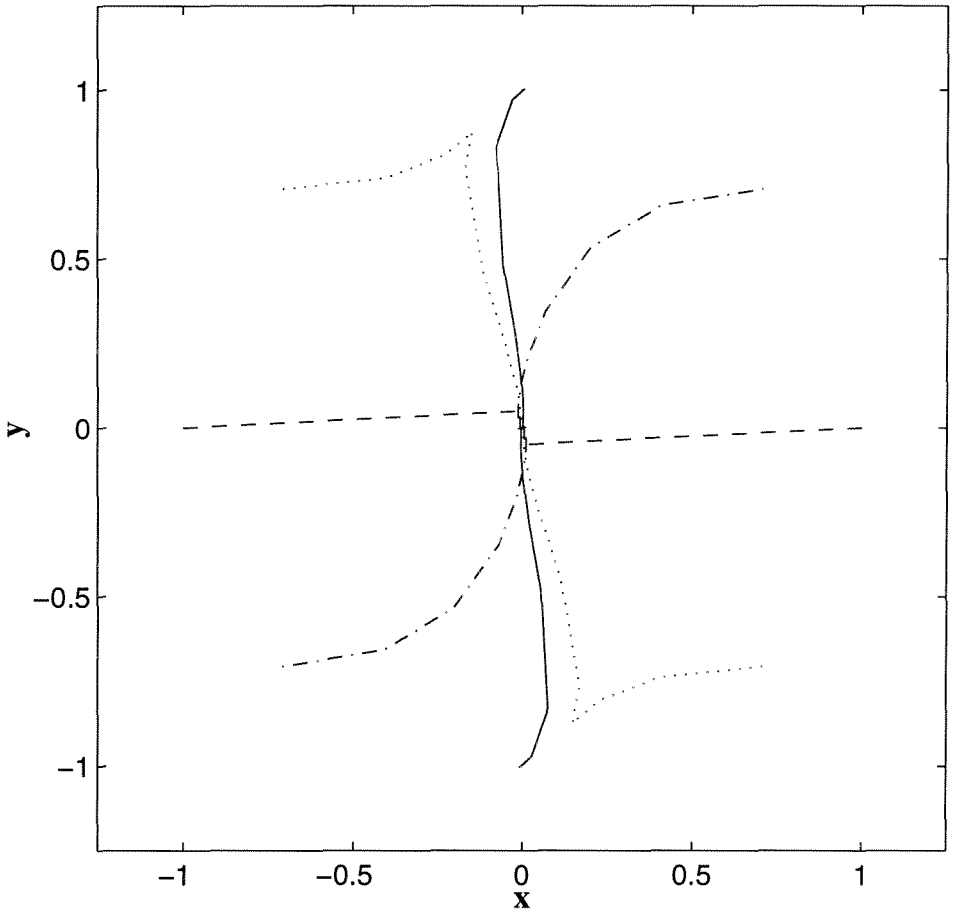

Figure 6.5: Resulting paths in the $xy-$plane using contractive MPC with local linearization when the car is initially on the unit circle and parallel to the $x-$axis.

The controller parameters used for simulations with the different initial conditions in figure 6.5 are given by:

1. **Initial conditions:** $[\mathbf{x_0},\ \mathbf{y_0},\ \theta_0] = [\pm\mathbf{1},\ \mathbf{0},\ \mathbf{0}]$

Controller Parameters (figure 6.5)		
$Q = \text{diag}([10\ \ 1\ \ 0])$	$R = 0$	$S = 0$
$P = 4$	$M = 2$	$\alpha = 0.8$

2. **Initial conditions:** $[\mathbf{x_0},\ \mathbf{y_0},\ \theta_0] = [\mathbf{0},\ \pm\mathbf{1},\ \mathbf{0}]$

Controller Parameters (figure 6.5)		
$Q = \text{diag}([5.9\ \ 1\ \ 0])$	$R = 0$	$S = 0$
$P = 3$	$M = 1$	$\alpha = 0.79$

3. **Initial conditions:** $[\mathbf{x_0},\ \mathbf{y_0},\ \theta_0] = \{[\sqrt{\mathbf{2}},\ \sqrt{\mathbf{2}},\ \mathbf{0}],\ [-\sqrt{\mathbf{2}},\ -\sqrt{\mathbf{2}},\ \mathbf{0}]\}$

Controller Parameters (figure 6.5)		
$Q = \text{diag}([7\ \ 1\ \ 0])$	$R = 0$	$S = 0$
$P = 3$	$M = 1$	$\alpha = 0.8$

4. **Initial conditions:** $[\mathbf{x_0},\ \mathbf{y_0},\ \theta_0] = \{[\sqrt{\mathbf{2}},\ -\sqrt{\mathbf{2}},\ \mathbf{0}],\ [-\sqrt{\mathbf{2}},\ \sqrt{\mathbf{2}},\ \mathbf{0}]\}$

Controller Parameters (figure 6.5)		
$Q = \text{diag}([7.5\ \ 1\ \ 0])$	$R = 0$	$S = 0$
$P = 3$	$M = 1$	$\alpha = 0.85$

The sampling time used is equal to $T = 0.1$.

Astolfi's discontinuous controller

The same kind of plot in the $xy-$plane for the controlled car using Astolfi's discontinuous controller has been presented in figure 3.7 and we reproduce it here in figure 6.6 for comparison with the results obtained using our contractive MPC scheme with local linearization.

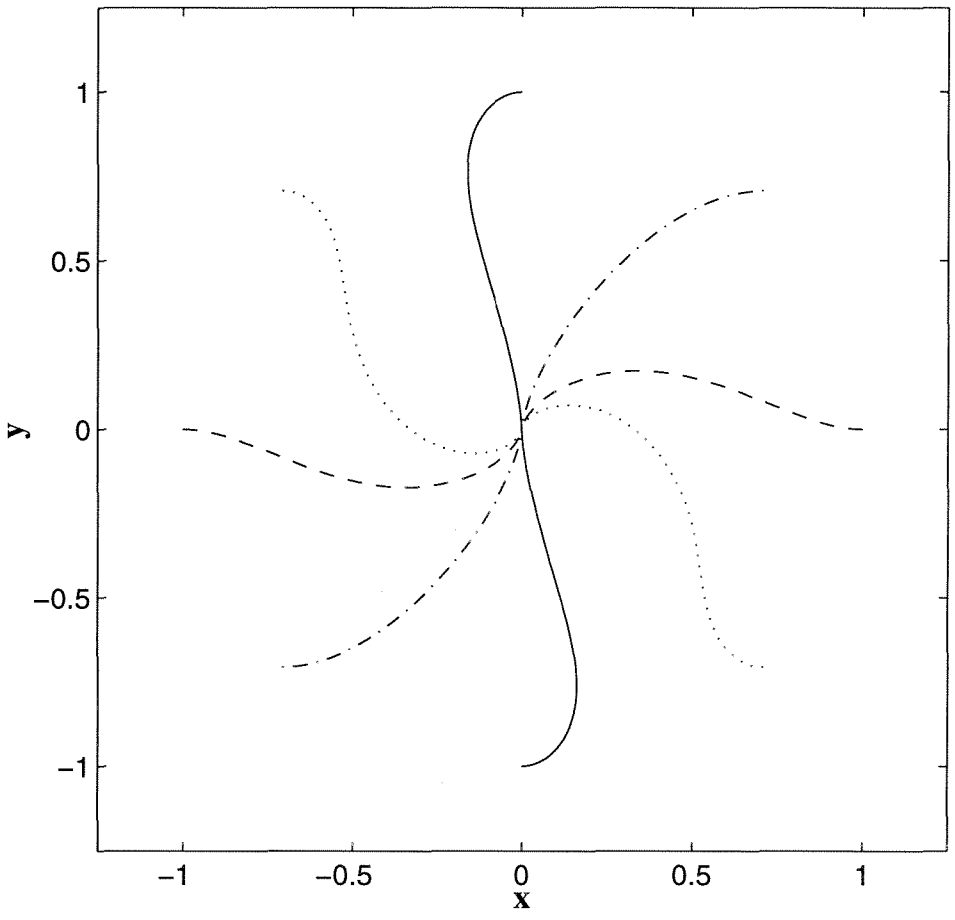

Figure 6.6: Resulting paths in the $xy-$plane using the analytical discontinuous controller when the car is initially on the unit circle and parallel to the $x-$axis.

Comparison of results in figures 6.4 and 6.6

The fact that contractive MPC with local linearization has been implemented here as a QP has reduced the time to compute the state trajectories dramatically and each simulation took on average between 3 and 5 seconds (compared to an average between 9 and 12 minutes for contractive MPC with a nonlinear prediction model).

We can see from figures 6.4 and 6.6 that, for both controllers, the car performs its maneuver towards the origin of the coordinate system in a very natural way.

We also observe that while the contractive MPC scheme with a nonlinear prediction model generates trajectories which approach the origin in a very optimized manner (as shown in figure 3.6 in chapter 3), the contractive MPC scheme with local linearization leads to a worse performance. The reason for this degradation in performance is that we are now optimizing a performance criterion which takes into consideration the state evolution of the local linearization of the system at each time step and not the states of the real nonlinear system. Besides, contraction after each set of P steps is now imposed on the states of the linear model computed at the beginning of the P steps and not on the nonlinear model states.

Comparing figures 6.4 and 6.6, we cannot really say that one performance is clearly superior to the other and it is obvious that we can improve (degrade) the performance of each controller by choosing different controller parameters (as shown for the contractive MPC controller in figure 6.5).

The fact that the linearization of this system around the origin is not controllable generates the same problem for contractive MPC which we discussed in detail in chapter 3. In order to prevent it, we set tolerances for the deviation of the final states with respect to the origin and stopped the control once these were satisfied.

Comparison between contractive and standard MPC controllers with local linearization (unconstrained and constrained cases)

Standard MPC with local linearization

In chapter 3, nominal stability and performance properties of contractive MPC (CNTMPC) were compared to those of a standard nonlinear finite horizon MPC (SNLMPC) scheme. There we noticed that certain controller parameter choices could destabilize SNLMPC while CNTMPC preserved its stability characteris-

tics as long as the optimization problem at the beginning of each horizon was feasible.

Now the existing model/plant mismatch makes it even easier to find controller parameters for which standard MPC with local linearization generates an unstable closed-loop response as we can see in figure 6.7.

The same experimental initial condition used in chapter 3 will be adopted in the simulations performed here. The sampling time for this example is equal to $T = 0.1$.

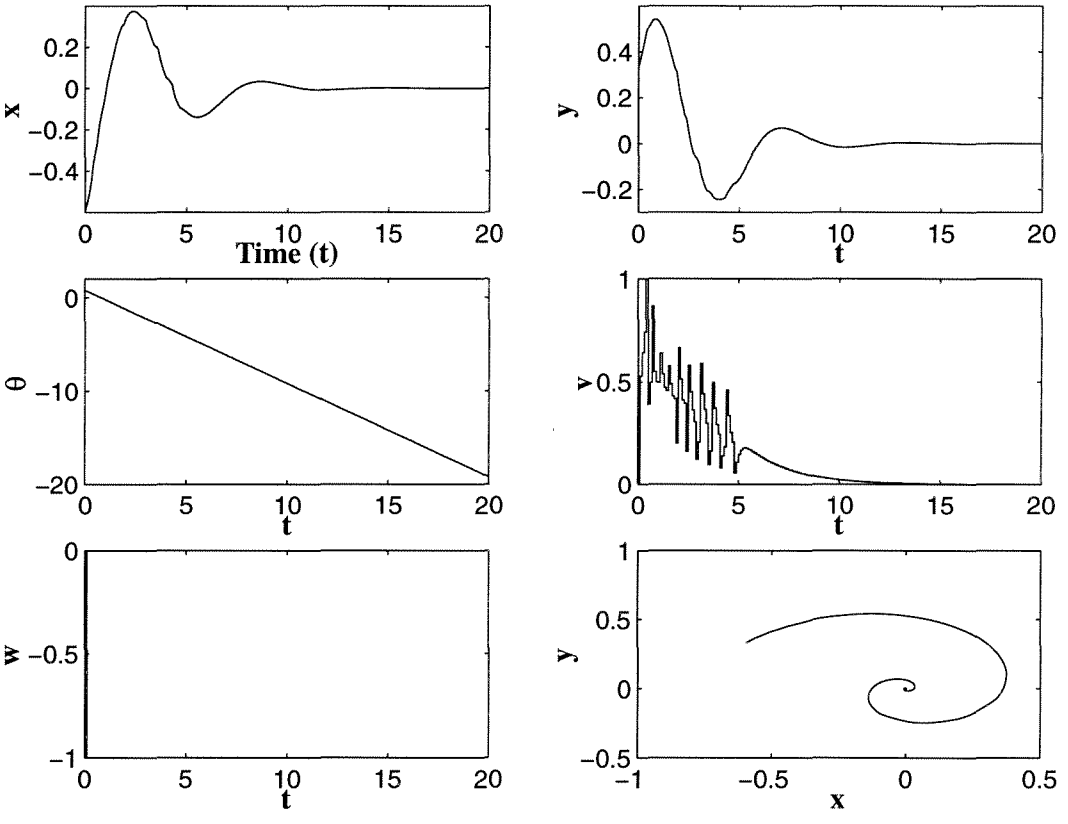

Figure 6.7: Car: State and control responses and $xy-$plot generated by standard MPC with local linearization in the constrained case.

The controller parameters used in these simulations are:

Controller Parameters (figure 6.7)		
$Q = \text{diag}([1 \;\; 1 \;\; 0])$	$R = 0$	$S = 0$
$P = 8$	$M = 5$	
$u_{min} = [-0.2 \quad -1.0]$	$u_{max} = [1.0 \quad 1.0]$	

From figure 6.7 we notice that the angle θ decreases linearly in time and goes unstable due to the fact that w is equal to -1 for all $t \geq 0.1$ and, from the equations of the model, $\dot{\theta} = w$. Thus, for this control parameter choice, the standard MPC controller with local linearization is unable to stabilize the angle of the car with respect to the $x-$axis.

Contractive MPC with local linearization

The unconstrained and constrained responses obtained with contractive MPC are shown in figure 6.8.

The controller parameters used in these simulations are given by:

Unconstrained case

Controller Parameters (figure 6.8)		
$Q = \text{diag}([1 \;\; 10 \;\; 1])$	$R = 0.1\, I_m$	$S = 0$
$P = 30$	$M = 18$	$\alpha = 0.8$

Constrained case

Controller Parameters (figure 6.8)		
$Q = \text{diag}([1 \;\; 10 \;\; 0])$	$R = 0.2\, I_m$	$S = 0$
$P = 32$	$M = 20$	$\alpha = 0.8$
$u_{min} = [-0.2 \quad -1.0]$	$u_{max} = [0.2 \quad 1.0]$	

The control and prediction horizons have been increased in the constrained case in order to guarantee feasibility of the QPs. We notice that the input constraints

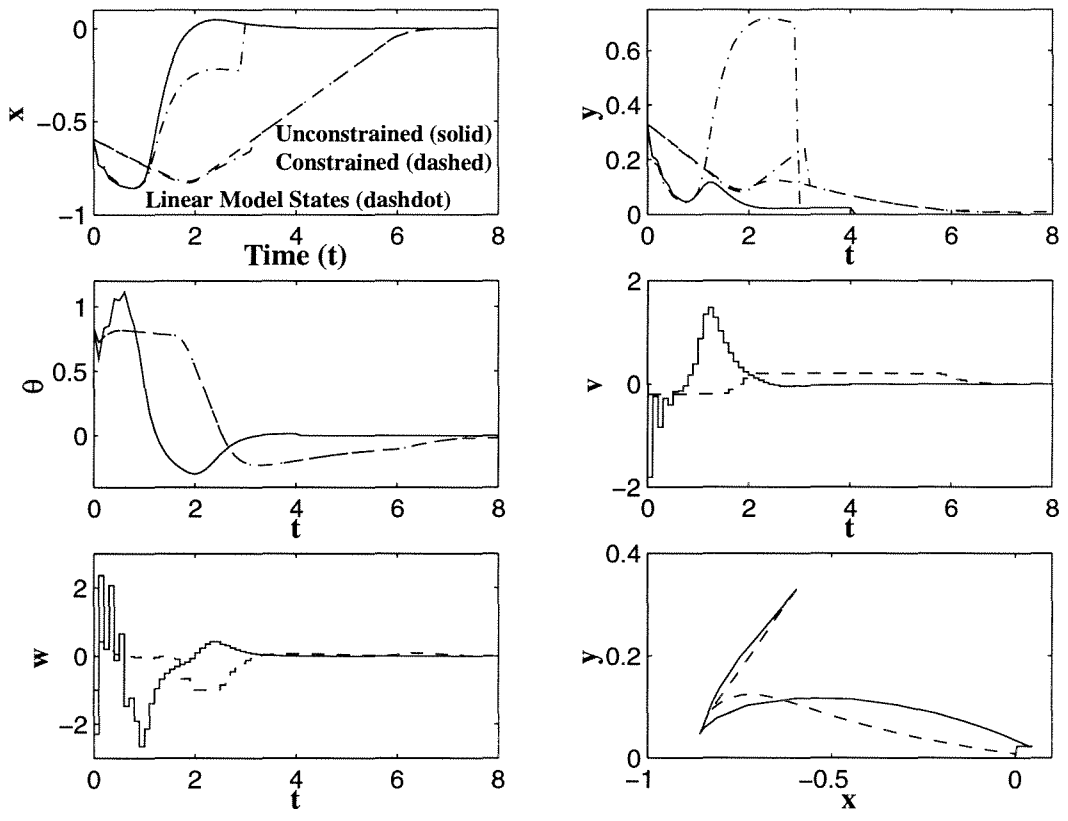

Figure 6.8: Car: State and control responses and $xy-$plot generated by contractive MPC in the unconstrained and constrained cases.

delay the closed-loop response but bring the responses of the linear model and of the original nonlinear system closer together.

In both cases, we notice that at time $t = 3$ ($t = 3.2$ in the constrained case), the states of the linear model are set to be equal to the states of the plant and the trajectory of the model (the "linear" trajectory) begins tangent to the "nonlinear" trajectory at this point (i.e., at the points where the contractive constraint is satisfied by the "linear" states). We also notice that the θ-response is matched exactly by the linear approximation. Naturally, this comes from the fact that the equation which governs the dynamics of this variable is linear and uncoupled with the other two equations of the system.

6.4.3 Example 2: Continuous Stirred Tank Reactor (CSTR) + Flash Unit

Here we will examine the same control problem of chapter 3 (**Case 1**), i.e., beginning at a steady state where the conversion of product in the distillate of the flash drum, C_3, is low and equal to the concentration of B in the reactor, C_2, we want to reach the point of maximum conversion. The parameters of the model and the sampling time are the same as the ones used in chapter 3.

The initial condition is a steady state of low conversion with the following coordinates:

Initial condition	
$T_{3,0} = 4.278166$	$V_0 = 8.3056 \times 10^{-2}$
$C_{2,0} = 0.428721$	$T_{2,0} = 4.43389$
$C_{3,0} = 0.428721$	

Case 1: No disturbances or uncertainty

The simulation results in the constrained case are depicted in figure 6.9.

The controller parameters used in **Case 1** are the following:

Controller parameters (figure 6.9)		
$Q = \text{diag}([1 \;\; 100 \;\; 1])$	$R = 0$	$S = 0$
$P = 1$	$M = 1$	$\alpha = 0.4$
$u_{min} = -0.1$	$u_{max} = 0$	

From figures 6.9 and 3.26 we can see that the mismatch between the linear system used in the and computation of the contractive constraint and the real nonlinear system does not compromise the responses of the states which still settle in two samples. However, this linear/nonlinear mismatch causes the input variable to have

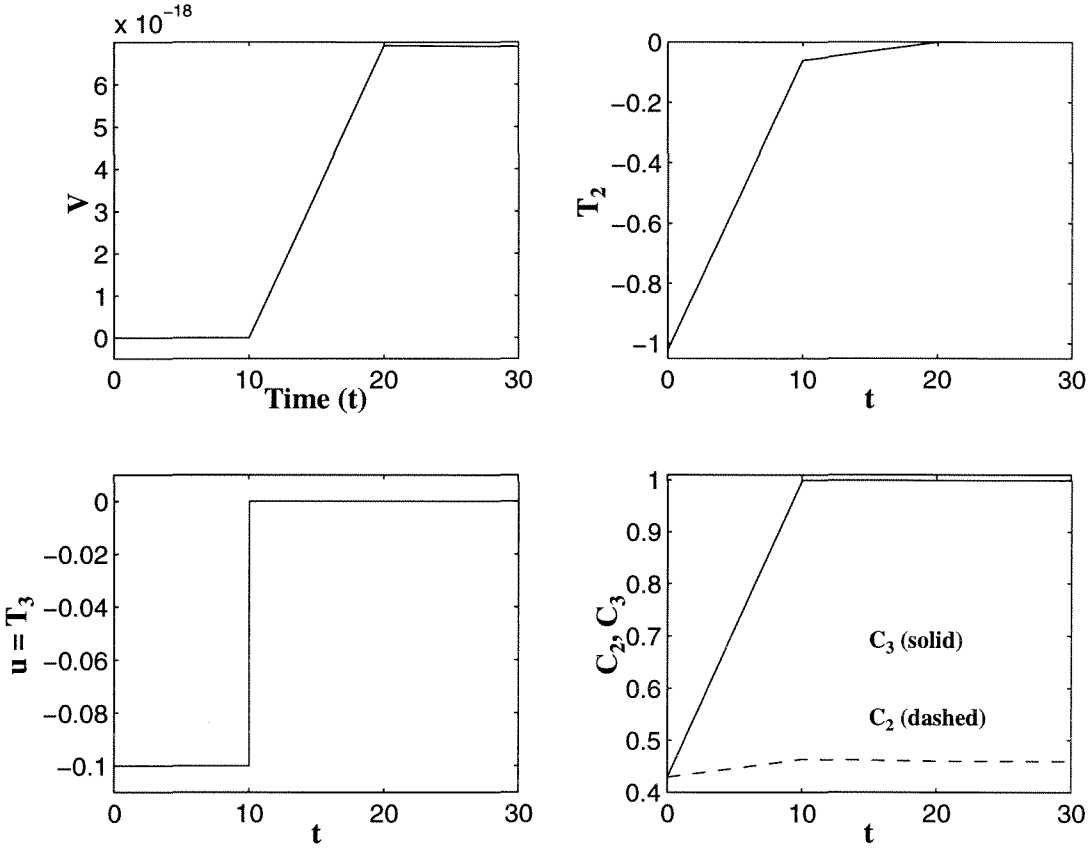

Figure 6.9: CSTR + Flash: State and control responses in the constrained **Case 1**.

opposite sign to what it has in the simulations where the nonlinear system is used for prediction (see figure 3.26).

Here we did not plot the states of the model used in the computation of the contractive constraint because the horizon is equal to $P = 1$ and since we set the states of the model equal to the states of the plant at every step, then the plots of the "linear" and "nonlinear" states coincide in this case.

Case 2: Parameter uncertainty

Here the linear model used in the prediction is computed at nominal parameter values while the plant is simulated with the real parameters. The set of uncertain parame-

ters is composed by the pre-exponential kinetic factors A_1, A_2 which are commonly unknown. In the simulations performed, the true parameters are 10% smaller than their nominal values. Simulation results in the constrained case are shown in figure 6.10.

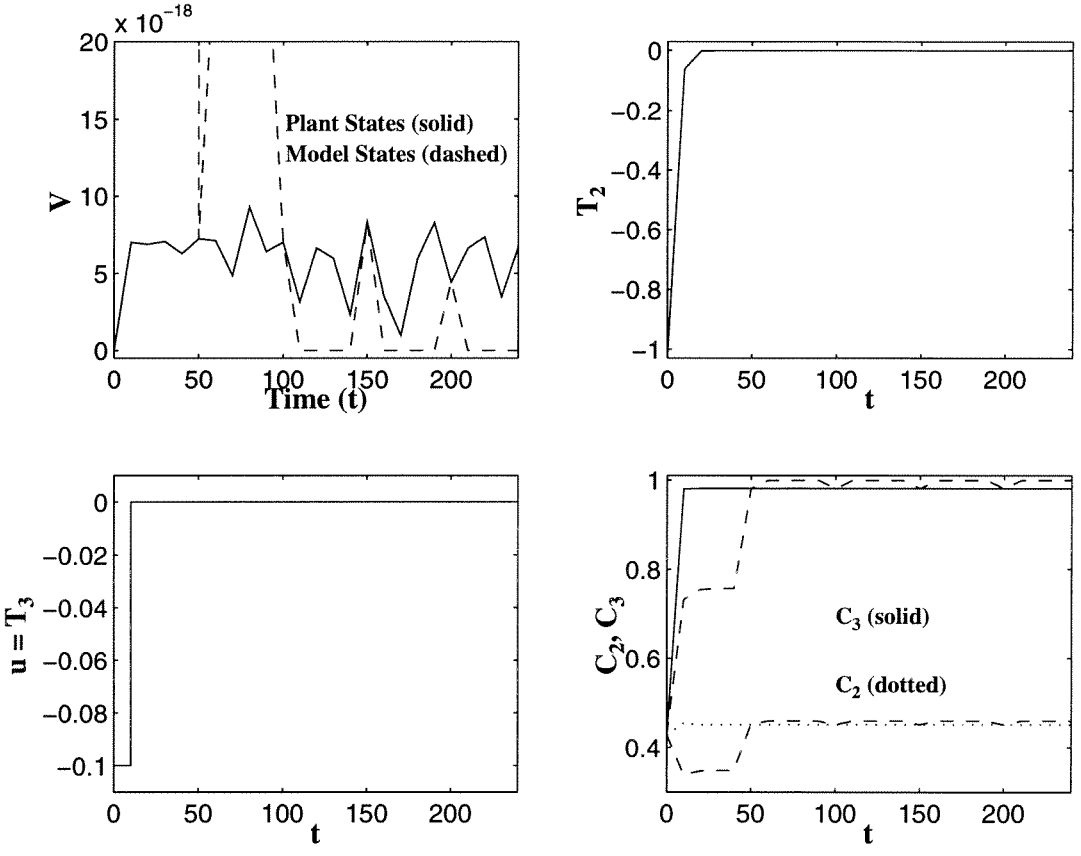

Figure 6.10: CSTR + Flash: State and control responses in the constrained **Case 2**.

The controller and model/plant parameters used in **Case 2** are as follows:

Controller parameters (figure 6.10)		
$Q = \text{diag}([1 \;\; 100 \;\; 1])$	$R = 0$	$S = 0$
$P = 5$	$M = 5$	$\alpha = 0.5$
$u_{min} = -0.1$	$u_{max} = 0$	

Model/Plant Parameters		
Parameters	**Plant**	**Model**
A_1	4.5×10^3	5.0×10^3
A_2	9.0×10^5	1.0×10^6

As we can see from figure 6.10, the parameter mismatch causes the state response to show offset. The states of the linear model show a tendency to converge to the origin, which is natural since they are computed using the nominal parameter values but they are brought to the states of the plant at every five time steps ($P = 5$). Thus, in this case, the closed-loop system is still stable but the states converge asymptotically to a small neighborhood of the origin and not to the origin itself.

The offset displayed by the output C_3 could not be reduced with various choices of controller parameters. The 10% deviation of the parameters with respect to their nominal values causes the plant to settle to another steady state, where the conversion of B in stream 3 is lower and equal to 98.14%, in only two samples.

Case 3: Exponentially decaying disturbances

Finally, we will study the effect of exponentially decaying disturbances on some of the non-manipulated input variables. The variables we have chosen to perturb are F_1 (input flow rate to the reactor) and T_1 (temperature of the input stream). These exponentially decaying disturbances are of the form:

$$d(t) \;=\; d^{ss}\,[1 + a\,e^{-bt}], \quad t \geq 0, \;\; a,\; b > 0 \tag{6.138}$$

where $d(t) := [F_1(t) \quad T_1(t)]$ and d^{ss} is the vector of nominal values of these input variables. The chosen values of a and b in the next simulations are $a = 0.5$ and $b = 0.01$, i.e., at $t = 0$ these variables are perturbed and assume values 50% larger than their nominal, steady state values. Then, they decay exponentially to these

steady state values. The theoretical prediction is that, if the sequence of successive local linear approximations mimic well the behavior of the original nonlinear system, then the states should converge to the desired steady state.

Simulation results in the constrained case are shown in figure 6.11. The disturbance behavior is depicted in figure 6.12.

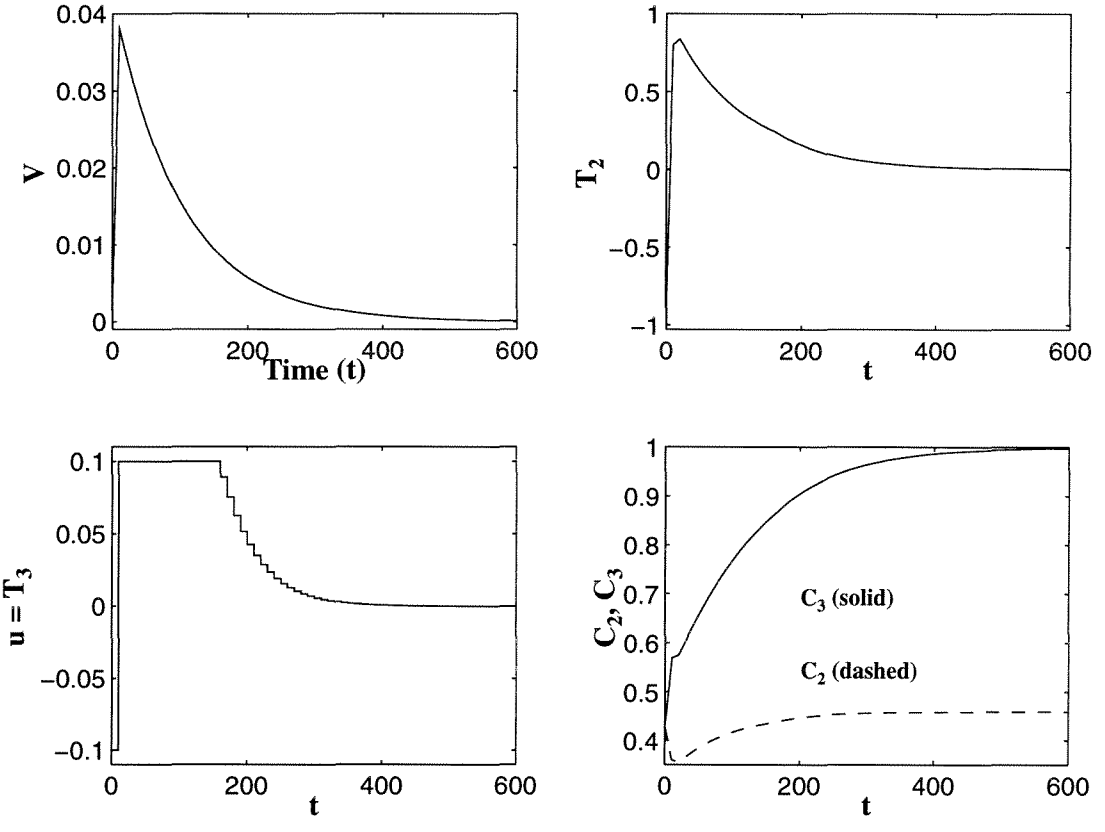

Figure 6.11: CSTR + Flash: State and control responses in the constrained **Case 3**.

The controller parameters used in **Case 3** are as follows:

Controller parameters (figure 6.12)		
$Q = \text{diag}([1 \ \ 100 \ \ 1])$	$R = 0$	$S = 0$
$P = 1$	$M = 1$	$\alpha = 0.4$
$u_{min} = -0.1$	$u_{max} = 0.1$	

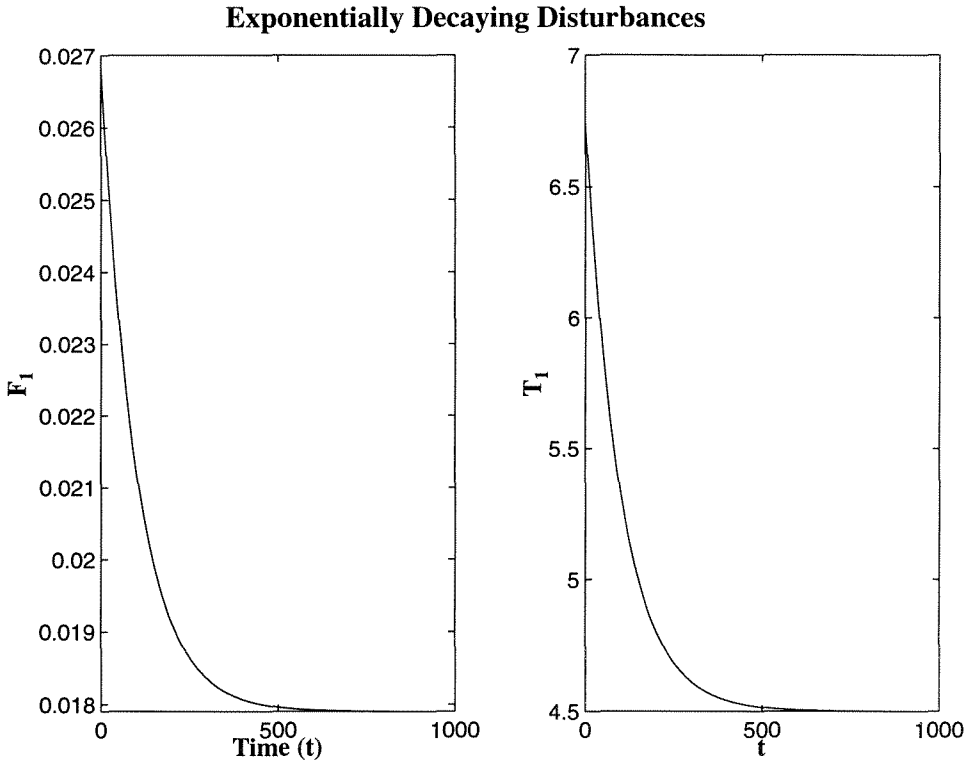

Figure 6.12: Exponentially decaying disturbances used in the simulations shown in figure 6.11.

From figures 6.11 and 6.12 we see that the controller is able to stabilize the system to the origin (in spite of the linear/nonlinear mismatch) as soon as the disturbances vanish. Comparison with figure 6.9 shows that the state response is considerably delayed by the disturbances.

6.4.4 Example 3: 2-Degree of Freedom Robot

For this example we will address the same setpoint tracking problem presented in chapter 3. The sampling time, the nominal parameter values and the initial and final states are the same as in that chapter.

Case 1: No disturbances or uncertainty

Unconstrained and constrained simulations for this system are depicted in figure 6.13.

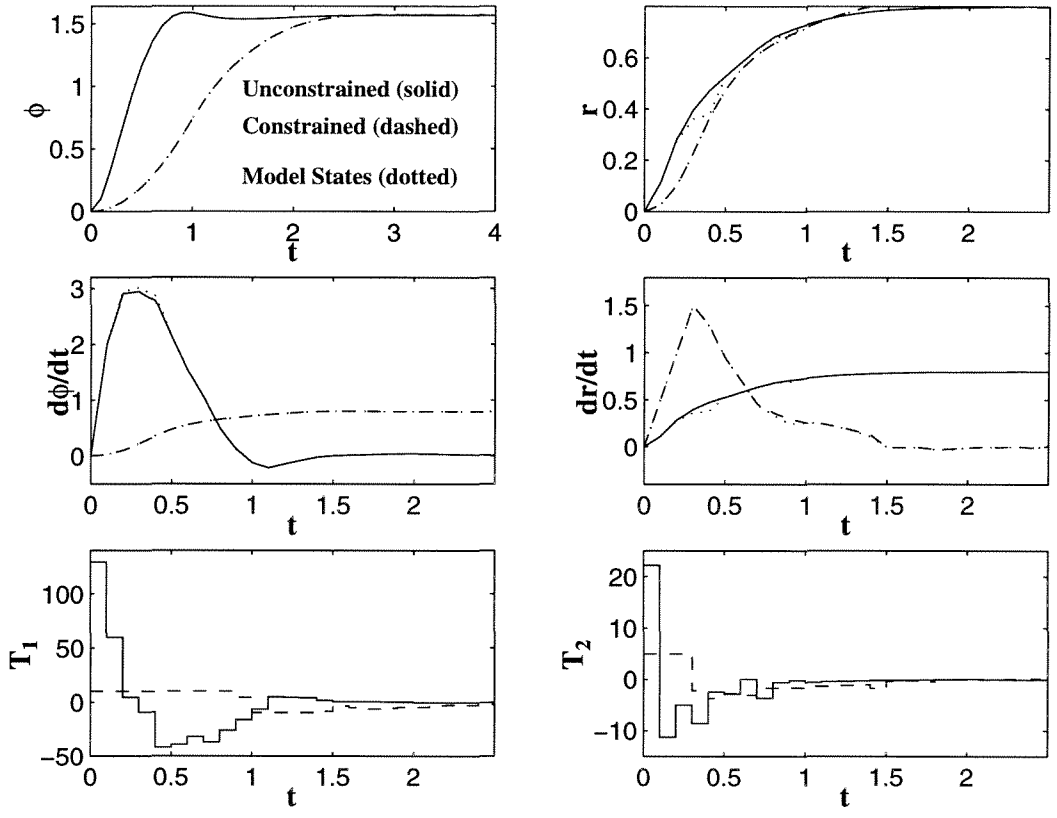

Figure 6.13: Robot: State and control responses in **Case 1**.

The controller parameters used in **Case 1** are the following:

Controller Parameters (figure 6.13)		
$Q = \text{diag}([10 \;\; 10 \;\; 1 \;\; 1])$	$R = 0$	$S = 0$
$P = 5$	$M = 5$	$\alpha = 0.8$
$u_{min} = [-10 \quad -5]$	$u_{max} = [10 \quad 5]$	

As we can see from figure 6.13, the state response of the local linearizations with the implemented control moves (one-step ahead response) represents very well the

response of the original nonlinear system. The presence of tight input constraints delays the response ever so slightly.

Case 2: Parameter uncertainty

Next we will examine the effect of computing the local linearizations at nominal parameter values and have the dynamics of the system evolve with true parameter values. Thus, besides the linear/nonlinear mismatch, we will introduce parameter uncertainty.

In the constrained simulations shown in figure 6.14, the linear model is computed using nominal parameter values (the same that we used in chapter 3) but the equations of the nonlinear system are integrated with $J = 3.2157$ (i.e., the true value of the moment of inertia is half the nominal value).

The controller parameters used in **Case 2** are given by:

Controller Parameters (figure 6.14)		
$Q = \text{diag}([10 \;\; 10 \;\; 1 \;\; 1])$	$R = 0$	$S = 0$
$P = 5$	$M = 5$	$\alpha = 0.9$
$u_{min} = [-10 \quad -5]$	$u_{max} = [10 \quad 5]$	

Figure 6.14 shows that even with this considerable parameter mismatch the linear model is a good approximation of the nonlinear dynamics especially for the output variables, ϕ and r. In this case, even with the sizeable constant parameter mismatch, and for our choice of controller parameters, it is still possible to drive the outputs to the setpoint exactly.

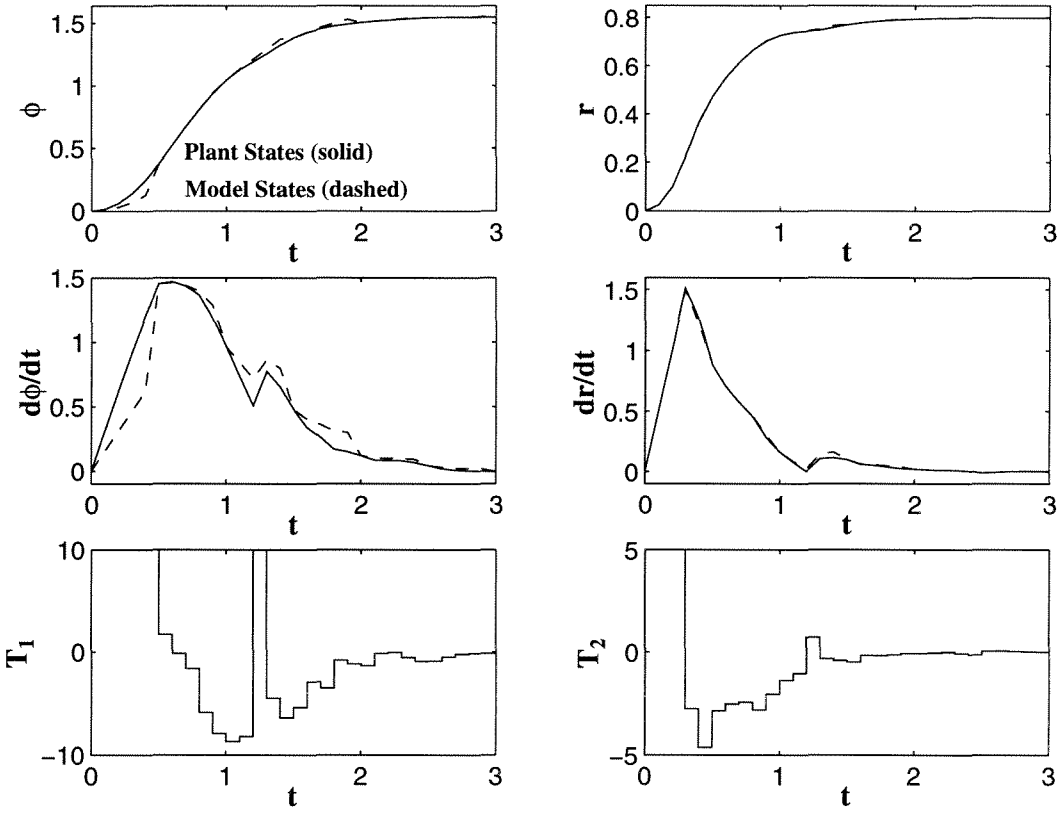

Figure 6.14: Robot: State and control responses in the constrained **Case 2**.

6.4.5 Example 4: Fluid Catalytic Cracking Unit (FCCU)

Transition 1: Step change from the OL unstable steady state to the OL stable steady state

Case 1.1: No disturbances or uncertainty

The parameters of the plant and the coordinates of the OL stable and unstable steady states are the same as used in chapter 3.

The simulation results in the unconstrained case are shown in figure 6.15.

The controller parameters used in **Case 1.1** are:

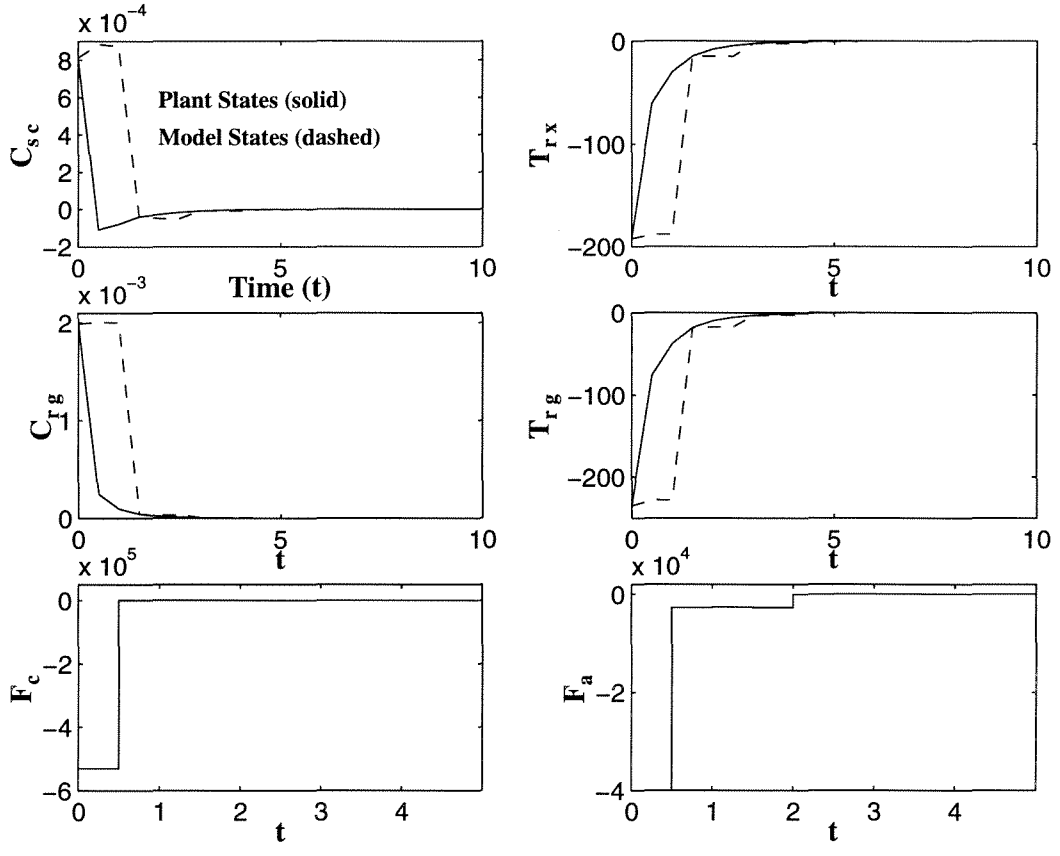

Figure 6.15: FCCU: State and control responses in the unconstrained **Case 1.1**.

Controller Parameters (figure 6.15)		
$Q = \text{diag}([0 \;\; 10^{-3} \;\; 1 \;\; 0])$	$R = 0.1\, I_m$	$S = 0$
$P = 3$	$M = 3$	$\alpha = 0.9$

The sampling time is equal to $T = 0.5$ h.

As we can see from figure 6.15, the use of local linear approximations of the original highly nonlinear FCC model for prediction and computation of the contractive constraint, does not at all compromise the performance obtained when there is no model/plant mismatch and the system operates in the stable regime (compare figures 6.15 and 3.15).

The reason why we will not examine the influence of input constraints on the closed-loop response comes from the fact that the control effort is very small

because the weight on u in the objective function is non-zero (this is the same behavior which we observed in chapter 3).

Case 1.2: Exponentially decaying disturbances

Next we will examine what happens when the three other input (non-manipulated) variables, namely, T_a (air temperature), T_f (feed temperature) and F_t (feed rate), are subjected to exponentially decaying perturbations. These variables behave as in equation (6.138) and, for the present example, we have: $d(t) := [T_a \quad T_f \quad F_t]$ and d^{ss} is the vector of nominal values of these input variables. Here we will use $a = [1 \;\; 1 \;\; 0.5]$ and $b = 0.1$.

The simulations in the presence of these exponentially decaying disturbances in the operational variables are represented in figure 6.16. The disturbances are plotted against time in figure 6.17.

The controller parameters used in **Case 1.2** are:

Controller Parameters (figure 6.16)		
$Q = \text{diag}([0 \;\; 10^{-3} \;\; 1 \;\; 0])$	$R = 0.1\, I_m$	$S = 0$
$P = 5$	$M = 3$	$\alpha = 0.9$

We notice that the contractive MPC controller is able to stabilize the system to the desired OL stable steady state as soon as the disturbances start to vanish. It is also clear that the linear model used in the prediction is a rather good approximation of the dynamics of the original system in this stable operating region, especially once the perturbed input variables approach their nominal values.

Case 1.3: Persistent disturbances

If the perturbed variables do not settle to their nominal values, but rather, to values 5% larger, then we should expect to see offset in at least two of

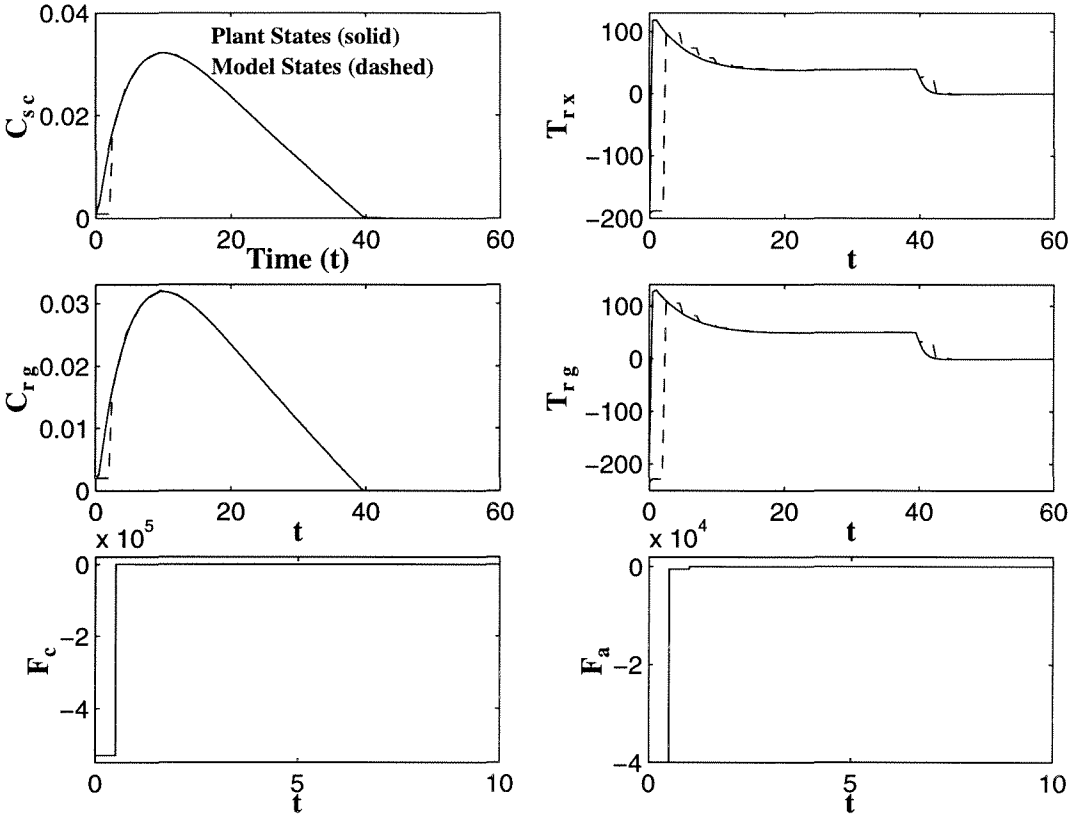

Figure 6.16: FCCU: State and control responses in the unconstrained **Case 1.2**.

the state variables. For the FCC, it turns out that the model equations are extremely sensitive to variations in these non-manipulated input variables and the resulting offset can be quite large, for a small deviation of these input variables with respect to their nominal values.

Here we have chosen exponentially decaying disturbances on T_a, T_f, F_t given by:

$$d(t) \;=\; c \;+\; a\, e^{-bt} \tag{6.139}$$

where $d(t) := [T_a(t) \quad T_f(t) \quad F_t(t)]$, $c = 1.05\; d^{ss}$ (with $d^{ss} := [T_a^{ss} \quad T_f^{ss} \quad F_t^{ss}]$ being the steady state coordinates), $b = 0.1$ and $a = [T_a^{ss} \quad T_f^{ss} \quad 0.5F_t^{ss}]$. Thus, this disturbance behavior is very similar to what we illustrated in figure 6.17

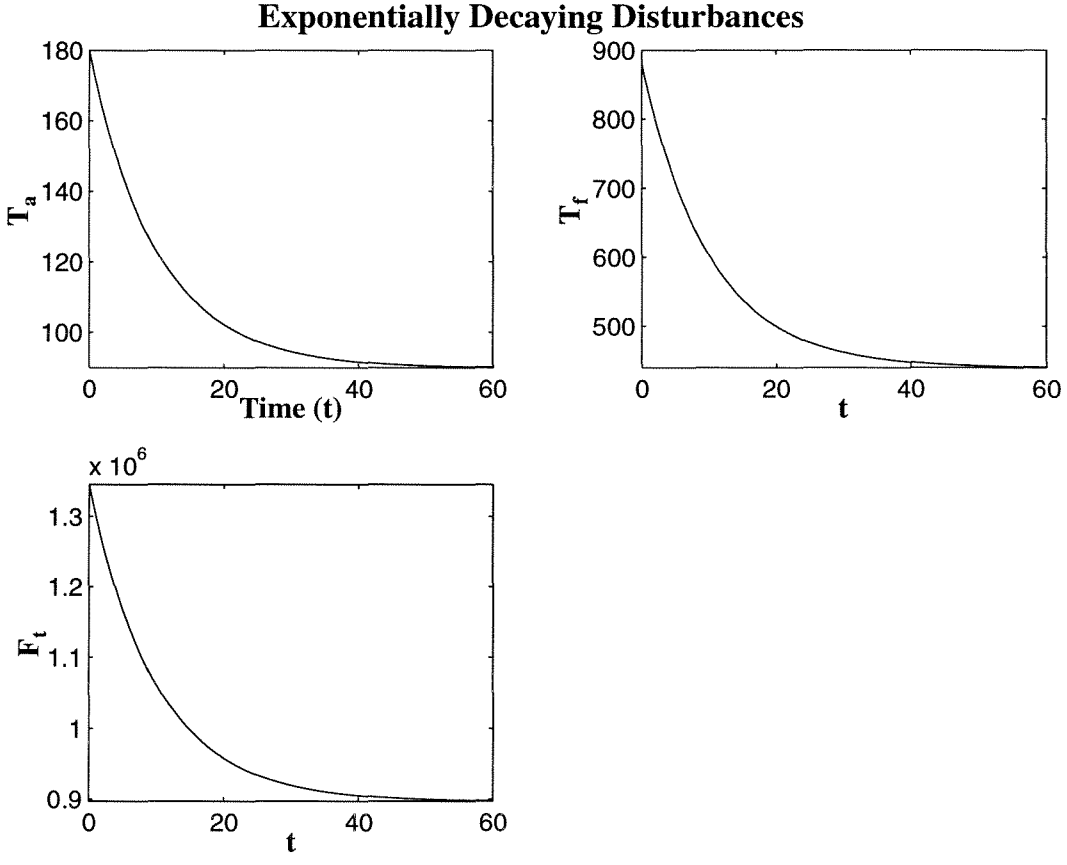

Figure 6.17: Exponentially decaying disturbances used in the simulations shown in figure 6.16.

except that a 5% error remains and the initial perturbation is slightly larger.

The simulation results are shown in figure 6.18.

The controller parameters used in **Case 1.3** are the following:

Controller Parameters (figure 6.18)		
$Q = \text{diag}([0 \;\; 10^{-3} \;\; 1 \;\; 0])$	$R = 0.1\, I_m$	$S = 0$
$P = 12$	$M = 8$	$\alpha = 0.9$

Figure 6.18 reveals that the temperatures T_{rg} and T_{rx} (which are highly correlated to one another, as observed in [36]) are very sensitive to this persistent constant disturbance in the input non-manipulated variables and show considerable deviations from their steady state coordinates. The concentrations C_{sc}

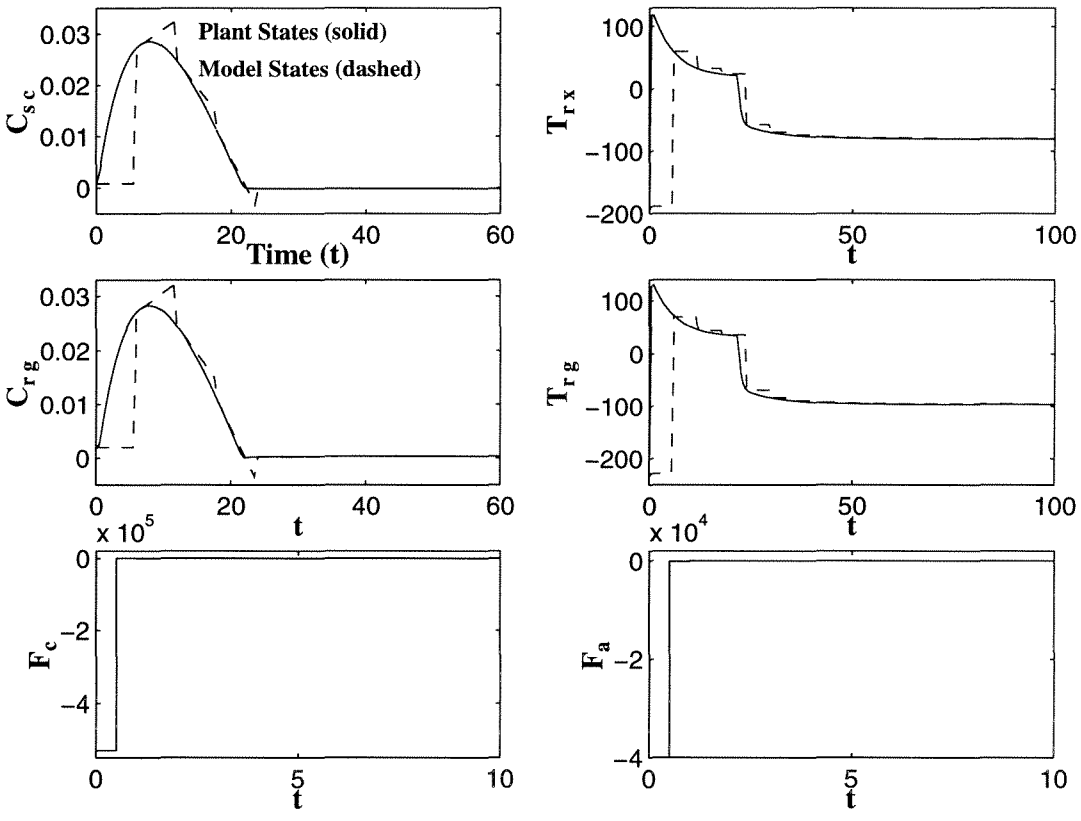

Figure 6.18: FCCU: State and control responses in the unconstrained **Case 1.3**.

and C_{rg} are much less sensitive and can in fact be brought to their steady state values in spite of the disturbance.

We have tried to eliminate or just reduce the offset on T_{rx} and T_{rg} with different controller parameter choices. One of the possibilities was obviously to increase their corresponding weights in the objective function, but if this is done, the other two states (the concentrations C_{sc} and C_{rg}) start showing offset and the improvement in the responses of the temperatures is very small. We have also tried using a weight $\hat{P}$ in the computation of the contractive constraint different from I_n, i.e., we weighted the temperatures with much smaller weights than the concentrations. This attempt did not award us much success either.

Transition 2: Step change from the OL stable steady state to the OL unstable steady state

Case 2.1

This is a much more challenging control problem, as we discussed in chapter 3. The simulation results are shown in figure 6.19.

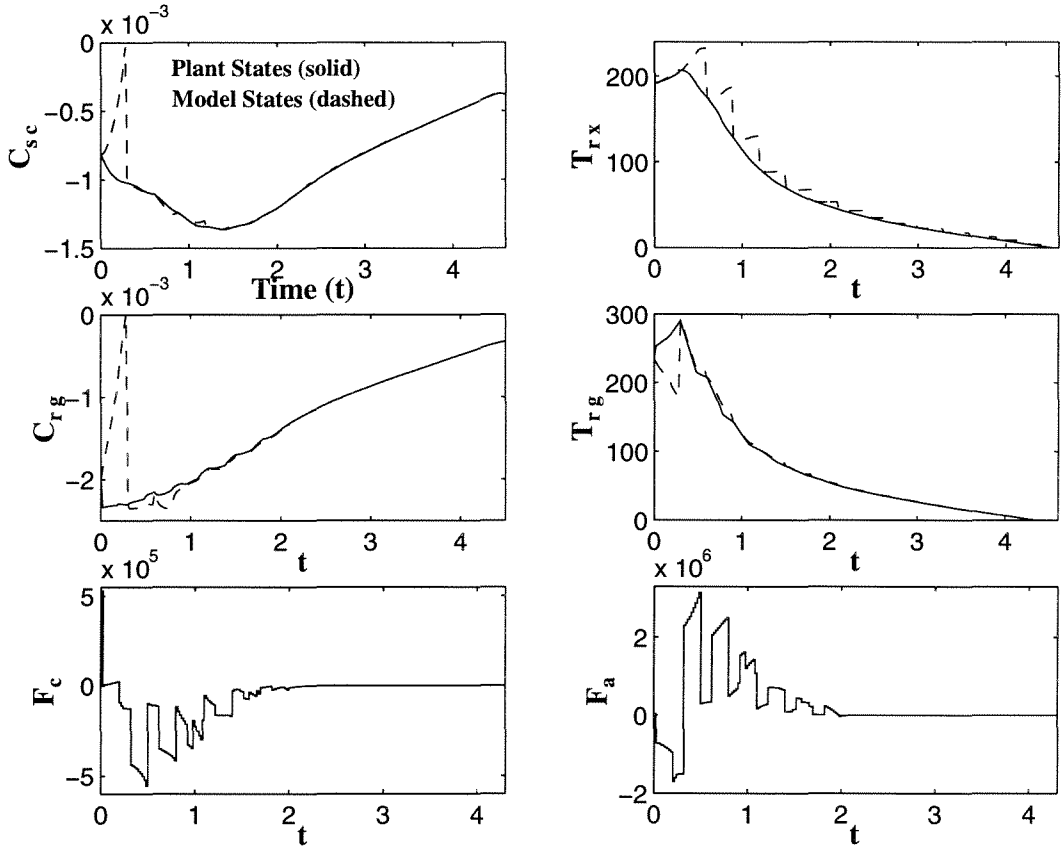

Figure 6.19: FCCU: State and control responses in the unconstrained **Case 2.1**.

The controller parameters used in **Case 2.1** are:

Controller Parameters (figure 6.19)		
$Q = \text{diag}([0\ \ 1\ \ 1\ \ 0])$	$R = 10^{-3}\ I_m$	$S = 0$
$P = 15$	$M = 10$	$\alpha = 0.9$

The sampling time used here is equal to $T = 0.02$ h. The reason why we needed to reduce the sampling time by a factor of 25 was due to the fact that local linear approximations do not represent very well the behavior of the highly ill-conditioned nonlinear model in the unstable operating regime. Therefore, we cannot afford to leave the linear model used in the computation of the contractive constraint open-loop for a very long period of time. In other words, we made the sampling time and the prediction horizon as small as possible within the region where feasibility can be guaranteed. Besides, we left α at a large value so as to be able to use as short an interval as possible for contraction of the "linear" states to occur and still retain feasibility.

Once again, when the exact nonlinear model was used in the prediction (see chapter 3), the algorithm breaks down once the states are very near their OL unstable steady state coordinates. This means that a feasible solution cannot be found with the chosen control parameters in a close-neighborhood of the OL unstable steady state.

We are able to drive both the temperatures in the reactor and in the regenerator to their steady state values (as one can see from figure 6.19) but the algorithm breaks (i.e., we cannot find a set of controller parameters which makes the optimization problem feasible from that point on) once the concentrations start approaching their coordinates at equilibrium. The control variables settle to the origin and show no offset.

Case 2.2

Simulations with a new set of control parameters are shown in figure 6.20.

The sampling time used in this case is equal to $T = 0.05$ h.

The controller parameters used in **Case 2.2** are:

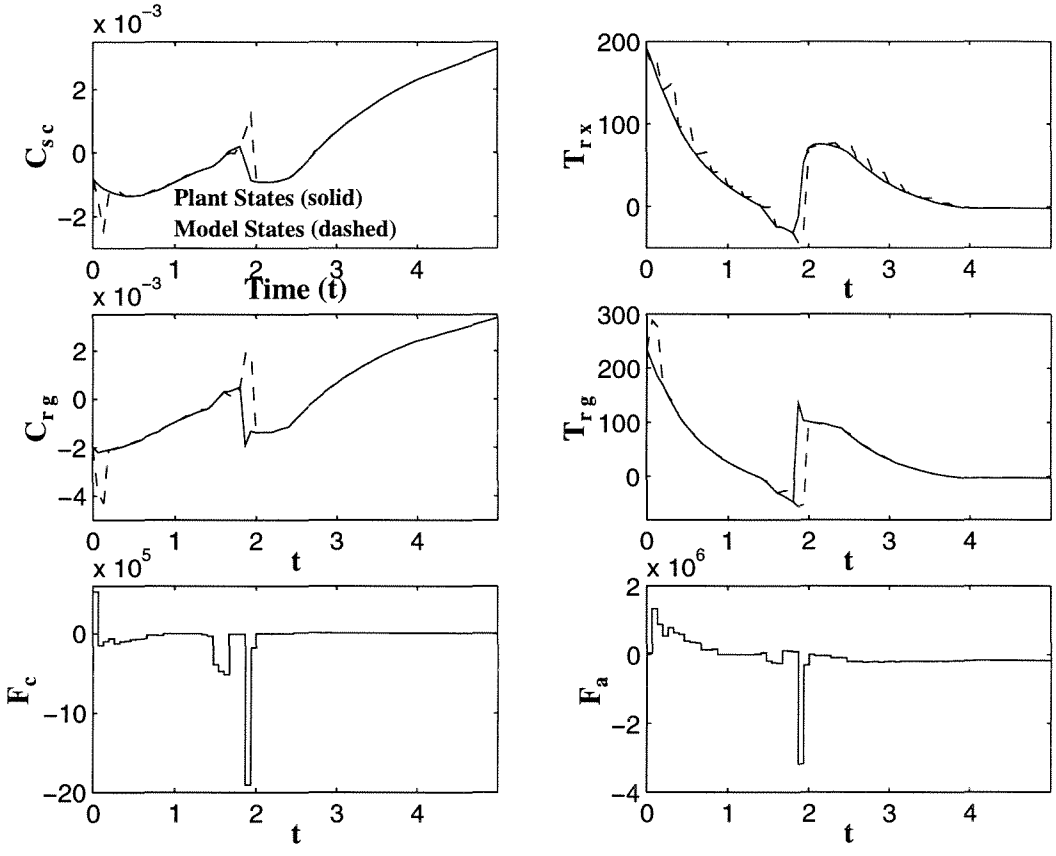

Figure 6.20: FCCU: State and control responses in the unconstrained **Case 2.2**.

Controller Parameters (figure 6.20)		
$Q = \text{diag}([0 \;\; 10^{-3} \;\; 1 \;\; 0])$	$R = 0.1\, I_m$	$S = 0$
$P = 3$	$M = 3$	$\alpha = 0.9$

Here, the code does not break down and, as we can see from figure 6.20, both the temperatures in the reactor and in the regenerator are brought to the origin. However, the concentrations C_{sc} and C_{rg} cannot be stabilized. This is mostly due to the fact that the state variables are of very different order of magnitude, so appropriate weighting in the contractive constraint (especially) and in the objective function has to be observed. Besides, since the system has only two manipulated variables and four states and the temperatures are so highly correlated, it is natural that, without appropriate weighting of the state variables,

the controller is only able to stabilize as many controlled variables as there are manipulated variables. Therefore, the contractive constraint is ineffective for the states C_{sc} and C_{rg} because of the difficulty in finding a proper weight $\hat{P}$. Trying to scale the problem through weights in the objective function and in the contractive constraint was proven to be very challenging and we could not obtain a set of weights for which the results were completely satisfactory.

6.4.6 Example 5: van der Vusse Reactor

Here we will investigate the same control problem as in chapter 4, i.e., beginning at certain arbitrary initial conditions, we want to be able to control the system to the point of maximum conversion of product B. The initial condition used here is $x_0 = [-2 \;\; 20 \;\; -200]$ for the deviation of the states with respect to the coordinates of the steady state of maximum conversion, unless otherwise indicated. The sampling time is $T = 0.1$ h.

Case 1: State feedback

Case 1.1: No disturbances or uncertainty

The results of the simulation in the constrained case are shown in figure 6.21.

The controller parameters used in **Case 1.1** are given by:

Controller Parameters (figure 6.21)		
$Q = \text{diag}([0.5 \;\; 1 \;\; 0.1])$	$R = 0$	$S = 0$
$P = 2$	$M = 2$	$\alpha = 0.7$
$u_{min} = 0$	$u_{max} = 0.5$	

Figure 6.21 reveals that the states settle to the origin very quickly (in approximately two samples) even in the presence of tight input constraints. The

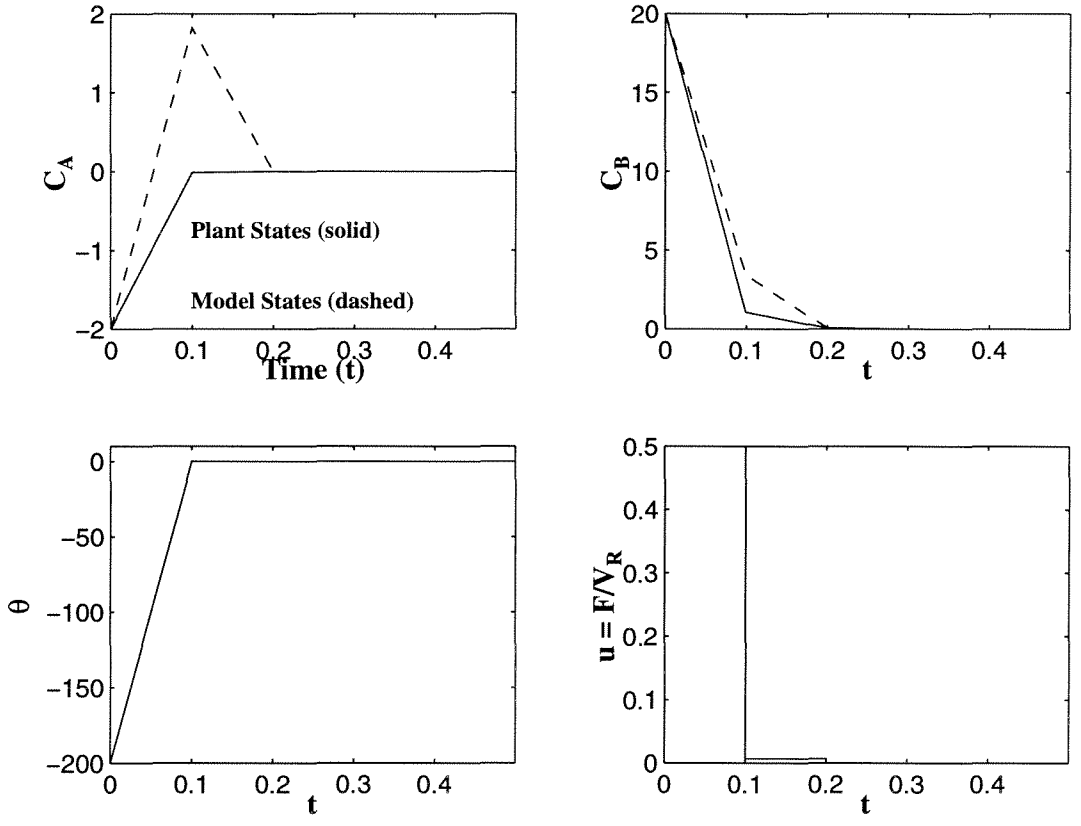

Figure 6.21: van der Vusse CSTR: State and control responses in the constrained **Case 1.1**.

temperature in the reactor θ has very fast dynamics and it settles to its steady state value in only one sampling time.

Case 1.2: Parameter uncertainty

The set of uncertain parameters is composed of k_{10}, k_{20}, k_{30} (kinetic constants or collision factors), A_R (surface of the cooling jacket) and k_W (heat transfer coefficient for the cooling jacket). These parameters are commonly unknown in true experimental set-ups of reactor systems. In the present simulations, we consider that the true parameter values are 10% larger than their nominal counterparts.

The simulation for the unconstrained case can be found in figure 6.22.

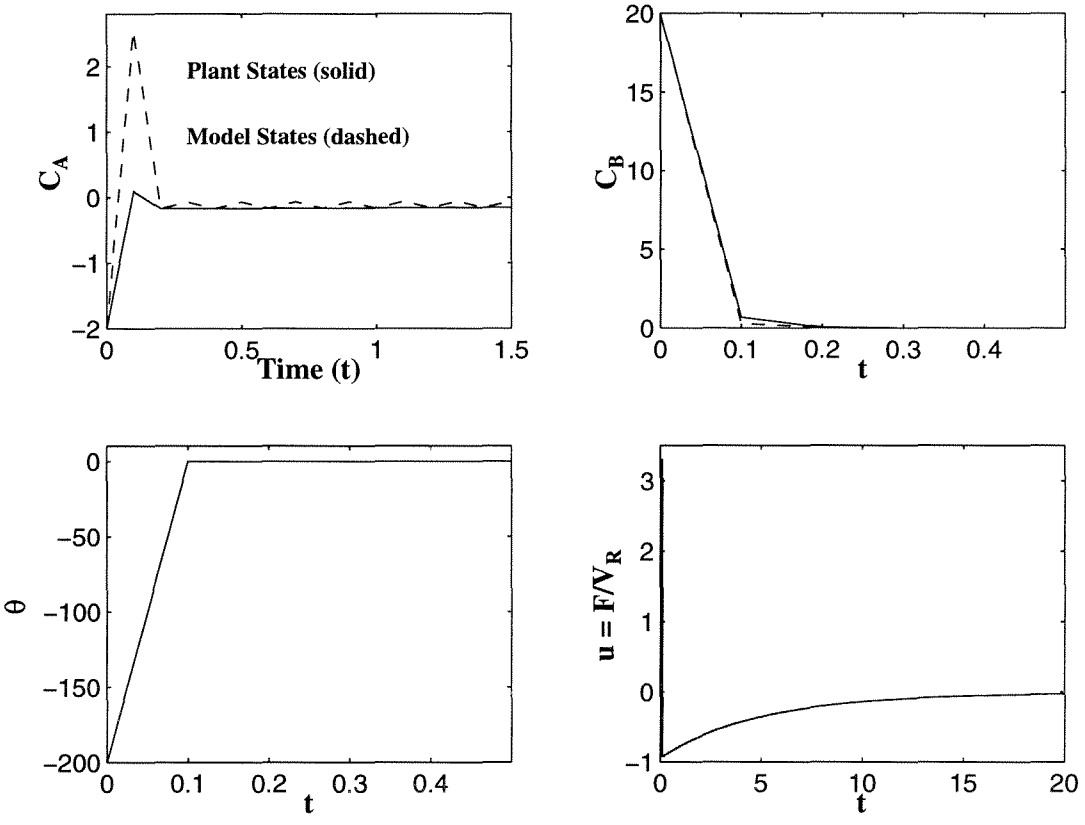

Figure 6.22: van der Vusse CSTR: State and control responses in the unconstrained **Case 1.2**.

The controller parameters used in **Case 1.2** are:

Controller Parameters (figure 6.22)		
$Q = \text{diag}([0.5 \;\; 1 \;\; 0.1])$	$R = 0$	$S = 0$
$P = 2$	$M = 2$	$\alpha = 0.9$

We notice from figure 6.22 that the first state variable, C_A, shows an offset with respect to its value at the steady state of maximum yield due to the parameter mismatch. The other variables, however, are not sensitive to this parameter uncertainty.

Case 1.3: Exponentially decaying disturbances

The perturbed variables are C_{A0} (concentration of reactant A in the feed) and θ_0 (inflow temperature) which are non-manipulated input variables. The disturbance behavior is as described by equation 6.138 but now $d(t) := [C_{A0} \quad \theta_0]$ and d^{ss} represents the vector of nominal values of these input variables. Now $a = [1 \quad 1]$ and $b = 0.1$. Thus, initially, due to some perturbation in the feed stream, C_{A0} and θ_0 increase to twice their values at the desired steady state and then they decrease exponentially to their nominal values. The constrained response under these disturbances is shown in figure 6.23. The disturbance behavior is also illustrated in figure 6.23.

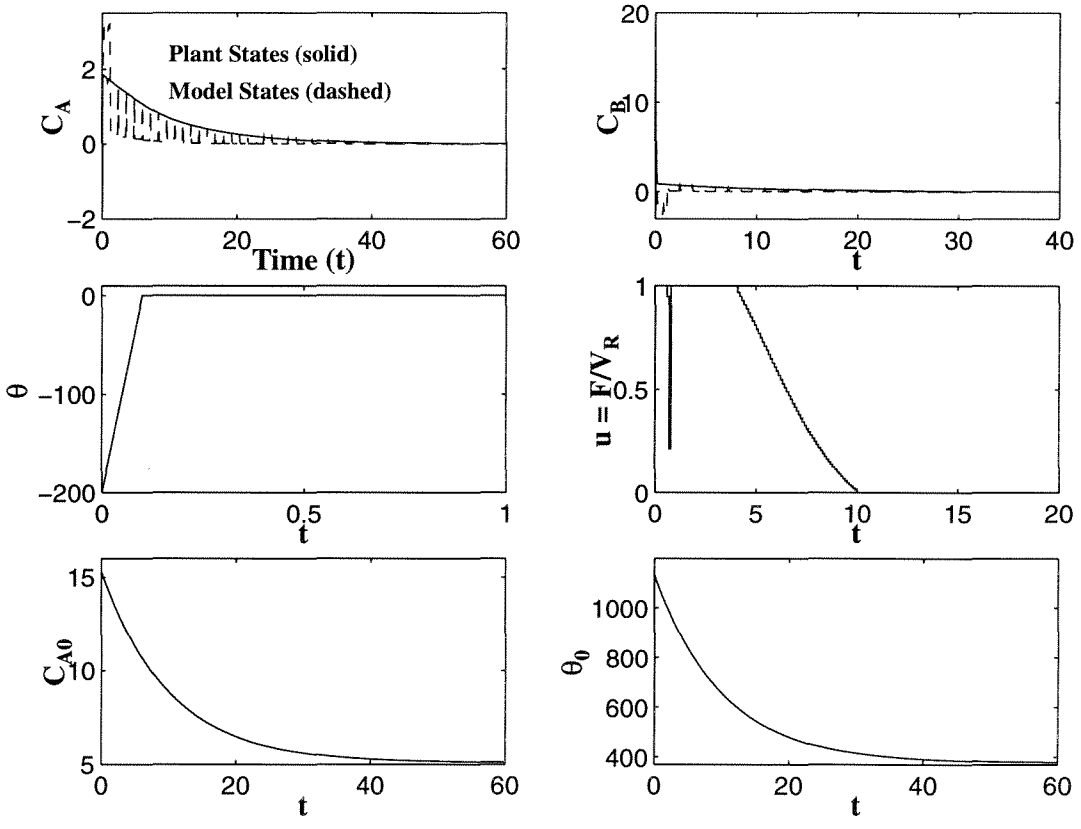

Figure 6.23: van der Vusse CSTR: State and control responses in the constrained **Case 1.3**.

The controller parameters used in **Case 1.3** are:

Controller Parameters (figure 6.23)		
$Q = \text{diag}([0.5 \ 1 \ 0.1])$	$R = 0$	$S = 0$
$P = 12$	$M = 8$	$\alpha = 0.9$
$u_{min} = 0$	$u_{max} = 1$	

Figure 6.23 shows that, since the states of the linear model are not affected by the disturbances, except every twelve steps when they are updated with the states of the plant, the model shows this behavior of "pushing" the nonlinear system towards the origin. This effect is felt more strongly in the first state, C_A. Once again, the temperature, θ, approaches the origin in only one time step.

The presence of these long lasting disturbances delay the response quite significantly compared to the response under no disturbances (look at the time scales in figure 6.23 and compare them with the ones in 6.21).

Case 1.4: Exponentially decaying disturbances (reactor operating initially at the desired steady state)

If the system is initially operating at the steady state of maximum conversion and the feed stream is perturbed as previously described (i.e., C_{A0} and θ_0 have their values doubled at $t = 0$ and decay exponentially to their nominal values in the fashion shown in figure 6.23), the constrained closed-loop response is illustrated in figure 6.24.

The controller parameters used in **Case 1.4** are the same as in **Case 1.3**.

As we notice from figure 6.24, the contractive MPC controller is able to re-stabilize the system back to the desired steady state as soon as the disturbances start to subside. The three states have approximately the same response time (opposite to what happens in the step change from a different initial condition,

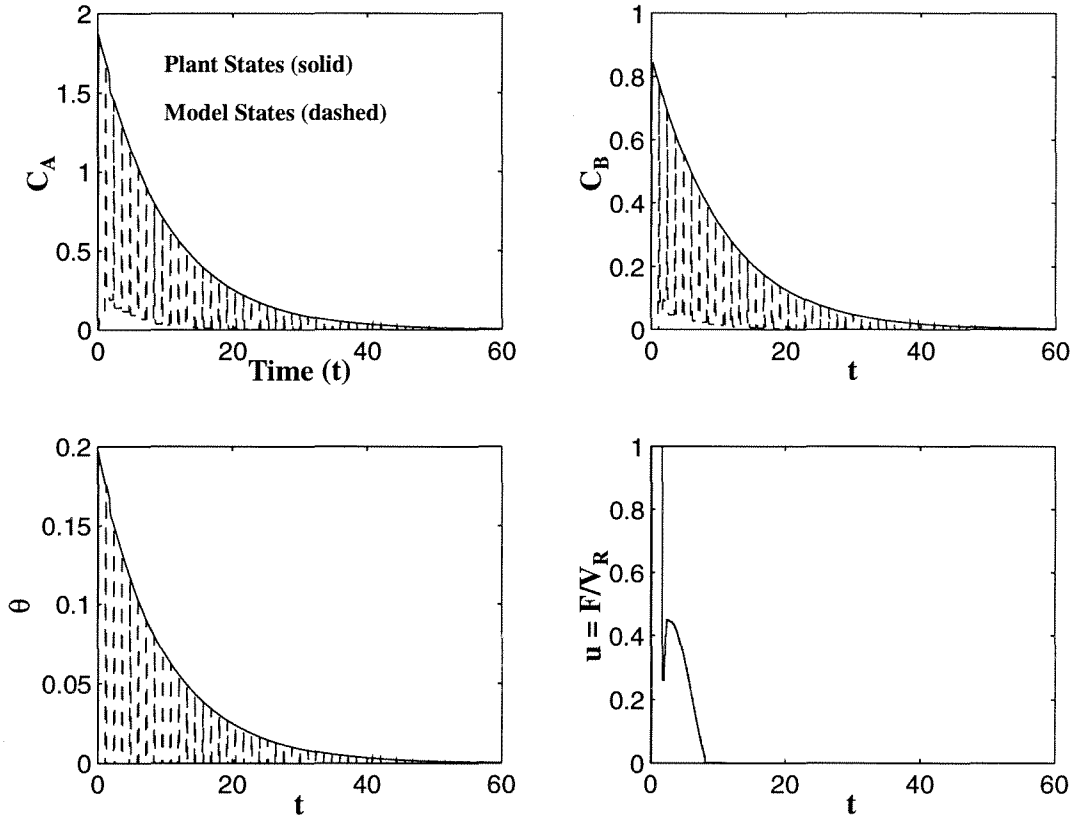

Figure 6.24: van der Vusse CSTR: State and control responses in the constrained **Case 1.4.**

where the dynamics of the temperature are always much faster than those of the concentrations of A and B in the reactor).

Case 2: Output feedback

Finally, we will analyze the closed-loop response to the step change in the states from $x_0 = [-2 \quad 20 \quad -200]$ to the origin. The least-squares moving horizon-based state estimator proposed in chapter 5 is used to provide state estimates, in the presence of asymptotically decaying random noise. C_B is the only (noisy) output variable.

The closed-loop response in the presence of input constraints is illustrated in figure 6.25. The dynamic and output noises are also plotted in figure 6.25.

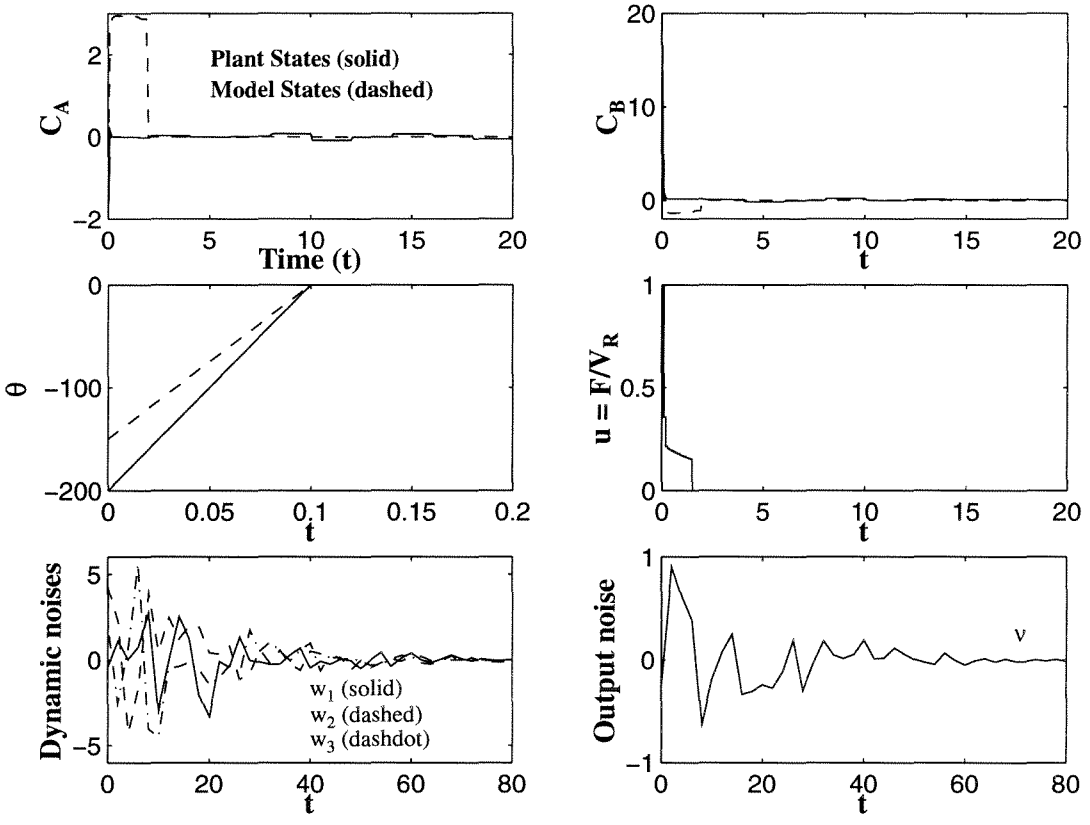

Figure 6.25: van der Vusse CSTR: State and control responses in the constrained **Case 2**.

The controller/estimator parameters and initial conditions used in **Case 2** are:

Controller and Estimator Parameters (figure 6.25)		
$Q = \text{diag}([0.5 \;\; 1 \;\; 0.1])$	$R = 0.01$	$S = 0$
$P = 20$	$M = 14$	$\alpha = 0.9$
$u_{min} = 0$	$u_{max} = 1$	
$m = 21$	$P_1 = 10^{-3}\, I_n$	$\bar{R}^{-1} = 10\, I_p$

Initial Conditions			
Plant:	$C_{A0} = -2$	$C_{B0} = 20$	$\theta_0 = -200$
Model/Observer:	$\bar{C}_{A0} = -1.5$	$\bar{C}_{B0} = 15$	$\bar{\theta}_0 = -150$

As we see from figures 6.25 the closed-loop system is stabilized to the origin and the estimator provides asymptotically convergent estimates. Notice that C_A is more sensitive to the dynamic noise than C_B and θ (which is not at all sensitive to the noise or initial state estimation error).

Bibliography

[1] M. Alamir and G. Bornard. New sufficient conditions for global stability of receding horizon control for discrete-time nonlinear systems. In D. Clarke, editor, *Advances in Model-Based Predictive Control*, pages 173–181. Oxford University Press, 1994.

[2] M. Alamir and G. Bornard. On the stability of receding horizon control of nonlinear discrete-time systems. *Syst. Control Lett.*, 23:291–296, 1994.

[3] M. Alamir and G. Bornard. Stability of a truncated infinite constrained receding horizon scheme: The general discrete nonlinear case. *Automatica*, 31(9):1353–1356, September 1995.

[4] V. M. Alekseev, V. M. Tikhomirov, and S. V. Fomin. *Optimal Control.* Consultants Bureau, New York, 1987.

[5] F. Allgöwer. Definition and computation of a nonlinearity measure and application to approximate I/O-linearization. Technical Report 95-1, Insitut für Systemdynamik und Regelungstechnik, Universität Stuttgart, 1994.

[6] F. Allgöwer. Analysis and controller synthesis for nonlinear processes using nonlinearity measures. In *AIChE Annual Meeting*, number 180h, Miami, FL, 1995.

[7] J. Arandes and H. de Lasa. Simulation and multiplicity of steady states in fluidized FCCUs. *Chem. Eng. Sci.*, 47(9-11):2535–2540, 1992.

[8] A. Arbel, Z. Huang, I. Rinard, and R. Shinnar. Partial control of FCC units: input multiplicities and control structures. In *AIChE Annual Meeting*, number 26f, St. Louis, MI, 1993.

[9] A. Arbel, I. Rinard, R. Shinnar, and A. Sapre. Dynamics and control of fluidized catalytic crackers. 2. Multiple steady states and instabilities. *Ind. Eng. Chem. Res.*, 34(9):3014–3026, 1995.

[10] A. Astolfi. *Asymptotic Stabilization of Nonholonomic Systems with Discontinuous Control.* PhD thesis, Swiss Federal Institute of Technology (ETH), 1995. Diss. ETH No. 10983.

[11] A. Astolfi. Discontinuous control of nonholonomic systems. *Syst. Control Lett.*, 27:37–45, 1995.

[12] A. Avidan, M. Edwards, and H. Owen. Fluid catalytic cracking: Past and future challenges. *Reviews in Chemical Engineering*, 6(1):1–71, 1990.

[13] V. Balakrishnan, Z. Zheng, and M. Morari. Constrained stabilization of discrete-time systems. In D. Clarke, editor, *Advances in Model-Based Predictive Control*, pages 205–216. Oxford University Press, 1994.

[14] J. S. Baras, A. Bensoussan, and M. R. James. Dynamic observers as asymptotic limits of recursive filters: Special cases. *SIAM J. Applied Mathematics*, 48(5):1147–1158, October 1988.

[15] B. R. Barmish, M. Corless, and G. Leitmann. A new class of stabilization controller for uncertain dynamical systems. *SIAM Journal of Control and Optimization*, 21:246–255, 1983.

[16] B. R. Barmish and G. Leitmann. On ultimate boundedness control of uncertain systems in the absence of matching condition. *IEEE Trans. Aut. Control*, 27:153–158, 1982.

[17] G. Becker, A. Packard, D. Philbrick, and G. Balas. Control of parametrically-dependent linear systems: A single quadratic Lyapunov approach. In *American Control Conf*, volume 3, pages 2795–2799, June 1993.

[18] S. Behtash. Robust output tracking for nonlinear systems. *Int. J. Control*, 51:1381–1407, 1990.

[19] B. W. Bequette. Nonlinear control of chemical processes: A review. *Ind. Eng. Chem. Res.*, 30:1391–1413, 1991.

[20] L. Biegler and J. Rawlings. Optimization approaches to nonlinear model predictive control. In *Conf. Chemical Process Control (CPC-IV)*, pages 543–571, South Padre Island, Texas, 1991. CACHE-AIChE.

[21] L. T. Biegler. Sensitivity analysis of QPs. Personal communication, 1994.

[22] R. R. Bitmead, M. Gevers, and V. Wertz. *Adaptive Optimal Control.* Prentice Hall, Englewood Cliffs, N.J., 1990.

[23] M. Bouslimani, M. M'Saad, and L. Dugard. Stabilizing receding horizon control: A unified continuous/discrete time formulation. In *Conf. on Decision and Control*, page 1298, 1993.

[24] R. Brockett. Asymptotic stability and feedback stabilization. In R. Brockett, R. Millman, and H. Sussman, editors, *Differential Geometric Control Theory*, pages 181–193. Birkhäuser, 1983.

[25] J. A. Bromley and T. J. Ward. Fluidized catalytic cracker control. A structural analysis approach. *Ind. Eng. Chem. Process Des. Dev.*, 20:74–81, 1980.

[26] P. J. Campo. *Studies in Robust Control of Systems Subject to Constraints.* PhD thesis, California Institute of Technology, 1990.

[27] P. J. Campo and M. Morari. Robust model predictive control. In *American Control Conf*, pages 1021–1026, 1987.

[28] C. Chen and L. Shaw. On receding horizon feedback control. *Automatica*, pages 349–352, 1982.

[29] H. Chen, A. Kremling, and F. Allgöwer. Nonlinear predictive control of a benchmark CSTR. In *European Control Conf*, pages 3247–3252, Rome, Italy, 1995.

[30] Y. H. Chen and G. Leitmann. Robustness of uncertain systems in the absence of matching assumptions. *Int. J. Control*, 45:1527–1544, 1987.

[31] L. Chisci and E. Mosca. Stabilizing predictive control: the singular transition matrix case. In D. Clarke, editor, *Advances in Model-Based Predictive Control*, pages 122–130. Oxford University Press, 1994.

[32] D. W. Clarke. Advances in model-based predictive control. In D. W. Clarke, editor, *Advances in Model-Based Predictive Control*, pages 3–21. Oxford University Press, 1994.

[33] D. W. Clarke, C. Mohtadi, and P. S. Tuffs. Generalized predictive control–I. The basic algorithm. *Automatica*, 23:137–148, 1987.

[34] M. Corless and G. Leitmann. Continuous state feedback guaranteeing uniform ultimate boundedness for uncertain dynamical systems. *IEEE Trans. Aut. Control*, 32:763–771, 1987.

[35] C. R. Cutler and B. L. Ramaker. Dynamic matrix control — A computer control algorithm. In *Joint Automatic Control Conf.*, San Francisco, California, 1980.

[36] N. M. de Oliveira. *Newton-type Algorithms for Nonlinear Constrained Chemical Process Control.* PhD thesis, Department of Chemical Engineering, Carnegie Mellon University, Pittsburgh, Pennsylvania, March 1994.

[37] S. L. De Oliveira. *Model Predictive Control (MPC) for Constrained Nonlinear Systems.* PhD thesis, California Institute of Technology, Pasadena, California, March 1996.

[38] J. J. Deyst and C. F. Price. Conditions for asymptotic stability of the discrete minimum-variance linear estimator. *IEEE Trans. Aut. Control*, 13(6):702–705, 1979.

[39] W. Eaton and J. Rawlings. Feedback control of nonlinear processes using on-line optimization techniques. *Comp. and Chem. Eng.*, 14:469–479, 1990.

[40] W. Eaton and J. Rawlings. Model-predictive control of chemical processes. *Chem. Eng. Sci.*, 47:705–720, 1992.

[41] C. Economou. *An Operator Theory Approach to Nonlinear Controller Design.* PhD thesis, California Institute of Technology, Pasadena, CA, 1985.

[42] W. Edwards and H. Kim. Multiple steady states in FCC unit operations. *Chem. Eng. Sci.*, 43(8):1825–1830, 1988.

[43] S. Engell and K. Klatt. Nonlinear control of a non-minimum-phase CSTR. In *American Control Conf*, pages 2941–2945, Los Angeles, CA, 1993.

[44] A. V. Fiacco. *Introduction to Sensitivity and Stability Analysis in Nonlinear Programming.* Academic Press, New York, 1983.

[45] A. V. Fiacco and G. P. McCormick. *Nonlinear Programming.* John Wiley & Sons, New York, 1968.

[46] R. Fletcher. *Practical Methods of Optimization.* John Wiley & Sons, 1987.

[47] L. C. Fu and T. L. Liao. Globally stable tracking of nonlinear systems using variable structure control and with an application to a robotic manipulator. *IEEE Trans. Aut. Control*, 35:1345–1351, 1990.

[48] C. E. García. Quadratic dynamic matrix control of nonlinear processes. An application to a batch reactor process. In *AIChE Annual Meeting*, San Francisco, CA, 1984.

[49] C. E. García and A. M. Morshedi. Quadratic programming solution of dynamic matrix control (QDMC). *Chem. Eng. Communications*, 46:73–87, 1986.

[50] C. E. García, D. M. Prett, and M. Morari. Model predictive control: Theory and practice — A survey. *Automatica*, 25(3):335–348, May 1989.

[51] G. Gattu and E. Zafiriou. Nonlinear quadratic dynamic matrix control with state estimation. *Ind. Eng. Chem. Res.*, 31(4):1096–1104, 1992.

[52] H. Genceli and M. Nikolaou. Robust stability analysis of constrained L_1-norm model predictive control. *AIChE Journal*, 39(12):1954–1965, 1993.

[53] P. E. Gill, W. Murray, M. A. Saunders, and M. H. Wright. User's guide for NPSOL 5.0: A FORTRAN package for nonlinear programming. Technical report, Stanford University, November 1994.

[54] G. H. Golub and C. F. V. Loan. *Matrix Computations.* Johns Hopkins University Press, Baltimore, Maryland, 1983.

[55] L. A. Gould, L. B. Evans, and H. Kurihara. Optimal control of fluid catalytic cracking processes. *Automatica*, 6:695–703, 1970.

[56] J. W. Grizzle and P. E. Moraal. Newton, observers and nonlinear discrete-time control. In *Conf. on Decision and Control*, pages 760–767, Hawaii, December 1990.

[57] P. Grosdidier, A. Mason, A. Aitolahti, P. Heinonen, and V. Vanhamaki. FCC unit reactor-regenerator control. *Comp. and Chem. Eng.*, 17(2):165–179, 1993.

[58] A. S. Householder. *The Theory of Matrices in Numerical Analysis.* Dover Publications, New York, 1974.

[59] M. Hovd and S. Skogestad. Controllability analysis for the fluid catalytic cracking process. In *AIChE Annual Meeting, Los Angeles, California*, November 1991.

[60] M. Hovd and S. Skogestad. Procedure for regulatory control structure selection with application to the FCC process. *AIChE Journal*, 39(12):1938–1953, 1993.

[61] A. H. Jazwinski. *Stochastic Processes and Filtering Theory.* Academic Press, New York, 1970.

[62] S. Keerthi and E. Gilbert. Optimal infinite-horizon feedback laws for a general class of constrained discrete-time systems: Stability and moving-horizon approximations. *Journal of Optimization Theory and Applications*, pages 265–293, 1988.

[63] L. Kershenbaum, D. Q. Mayne, R. Pytlak, and R. B. Vinter. Receding horizon control. In *Advances in Model-Based Predictive Control*, pages 233–246. Oxford University Press, 1993.

[64] K. Klatt and S. Engell. Rührkesselreaktor mit Parallel- und Folgereaktion: Testbeispiel des GMAFA 1.4 zur nichtlinearen Regelung. In *VDI-Bericht Nr. 1026.* VDI-Verlag, Düsseldorf, Germany, 1993.

[65] K. Klatt, S. Engell, A. Kremling, and F. Allgöwer. Testbeispiel: Rührkesselreaktor mit Parallel- und Folgereaktion. In S. Engell, editor, *Entwurf nichtlinearer Regelungen*, pages 425–432. Oldenbourg Verlag München, 1995.

[66] M. V. Kothare, V. Balakrishnan, and M. Morari. Robust constrained model predictive control using linear matrix inequalities. *Automatica (in press)*, 1996.

[67] H. W. Kuhn and A. W. Tucker. Nonlinear programming. In J. Neyman, editor, *2nd Berkeley Symposium on Mathematical Statistics and Probability.* University of California Press, 1951.

[68] O. K. Kwon, W. H. Kwon, K. S. Yoo, and M. J. Kim. Receding horizon LQG controller using optimal FIR filter with control input. In *Conf. on Decision and Control*, volume 2, pages 1292–1297, December 1993.

[69] W. Kwon and A. Pearson. A modified quadratic cost problem and feedback stabilization of a linear system. *IEEE Trans. Aut. Control*, 22(5):838–842, 1977.

[70] W. H. Kwon. Advances in predictive control: Theory and application. In *1st Asian Control Conf*, Tokyo, July 1994. Updated in October, 1995.

[71] W. H. Kwon, A. N. Bruckstein, and T. Kailath. Stabilizing state feedback design via the moving horizon method. *Int. J. Control*, 37(3):631–643, 1983.

[72] L. S. Lasdon. *Numerical Optimization 1984*, chapter Nonlinear programming algorithms - Applications, software and comparisons. SIAM publications, Philadelphia, 1985.

[73] J. H. Lee, M. S. Gelormino, and M. Morari. Model predictive control of multi-rate sampled-data systems: A state-space approach. *Int. J. Control*, 55:153–191, 1991.

[74] J. H. Lee and N. L. Ricker. Extended Kalman filter based on nonlinear model predictive control. *Ind. Eng. Chem. Res.*, 33:1530–1541, 1994.

[75] W. Lee and A. Kugelman. Number of steady-state operating points and local stability of open-loop fluid catalytic cracker. *Ind. Eng. Chem. Process Des. Dev.*, 12(2):197–204, 1973.

[76] F. L. Lewis. *Optimal Estimation.* John Wiley & Sons, New York, 1986.

[77] T. L. Liao, L. C. Fu, and C. F. Hsu. Adaptive robust tracking of nonlinear systems and with an application to a robotic manipulator. *Syst. Control Lett.*, 15:339–348, 1990.

[78] L. Ljung. Asymptotic behavior of the extended Kalman filter as a parameter estimator for linear systems. *IEEE Trans. Aut. Control*, 24(1):36–50, Feb. 1979.

[79] A. I. Lur'e. *Some nonlinear problems in the theory of automatic control.* Her Majesty's Stationery Office, London, 1957. In Russian, 1951.

[80] A. I. Lur'e and V. N. Postnikov. On the theory of stability of control systems. *Applied Mathematics and Mechanics*, 8(3), 1944.

[81] D. Mayne and H. Michalska. An implementable receding horizon controller for the stabilization of nonlinear systems. In *Conf. on Decision and Control*, pages 3396–3397, Honolulu, HI, 1990.

[82] D. Mayne and H. Michalska. Receding horizon control of nonlinear systems. *IEEE Trans. Aut. Control*, 35:814–824, 1990.

[83] D. Mayne and H. Michalska. Approximate global linearization of nonlinear systems via on-line optimization. In *European Control Conf*, pages 182–187, Grenoble,France, 1991.

[84] D. Mayne and H. Michalska. Model predictive control of nonlinear systems. In *American Control Conf*, pages 2343–2348, Boston, MA, 1991.

[85] D. Mayne and H. Michalska. Receding horizon control of nonlinear systems without differentiability of the optimal value function. *Syst. Control Lett.*, 16:123–130, 1991.

[86] D. Q. Mayne. Optimization in Model Based Control. In J. B. Rawlings, editor, *4th IFAC Symposium on Dynamics and Control of Chemical Reactors, Distillation Columns, and Batch Processes (DYCORD+ '95)*, pages 229–242. Danish Automation Society, June 1995.

[87] D. Q. Mayne and H. Michalska. Moving horizon observer-based control. In *Conf. on Decision and Control*, pages 1512–1517, Tucson, Arizona, December 1992.

[88] D. Q. Mayne and H. Michalska. Adaptive receding horizon control for constrained nonlinear systems. In *Conf. on Decision and Control*, pages 1286–1291, San Antonio, Texas, December 1993.

[89] D. Q. Mayne and E. Polak. Optimization based design and control. In *12th IFAC World Congress*, pages 129–138, Sydney, Australia, 1993.

[90] R. M'Closkey and R. Murray. Experiments in exponential stabilization of a mobile robot towing a trailer. In *American Control Conf*, volume 1, pages 988–993, Baltimore, Maryland, June 1994.

[91] E. Meadows, M. Henson, J. Eaton, and J. Rawlings. Receding horizon control and discontinuous state feedback stabilization. *Int. J. Control*, 62(5):1217–1229, 1995.

[92] E. Meadows and J. Rawlings. Receding horizon control with an infinite horizon. In *American Control Conf*, pages 2926–2930, San Francisco, California, 1993.

[93] E. S. Meadows and J. B. Rawlings. Topics in model predictive control. In E. Ridvan Berber, editor, *NATO Advanced Study Institute on Methods of Model Based Control Proceedings*, Antalya, Turkey, 1994. Kluwer Academic Publishers.

[94] R. K. Mehra, R. Rouhani, J. Eterno, J. Richalet, and A. Rault. Model algorithmic control: Review and recent development. In *Conf. Chemical Process Control (CPC-II)*, pages 287–310. United Engineering Trustees, 1982.

[95] H. Michalska and D. Mayne. Robust receding horizon control of constrained nonlinear systems. *IEEE Trans. Aut. Control*, 38(11):1623–1633, Nov. 1993.

[96] H. Michalska and D. Q. Mayne. Moving horizon observers. In M. Fliess, editor, *IFAC Nonlinear Control Systems Design Symposium (NOLCOS '92)*, pages 576–581, Bordeaux, France, 1992.

[97] H. Michalska and D. Q. Mayne. Moving horizon observers and observer-based control. *IEEE Trans. Aut. Control*, 40(6):995–1006, June 1995.

[98] M. Morari. Robust stability of systems with integral control. In *Conf. on Decision and Control*, pages 865–869, San Antonio,TX, 1983.

[99] M. Morari, C. E. García, J. H. Lee, and D. M. Prett. *Model Predictive Control.* Prentice-Hall, Englewood Cliffs, N.J., 1997. in preparation.

[100] K. R. Muske and J. B. Rawlings. Nonlinear moving horizon state estimation. In E. Ridvan Berber, editor, *NATO Advanced Study Insitute on Methods of Model Based Control Proceedings*, Antalya, Turkey, 1994. Kluwer Academic Publishers.

[101] G. D. Nicolao and R. Scattolini. Stability and output terminal constraints in predictive control. In *Advances in Model-Based Predictive Control*, pages 105–121. Oxford University Press, 1994.

[102] A. Packard and J. Doyle. The complex structured singular value. *Automatica*, 29(1):71–109, 1993.

[103] A. Palazoglu and T. Khambanonda. Dynamic operability analysis of a fluidized catalytic cracker. *AIChE Journal*, 33(6):1037–1040, 1987.

[104] L. R. Petzold. A description of DASSL: a differential/algebraic system solver. Technical Report 82-8637, Sandia National Laboratories, Livermore, California, 1982.

[105] J. Pomet. Explicit design of time-varying stabilizing control laws for a class of controllable systems without drift. *Syst. Control Lett.*, 18:147–158, 1992.

[106] V. M. Popov. *Hyperstability of Control Systems.* Springer-Verlag, Berlin, 1973.

[107] D. M. Prett and R. D. Gillette. Optimization and constrained multivariable control of a catalytic cracking unit. In *AIChE Meeting*, Houston, TX, 1979.

[108] A. I. Propoi. Use of LP methods for synthesizing sampled-data automatic systems. *Automation and Remote Control*, 24:837, 1963.

[109] J. B. Rawlings and K. R. Muske. The stability of constrained receding horizon control. *IEEE Trans. Aut. Control*, 38(10):1512–1516, Oct. 1993.

[110] N. L. Ricker and J. H. Lee. Nonlinear model predictive control of the Tennesee Eastman challenge process. *Comp. and Chem. Eng.*, 19(9):961–981, 1995.

[111] D. G. Robertson, J. H. Lee, and J. B. Rawlings. A moving horizon-based approach to least squares estimation. *AIChE Journal (in press)*, 1996.

[112] C. Schmid and L. Biegler. Application of multistep Newton-type controllers to fluid catalytic cracking. In *American Control Conf*, pages 581–586, S. Diego, CA, 1990.

[113] P. Scokaert and D. Clarke. Stability and feasibility in constrained predictive control. In D. Clarke, editor, *Advances in Model-Based Predictive Control*, pages 217–229. Oxford University Press, 1994.

[114] P. O. M. Scokaert and J. B. Rawlings. Stability of model predictive control under perturbations. In *IFAC Nonlinear Control Systems Design Symposium (NOLCOS '95)*, volume 1, pages 21–26, Tahoe City, California, June 1995.

[115] S. N. Singh and A. R. Coelen. Nonlinear control of mismatched uncertain linear systems and application to control of aircrafts. *ASME J. Dynamic System and Control*, 106:203–210, 1984.

[116] S. Skogestad, M. Morari, and J. C. Doyle. Robust control of ill-conditioned plants: High purity distillation. *IEEE Trans. Aut. Control*, 33:1092–1105, 1988.

[117] Y. Song. *Estimation and Control in Discrete-Time Nonlinear Systems.* PhD thesis, Dept. of Aerospace Engineering, Univeristy of Michigan, 1992.

[118] Y. Song and J. W. Grizzle. The extended Kalman filter as a local asymptotic observer for nonliner discrete-time systems. *J. Math. Syst., Estim. and Control*, 5(1):59–78, 1995.

[119] L. C. F. T. L. Liao and C.-F. Hsu. Output tracking control of nonlinear systems with mismatched uncertainties. *Syst. Control Lett.*, 18:39–47, 1992.

[120] A. Teel, R. Murray, and G. Walsh. Nonholonomic control systems: from steering to stabilization. In *Conf. on Decision and Control*, pages 1603–1609, 1992.

[121] S. Wiggins. *Introduction to Applied Nonlinear Dynamic Systems and Chaos.* Springer-Verlag, 1990.

[122] T. H. Yang and E. Polak. Moving horizon control of linear systems with input saturation and plant uncertainty.1. Robustness. *Int. J. Control*, 58(3):613–638, September 1993.

[123] T. H. Yang and E. Polak. Moving horizon control of linear systems with input saturation and plant uncertainty.2. Disturbance rejection and tracking. *Int. J. Control*, 58(3):639–663, September 1993.

[124] T. H. Yang and E. Polak. Moving horizon control of nonlinear systems with input saturation, disturbances and plant uncertainty. *Int. J. Control*, 58(4):875–903, 1993.

[125] E. Zafiriou. Robust model predictive control of processes with hard constraints. *Comp. and Chem. Eng.*, 14(4/5):359–371, 1990.

[126] S. H. Zak. On the stabilization and observation of nonlinear uncertain dynamic systems. *IEEE Trans. Aut. Control*, 35:604–607, 1990.

[127] Z. Q. Zheng. *Robust Control of Systems Subject to Constraints.* PhD thesis, California Institute of Technology, Pasadena, California, 1995.

[128] Z. Q. Zheng and M. Morari. Stability of model predictive control with mixed constraints. *IEEE Trans. Aut. Control*, 40(10):1818–1823, October 1995.